HPLC-AAS INTERFACES FOR THE DETERMINATION OF IONIC ALKYLLEAD, ARSONIUM AND SELENONIUM COMPOUNDS.

© Jean-Simon Blais

Department of Food Science and Agricultural Chemistry

Faculty of Agriculture

McGill University, Montreal

February 1990

A thesis submitted to the Faculty of Graduate Studies and Research in partial fulfillment of the requirements for the degree of Ph.D.

Suggested Short Title:

HPLC-AAS INTERFACES

Table of Contents

ABSTRACT

Ph.D. Jean-Simon Blais Fd. Sc. and Agr. Chem.

HPLC-AAS INTERFACES FOR THE DETERMINATION OF IONIC ALKYLLEAD, ARSONIUM AND SELENONIUM COMPOUNDS.

Three direct interfaces for coupling high performance liquid chromatography (HPLC) with atomic absorption spectrometry (AAS) were developed and optimized for the determination of ionic organolead, organoselenium and organoarsenic compounds. The first all-quartz interface consisted of a thermospray nebulizer and a flame microatomizer in which ionic alkyllead analytes ($R_nPb^{(4-n)+}$; R = CH_3, C_2H_5) were atomized by a methanol(from HPLC eluent)-oxygen kinetic flame, and channeled in a quartz tube (atom keeper) mounted into the AAS optical beam. Alternately, the classical electrothermal atomization technique for organolead species (quartz furnace under hydrogen atmosphere) was coupled with a post-column derivatization-volatilization apparatus based on the ethylation of ionic alkylleads by sodium tetraethylborate. The limits of detection provided by these two approaches were 1.0-3.4 ng and 0.10-0.15 ng, respectively. Arsonium [$(CH_3)_3RAs^+$; R = CH_3, CH_2CH_2OH, CH_2COOH] and selenonium [$(CH_3)_2RSe^+$; R = CH_3, CH_2CH_2OH] species were quantified using a novel HPLC-AAS approach based on a direct coupling of three processes: thermospray nebulization, thermochemical hydride generation using hydrogen gas, and diffuse flame atomization. Direct evidences for the thermochemical hydride generation process was obtained by injecting $(CH_3)_3SeI$ and SeO_2 into the interface and capturing the gaseous end products in liquid chemical traps specific for SeH_2 and Se(IV). Both analytes were derivatized to SeH_2 only in the presence of hydrogen in the interface. Reverse- and normal-phase high pressure liquid chromatographic methods were also developed and adapted for the HPLC-AAS analyses of alkyllead, arsonium and selenonium compounds in real samples. The limit of detection of the arsonium and selenonium cations were 7.6-13.3 ng and 31.0-43.9 ng, respectively.

Résumé
Ph.D. Jean-Simon Blais Fd. Sc. and Agr. Chem.

COUPLAGE CLHP-SAA POUR LA DETERMINATION DE COMPOSES ALKYLPLOMBS, ARSONIUMS ET SELENONIUMS.

Trois interfaces directes entre la chromatographie liquide à haute pression (CLHP) et la spectrométrie d'absorption atomique (SAA) ont été developpées et optimisées pour la détermination de composés organoplombs, organoarseniques et organosélénium. La première de ces interfaces de quartz comprenait un thermonébulisateur dans lequel les alkylplombs ioniques ($R_nPb^{(4-n)+}$; R = CH_3, C_2H_5) étaient atomisés par une flame supportée par le méthanol (phase mobile CLHP) et l'oxygène. Les limites de détection obtenues ont variés de 1.0-3.4 ng. Une seconde interface dans lequel les composés organoplombs ioniques étaient dérivés en tétraalkylplombs avec le sodium tétraéthyleborate, et volatilisés dans une fournaise éléctrothermale de quartz à donné des limites de détections de l'ordre de 0.10 à 0.15 ng. Les composés arsonium [$(CH_3)_3RAs^+$; R = CH_3, CH_2CH_2OH, CH_2COOH] et sélénonium [$(CH_3)_2RSe^+$; R = CH_3, CH_2CH_2OH] ont été quantifiés par le couplage direct de trois procédés: (a) thermonébulisation, (b) génération thermochimique d'hydrure (MH_2; M = As, Se) avec l'hydrogène et (c) atomisation par flame diffuse. Des évidences directes de la génération thermochimique d'hydrure ont été obtenues par la capture des produits de pyrolyse dans des trappes chimiques spéfifiques pour SeH_2 et Se^{4+}. Les deux composés étudiés [$(CH_3)_3SeI$ et SeO_2] ont été dérivés en SeH_2 seulement en présence d'hydrogène dans l'interface. Les limites de détection obtenues pour les cations arsonium et sélénonium ont été de l'ordre de 7.6-13.3 ng et 30.0-43.9 ng, respectivement. Des nouvelles méthodes de séparations par CLHP en phases normale et inversée ont été développées et optimisées pour l'analyses des trois classes de composés organométaliques (Pb, As, Se).

Acknowledgements

The author gratefully acknowledges Dr. William D. Marshall for the scientific, morale and financial support provided throughout these studies.

Many thanks to my fellow graduate students, Ms Georges-Marie Momplaisir and Mr. Alexis Huyghes-Despointes, and to Dr. I Wharf for helpful suggestions during the development of the HPLC-AAS interfaces.

I wish to dedicate this work to my wife Josée and my daughter Renée-Anne; endless sources of inspiration.

List of Tables.

List of Figures.

---

1. Liquid Chromatography-Atomic Absorption Spectrometry for the Determination of Ionic Alkyllead, Organoselenium and Organoarsenic Species

1.1 Introduction

The objectives of this research have been to develop and optimize direct interfaces between high pressure liquid chromatography (HPLC) and atomic absorption spectrometry (AAS) instruments for speciating organolead, organoselenium and organoarsenic compounds. These interfaces were to be developed according to criteria which would allow a determination of the analytes at environmentally relevant concentrations. In addition to providing low- to sub-nanogram limits of detection, the resulting interfaces had to be robust, inexpensive and compatible with an automated HPLC system. Three original designs involving different derivatization or atomization principles were considered capable of fulfilling these criteria. Ionic organolead analytes were atomized in a methanol-oxygen kinetic flame maintained in a miniaturized quartz thermospray-atomizer (section 2). Alternately, the classical electrothermal atomization technique for organolead species (quartz furnace under hydrogen atmosphere) was coupled with a post-column derivatization-volatilization apparatus based on the ethylation of ionic alkylleads by sodium tetraethylborate (section 3). Arsonium and selenonium species were quantified using a novel approach based on thermochemical hydride generation coupled with a diffuse hydrogen/oxygen flame atomizer (section 4).

Original reversed- and normal-phase high pressure liquid chromatography methods were also developed and adapted for the HPLC-AAS analyses of alkyllead, arsonium and selenonium compounds in real samples.

1.2 Organolead Speciation

1.2.1 Early Approaches

Since their introduction into gasoline as antiknock agents in the early 1920's, there has been considerable interest in the determination of alkylleads in petroleum products as well as in biological and environmental samples. An impressive number of techniques have been developed for this purpose. Early extraction methodologies included wet chemical trapping (Griffing et al., 1957; Snyder and Henderson, 1961; Purdue et al. 1973; Harrison and Laxen, 1978) followed by oxidation of the extracts to transform the alkyllead species to a common physico-chemical state (inorganic lead cation), which was then quantified by AAS (Purdue et al., 1973; Harrison and Laxen, 1978), complexometric spectrophotometry (Griffing et al., 1957; Snyder and Henderson, 1961), or by polarography (Hubis and Clark, 1955). Another technique involved cryogenic trapping and analyses of the condensates by conventional gas chromatography-atomic absorption spectrometry (GC-AAS; Chau et al. 1976a) or GC-graphite furnace AAS (Robinson and Kiesel, 1977; Chakraborti et al., 1981). These early approaches suffered from only moderate selectivity and, in some cases, from relatively low sensitivity.

1.2.2 Hyphenated GC-Atomic Spectrometry

A growing knowledge of the relative toxicities and bioavailabilities of the different physico-chemical forms of alkyllead species (Greanjean and Nielsen, 1979) and other organometallic pollutants has emphasized the need for more accurate and sensitive speciation techniques. This search became successful in the mid 70's, with the development of flameless GC-AAS interfaces. Gas chromatographic effluent containing alkyllead compounds (R_4Pb and/or R_3PbCl; R = CH_3, C_2H_5) have been directly channeled into graphite furnaces (Robinson and Kiesel, 1977; De Jongue et al., 1980; Chakraborti et al., 1981), plasma furnaces (Estes et al., 1981,

1982a), or electrothermal quartz atomizers (QTAAS; Chau et al., 1976b, 1979, 1980; Chakraborti et al., 1984; Forsyth and Marshall, 1985), which provided limits of detection in the sub-nanogram range. Automation GC-QTAAS instrument has been developed successfully (Forsyth and Marshall, 1985).

In order to achieve high gas chromatographic efficiencies, ionic trialkyllead (Estes et al., 1982b) and dialkyllead compounds (Chau et al., 1983) have been derivatized to their corresponding volatile n-butylates using the n-butyl Grignard reagent. Complexometric extraction of ionic alkylleads with sodium diethyldithiocarbamate (NaDEDTC) (Chau et al., 1983, 1984; Chakraborti et al., 1984) or diphenylthiocarbazone (Forsyth and Marshall, 1986) followed by n-butyl derivatization and GC-QTAAS speciation has been applied to a variety of environmental and biological samples. A selective procedure has also been developed for the sequential extraction of tetraalkylleads, ionic alkylleads and inorganic lead in soil, water and street dust samples containing high levels of inorganic lead (Blais and Marshall, 1986).

Because of the requirement for derivatization and the relatively long GC-AAS analysis time, this analytical approach is labor intensive and time consuming. The derivatization step can be problematic since NaDEDTC extracts from lead polluted urban samples have been shown to contain a mixed tetraalkyllead artifact which was produced during the butylation reaction (Blais and Marshall, 1986). A promising alternative to avoid a derivatization step and to decrease chromatographic analysis time would be to use a hyphenated high pressure liquid chromatography-AAS (HPLC-AAS) instrument. This approach would allow a direct speciation of ionic alkylleads from complexometric extracts.

1.3 Hyphenated HPLC-Atomic Spectrometry Techniques

1.3.1 Rationale

It has been noted that only about 10 % of the approximately two million known compounds are amenable to analysis by GC (Gouw et al., 1979). In gas chromatography, the mobile phase contributes only for zone movement and temperature is the parameter used to control analyte concentration in the mobile phase. Because a liquid mobile phase serves two purposes; solvation and zone movement, high pressure liquid chromatography is suitable for the separation of non-volatile and thermally labile compounds. A high resolution HPLC column (6 μm particles, 25 cm long) is equivalent to about 42,000 theoretical plates (168,000 plates/m) whereas a 50 m capillary GC column can yield more than 250,000 theoretical plates (5000 plates/m). The lower total efficiency of HPLC relative to GC columns results in band broadening which is reflected by lower signal maxima and consequently higher limits of detection.

In many situations, e.g. clinical chemistry, toxicology, environmental modeling, forensic chemistry, food chemistry and petrochemistry, a precise knowledge of the physico-chemical forms and the relative amounts of trace elements can be vital. Characteristically, metal-containing organic species occur at very low concentrations (typically sub-parts per billion) in highly polar and complex media, such as biological fluids. Paralleling reports of efficient GC-AAS instruments for the analysis of thermally stable organometallic species and metal complexes (Ebdon et al., 1986) was the rapid development of LC-atomic spectrometry techniques (Ebdon et al., 1987). Adsorption, ion exchange, gel permeation, normal- and reversed-phase liquid chromatographs have all been interfaced with atomic spectrometry detectors.

The requirements for the successful coupling of HPLC and AAS instruments for applications to real samples are demanding. The atomization cells, e.g. kinetic flame, electrothermal furnace or plasma, must be capable of handling voluminous solvent flows (typically 0.1 to 3 mL/min of liquid are vaporized into liters of gases\min in these detectors). In order to survive contemporary financial constraints, the interface module should be inexpensive to construct, to operate, and to automate. Finally, the atomization cell must be sufficiently efficient to allow the spectrometric quantification of low- to sub-nanogram amounts of trace elements emerging from the HPLC column.

Usually, different nebulization techniques are used to convert the liquid effluent from the chromatograph into an aerosol suitable for introduction into a flame or a plasma. This step is often regarded as the most inefficient process in atomic spectrometry and considerable attention has been given to modify and optimize this aspect of coupling (Ebdon et al., 1987).

1.3.2 Plasma Atomic Emission Spectrometry Detection

Both the direct current plasma (DCP) and inductively coupled plasma (ICP), with their ability to withstand organic and aqueous solvent flows, have found application as excitation sources for spectroscopic LC detectors (Boorn and Browner, 1982; Jinno et al., 1983; Lawrence et al., 1984; LaFreniere et al., 1987). This coupling is normally direct through standard or modified nebulizer configurations. Although the capability for simultaneous multi-element detection (including many non-metals) makes plasma atomic emission spectroscopy an attractive detection system for trace elements, the techniques have two major economic and technical disadvantages. The DCP or ICP technologies require heavy financial investments and the operating cost of plasma detectors is prohibitive since

the argon supporting the plasma has to be introduced into the atomization cell at flow rates of several liters/min. Generally, these detectors are characterized by limits of detection which can be several orders of magnitude higher than flameless furnace detectors. It may be anticipated that design improvements in sample introduction devices and in micro torches will appreciably lower the limits of detection and the operating cost, respectively. However, given the cost of acquiring and operating current models, it has often been difficult to rationalize their dedication to a single chromatographic analysis.

Applications of this technique have included analysis of organoarsenic compounds (Korusawa et al., 1980; Hausler and Taylor 1981; Irgolic et al., 1983; Francescony et al., 1985; Low et al., 1986; Shiomi et al., 1987) speciation of alkylleads (Gast et al., 1979) and detection of selenium species (Irgolic et al., 1983).

1.3.3 Flame Atomic Absorption Spectrometry Detection

Because it is relatively simple to achieve, post-column flame atomic absorption spectrometry (FAAS) has been used in a number of metal speciation surveys. The FAAS technique readily accepts liquid samples and 100 % nebulization efficiencies of organic solvents (32 % for water) have been achieved (Jones et al., 1976). Organic mobile phases also act as secondary fuel to support the analytical flame. The most widely used coupling technique is a direct connection to a commercial FAAS nebulizer (Ebdon et al., 1987). The very short residence time of the atomized metal in the analytical flame and the relatively low signal to noise ratio observed in FAAS are the factors which limit the sensitivity of the technique. Additionally, conventional FAAS nebulizers contribute excessively (up to 80 % of total) to peak dispersion (Katz and Scott, 1985). Thus, the resolving power of 3 and 5 μ chromatographic packing cannot be realized for rapidly eluting analytes.

Several of the more recent reports on coupled LC-FAAS have stressed simple interface systems and have demonstrated increased sensitivity by attention to the atomization cell. One technique, developed for the analysis of alkyltin compounds, was to install a slotted-tube atom trap above the flame to increase the residence time of tin atoms in the optical beam of the detector (Ebdon et al., 1985). A more complicated approach was the use of a series of rotating platinum spirals which, under microprocessor control, transport the effluent from the end of the column successively to a warm flame, to dry the spiral, and a conventional air-acetylene flame to atomize the metal. Because this coupling was not direct, chromatographic data were presented as integrated histograms. Again, a slotted quartz tube was used as an atom trap to enhance the sensitivity (Hill et al., 1986).

1.3.4 Graphite Furnace-Atomic Absorption Spectrometry Detection

Graphite furnace atomic absorption spectrometry (GFAAS) offers the advantage of high sensitivity for a single atomization. However, the necessity to dry and ash a sample prior to atomization makes the direct coupling of HPLC to GFAAS especially difficult. Organotin compounds have been analyzed successfully by direct HPLC-GFAAS in which the eluate (0.2-0.3 mL/min) was pre-heated in a capillary tube and transferred quantitatively into a modified graphite cup maintained at 1100 ^{o}C (Nygren et al., 1988). However, most transition and metalloid elements are not predicted to be atomized in such mild conditions.

Various indirect HPLC-GFAAS couplings based on periodic sampling of the column eluate have been developed, providing sub-nanogram sensitivities (Ebdon et al., 1987). In the on-line mode (also called pulsed-mode), the synchronization of the sampling rate and graphite furnace cycles has been achieved using sampling devices such as actuated sampling valves (Stockton et al., 1979; Vickrey and Eue, 1979).

Another somewhat simpler pulsed-mode interface was a low dead-volume flow-through PTFE cup connected to the column outlet, which was periodically sampled by the GFAAS-autosampler unit (Brinckman et al., 1977; Iadevaia et al., 1980). The interference caused by background absorption was best avoided using Zeeman effect background correction (Stockton et al., 1979; Vickrey et al. 1980).

Although GFAAS appears to provide the best conditions of sensitivity, it remains an economically and technically demanding technique. Because the lifetime of the graphite tube is limited to a few hundreds of cycles, the instrument would be difficult to automate for long term applications and would suffer appreciable periods of down-time. Another disadvantage of on-line coupling which makes the technique less attractive is that the chromatographic information is recorded in a pulsed mode. This implies a lower precision (relative to the continuous information sampling mode using direct interfaces) of the resulting integrated histogram, especially for highly resolved peaks. With the capacity of decreasing the GF temperature cycle to 20 s, the flow injection thermospray deposition-GFAAS technique might help in improving the precision of this method (Bank et al., 1988). Also problematic is the possibility of changes in sensitivity resulting from tube deterioration during a chromatographic run. In this respect, off-stream collection and subsequent analyses of the fractions, with periodic calibrations, appears to be a more accurate approach (Brinckman et al., 1977, 1980; Koizumi et al., 1978; Parks et al., 1979; Lawrence et al., 1986).

1.3.5 Hydride Generation-Quartz Tube Atomization-AAS

One sensitive approach developed for arsenic (Ricci et al., 1981; Tye et al., 1985) and tin (Burns et al., 1981) speciation was to volatilize the species as their hydride derivatives in an electrothermally (Burns et al., 1981; Ricci et al., 1981) or

flame (Tye et al., 1985) heated quartz tube, using a continuous-flow hydride generator serially connected to the analytical column. The use of hydride generation circumvents the problems of low nebulization efficiency and low signal to noise ratio (S/N) normally encountered with FAAS. However, the technique is limited to the reducible physico-chemical forms of the metals and metalloids which can be volatilized as stable hydrides, including some organic compounds of selenium, arsenic, and tin. In a study on organotin compounds, a 1,000 fold increase in the response to tin has been observed when using on-line hydride generation-quartz tube atomization-AAS as opposed to coupling the eluent directly to the nebulizer for FAAS (Burns et al., 1981).

---

2. Optimization of a Thermospray-Microatomizer Interface for HPLC-AAS

2.1 Synopsis

An on-line HPLC-AAS interface has been designed and optimized for the analysis of ionic alkyllead compounds. The interface consists of a thermospray unit in which the chromatographic eluent is quantitatively nebulized by electrothermal thermospray effect, and ignited in the presence of oxygen. The resulting flame appears to efficiently support the atomization of lead species.

2.2 Materials and Methods

2.2.1 Thermospray-Microatomizer Interface

The thermospray-microatomizer unit shown in Figure 1 consists of an atom keeper (A), a microatomizer (B) and a thermospray tube (C) (Clear fused quartz, A = 10 cm x 7 mm i.d. x 9 mm o.d.; B and C = 6 cm x 4 mm i.d. x 6 mm o.d.). The thermospray tube (C) meets the microatomizer tube (B) 3 cm below the intersection of tubes A and B at an angle of 80^{o} relative to the axis of tube B. Quartz tube joints were made using an oxygen-butane flame. Thermoelectric elements (D = 2 x 1 m, E = 40 cm, Alloy 875, 21-gauge, 1.108 ohms, Hoskins Alloys Can. Ltd, Toronto) were coiled around tubes A-B and C and their surfaces were oxidized at approx. 900 ^{o}C for 1h prior to encasing. The atom keeper (A) and thermospray (E) elements were insulated with refractive wool (Fiberfrax, The Carborundum Co. Niagara Falls, N.Y.) and encased in shaped firebrick. The optical tube (atom keeper, A) was mounted within a hinged aluminum tube (10 cm x 4 cm i.d.), which was provided with insulated entry ports for electrical connections and for a thermocouple (Forsyth and Marshall, 1985).

The assembly was positioned so that the longitudinal axis of the upper T-tube coincided with the optical beam of the AAS detector. The temperature of the heating element D was monitored using an insulated thermocouple (Omega Engineering Inc.,

Figure 1. Thermospray-microatomiser interface: (A) Atom keeper (quartz); (B) microatomizer tube (quartz); (C) thermospray tube (quartz); (D,E) thermoelectric elements; (F) ceramic insert; (R) quartz insert; (G-Q) Swagelok fittings; (J,N) gas inlets; (S) silica capillary transfer line from HLPC column.

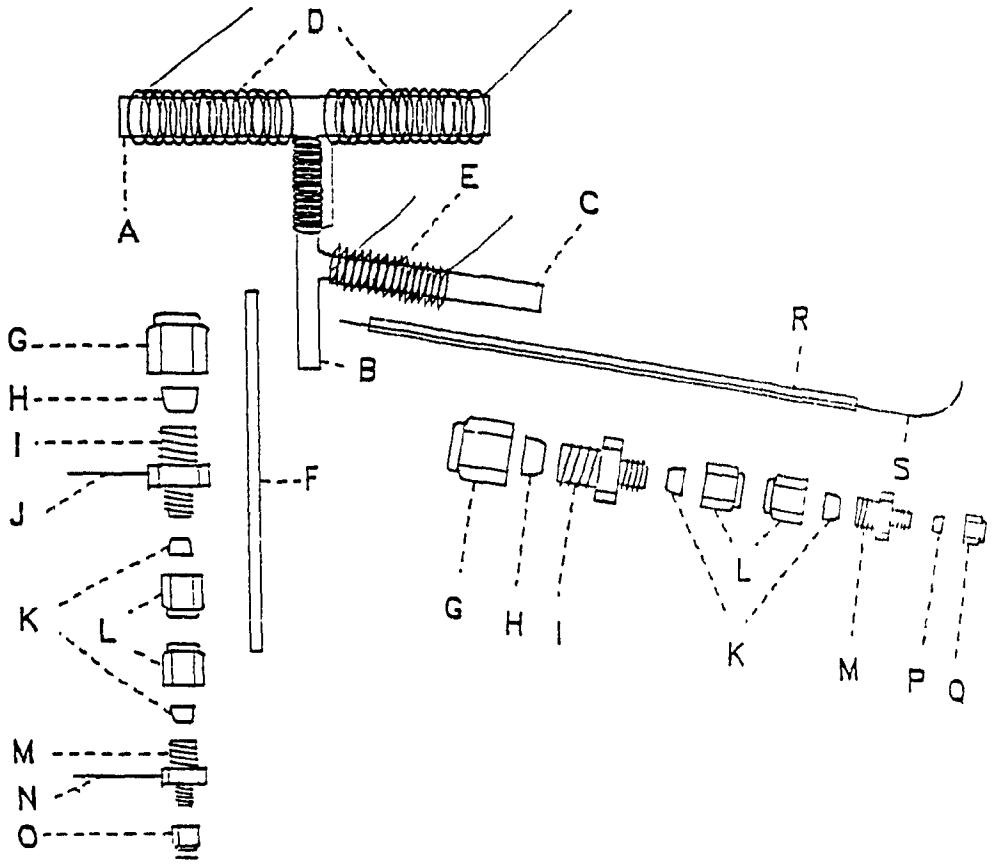
D
A
E
C
B
R
S
G
H
I
J
F
K
L
M
N
O
G
H
I
L
K
M
P
Q

Stamford; CT) positioned 3 cm from the right end of the optical tube (A) at about 2 mm from the coil. Heating elements were energized using two variable transformers and currents were measured using ampmeters.

A 50 µm I.D. fused silica capillary tube (S) (DB-1,SP thickness 0,05 µ, J&W Co., Rancho Cordova, CA) was connected to the analytical column via a reducing union (0.16 cm SS ferrule to 0.08 cm capillary vespel ferrule, Chromatographic Specialties Inc. Brockville, Ont.). The capillary was positioned within the thermospray tube (C) at 0 to 2 cm from intersection (C-B) using a quartz insert (R) (5 cm x 2 mm i.d. x 3.2 mm o.d.). During operation, the thermoelectric element (E) overheated the chromatographic eluent, forcing it to flash-evaporate as it emerged from the capillary column. Then, the vaporized mobile phase met a flow of oxygen which was introduced in the microatomizer inlet tube (B) via a modified Swagelok fitting (I,J). The resulting mixture ignited at the intersection (C-B).

If necessary, an acetylene-air or hydrogen-air flame could be maintained in the microatomizer by introducing the fuel-oxidant mixture via the ceramic insert (F) (5 cm x 0.32 cm o.d. x 0.16 cm i.d.) through the modified Swagelok fitting (M,N). Inserts (F) and (R) were positioned by Swagelok fittings (Nuts G = 0.64 cm; L = 0.32 cm; Q = 0.16 cm; O = stopper 0.16 cm; Reducing unions M = 0.32 cm to 0.16 cm; I = 0.64 cm to 0.32 cm with i.d. oversized to 0.32 cm) and Vespel-graphite ferrules (H = 0.64 cm; K = 0.32 cm; P = 0.16 cm; Chromatographic Specialties, Brockville, Ont.). Gases were introduced into microatomizer and ceramic insert (F) using stainless steel (0.16 cm o.d. x 0.32 cm i.d.) tubes (J and N) which had been silver soldered on to modified (bored) reducing unions (I and M).

Preliminary tests of the thermospray assembly were performed using a quartz T-tube atomizer without side arm (Figure 2). In this design, the capillary tube (S) was introduced in the atomizer via the ceramic insert (R). The thermospray effect was obtained by positioning the capillary in the electrothermally heated portion of the inlet tube (B). Other components were as described above.

2.2.2 Chromatography

2.2.2.1 Instrumental Components

The chromatographic system is presented schematically in Figure 3. The mobile phase was delivered by a dual-piston high pressure pump (Beckman model 100A) which was serially connected to an autoinjector (LKB-Bromma model 2157), a precolumn filter (Waters Guard-PAK with C_{18} Bondapak or Nucleosil C_{18} inserts) and the analytical column (Shandon Hypersil C_{18} or Macherey-Nagel Nucleosil C_{18}; particles diameter 5 u; length 15 cm; Chromatography Sciences Co., Montreal, Que.).

A simple automated pre-pump mobile phase selection system was constructed from an inert two-way manual solvent selector (Altex, Toronto, Ont.), a double acting pneumatic cylinder (Festo Pneumatic, Hauppauge, N.Y.) and two 2-way solenoid valves (ASCO, Florham Park, N.J). The solenoid valves were energized by solid-state relays (Amprotech, Montreal, Que.) triggered by TTL signals programmed in real-time from the data acquisition interface (Nelson Analytical model 706). The solvent selector and pneumatic cylinder were mounted, respectively, on the opposite walls of a metallic rectangular frame. The piston was connected to the solvent selector lever with a metallic wire, so that the piston could push the selector lever directly, or pull on the wire to return the lever to its original position.

Figure 2. Preliminary thermospray interface: (A) Quartz T-tube; (D) thermoelectric element; (G-Q) Swagelok fittings; (J,N) gas inlets; (R) quartz insert; (S) silica capillary transfer line from HLPC column.

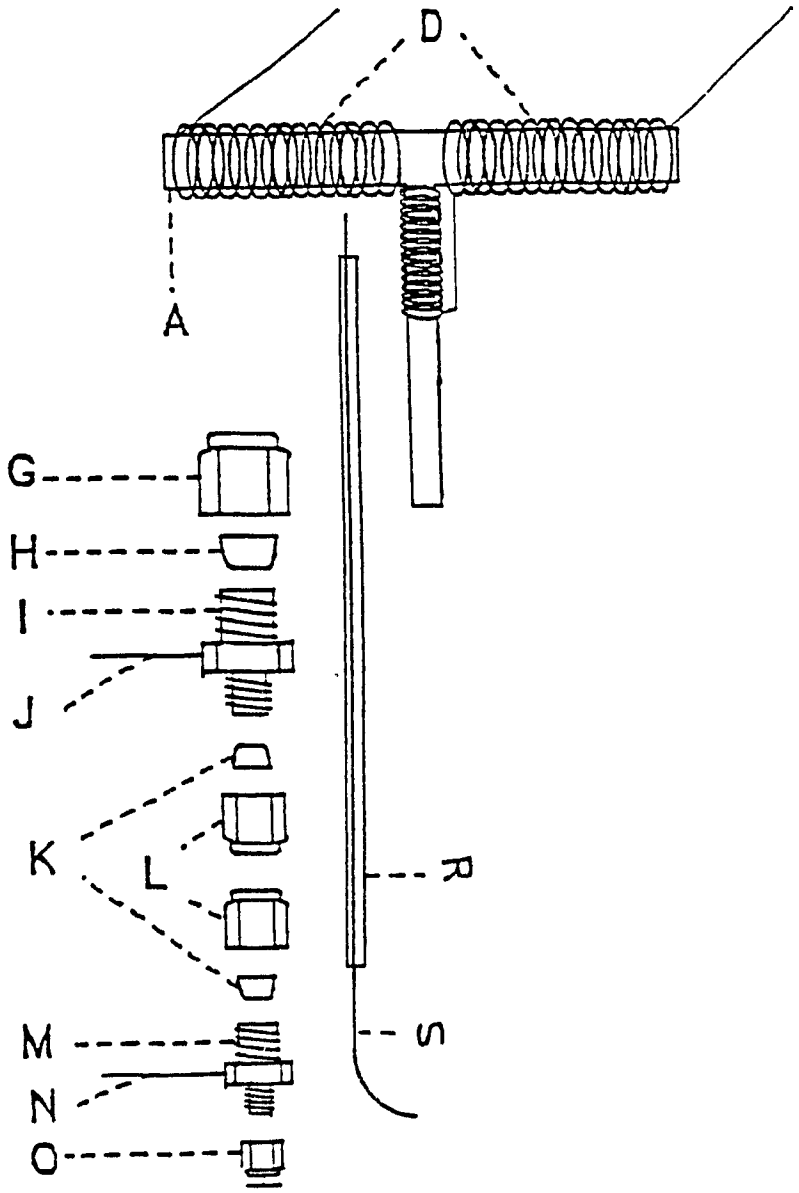
D
A
G
H
I
J
K
L
R
S
M
N
O

Figure 3. Block diagram of the HPLC-AAS instrument: (A) thermospray-microatomizer interface; (B) analytical column; (C) pre-column filter.

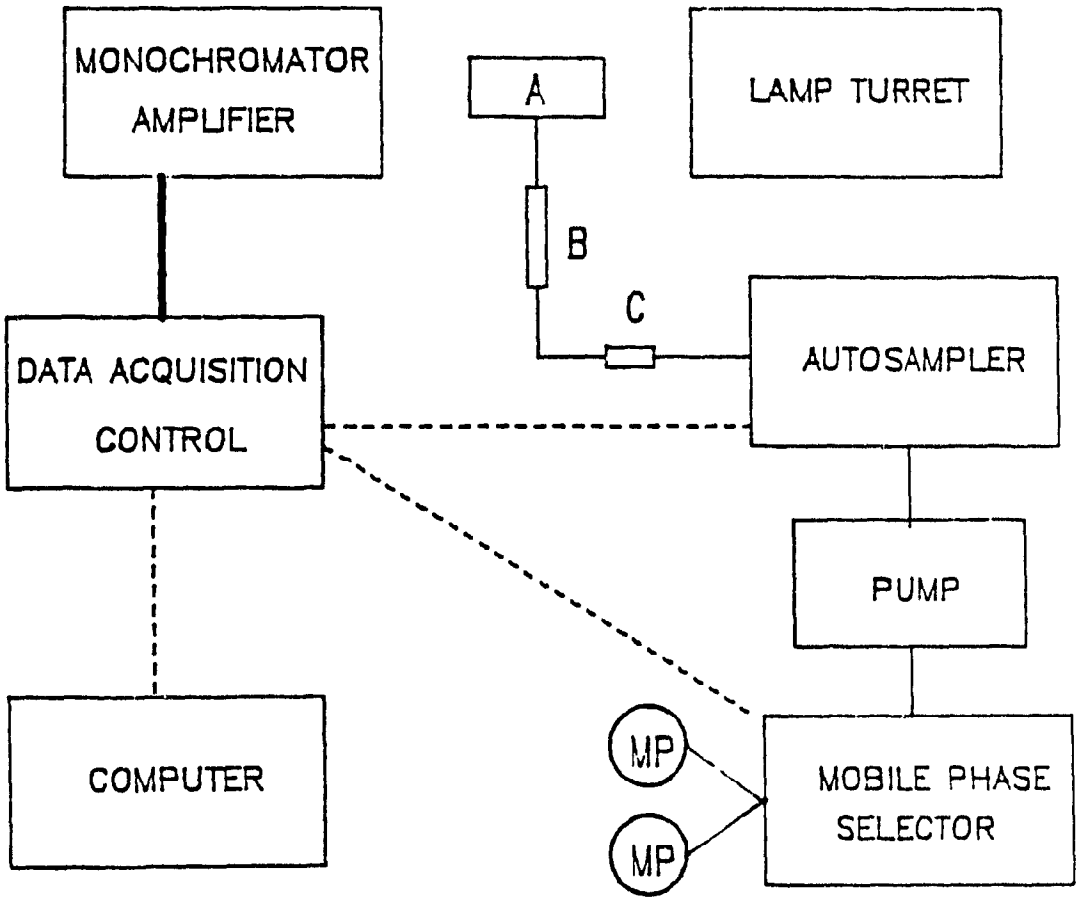
MONOCHROMATOR
AMPLIFIER
A
LAMP TURRET
B
C
AUTOSAMPLER
DATA ACQUISITION
CONTROL
PUMP
COMPUTER
MP
MP
MOBILE PHASE
SELECTOR

Detection of the atomized metallic lead was performed by a Perkin-Elmer model 303 or a Zeiss FMD-3 atomic absorption spectrometer (AAS). Detector signals (Pb AAS wavelength = 283.3 nm) were integrated using a recording integrator (HP Model 3390A) or a data acquisition system (Nelson Analytical model 706) interfaced with a microcomputer (IBM model XT). Sample injection, mobile phase selection and data acquisition were automated in a timed cycle initiated by the autosampler.

2.2.2.2 Reagents and Chemicals

Mobile phase organic components (methanol, dioxane, acetic acid; Caledon Laboratories, Georgetown, Ont.) were "distilled in glass" grade or better, and water was distilled-deionized. Complexing agents and adsorption competitive agents investigated were sodium diethyldithiocarbamate (NaDEDTC), sodium dimethyldithiocarbamate (NaDMDTC) (Aldrich Chemicals Co., Milwaukee, Wis.); diphenylthiocarbazone (dithizone, Dz), disodium ethylenediaminetetraacetate (Na_2EDTA), ammonium pyrrolidinedithiocarbamate (APDTC), ammonium citrate, cysteine hydrochloride, zinc chloride, cupric acetate (Anachemia Co., Montreal, Qc), 1,2-ethanedithiol (American Chemicals Co., Toronto, Ont.). Mobile phase components were mixed together, deoxygenated with nitrogen and degassed by ultrasonication.

2.2.2.3 HPLC Eluent Composition Programs

Mobile phase flow rate was kept constant at 1 mL/min. Using the Shandon Hypersil C_{18} column, separation of the analytes (Pb^{2+}, R_2Pb^{2+}, R_3Pb^{+}, R = CH_3 or C_2H_5) was obtained with the following mobile phase cycle: Mobile phase A = 85 % (v/v) methanol, 5 % water, 10 % 1,4-dioxane, 300 µg/mL dithizone; mobile phase B = 80 % (v/v) methanol, 5 % water, 10 % 1-4 dioxane, 5% acetic acid, 300 µg/mL sodium dimethyldithiocarbamate; cycle: solvent A before t=0 min, B at t=0 min, A at t=6min, subsequent injection at t=12 min.

Mobile phase cycles used to separate the lead species with the Nucleosil C_{18} column were; Mobile phase A = 75 % (v/v) methanol, 15 % water, 10 % 1-4 dioxane, 300 µg/mL dithizone; Mobile phase B = 80 % (v/v) methanol, 10 % water, 10 % 1,4-dioxane, 300 µg/mL dithizone; cycle: A before t=0 min, B at t=4 min, A at t=10 min, next injection at t=20 min. A more flexible chromatographic system was subsequently developed for applications to environmental samples. An optimum separation of extracted analytes (from hexane) was obtained using the Nucleosil C_{18} column eluted isocratically with a 75 % methanol:25 % water (v/v) mobile phase containing 600 µg/mL of ammonium pyrrolidinedithiocarbamate.

2.2.3 Analytical Standards

Alkyllead chlorides (R_3PbCl, R_2PbCl_2; R = CH_3, C_2H_5) and alkyllead butylates (R_3BuPb, R_2Bu_2Pb, Bu = C_4H_9) were prepared and purified as described previously (Forsyth and Marshall, 1983, 1985). Stock solutions of these alkyllead compounds were prepared as follow: Me_3PbCl (1.10 x 10^{-4} g/mL), Me_2PbCl_2 (1.06 x 10^{-4} g/mL), Et_3PbCl (1.06 x 10^{-4} g/mL), Et_2PbCl_2 (1.01 x 10^{-4} g/mL), $Pb(NO_3)_2$ (1.00 x 10^{-4} g/mL) in 1:1 methanol/water; Me_3BuPb (2.29 x 10^{-5} g/mL), Me_2Bu_2Pb (2.29 x 10^{-5} g/mL), Et_3BuPb (2.54 x 10^{-5} g/mL), Et_2Bu_2Pb (2.46 x 10^{-5} g/mL) and Bu_4Pb (2.40 x 10^{-5} g/mL) in hexane. Dilution of these stock solutions with their original solvents (or 100 % methanol for ionic alkylleads) provided working standards. Ionic alkyllead chelates were prepared by reacting a known quantity of the alkyllead chloride with a 100 fold excess of the complexing agent Dz, NaDMDTC or NaDEDTC in distilled-deionized water. The resulting chelates were extracted with three (5 mL) aliquots of benzene; the combined extracts were centrifuged, dried with Na_2SO_4, decanted (with rinsing), and diluted to volume. Analytical standards for the APDTC-Nucleosil C_{18} system were prepared by injecting 50 µl of the ionic alkylleads solution in 1 mL of hexane containing approx. 1 µg of APDTC.

2.3 Results and Discussion

2.3.1 Thermospray-Microatomizer Unit

One important criterion in interfacing a detector directly with a chromatographic device is the necessity of introducing the column eluate in a continuous and pulseless mode. In atomic absorption spectroscopy (AAS), an efficient atomization of the analytes, prior to detection, requires a complete and uniform nebulization (and pyrolysis) of the solvent. Thus, efficient HPLC-AAS coupling have been achieved using a variety of eluate nebulization techniques (Ebdon et al., 1987).

The thermospray effect was a promising approach for nebulizing the chromatographic eluent prior to a direct interfacing with spectroscopic instruments. The technique has been first developed for the coupling of HPLC with mass spectroscopy (HPLC-MS) to nebulize the eluent prior to chemical or electron impact ionization (Blakley et al., 1980). The HPLC effluent was forced into a stainless steel capillary (0.3 cm x 150 u i.d.) which was heated at ca. 1000^{o}C by oxy-hydrogen microburners. Pressurized and overheated in the capillary, the eluent (methanol-water mixtures) emerged into a continuously evacuated vessel where it was flash-evaporated and vented through a vacuum pump. Under these conditions, more than 50 % of the analyte was projected by inertia through a 750 μ skimmer (access to the MS ionization chamber) facing the capillary.

Thermospray sample introduction has been also applied successfully to conventional flame AAS (Robinson and Choi, 1987), ICP-AES and ICP-MS (Mayer et al., 1985; Elgershma et al., 1986; Vermeiren et al., 1987) as well as graphite furnace AAS (Bank et al., 1988). The higher sensitivities provided by thermospray introduction (relative to conventional pneumatic nebulizers) has been attributed to improved analyte transport (Vermeiren et al., 1987). The thermospray mechanism is

described schematically in Figure 4. Models for thermospray aerosol generation (Schwartz and Meyer, 1986; Koropchack et al., 1988) suggest that this improvement results from a higher sonic velocity of the gas jet leaving the thermospray capillary than can be attained for gas jets emerging from pneumatic nebulizers. Thermospray droplets are also relatively hot and the analyte rapidly desolvates, increasing transport efficiency (Koropchak et al., 1988). Both stainless steel and silica capillary have been used in this technique.

A similar thermospray effect was obtained in this work using a fused silica capillary (50 µm i.d.) positioned inside an electrothermally heated quartz tube. Preliminary tests were performed by inserting the capillary in the electrothermally heated inlet of a quartz T-tube furnace usually dedicated to GC-AAS (Figure 2). The capillary was connected to the outlet of a C_{18} Hypersil HPLC column which was used to separate tetraalkyllead compounds. The solvent (methanol/water 0 to 30 %) appeared to be completely vaporized when the quartz furnace inlet was maintained at approx. 900^{o}C. The vapors self-ignited in the optical tube and the lead species were detected with an approximate limit of detection of 50 ng.

Attempts to decrease this limit of detection by introducing fuel or oxidant gases (H_2, C_2H_2 or O_2) in the furnace (via inlet J or N; Figure 2) at 100 - 300 mL/min disrupted the thermospray effect, presumably by cooling the capillary. Decreasing gases flow rates (10-50 mL/min) and increasing the thermoelectric element temperature reestablished the thermospray effect. In contrast to hydrogen or acetylene, which did not seem to influence the response of the lead compounds, oxygen decreased their limit of detection appreciably. The presence of oxygen in the thermospray environment resulted in a fireball which apparently sustained the atomization of lead

Figure 4. Vaporization process which occurs in the thermospray.

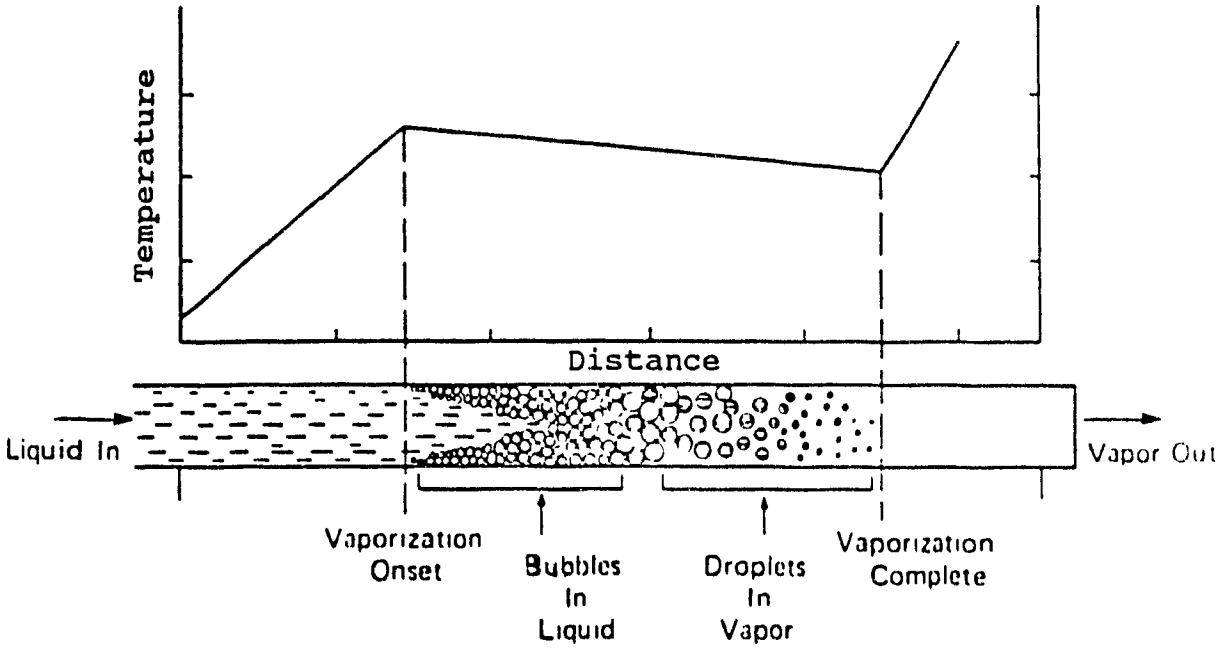

(Schwartz and Meyer, 1986)

atoms from tetraalkyllead compounds. However, this fireball overheated the silica capillary, causing in-column pyrolysis of the eluent (only for 90-100 % methanol), forming deposits which eventually blocked the line. Although the addition of more than 10% H_2O in the eluent solved this problem, the elution of heavier tetraalkyllead compounds still required a 100 % methanolic mobile phase. Increasing the flow rate of oxygen appeared to initiate the fireball remote from the capillary tip but it was not possible to introduce this gas at flow rates higher than 100mL/min without disrupting the thermospray effect.

It became necessary to physically separate the thermospray unit from the oxygen inlet so that ignition of the eluent vapor-oxygen mixture would occur away from the capillary tip. The thermospray tube (Figure 1, C) was positioned half-way and nearly perpendicular to the inlet tube (B) of the quartz T-tube. Using this configuration, the heat transfer from the thermoelement (E) and the capillary (S) was not affected by the make-up gas, which was introduced through inlet tube (B). With this configuration, the fireball was initiated downstream (0.5 - 1.5 cm) from the capillary tip; i.e. at the intersection of tube (B) and (C) where the vaporized chromatographic eluent and oxygen gas met. With this design, it was possible to maintain the thermospray effect with mobile phases containing 0-50 % water.

It appeared that long-term exposure of the quartz microatomizer to chromatographic eluent resulted in devitrification of the quartz surface. The devitrification was appreciably accelerated by the presence of sodium dimethyldithiocarbamate which was added to the mobile phase to elute R_3Pb^+ from the Hypersil C_{18} column. Although the devitrification process did not affect the atomization efficiency of lead compounds, it resulted in a modified silica which spontaneously desintegrated when

the assembly was cooled down. Devitrification was much slower when dithizone was used exclusively as complexing agent (using the Nucleosil C_{18} column).

Reports on the use of water cooled or slotted quartz tube as atom traps demonstrated that samples containing moderate concentrations of sodium quickly devitrified the quartz tube. It was suggested that sodium atoms in the flame may migrate into hot quartz, forming Na silicates which contract heterogeneously on cooling and destroy the tube (Brown et al., 1987). It was found that tube lifetime increased substantially when the exposed surface was coated with a refractory oxide (lanthanum, vanadium or aluminum). The coating acted as a physical barrier, preventing the Na atoms from contacting the quartz.

In this work, a refractory aluminum oxide coating was obtained by pumping a 1000 µg/mL methanolic aluminum nitrate solution through the thermospray-microatomizer assembly. This treatment efficiently protected the quartz surface when exposed to dithizone (using the Nucleosil C_{18} column). With these conditions, the assembly was cooled down periodically during three weeks of intensive use, without apparent modification of the quartz surface. However, the refractory coating had little effect on the rate of quartz devitrification when exposed to NaDMDTC (300 µg/mL in mobile phase).

If NaDMDTC was to be added to the mobile phase (Hypersil C_{18} column), it was imperative to maintain the temperature of the microatomizer and thermospray units higher than 500-600^{o}C when the instrument was not in use. During down time, the thermospray-microatomizer joint [Figure 1, intersection of tubes (B) and (C)] was also maintained at high temperature using an air-acetylene microflame located at the tip of the ceramic insert (F). With these conditions, the useful lifetime of the

thermospray-microatomizer unit was at least 120 hours of operation. Replacement of the unit took about 1 hour and the original sensitivity was restored after 2-3 chromatographic runs. The aluminum oxide coating was found useful only if NaDMDTC was not used in the mobile phase and this coating did not affect the response of lead containing analytes. The latter observation suggest that the quartz tube surface may not have a chemically active role in the atomization of the lead species.

2.3.2 Optimization of the Thermosray-Microatomizer Unit

Three operating parameters of the thermospray-microatomizer unit were optimized by altering one parameter while the others were kept constant (univariate optimization). Parameters optimized were, in order: temperature of the optical tube (Figure 1, A), flow rate of air introduced through the ceramic insert (F), and flow rate of oxygen introduced through inlet tube (B).

Chromatographic integrations from triplicate 20 µl injections of benzene containing approximately 20 ng of $Pb(DMDTC)_2$, $Me_2Pb(DMDTC)_2$ and $Me_3Pb(DMDTC)$ were recorded for each experimental condition. The lead species were separated using the Hypersil C_{18} column and the eluent cycles described previously (section 2.2.2.3). The temperature of the thermospray unit was adjusted to obtain a stable thermospray effect. Once a stable thermospray effect was established, moving the capillary 0.5 cm back and forth did not affect analytes responses. The working temperature range of the thermospray unit (inner surface) varied between $700^{o}C$ and 1000^{o} C, depending on the water content of the chromatographic eluent.

The relative temperature of the optical tube was measured using an isolated thermocouple located 2 mm from the heating element. This relative temperature was related to the inner surface temperature as determined with a bare thermocouple inserted inside the optical tube. The later measurements were performed after the optimization experiments since trace amounts of foreign metals deposited in quartz tube atomizers may decrease their atomization efficiency (Welz and Melcher, 1983). This technique was also used to measure the temperature of the thermospray unit.

The inner temperature of the optical tube was varied between 680 and 960^{o}C while gas flow rates were maintained as follows: air 400 mL/min and acetylene 80 mL/min (introduced through the ceramic insert); oxygen 200 mL/min (introduced through the microatomizer inlet tube). Operating the optical tube at temperatures lower than 650^{o}C resulted in extensive deposition of carbon which peeled off and interfered with the hollow cathode optical beam of the AAS detector.

Response of the three lead compounds versus optical tube temperature are presented graphically in Figure 5. The temperature influenced the sensitivity only slightly over the range studied. The fact that sensitivity decreased at higher temperatures may be attributed to the increased thermal expansion of gas at high temperatures, resulting in a shorter residence time of the atomized lead in the optical tube. Although slightly higher responses were observed at 680^{o}C, it was decided to operate at 800^{o}C to avoid carbon deposits at the extremities of the optical tube.

The thermospray-microatomizer unit was originally operated with an air-acetylene microflame at the tip of the ceramic insert (Figure 1, F). It was originally anticipated that this flame would promote ignition of the chromatographic eluent and atomization of the lead species. The flame was maintained by introducing air (400

Figure 5. Effect of atom keeper tube temperature on analytes response: (A) Pb^{2+}; (B) Me_2Pb^{2+}; (C) Me_3Pb^{+}.

A

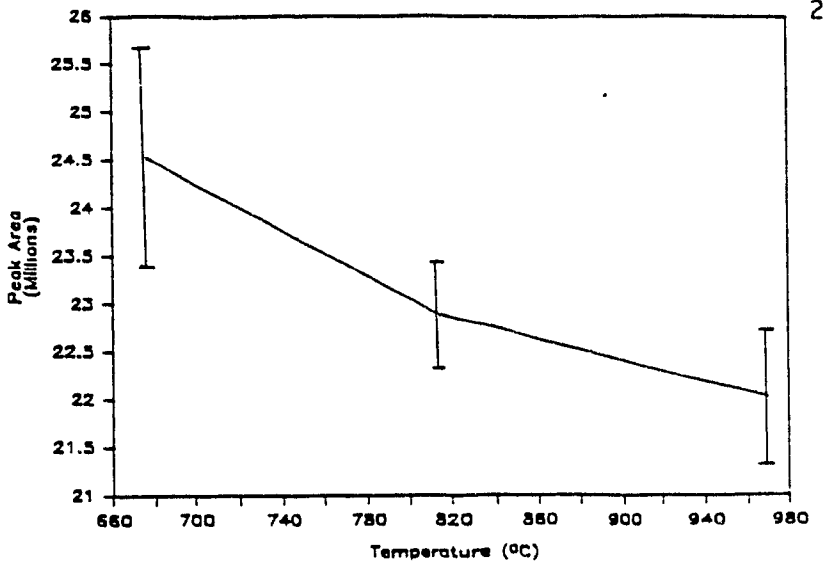
26
25.5
25
24.5
24
23.5
23
22.5
22
21.5
21
Peak Area (Millions)
660
700
740
780
820
860
900
940
980
Temperature (°C)

B

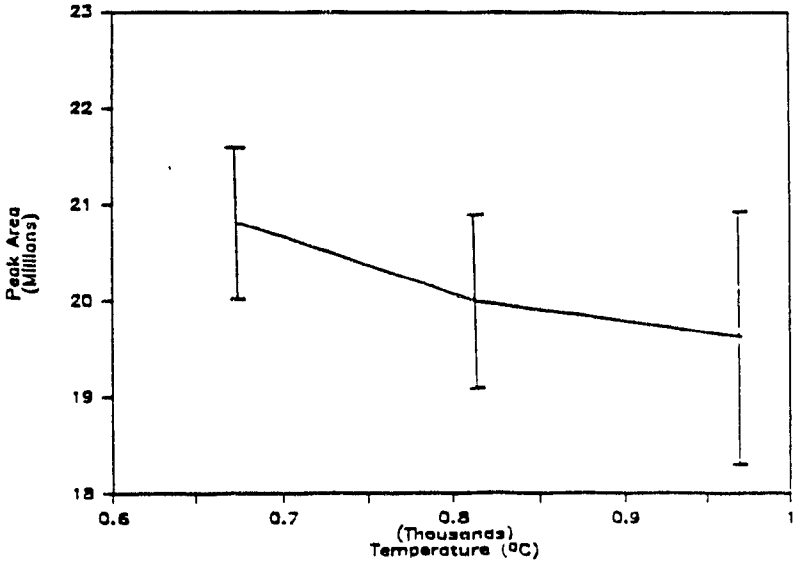
23
22
21
20
19
18
Peak Area (Millions)
0.6
0.7
0.8
0.9
1
(Thousands)
Temperature (°C)

C

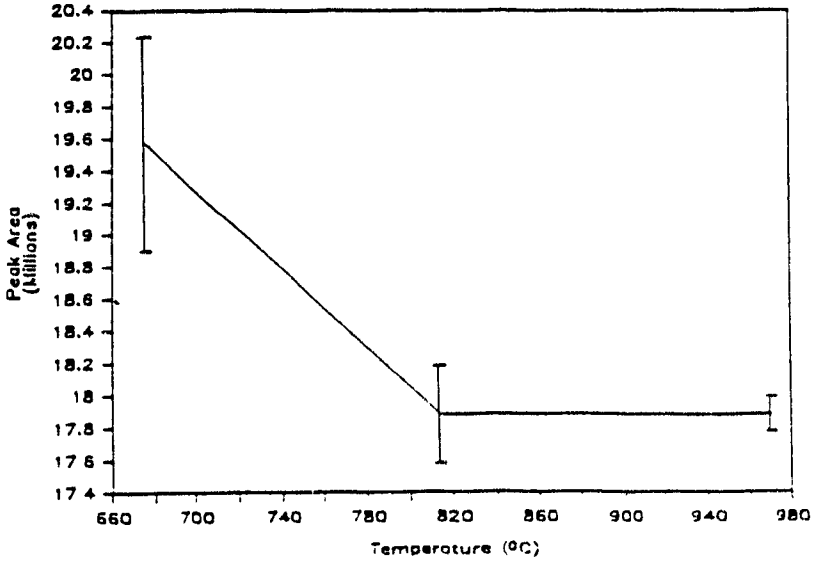
20.4
20.2
20
19.8
19.6
19.4
19.2
19
18.8
18.6
18.4
18.2
18
17.8
17.6
17.4
Peak Area (Millions)
660
700
740
780
820
860
900
940
980
Temperature (°C)

mL/min) and acetylene (80 mL/min) through the ceramic insert and oxygen (200 mL/min) through inlet tube. For economy, oxygen flowing through inlet tube (B) was replaced by air (400 mL/min) during standby (to maintain the acetylene microflame).

It was found that the presence of fuel (acetylene or hydrogen) had little effect on analyte response, and consequently the acetylene valve was turned-off. The effect of air flow rate (originally added to support combustion of acetylene) on the response of the three lead species is presented in Figure 6. The sensitivity was significantly affected by air, in a linear relationship. Once again the reasons for this appear to be directly related to analyte residence time inside the optical tube. The interface was subsequently operated without addition of either air or acetylene.

The effect of oxygen flow rate on sensitivity was more dramatic. An optimal flow rate of 200 mL/min was determined visually, to obtain a bright-yellow fireball at the thermospray-microatomizer intersection. Carbon deposits (which eventually peeled-off and reached the optical tube) occurred at flow rate between 100 and 150 mL/min. Flow rates between 200 and 300 mL/min resulted in lower responses of the lead species (possibly the result of a decreased residence time). The quartz walls started to soften at flow rates above 300 mL/min, which reflected a flame temperature exceeding 1665^{o}C. The optimal oxygen flow rate appeared to be 200 mL/min.

The linearity of response and the limit of detection of the system were characterized by injecting serial dilutions of a fresh standard solution containing $Pb(NO_3)_2$, Me_3PbCl, Me_2PbCl_2, Et_3PbCl and Et_2PbCl_2. The compounds were separated using the Nucleosil C_{18} column and the solvent cycles described previously (section 2.2.2.3).

Figure 6. Effect of air flow rate on analytes response: (A) Pb^{2+}; (B) Me_2Pb^{2+}; (C) Me_3Pb^{+}.

A

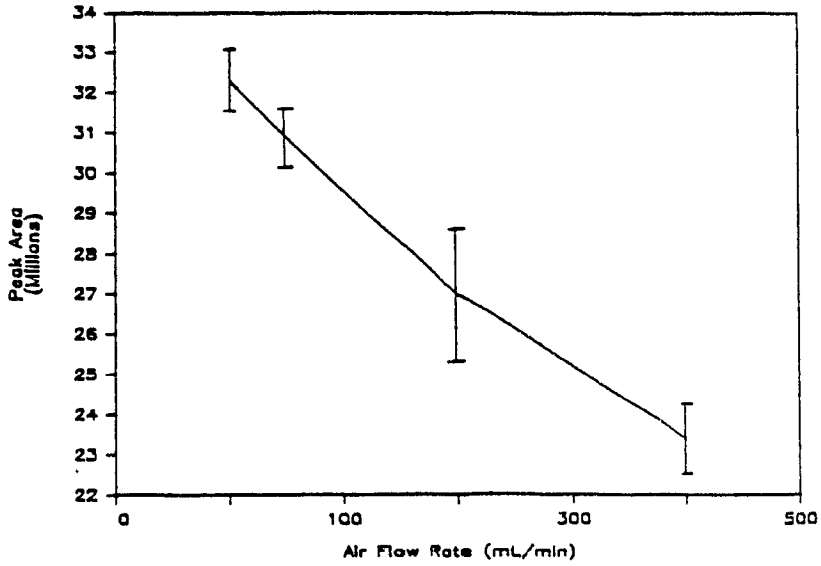
Peak Area (Millions)
34
33
32
31
30
29
28
27
26
25
24
23
22
0
100
300
500
Air Flow Rate (mL/min)

B

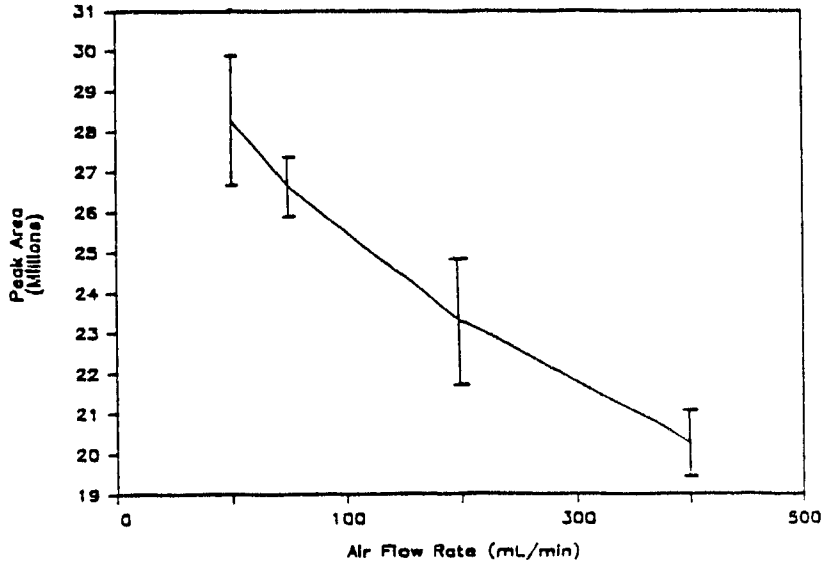
Peak Area (Millions)
31
30
29
28
27
26
25
24
23
22
21
20
19
0
100
300
500
Air Flow Rate (mL/min)

C

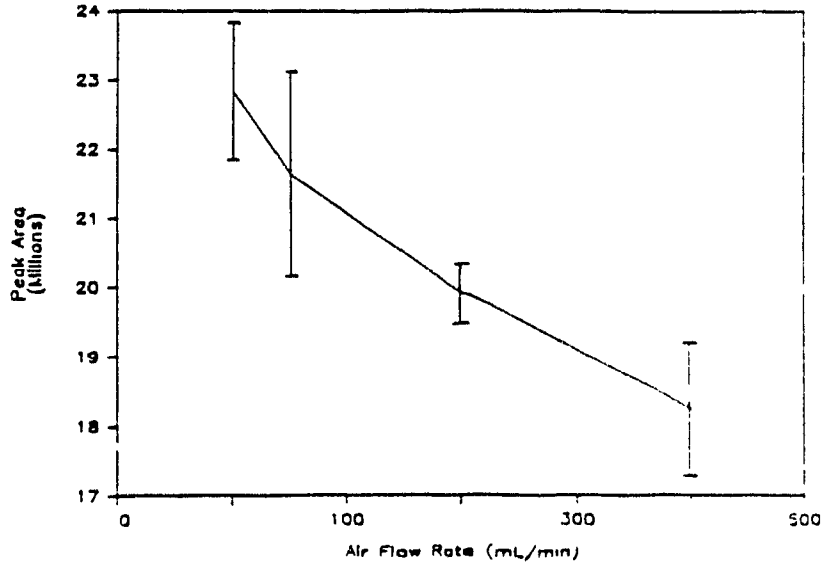
Peak Area (Millions)
24
23
22
21
20
19
18
17
0
100
300
500
Air Flow Rate (mL/min)

Preliminary experiments demonstrated that appreciable portions of diluted Pb^{2+} and Me_2Pb^{2+} (at 0.5 μg/mL) were adsorbed on the walls of the borosilicate glass vials used by the autosampler. Repeated chromatography of these standards from the same vial showed a slow decrease of Pb^{2+} and Me_2Pb^{2+} responses, whereas Me_3Pb^{3+} response remained unchanged. Adsorption of the divalent lead compounds on the borosilicate surface was corroborated by the addition of a crystal of NaDMDTC to the vial, which resulted in responses for these analytes which were equal to their original values. This problem was not observed when the standard was sampled from an inert Teflon vial. Therefore, the sample tray of the autosampler was removed and the standards were diluted in Teflon vials which were positioned under the metering syringe.

The calibration regressions and related statistics for the five analytes studied are presented in Appendix 1. The limits of detection (LOD) of these lead compounds were determined using a model based on first order error propagation (Foley and Dorsey, 1984). Analyte responses were linear ($0.99947 < r < 0.99997$) in the 5 - 250 ng range.

The predicted limits of detection of the analytes were: $Pb(NO_3)_2$ = 3.4 ng, Me_3PbCl = 1.0 ng, Me_2PbCl_2 = 1.7 ng, Et_3PbCl = 1.5 ng, Et_2PbCl_2 = 1.8 ng. The higher limit of detection of inorganic lead may be attributed to higher baseline noise in this area of the chromatogram, due to the proximity of the solvent front. These limits of detection were 10-100 fold lower than those observed using conventional flame-AAS detectors (Botre et al., 1976; Messman and Rains, 1981).

Table 1.Reproducibility of the HPLC-AAS at Varying Analyte Levels.

Amount (ng)	Pb^{2+} r.s.d.(%)[a]	Me_3Pb^+ r.s.d.(%)	Et_3Pb^+ r.s.d.(%)	Me_2Pb^{2+} r.s.d.(%)	Et_2Pb^{2+} r.s.d.(%)
5	11.0	5.3	8.2	3.1	4.2
20	4.6	3.3	1.0	2.1	2.6
50	0.5	0.8	2.5	2.0	2.1
100	1.5	0.7	1.6	1.0	0.9
250	2.2	0.4	0.5	0.2	0.3

[a] r.s.d. = relative standard deviation based on triplicate analyses.

The long-term reproducibility of the instrument was determined by periodically analyzing the standard mix (at levels of 5 x LOD) for 20 hours. The relative standard deviations (N = 10) for the five compounds were: $Pb(NO_3)_2$= 5.8 %, Me_3PbCl = 2.8 %, Me_2PbCl_2 = 7.1 %, Et_3PbCl = 6.6 %, Et_2PbCl_2 = 7.7 %. The short term reproducibility of the instrument was assessed after three consecutive injections of standards at levels of 5, 20, 50, 100 and 250 times their limits of detection (Table 1). The relative standard deviations of the alkyllead standards were less than 8.2 % at the 5 x LOD level and less than 1.6 % at 100 x LOD.

In contrast to the hydrogen radical mediated atomization observed in a quartz electrothermal atomizer (Forsyth and Marshall 1985), the atomization efficiency of lead in this interface did not appear to be affected by the condition of the quartz tube surface and was maximized by the presence of oxygen. Thus, in this interface, the atomization process appears to be mediated by a kinetic flame ($1400^{o}C < T < 1600^{o}C$) which is supported by the chromatographic eluent (fuel) and oxygen. This interface is inexpensive, robust and provided sensitivities 1-2 orders of magnitude higher than those observed using conventional flame AAS detectors (Botre et al., 1976; Messman and Rains, 1981).

2.3.3 Optimization of Chromatography

2.3.3.1 Separation of Tetraalkylleads

Preliminary experiments using a thermospray unit in the inlet tube of a quartz T-furnace (Figure 2) was performed using mixed alkyllead butylate standards (Me_3BuPb, Me_2Bu_2Pb, Et_3BuPb, Et_2Bu_2Pb and Bu_4Pb; Me=CH_3, Et=C_2H_5, Bu=C_4H_9), usually dedicated to GC-AAS analyses. For preliminary tests R_4Pb compounds were preferred to ionic alkylleads because of their relative inertness and low polarity.

Three of the five lead compounds were separated (based on molecular weight) on the Hypersil C_{18} column eluted with 100 % methanol (Figure 7, 1). The two isomers (Me_2Bu_2Pb and Et_3BuPb) were only partially resolved under these conditions. Addition of water (5% v/v) in the mobile phase resulted in partial separation of the isomers. The drastic effect of water on the retention times and resolution of heavier tetraalkyllead peaks confirmed the hydrophobic mechanism for this chromatography (Nahum and Horvath, 1983). Almost baseline separation of the isomers and optimum resolution of Et_2Bu_2Pb and Bu_4Pb peaks was obtained using a dual-pump solvent program (Figure 7,2).

2.3.3.2 Separation of Ionic Alkylleads

The separation of trace metals and metalloids by chromatographic techniques has been investigated. There are several reports on the determination of chelated metals by gas chromatography (GC). Several divalent transition and heavy metals have been complexed with dialkylthiophosphates, acetylacetonates, beta-diketonates or beta-ketonates and subjected to GC-separation with varying degrees of success, generally limited by the low volatility and thermal stability of the chelates (Lederer, 1955; Belcher et al., 1971; Uden et al., 1974; Cardwell et al., 1980).

Figure 7. HPLC-AAS chromatograms of tetraalkylleads (200ng) (A) Me_3PbBu; (B) Me_2PbBu_2; (C) Et_3PbBu; (D) Et_2PbBu_2; (E), Bu_4Pb ($Me=CH_3$, $Et=C_2H_5$, $Bu=C_4H_9$) using the Hypersil C_{18} column. Chromatograms 1 was obtained using methanol. Chromatogram 2 was obtained using methanol + 30 % water followed by 30-0 % water (6%/min) at 15 min.

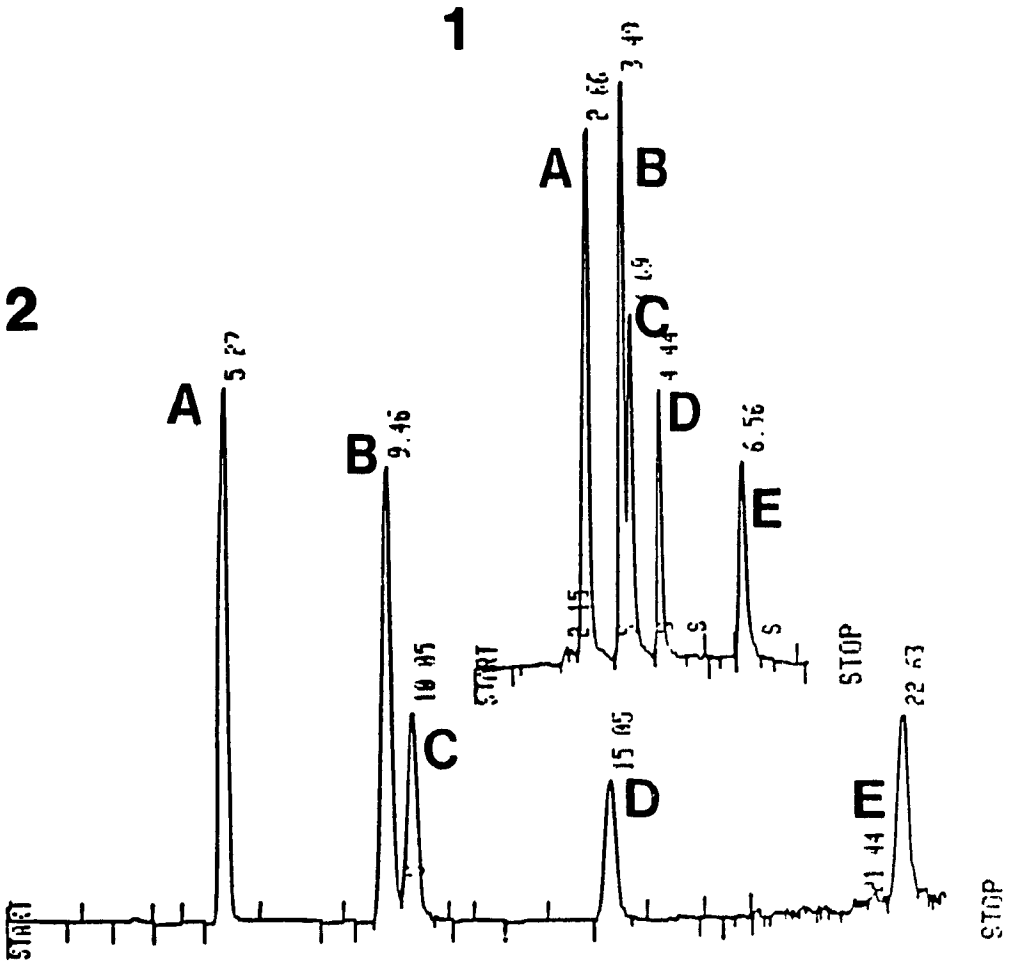
1
2
A
B
C
D
E
START
STOP
2.66
3.43
6.56
5.27
9.46
10.85
15.05
22.63

Dialkydithiocarbamate (DADTC) species form thermally stable complexes with some divalent metals which have been successfully separated by GC (Masaryk et al., 1975; Cardwell et al.,1976; Tavlaridis and Neeb, 1978; Carvajal and Zienius, 1986). The accuracy of the technique was uncertain because of the low resolution, peak asymmetry and analyte degradation which has been observed using a variety of chromatographic packing.

High pressure liquid chromatography (HPLC) appears to be more suitable for the separation and determination of extracted metal complexes, especially when coupled with AAS detection. Several metal chelates have been successfully chromatographed by normal- or reversed-phase HPLC, including those with diphenylthiocarbazone (Lohmuller et al., 1977), 1,2-diketobisthiobenzylhydrazone, 1,2-diketobisthiosemicarbazone (Heizmann and Ballschmiter, 1977), 8-hydroxyquinoline (Bond and Nagaosa, 1985; Mooney et al., 1987), diethyldithiocarbamate (Bond and Wallace, 1981; Drash et al., 1982) and pyrrolidinedithiocarbamate (Bond and Wallace, 1981). Direct injection of metallic cations into the chromatographic system, followed by *in situ* formation of their complexes has been accomplished by incorporating sodium diethyldithiocarbamate into the mobile phase (Bond and Wallace, 1981).

The reversed-phase chromatographic behavior of metal-diethyldithiocarbamates ($M(DEDTC)_2$) has been studied. With a reversed-phase (RP) Separon C_{18} column the capacity ratios k' and log k'of Cu-, Co-, Ni-, and Hg-$(DEDTC)_2$ complexes were linearly correlated with their liquid-liquid extraction distribution ratios (Dc) and with the volume fraction of water in the methanolic mobile phase, respectively (Vlacil and Hamplova, 1985). For these metals, it was concluded that their RP chromatographic retention was caused by hydrophobic interactions. The Pb^{2+} chelate was retained on the column longer than would have been predicted from the linear dependence of k'

on Dc so that the occurrence of a secondary silanophilic interaction during the chromatographic process was suggested. This was corroborated by a high peak asymmetry factor for this analyte. The addition of an organic polar modifier (chloroform) to the mobile phase has been demonstrated to reduce peak tailing during the RP(C_8) separation of $Pb(DEDTC)_2$ (Drash et al., 1982).

The "hydrophobic theory" of reversed-phase chromatography neglects the role of underivatized silica (at least 50 % of silanol groups (Bayer and Paulus, 1987)) in the chromatographic behavior on these stationary phases. High resolution chromatography methodologies often require the neutralization of surface silanol by adding protonated amines in the mobile phase to reduce tailing of cationic compounds (Bayer and Paulus, 1987).

Since the HPLC-AAS analysis of environmental samples for ionic alkylleads was to be preceded by a complexometric extraction of the lead compounds into an organic solvent and by a concentration step (evaporation of the solvent), it was preferable to inject the analytes directly into the chromatograph as their complexed forms. Sodium dimethyldithiocarbamate (NaDMDTC) was selected for this study because: (a) in contrast with dithizone, NaDMDTC is water soluble and can be extracted from the organic phase (hexane) before the evaporation step, which allows a 100 fold concentration of the organic extract (from water or soil) without formation of precipitate; (b) when used with hexane, this complexing agent is highly selective toward ionic alkylleads (Blais and Marshall, 1986), and can be used to extract matrices containing high levels of Pb^{2+}, and (c) preliminary thin layer chromatographic studies suggested higher selectivities between ionic alkylleads-DMDTC complexes versus DEDTC or pyrrolidinedithiocarbamate complexes.

Preliminary work was undertaken using the thermospray-microatomizer interface described previously (Figure 1). The chromatographic system comprised a Hypersil C_{18} stationary phase and a methanolic mobile phase containing varying proportions of water and dioxane. Dioxane was selected as the organic polar modifier because it was transparent to the detection system whereas halogenated hydrocarbons, ketones and acetonitrile contributed appreciably to the background noise. Dimethyldithiocarbamate (DMDTC) complexes of Pb^{2+}, Me_2Pb^{2+} and Me_3Pb^{+} were used as test compounds. Using a pure methanolic phase, $Pb(DMDTC)_2$ (50 ng) was only partially eluted and the ionic alkylleads remained immobilized from the column. The lead compounds were quantitatively eluted by adding DMDTC (200 µg/mL) to the mobile phase, which indicated that the original complexes had been degraded, leaving cationic lead species adsorbed to acidic sites in the column.

From previous thin layer chromatographic studies (Blais and Marshall, 1987, 1988a), it was known that SiO_2, Al_2O_3 and even the relatively inert polyamide stationary phases degrade alkyllead complexes (dialkyldithiocarbamates or dithizonates) and immobilize the lead species. Thus, the addition of a complexing agent in the HPLC mobile phase was required to desorb and elute the lead species.

Varying methanolic mobile phases composed of water (1-40 % v/v), dioxane (5-40 % v/v) and NaDMDTC (100-500 µg/mL), failed to completely resolve the analytes. Other complexing agents added to the mobile phase (disodium ethylenediaminetetraacetate, ammonium citrate, cysteine hydrochloride, and 1,2-ethanedithiol) at 10-200 µg/mL, desorbed the analytes from the stationary phase but did not provide adequate selectivity. Both zinc and cupric cations (10 µg/mL) also desorbed the lead species (presumably by competition for adsorption sites) which were co-eluted in a single broad peak.

Dithizone (Dz) appeared to be a more promising complexing agent for appropriate selectivity and resolution of (in order of retention times) the inorganic lead, dimethyllead, and diethyllead cations. The addition of 10 % water in the mobile phase resulted in longer retention times for these analytes with no appreciable effect on resolution, which suggested a hydrophobic chromatography mechanism. Monovalent trimethyl- and triethyllead were not eluted under optimum conditions for chromatography of the divalent lead compounds. The trialkyllead compounds were eluted as sharp peaks by shifting during the chromatographic run, to a mobile phase of similar composition containing NaDMDTC, using a pre-pump mobile phase selector (Figure 8). The two complexing agents, used sequentially in this chromatographic procedure (Dz and NaDMDTC), were virtually transparent to the detector, causing a negligible fluctuation of the baseline during the mobile phase shift. Optimum reproducibility of retention times was achieved only if a small proportion of acetic acid (5% v/v) was present in the second mobile phase (containing NaDMDTC). It was found essential to handle and store the 1-4 dioxane added in the mobile phase under nitrogen since this solvent reacts with oxygen to form reactive peroxides which rapidly degrade dithizone (Irving and Manhot, 1968). Whether these cationic lead species were injected as their chloride salts (in methanol) or as the DMDTC complexes (in benzene) only slightly affected their retention times and resolutions (Figure 8 a-b).

Figure 8. HPLC-AAS chromatograms of (a) Pb^{2+}; (b) Me_2Pb^{2+}; (c) Me_3Pb^{+} (10 ng) using the Hypersil C_{18} column, Dz (300 μg/mL) and DMDTC (300 μg/mL) sequentially in the mobile phases. Chromatogram (A) analytes injected as chlorides from methanol; (B) analytes injected as DMDTC complexes from benzene.

A

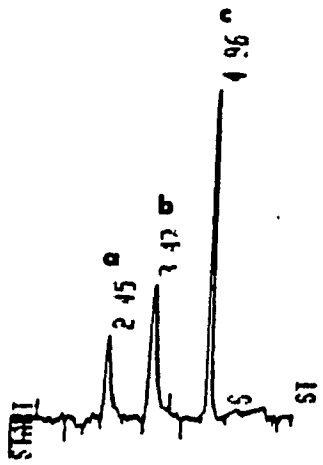

B

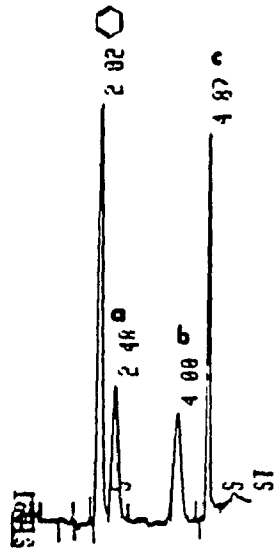

The fact that dithizone failed to desorb trimethyllead while complexing the divalent lead species and eluted them in an apparent hydrophobic chromatography suggested the occurence of a strong silanophilic interaction between the former analytes and the Hypersil stationary phase. The $Pb(Dz)_2$ complex is known to be relatively stable on bare silica and alumina gels (Lohmuller et al., 1977), and it would be reasonable to assume that $R_2Pb(Dz)_2$ complexes are relatively stable, as suggested by their chromatographic behavior. The elution of adsorbed trialkylleads using NaDMDTC but not Dz most probably reflects the fact that the stability constants of monovalent and divalent metal dithizonates (as predicted from their extraction constants) are generally lower than the constants of the corresponding metal dialkyldithiocarbamates (Stary and Ruzicka, 1968), especially at low pH. Because it was not possible to discriminate between the triethyl- and trimethyllead compounds, this chromatographic system was of no practical use for speciating lead in environmental extracts since both species may be present. However, this method has been applied successfully for the preparative isolation of radiolabeled ionic methyllead tracers (Blais and Marshall, 1989a).

The Nucleosil C_{18} stationary phase appeared to be a promising alternative for the selective chromatography of trimethyl- and triethyllead. It was known that microgram amounts of the five cations of interest could be separated on the Nucleosil C_{18} packing using a 9:1 aqueous acetate buffer (pH 4.6):methanol mobile phase (Blaszkewicz et al., 1984). However, the high water content of this mobile phase was not compatible with the AAS interface described earlier. In contrast to other reversed-phase packing, the Nucleosil C_{18} microspheres have been shown to produce virtually no silanophilic interactions with basic compounds. Surprisingly, this phenomenon was shown to be independent of the C_{18} derivatization procedures and was attributed to the microstructural properties of the Nucleosil bare silica (Bayer and

Paulus, 1987). From this background, it was postulated that addition of a complexing agent (NaDMDTC or Dz) in the mobile phase would result in a selective chromatography of the five complexed analytes.

Using a methanolic mobile phase, only the $Pb(DMDTC)_2$ complex (50 ng) was eluted from the Nucleosil C_{18} packing. The four other lead species were desorbed non-selectively after addition of NaDMDTC or Dz (300 µg/mL) to the mobile phase. Once again the DMDTC complexes were chromatographed with poor selectivity using methanolic eluents containing various proportions water (5-40 % v/v) and dioxane (5-25 % v/v). A selectivity for the five lead compounds was obtained with a methanolic mobile phase containing Dz (300 µg/mL), water (15 %) and dioxane (15 %). Optimum resolution and retention times were achieved by shifting to a mobile phase containing less water (10 %) during the chromatographic run using the automated mobile phase selector. A chromatogram resulting from this combination is presented in Figure 9.

As shown in Figures 8 and 9, the elution order of the dithizone complexes from the nucleosil C_{18} column ($PbDz_2$, Me_3PbDz, Et_3PbDz, Me_2PbDz_2, Et_2PbDz_2) was different from the order observed on the Hypersil C_{18} stationary phase ($PbDz_2$, Me_2PbDz_2, Et_2PbDz_2). The elution order on the nucleosil C_{18} packing and the retarding effect of increased proportions of water suggested a purely hydrophobic mechanism. The postulated structures of these complexes are presented in figure 10.

Figure 9. HPLC-AAS chromatogram of (a) Pb^{2+} (20 ng); (b) Me_3Pb^+; (c) Et_3Pb^+; (d) Me_2Pb^{2+}; (e) Et_2Pb^{2+} (10ng) using the Nucleosil C_{18} column and Dz in the mobile phase.

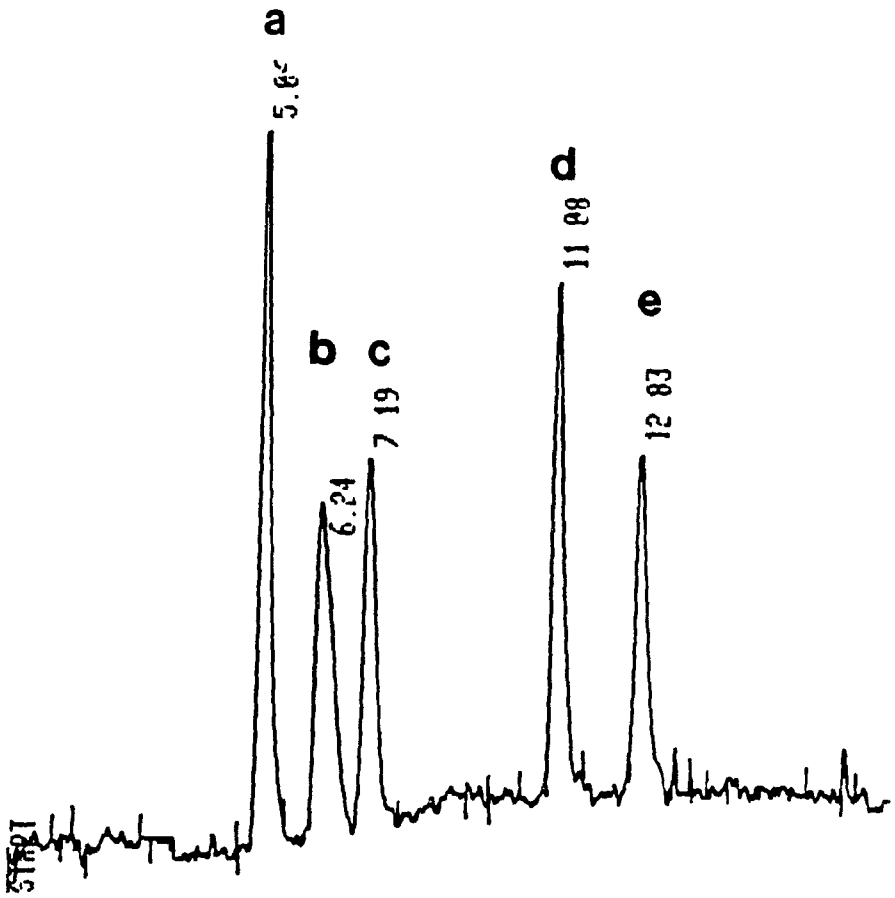
a
5.6
b
6.24
c
7 19
d
11 88
e
12 83

Figure 10. Postulated structures of (A) dithizone (Dz); (B) $Pb:Dz_2$; (C) $Me_2Pb:Dz_2$; (D) $Me_3Pb:Dz$.

A

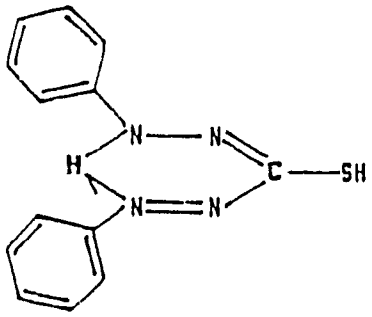

B

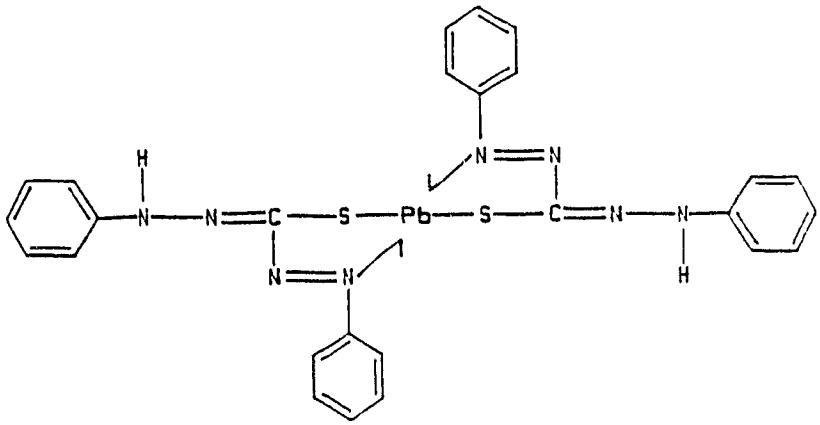

C

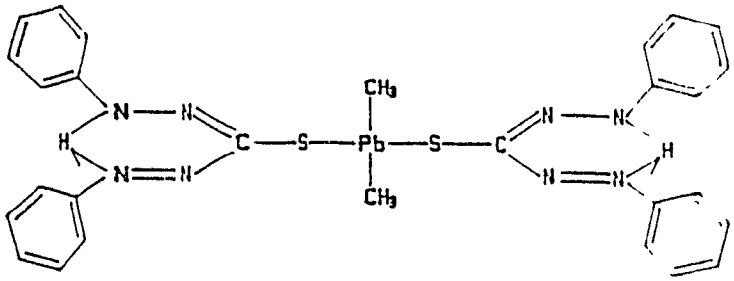

D

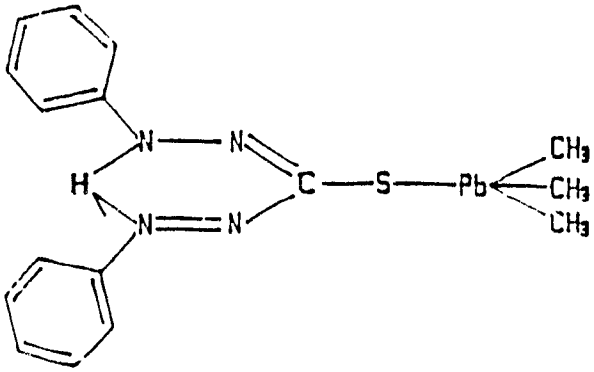

2.3.4 Application to Environmental Samples

The applicability of the optimized HPLC-AAS instrument for the analysis of real samples was investigated by extracting water (10 mL) or soil (5 g of a sandy clay loam + 5 mL water) which had been spiked with 100 ng of each of the four ionic alkylleads of interest. The complexometric extraction systems studied were combinations of NaDMDTC with hexane or benzene (Blais and Marshall, 1986). The resulting organic extracts were washed with water, dried with Na_2SO_4, transferred in dry graduated tubes and evaporated to 0.2 mL (75 fold concentration step) under a gentle flow of N_2. The resulting extracts were injected (50 μL) directly into the HPLC-AAS system.

The more efficient complexometric extraction system was found to be benzene-DMDTC. Resulting chromatograms are presented in Figure 11. The extraction efficiencies of the four compounds from water were: Me_3Pb^+ = 95 % ± 4, Me_2Pb^{2+} = 84 % ± 6, Et_3Pb^+ = 98 % ± 3, Et_2Pb^{2+} = 92 % ± 4. Chromatograms of hexane-DMDTC water extracts (Figure 11, A) were unacceptable because the dialkylleads were presumably co-eluted as their DMDTC complexes. The reason for this is unclear since chromatograms of benzene-DMDTC water extracts were similar (except for lower peak resolution) to those observed using ionic alkyllead standards (Figure 9 vs 11,B). A possible explanation for this difference is a masking effect of hexane (but not benzene) on silanol active sites which would normally degrade the original DMDTC complexes and consequently allow the alkyllead cations to complex with the complexing agent (dithizone).

Chromatograms of soil extracts were characterized by a degraded chromatographic behavior of the analytes which were co-eluted with the solvent front (Figure 11, C). In this case, foreign organic or metallic species (co-extracted by the complexometric

Figure 11. HPLC-AAS chromatograms of (a) Pb^{2+}; (b) Me_3Pb^+; (c) Et_3Pb^+; (d) Me_2Pb^{2+}; (e) Et_2Pb^{2+} which had been added at 10 ng/g to (A-B) water or (C) soil and extracted with (A) DMDTC-hexane or (B-C) DMDTC-benzene.

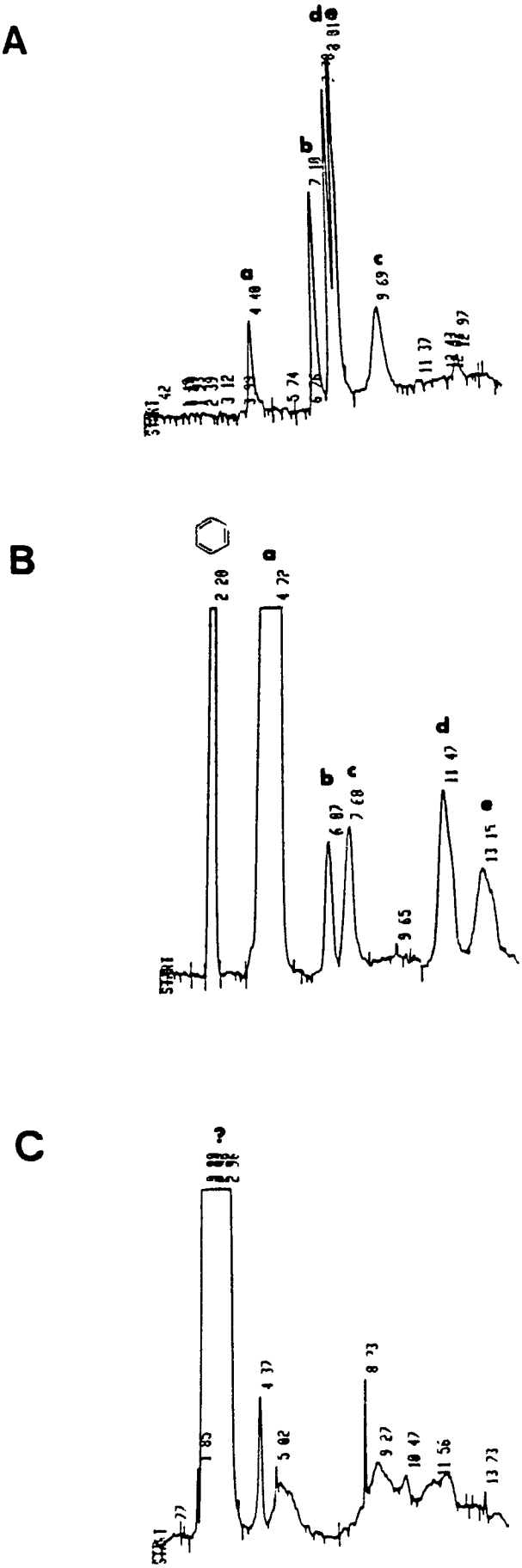
A
B
C

system), were most probably responsible for this deterioration of chromatographic performances.

In a tentative approach to solve this problem, a first extraction of the ionic alkylleads with the highly selective Dz-hexane system (Blais and Marshall, 1986) was followed by the back extraction of the alkyllead cations in dilute HNO_3(aq) leaving non-polar interferents in the organic phase (back-extraction technique; Forsyth and Marshall, 1983). The resulting aqueous solution was made alkaline, re-extracted with benzene-DMDTC and chromatographed as described above. The resulting chromatograms were characterized by unacceptable variations in peraks resolutions and retention times for replicate samples. Although the reasons for this behaviour were not investigated, it was postulated that variations were the result of the low stability of the dithizone-lead complexes relative to other co-extracted metal-dithizonates. Because the chromatographic characteristics of the lead compounds were believed to vary with the concentration (and possibly the nature) of metallic co-extractives, the use of dithizone as complexing agent was abandoned.

Among the dialkyldithiocarbamates evaluated as complexing agents on the Nucleosil C_{18} stationary phase, only ammonium pyrrolydinedithiocarbamate (PDTC) was highly compatible with the thermospray-microatomizer AAS interface (other dialkyldithiocarbamates were commercially available only as their sodium salts). The PDTC complexes of the five analytes of interest were separated efficiently by hydrophobic interactions (Figure 12). The optimum mobile phase for baseline separation of the lead species from hexane (50 µl injection) was 75% methanol:25% water containing 600 µg/mL PDTC. The reproducibility of the system was comparable to the figures observed using the dithizone-Nucleosil C_{18} system (Table 1.).

Figure 12. HPLC-AAS chromatograms of (a) Me_3Pb^+; (b) Pb^{2+}; (c) Et_3Pb^+; (d) Me_2Pb^{2+} and (e) Et_2Pb^{2+} (injected from methanol) obtained using a Nucleosil C_{18} column eluted with methanol containing 600 µg/mL of PDTC and (A) 5%, (B) 10%, (C) 15% and (D) 20% water. Chromatograms (E) and (F) represents 25 ng and 5 ng of each standards respectively, injected from hexane and chromatographed using 75 % methanol:25 % water containing 600 µg/mL of PDTC.

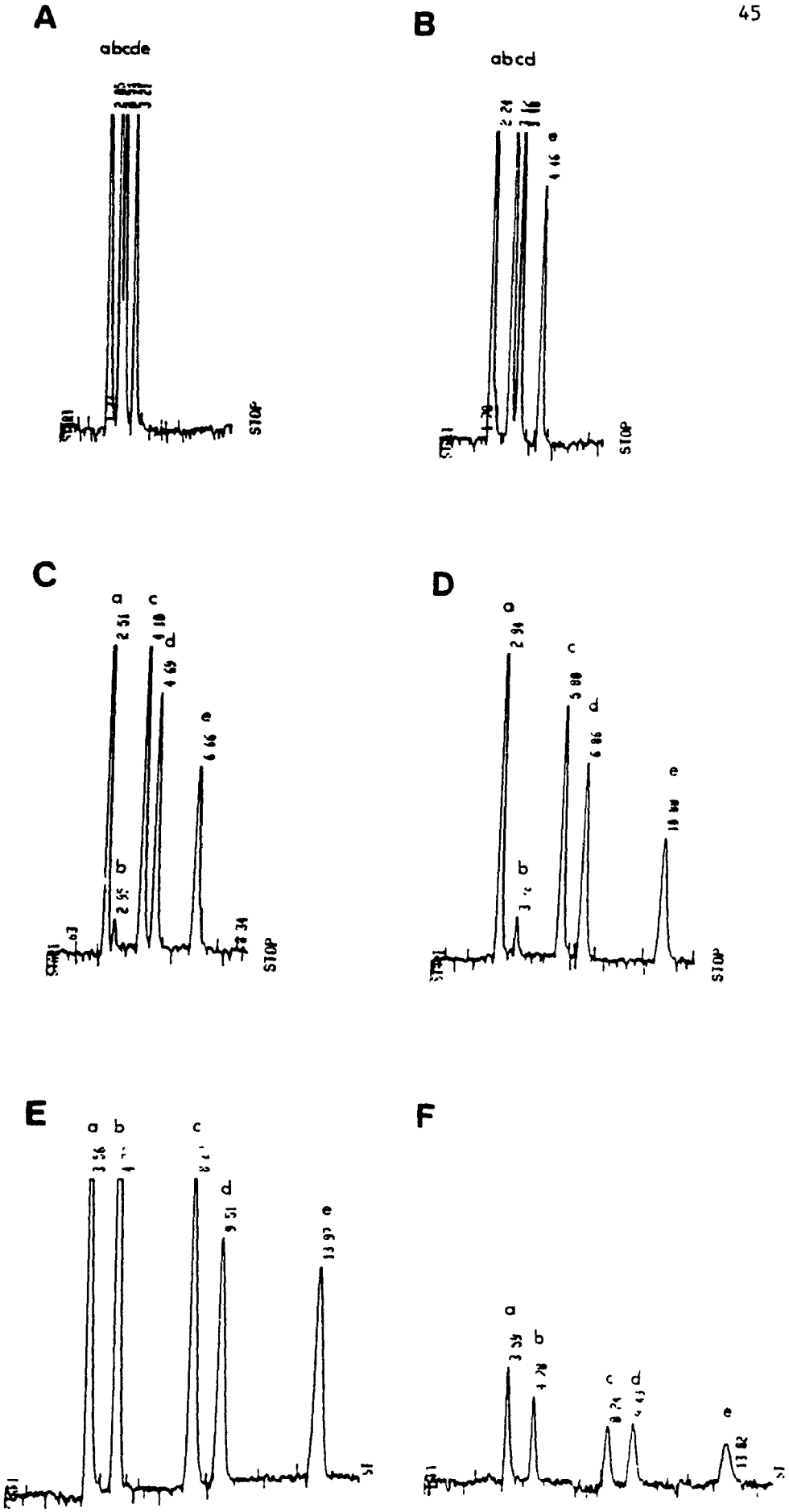
A
abcde
STOP
B
abcd
STOP
C
a
c
d
e
STOP
D
a
c
d
e
STOP
E
a
b
c
d
e
F
a
c
e

To demonstrate the applicability of this chromatographic system, water, soil (Blais and Marshall, 1986,) and anoxic sediments (Blais and Marshall, 1988b) were spiked at 10 ng/g with the four ionic alkyllead compounds and extracted with PDTC-hexane as described previously (Blais and Marshall, 1986). Prior to this complexometric extraction, the samples were pre-extracted with hexane (in an effort to remove organic non-polar species) and the hexane extracts were combined and back-extracted with water. The latter aqueous extract was combined with the samples prior to complexometric extraction with PDTC-hexane. The final hexane extracts were concentrated to 0.2 mL and injected (25-75 μL) in the HPLC-AAS instrument. Recovery efficiencies of this method are presented in Table 2 (method 1).

Using this method the lead compounds were recovered efficiently only from water. The chromatograms of sediment extracts were unacceptable because of the presence of an organic yellowish co-extractive which eluted as an off-scale tailing peak with inorganic lead. It was decided to apply the double extraction technique to these matrices to remove organic co-extractives from the final extract. Ionic alkylleads were extracted with dithizone and 1:1 benzene-hexane and then back extracted in dilute HNO_3 (Forsyth and Marshall, 1983). The resulting aqueous solution was made alkaline and re-extracted with the ionic alkyllead selective hexane-PDTC system (Blais and Marshall, 1986). As shown in Table 2 (method 2), the analytes were recovered relatively efficiently from water and sediments but not from soil. Chromatograms of these extracts are presented in Figure 13.

The low recoveries from soil (Figure 13, C) were rather surprising since a simple PDTC-hexane extraction followed by n-butyl derivatization and analysis by GC-AAS has been proven to be efficient (Blais and Marshall, 1986), indicating that the species were present in the complexometric extract. A direct PDTC-hexane extraction of the

Table 2. Percent Recoveries (± 1 S.D.) of ionic alkylleads from Water, Soil or Anoxic Sediments using Different Extraction Procedures.

Sample	Method	Me_3Pb^+ (%)	Et_3Pb^+ (%)	Me_2Pb^{2+} (%)	Et_2Pb^{2+} (%)
Water	1	96 ± 3	90 ± 5	86 ± 6	91 ± 4
Soil	1	50 ± 7	25 ± 4	ND[a]	ND
Sediment	1	UC[b]	UC	UC	UC
Water	2	98 ± 4	95 ± 3	92 ± 8	94 ± 4
Soil	2	66 ± 1	52 ± 4	ND	ND
Sediment	2	90 ± 0.5	86 ± 2	72 ± 4	75 ± 5
Soil	3	83 ±(6)	83 ± 2	73 ± 6	74 ± 3

[a] ND = Not detected.
[b] UC = Unacceptable chromatography.

Figure 13. HPLC-AAS chromatograms of (a) Me_3Pb^+; (b) Pb^{2+}; (c) Et_3Pb^+; (d) Me_2Pb^{2+} and (e) Et_2Pb^{2+} which had been spiked (10 ng/g) and extracted (double extraction) from (A) water, (B) sediments and (C) soil. Chromatogram (D) was obtained using a direct extraction procedure for the soil samples.

A

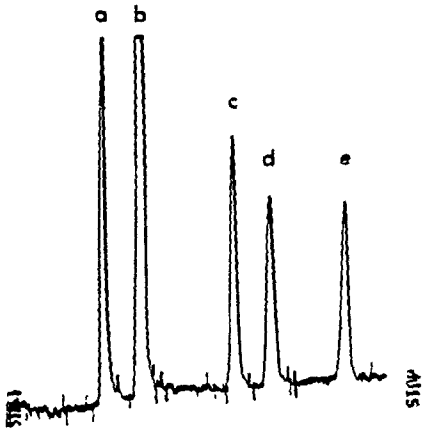

B

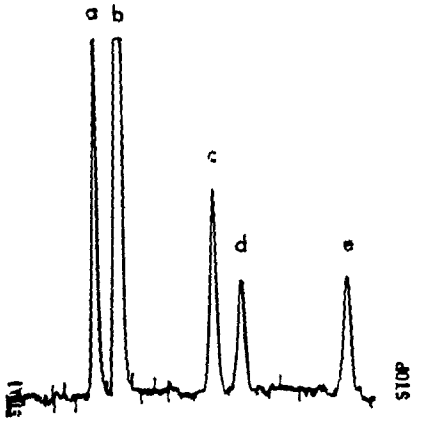

C

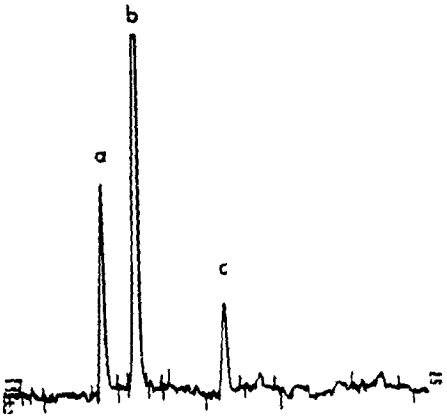

D

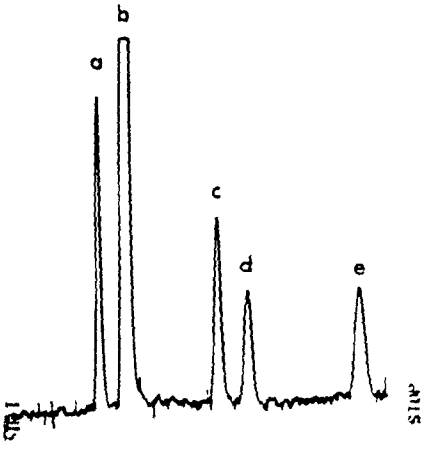

lead species from soil (without pre-extraction with hexane) was subsequently found to extract the lead compounds (Figure 13, D) with yields (Table 2, method 3) which were comparable to those previously reported (Blais and Marshall, 1986). This result indicated that this soil contained species which can co-ordinate ionic alkylleads (especially dialkylleads) to form hexane soluble complexes. These complexes were relatively stable since they were not degraded by the dilute acid used in the double extraction technique.

2.3.5 Conclusion

Using the PDTC-Nucleosil C_{18} chromatographic system, the limits of detection (LOD) of the analytes were similar to those observed using the dithizone-Nucleosil C_{18} combination (1-2 ng), which represents 0.2 ng/g (0.2 ppb) for a 5 g sample. This LOD was at least 10 fold higher than those provided by GC-AAS techniques. On the other hand, this approach does not requires artifact prone derivatization steps and allows faster analyses.

3. HPLC-Quartz Tube-AAS for the Determination of Ionic Alkylleads

3.1 Synopsis

At low- or sub-ppb levels, organoleads and other organometallic compounds may affect biological systems (Grandjean and Nielsen, 1979). Thus, it is imperative to speciate these chemicals with the lowest limit of detection one can achieve, especially in environmental and biological compartments which are at the base of the food chain (waters, sediments, soils, microbiota).

The miniaturized FAAS atomization interface presented in section 2 provided a practical limit of detection (0.2 ppb for a 5 g samples) which was from 1 to 2 orders of magnitude lower than other reported HPLC-FAAS direct interfaces (Botre et al., 1976; Messman and Rains, 1981). In the atomic absorption technique, the analytical flame of a flame atomizer is intrinsically less efficient than flameless atomization cells, because (a) it usually does not atomize the analyte quantitatively, (b) the atomic species spend a very short time within the optical beam of the spectrometer, and (c) it radiates a relatively high spectral background in the ultra-violet range (resulting in a low signal to noise ratio). Post-column volatilization of the metallic compounds in a chemically active electrothermal quartz furnace (QTAAS) is a promising alternative for an HPLC-AAS interface since virtually absolute sensitivities have been observed in these atomization cells (Siemer amd Hageman, 1975; Siemer et al., 1976; Siemer and Koteel, 1977). This approach has been used to speciate different physico-chemical forms of those metallic elements which can be reduced by sodium borohydride to form volatile hydrides (Ebdon et al., 1987).

However, most organometallics either do not react with reducing agents such as sodium borohydride or do not form stable hydride derivatives. Two volatilization techniques for Pb^{2+}, R_2Pb^{2+} and R_3Pb^{+} have therefore been evaluated; (a) formation of hydride derivatives with sodium borohydride and (b) formation of volatile ethylated tetraalkyl-derivatives using sodium tetraethylborate. A post-column ethylation/volatilization approach based on $NaBEt_4$ was then developed for the analysis of ionic alkylleads by HPLC-QTAAS.

3.2 Materials and Methods

3.2.1 Chemicals and Reagents

Methanol (Caledon Laboratories, Georgetown, Ont.) and water used for HPLC mobile phases preparation were "distilled in glass" grade and distilled-deionized, respectively. Mobile phase components were mixed, deoxygenated with nitrogen and degassed by ultrasonication. The complexing agent ammonium pyrrolidinedithiocarbamate (PDTC) was purchased from Anachemia (Montreal, Qc).

Alkyllead chlorides (R_3PbCl, R_2PbCl_2; R = CH_3, C_2H_5) were prepared and purified as described previously (Forsyth and Marshall, 1983, 1985). Stock solutions of these alkyllead compounds were prepared as follows: Me_3PbCl (1.10×10^{-4} g/mL), Me_2PbCl_2 (1.06×10^{-4} g/mL), Et_3PbCl (1.06×10^{-4} g/mL, Et_2PbCl_2 (1.01×10^{-4} g/mL), $Pb(NO_3)_2$ (1.00×10^{-4} g/mL) in 1:1 methanol:water. Dilution of these stock solutions with methanol provided working standards.

3.2.2 Formation of Volatile Alkyllead Hydride Derivatives

Preliminary experiments were performed in a hydride generation cell (Figure 14) composed of a pyrex test tube sealed with a suba-seal septum (Suba-Seal # 17, W. Freeman and Co. Barnsley, U.K.). The reaction medium containing the sample was continuously flushed with 50-100 mL/min of N_2 (using a stainless steel needle), and the gaseous effluent was channeled to the electrothermal quartz furnace-AAS (QTAAS) assembly described previously (Forsyth and Marshall, 1985) using a 0.3 cm i.d. teflon tube. Reactants and analytes were injected into the cell through the septum using a syringe. Ten ng of the analyte was added in 1 mL of 1 N HCl or HNO_3(0.5 M)-H_2O_2 [10% (v/v)] and, subsequently, 2 mL of 1 % (w/v) sodium borohydride was rapidly injected. The AAS response (Perkin-Elmer AAS, model 303, 283.3 nm) was recorded with a recording integrator (Hewlett-Packard, model 3390-A).

3.2.3 Formation of Volatile Ethylated Tetraalkyllead Derivatives

The derivatization reaction with sodium tetraethylborate was investigated using the apparatus described above (section 3.2.2) by adding 2 mL of 5 % (w/v) aqueous $NaBEt_4$ into 1 mL of water containing 10 ng of the compound.

3.2.4 Continuous-Flow Ethylate Generator Interface

A diagram of the interface is presented in Figure 15. The HPLC eluate was mixed with aqueous $NaBEt_4$ (metered by a Beckman model 100A HPLC pump) in a stainless steel T-union (0.16 cm, zero dead volume; Chromatographic Specialties, Brockville,Ont.). The resulting mixture was channeled in a Pyrex heating coil (Figure 15, B; 0.64 cm o.d. x 0.4 cm i.d. x 10.3 cm^3 i.v.) via a capillary Teflon tube (A; 0.16 cm o.d. x 0.03 cm i.d.) secured within the glass coil by reducing Swagelok unions (C; 0.64 cm x 0.16 cm). Heating water (from a thermostatted bath) was circulated in the coil with a centrifugal pump (2 L/min). The other end of the Teflon

Figure 14. Hydride generation Cell: (A) Suba-Seal septum (#17) fitted to a pyrex tube; (B) nitrogen input (stainless steel needle); (C) gas output to QTAAS.

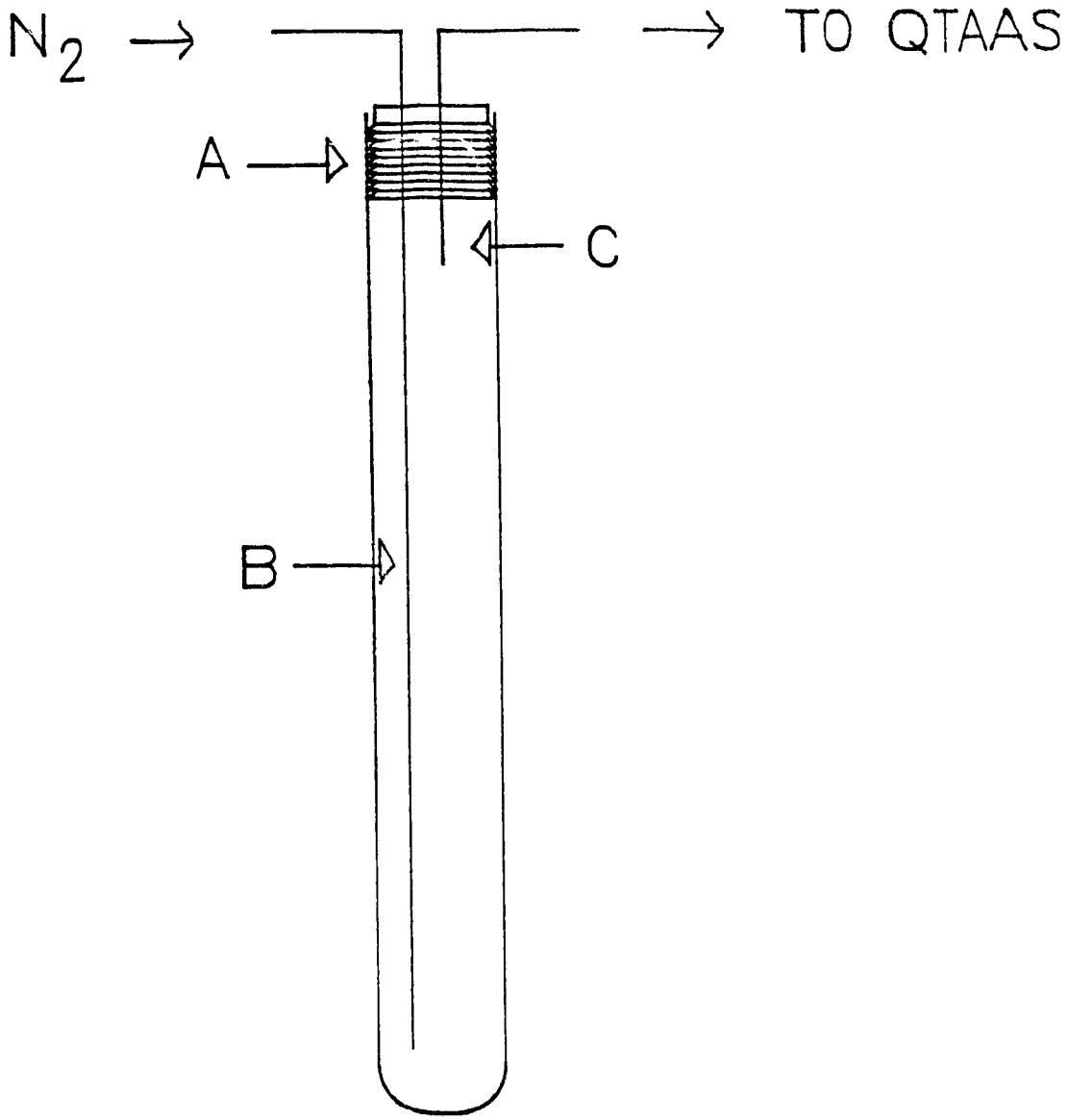
N_2
TO QTAAS
A
C
B

Figure 15. Continuous flow ethylate generation interface: (A) capillary Teflon tube; (B) glass heating coil; (C, D, F) Swagelok fittings; (G) 320 μm silica transfer line to QTAAS. The gas liquid separator (insert) comprised: (a) inlet tube; (b) main body; (c) gas outlet; (d) liquid disposal vessel; (e) liquid outlet; (f) mercury column.

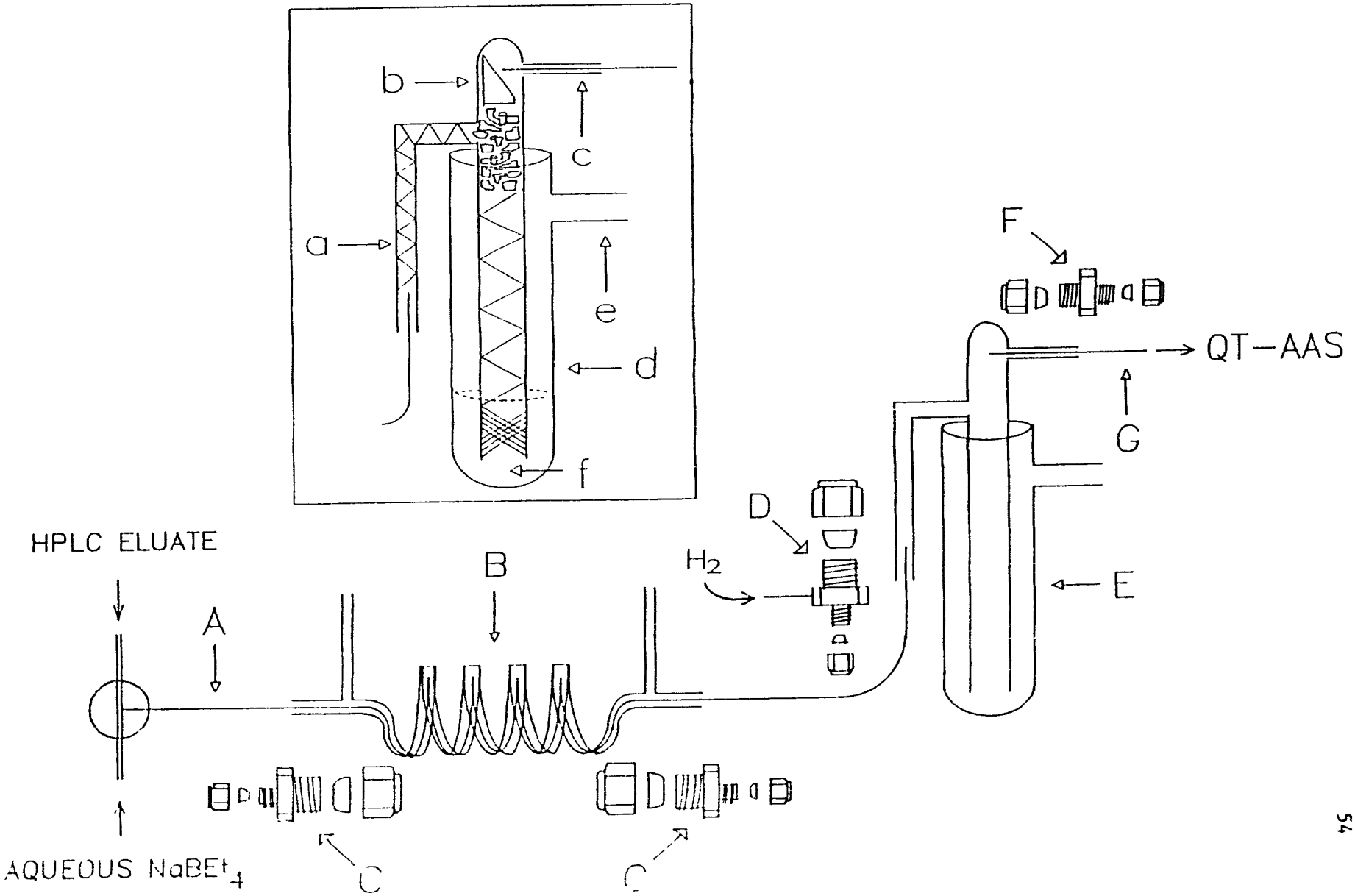
b
c
a
e
d
f
F
QT–AAS
G
D
H2
E
HPLC ELUATE
B
A
AQUEOUS NaBEt4
C
C

line (A) was connected to the inlet of a gas-liquid separator (GLS) assembly (E) using a reducing Swagelok union (D; 0.64 cm x 0.16 cm) modified for gas introduction. Hydrogen was introduced in the GLS at this point via a 0.16 cm o.d. stainless steel tube soldered in an inlet bored through the reducing union (D). The gases emerging from the GLS were channeled in a 0.32 mm i.d. deactivated quartz capillary (Chromatographic Specialties, Brockville, Ont.) to a QTAAS unit (Forsyth and Marshall, 1985) adjusted to the Pb specific wavelength (283.3 nm). The capillary was fixed to the GLS outlet using a reducing union (0.32 cm x 0.16 cm).

The GLS (Figure 15, insert) consisted of a quartz tube (b, 8 cm x 12 mm o.d. x 10 mm i.d.) fitted with an inlet (a, quartz tube, 8 cm x 6 mm o.d. x 4 mm i.d.) and a gas outlet (c, quartz tube, 3 cm x 3.2 mm o.d. x 2 mm i.d). The GLS was placed in a liquid disposal vessel made from a Pyrex test tube (d, 6 cm x 3 cm o.d. x 2.6 cm i.d.) fitted with a liquid outlet (e, 3 cm x 0.64 cm o.d. x 0.5 cm i.d.).

A positive pressure was maintained inside the GLS by adding metallic mercury (f) in the liquid disposal vessel. The dead volume of the GLS was filled with sand (schematized by triangulations; Ottawa standard sand 2170, Canlab, Montreal P.Q.) and Teflon chips (intersection of inlet and main tubes; Norton Performance Plastics. Norton , N.J., USA). The upper section of the GLS was configured with a solid Teflon insert (shaped from a 6 mm Teflon stopcock; Cole Parmer Instrum. Co., Windsor Ont.) cut diagonally so that the tip of the capillary transfer line could be centered in the GLS main body. The other end of the GLS (liquid outlet) was fitted with a glass wool plug.

3.2.5 Chromatography

The chromatographic and data acquisition systems used for this study were as described previously (section 2.2.2). The analytes were separated in two Nucleosil C_{18} columns (5 µ, 0.46 cm i.d. x 15 cm) connected serially with a capillary stainless steel tube (4 cm x 0.16 cm o.d. x 0.02 cm i.d.). The chromatographic eluent (1 mL/min) was composed of a methanolic solution containing 20 % (v/v) water and 600 µg/mL of ammonium pyrrolidinedithiocarbamate.

3.2.6 Optimisation

Five variables of the ethylate generator-QTAAS system [NaBEt4 concentration (0.1-1 % [w/v]) and flow rate (0.1-1 mL/min), reaction coil temperature (25-70 ^{o}C, hydrogen flow rate (10-100 mL/min and quartz furnace temperature (869-1145 ^{o}C)] were optimised simultaneously. The temperature of the furnace was expressed as current since a direct measurement of the inner surface temperature was not possible. The outer surface temperature was continuously monitored using a thermocouple as described elsewhere (Forsyth and Marshall, 1985). This temperature was found to be proportional to the current applied to the heating element, and independent of the hydrogen flow rate in the range studied (10-100 mL/min). As metallic contamination from thermocouple was know to affect the sensitivity, the current was correlated with inner temperature after the optimization trials.

A multivariate methodology was designed to obtain the estimates of optimum parameters (Box and Wilson, 1951, Hill and Hunter, 1966). This approach allows the determination of a quadratic model which accounts for simple and interaction effects of the variable studied. A detailed description of this method is presented in Appendix 2. A half-replicate 2^5 (2 levels, 5 variables) factorial design

(16 observations) was augmented by 11 points to form a composite design, with a total of 81 observations (triplicate observations/data point + three additional observations for the central data point). The design matrix of the augmented half-replicate 2^5 factorial experiment is outlined in Appendix 2. The HPLC column was removed for these experiments. No AAS response was observed upon injection of methanol in these conditions. A standard solution of the five species (0.5 ng) of interest was injected into the chromatograph and the resulting signal was recorded. An equilibration time of 10 min was allowed between each data point trials. The linearity, stability and limits of detection provided by this instrument were determined as described previously (Section 2.3.2, Appendix 1).

3.3 Results and Discussion

3.3.1 Formation of Volatile Alkyllead Hydride Derivatives

Only trimethyl- and triethyllead were volatilized as the hydride derivatives in the concentration range studied. Assuming a linear calibration curve, the limit of detection of these compounds was estimated to be 50-100 pg. Difficulties with inorganic lead(II) hydride generation have been documented (Vijan and Wood, 1976; Godden and Thomerson, 1980; Smith, 1981), and a similar problem has been observed in the case of dialkyllead(IV) species (D'Ulivo et al., 1986). The causes are considered to be the poor yields of the volatile hydride and the low thermal stability of the product. It has been reported that the efficiency of the lead hydride generation technique increases if oxidants, such as potassium dichromate (Ikeda et al., 1981), malic acid- or tartaric acid-$K_2Cr_2O_7$ (Flemming and Ide, 1976, HNO_3- or HCl-H_2O_2 (Bonilla et al., 1987), or HNO_3-$(NH_4)_2S_2O_8$ (Jin and Taga, 1982) are added to the solution. For the concentration range studied, the response of inorganic lead or dialkyllead(IV) hydrides from the HNO_3-H_2O_2 solutions was still

very low (0.5-1 %) relative to trialkylleads responses. Consequently, this approach to the post column volatilization of ionic alkylleads was abandoned.

3.3.2 Ethylate Generation

Ethylation of lead(II) (reaction 1) and lead(IV) organometallic salts (reactions 2-3) using sodium tetraethylborate was considered a more promising route to the post-column volatilization of these species. These reaction is considered to be mediated by the thermodynamic feasibility of the transmetalation.

$$2\ Pb^{2+} + 4\ NaB(C_2H_5)_4 \longrightarrow 2\ [(C_2H_5)_2Pb(II)]$$

$$2\ [(C_2H_5)_2Pb(II)] \longrightarrow (C_2H_5)_4Pb + Pb^{o} \qquad (1)$$

(Honeycutt and Riddle, 1961)

$$R_3Pb^{+} + NaB(C_2H_5)_4 \longrightarrow R_3Pb(C_2H_5) \qquad (2)$$

$$R_2Pb^{2+} + 2\ NaB(C_2H_5)_4 \longrightarrow R_2Pb(C_2H_5)_2 \qquad (3)$$

(Rapsomanikis et al., 1986)

The stoichiometry of these transmetalation reactions is uncertain, since triethylborane can also ethylate lead(II) and most probably lead (IV) compounds (Honeycutt and Riddle, 1960).

Ionic methylleads in water have been speciated in the low picogram range by *in-situ* ethylation in a closed cell followed by dynamic purging of the derivatives on a gas chromatographic packing and mild thermal desorption to a QTAAS system (Rapsomanikis et al., 1986). Addition of $NaEt_4B$ to the head of a GC column was sufficient to result in successful chromatography of Pb^{2+} and well as $Me_nPb^{(4-n)}$ (n=2,3) as their corresponding ethylates (Ashby et al., 1988). The latter methods did not permit the speciation of alkyllead in environmental samples, because of ambiguities associated with the ethylation procedure. Both diethyl- and triethyllead (also Me_2Pb^{2+} and Me_2EtPb^{+}) would form the same derivative. However, this reagent was promising for a post-HPLC derivatization/volatilization approach.

Using a simple ethylate generator (Figure 14), both monovalent and divalent methyllead and ethyllead species studied were successfully volatilized as tetraalkyllead derivatives from aqueous solutions to a QTAAS system, with estimated limits of detection (LOD) in the low nanogram range. Inorganic lead was also volatilized, but with a relatively poor LOD (0.1-1% relative to ionic alkylleads) in the concentration range studied. This low efficiency may be attributed to (a) the low theoretical yield (50 %) of the macroscale reaction, and (b) the high dilution of the reaction mixture which causes the unstable organolead(II) intermediate to decompose instead of disproportionating.

3.3.3 Continuous-Flow Ethylate Generator Interface

A continuous-flow reactor (Figure 15) was developed to volatilize chelated ionic alkyllead species (emerging from an HPLC column) in a quartz tube-atomic absorption (QTAAS) system. The HPLC eluate was continuously mixed with aqueous $NaBEt_4$ in a T-union and channeled to a glass reaction coil (Figure 15, B) in which water was circulated at controlled temperature. After separation from the

liquid matrix (using H_2 as carrier gas) in a gas-liquid separator (GLS) (E), the resulting volatile derivatives were transferred to the QTAAS unit via a deactivated capillary silica transfer line (F).

In order to obtain a constant head space (or liquid level) in the GLS, the gas pressure was to be equilibrated with an hydrostatic pressure applied to the liquid disposal outlet. Small differential between these pressures in the GLS resulted in heterogeneity of chromatographic peaks widths and, ultimately, either loss of gaseous analytes through the liquid disposal outlet or transfer of liquid in the quartz furnace via the capillary transfer line. Pressure differential became a problem during preliminary optimisation trials where the hydrogen flow rate and pressure were varied extensively. This problem was not observed in GLS designs including a larger transfer line (2 mm i.d. quartz tube) to the QTAAS unit, but this approach was abandoned because of extensive deposition of analyte (as metallic Pb) inside the tube. The use of a 0.32 mm silica capillary as a transfer line was a successful solution because higher gas linear velocities were achieved, resulting in a more efficient cooling of the silica wall and shorter residence time of the species in the hot portion of the line. On the other hand, this capillary transfer line induced an appreciable back-pressure in the GLS.

Different approaches were investigated for maintaining a constant hydrostatic pressure in the GLS, through the liquid disposal outlet (needle valves, water columns) with irreproducible results. A stable head volume in the GLS was successfully maintained using a mercury column to counteract H_2 pressure. For this purpose, the required amount of mercury (Figure 15, f) was added or removed from the liquid disposal vessel (d) using a syringe fitted with a long stainless steel needle. Although metallic mercury was known to be inert to $NaBEt_4$, it was reasonable to

assume that trace amounts of mercury(II) would be produced at the mercury-aqueous interface. Since ionic mercury reacts with $NaBEt_4$ (Honeycutt and Riddle, 1961), the presence of trace diethyl mercury species in the liquid waste container was anticipated and the latter was ventilated.

The dead volume of the GLS was minimized by filling it with standard Ottawa sand. The sand in the GLS inlet (a) was stabilized with teflon chips added in the GLS main body. A diagonally shaped teflon bar was seated above the bed of teflon chips so that the capillary transfer line tip could be centered in the GLS main body. Because a small proportion of methanol was continuously distilled and condensed in the GLS gas outlet (c), positioning the transfer line in this tube resulted in random bursts of liquid in the furnace, causing fluctuations of the AAS signal.

More reproducible results were observed if the GLS inlet (a) was bent (in a smooth 90^{o} arc) to parallel the GLS main body. This observation was attributed to a more homogeneous diffusion of H_2 through the sand in a vertical configuration relative to an horizontal one, in which the gas and liquid phases tend to flow separately.

3.3.4 Optimisation

Because preliminary experiments showed that some variables may interact with others, a multivariate optimisation methodology was designed (Box and Wilson, 1951; Hill and Hunter, 1966). Since excessive experimentation would have resulted from a complete 3^5 (5 variables;3 levels) factorial design (triplicated observations would have required 729 experiments), a half-replicate 2^5 factorial design (16 observations) was augmented by 11 points to form a composite design. The statistical analyses required to define the factorial model were performed by least

squares regression using the RSREG procedure of the SAS software (SAS institute, Cary, NJ, USA). Details of the statistical analysis are presented in Appendix 2.

The different $NaBEt_4$ concentrations (0.1-1 % w/v) and furnace temperatures (869-1145 ^{o}C) studied did not significantly affect (at the 0.01 confidence level) the response of the analytes. However, the effect of $NaBEt_4$ concentration was significant at the 0.05 confidence level. These results are in agreement with previous studies which showed that (a) $NaBEt_4$ concentrations as low as 0.03 % were sufficient to volatilize trace levels of alkyllead salts from water at room temperature (Rapsomanikis et al., 1986) and (b) the response of alkylleads in a GC-AAS quartz furnace reach a plateau at furnace temperatures exceeding 800-900 ^{o}C (Forsyth and Marshall, 1985). The effects of reaction coil temperature (25-70 ^{o}C) and hydrogen flow rate (10-100 mL/min) were significant at the 0.01 level of confidence. The most surprising effect on the analyte signal was due to changing the flow rate of aqueous $NaBEt_4$ ($p = 0.0001$).

Three dimensional response surfaces describing the predicted effects of the most significant variables were obtained from the resulting factorial equation parameters (Appendix 2). The resulting response surface plots are presented in Figure 16. As indicated by these these figures the response decreased with increases in the hydrogen flow rate and $NaBEt_4$ concentration, and increased with rises in $NaBEt_4$ solution flow rate and reaction coil temperature.

The increased response at higher reaction coil temperature may be explained, in part, by the Arrhenius law (more rapid derivatization of the species at higher temp.), but is also likely a result of a more efficient volatilization of the derivatives from the methanolic solution. The positive effect of higher $NaBEt_4$ flow rates

squares regression using the RSREG procedure of the SAS software (SAS institute, Cary, NJ, USA). Details of the statistical analysis are presented in Appendix 2.

The different $NaBEt_4$ concentrations (0.1-1 % w/v) and furnace temperatures (869-1145 ^{o}C) studied did not significantly affect (at the 0.01 confidence level) the response of the analytes. However, the effect of $NaBEt_4$ concentration was significant at the 0.05 confidence level. These results are in agreement with previous studies which showed that (a) $NaBEt_4$ concentrations as low as 0.03 % were sufficient to volatilize trace levels of alkyllead salts from water at room temperature (Rapsomanikis et al., 1986) and (b) the response of alkylleads in a GC-AAS quartz furnace reach a plateau at furnace temperatures exceeding 800-900 ^{o}C (Forsyth and Marshall, 1985). The effects of reaction coil temperature (25-70 ^{o}C) and hydrogen flow rate (10-100 mL/min) were significant at the 0.01 level of confidence. The most surprising effect on the analyte signal was due to changing the flow rate of aqueous $NaBEt_4$ ($p = 0.0001$).

Three dimensional response surfaces describing the predicted effects of the most significant variables were obtained from the resulting factorial equation parameters (Appendix 2). The resulting response surface plots are presented in Figure 16. As indicated by these these figures the response decreased with increases in the hydrogen flow rate and $NaBEt_4$ concentration, and increased with rises in $NaBEt_4$ solution flow rate and reaction coil temperature.

The increased response at higher reaction coil temperature may be explained, in part, by the Arrhenius law (more rapid derivatization of the species at higher temp.), but is also likely a result of a more efficient volatilization of the derivatives from the methanolic solution. The positive effect of higher $NaBEt_4$ flow rates

Figure 16. Predicted response surfaces derived from the quadratic response model: H2 = hydrogen flow rate (mL/min); TC = heating coil temperature (^{0}C), CD = concentration of $NaBEt_4$ (% w/v); FD = flow rate of the $NaBEt_4$ solution (mL/min). The quadratic equations describing these surfaces are presented in Table A-4.

PLot of Peak Area vs H2 and FD

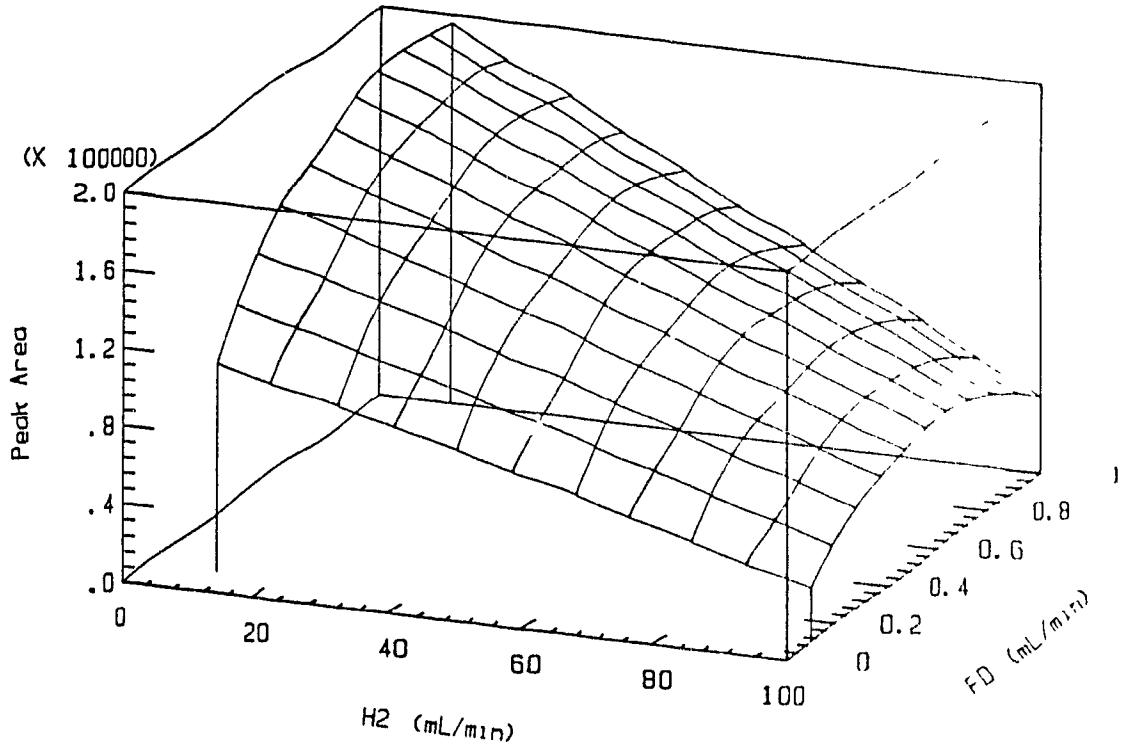

Plot of Peak Area vs FD and TC

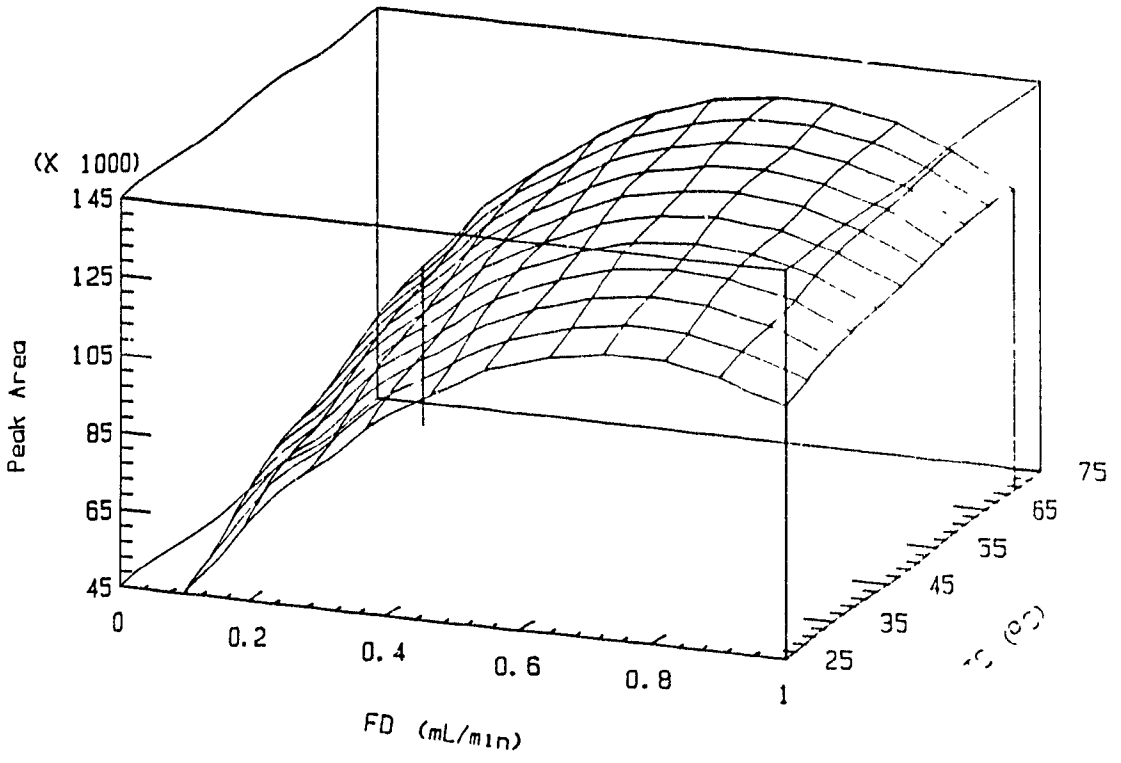

Figure 16. Predicted response surfaces derived from the quadratic response model: H2 = hydrogen flow rate (mL/min); TC = heating coil temperature (^{o}C), CD = concentration of $NaBEt_4$ (% w/v); FD = flow rate of the $NaBEt_4$ solution (mL/min). The quadratic equations describing these surfaces are presented in Table A-4.

Plot of Peak Area vs CD and TC

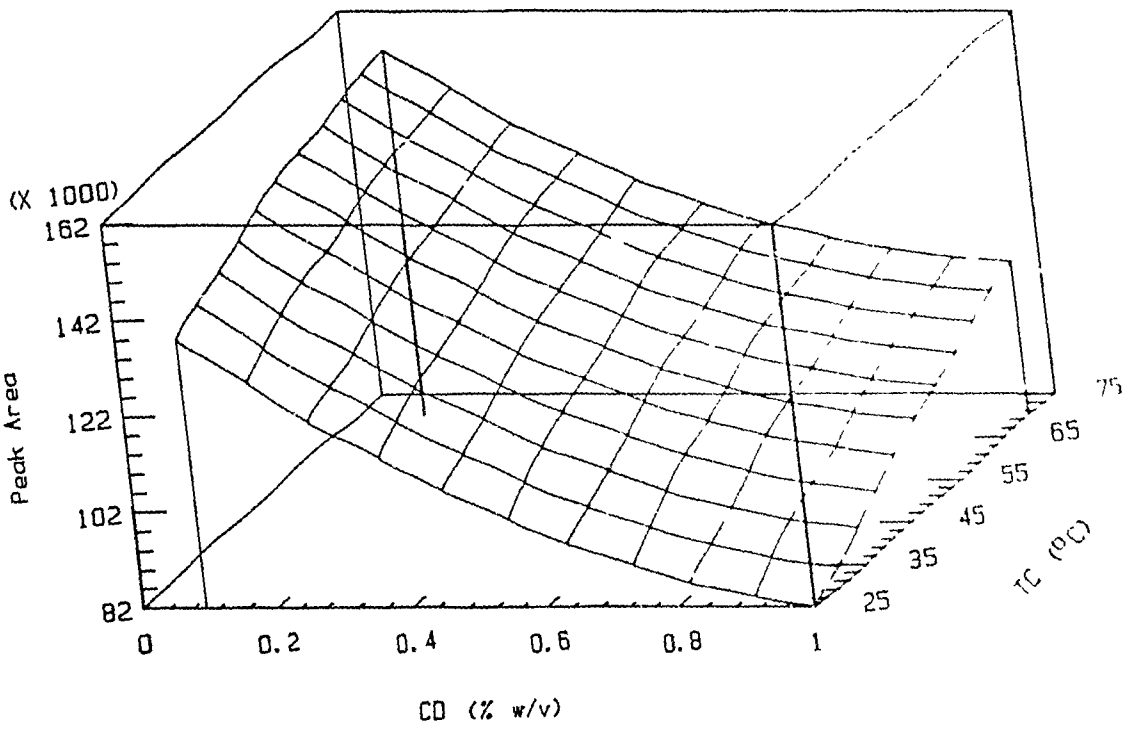

Plot of Peak Area vs H2 and TC

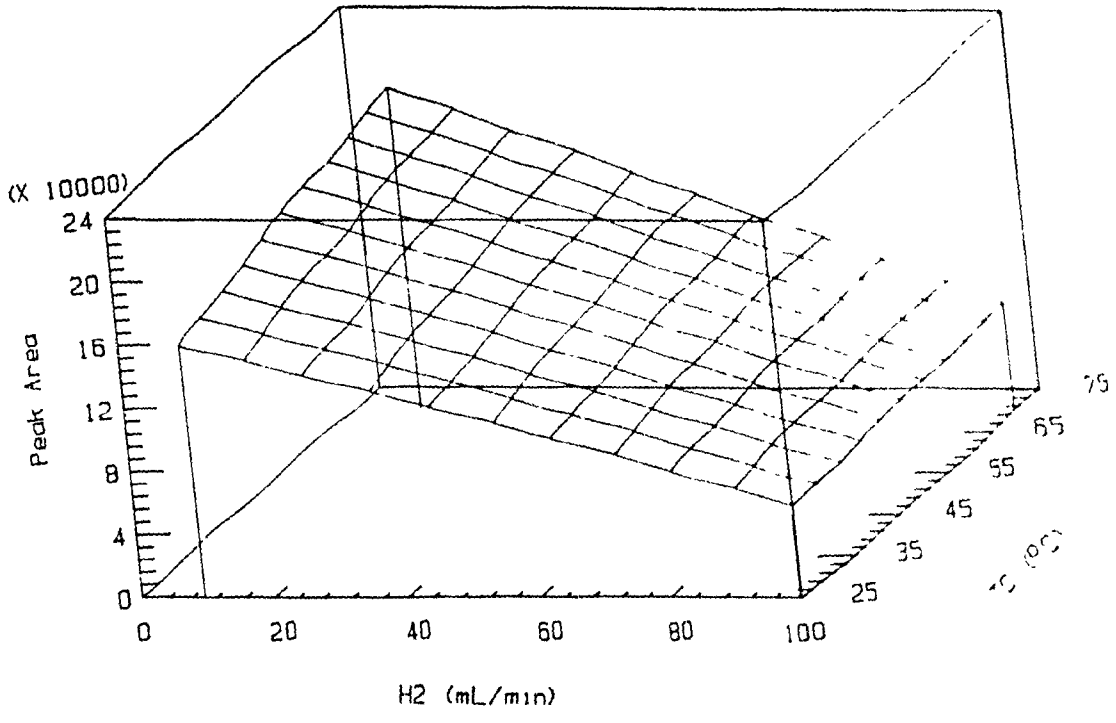

Figure 16. Predicted response surfaces derived from the quadratic response model: H2 = hydrogen flow rate (mL/min); TC = heating coil temperature (^{O}C), CD = concentration of $NaBEt_4$ (% w/v); FD = flow rate of the $NaBEt_4$ solution (mL/min). The quadratic equations describing these surfaces are presented in Table A-4.

Plot of Peak Area vs CD and FD

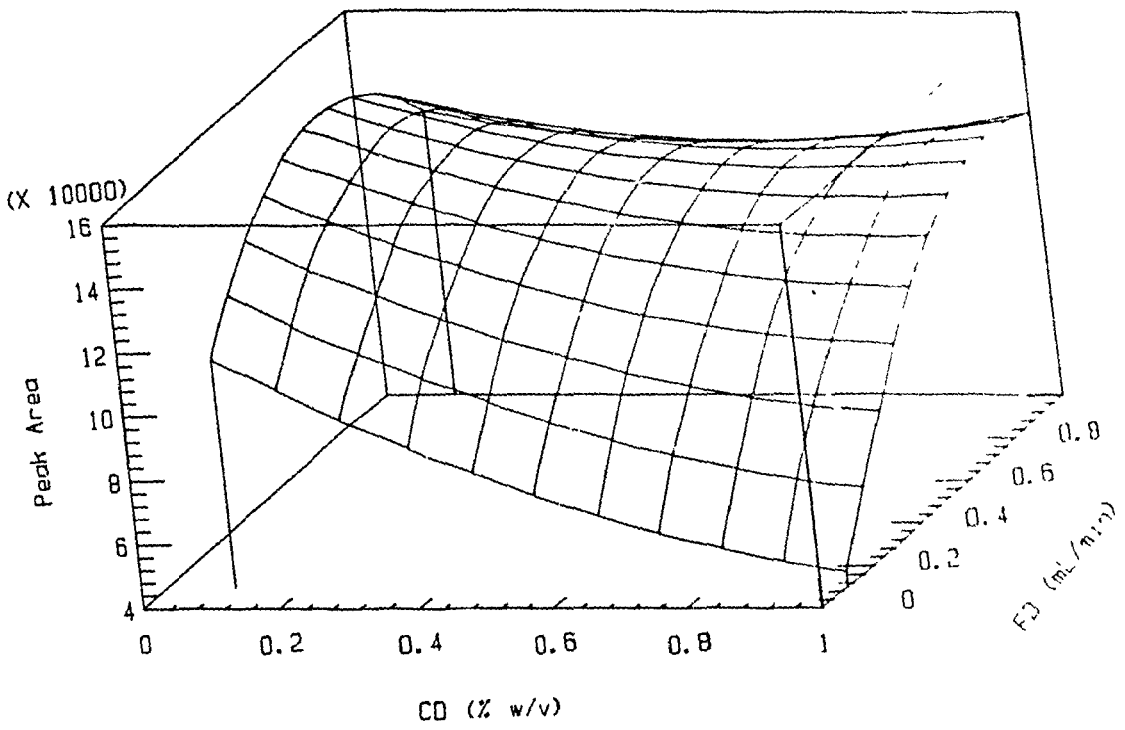

Plot of Peak Area vs H2 and CD

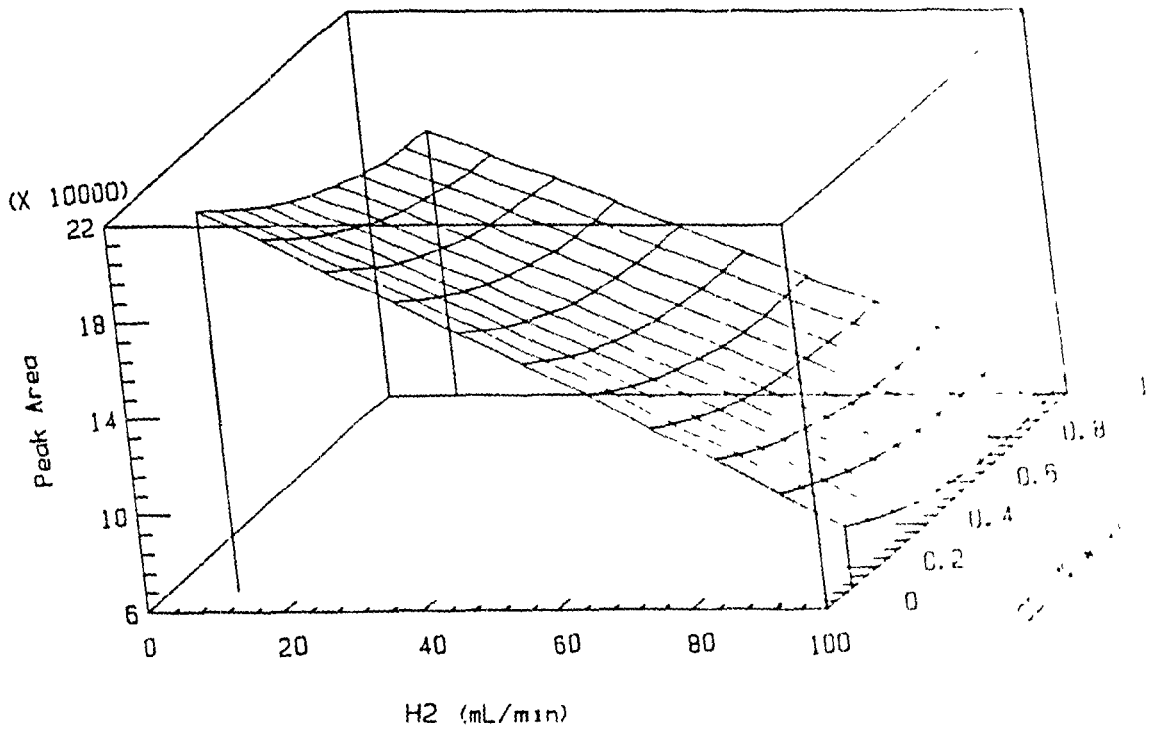

(which might have been predicted to be detrimental due to analyte dilution) can be explained by the low solubility of the tetraalkyllead derivatives in water, promoting an increased partition of these derivatives into the gaseous phase.

Hydrogen was circulated in the interface both as a carrier gas and as an active species to promote the silica-catalyzed lead atomization reaction in the electrothermal quartz furnace (Forsyth and Marshall, 1985). Hydrogen flow rates as low as 10 mL/min were sufficient to transport the analytes to the furnace, reflecting the efficiency of the gas-liquid separator. The inverse effect of hydrogen flow rate on analyte response may be explained in term of the reduced residence time of atomized lead within the optical tube of the quartz furnace. However, low hydrogen flow rates were not considered optimal since dissymetry and lower reproducibility of the AAS peak were observed.

The negative effect of increasing $NaBEt_4$ concentration was explained by a detrimental interaction between carbon (ethane from $NaBEt_4$ degradation) and one component of the atomization reaction (possibly the active quartz surface).

From this model (Appendix 2), the optimum values of the five variables studied were considered to be: Hydrogen flow rate, 50 mL/min; $NaBEt_{4(aq)}$ flow rate and concentration, 1 mL/min and 0.1 % w/v, respectively; reaction coil and quartz furnace temperature, 70 ^{o}C and 1000 ^{o}C respectively.

3.3.5 Calibration and Reproducibility

The response, linearity and the limits of detection of the species were determined by injecting serial dilutions of a standard solution in the chromatographic system. The resulting calibration curves and related regression statistics are presented in Appendix 2. The analyte responses varied linearly ($0.9981 < r < 0.9991$) with the mass of analyte injected in the range studied (0.5 - 5 ng). The limits of detection (LOD) of these compounds were determined using a model based on first order error propagation with background noise normally distributed (Appendix 1). The resulting LOD's were as follows: Me_3PbCl = 0.12 ng; Et_3PbCl = 0.15 ng; Me_2PbCl_2 = 0.10 ng; Et_2PbCl_2 = 0.13 ng. The longer-term reproducibility of the system was studied by analyzing periodically the standard (10 x LOD) for 10 hours. The HPLC-AAS system was highly reproducible as shown by the relative standard deviations (n = 10) calculated for each species: Me_3PbCl = 4.4 %; Et_3PbCl = 3.9 %; Me_2PbCl_2 = 4.3 %; Et_2PbCl_2 = 5.2 %. The short term reproducibility of the instrument was assessed after three consecutive injections of standards at levels of 1, 3, 10 and 50 times their limits of detection (Table 3), with results approaching the long term reproducibility values.

Chromatograms recorded during the calibration study are presented in figure 17. Injecting more than 3 ng of the analytes in the optimised instrument resulted in appreciable peak tailing, causing Et_3Pb^+ and Me_2Pb^{2+} peaks to overlap and decreasing the reproducibility and precision of the analysis (Figure 17, A). This situation caused a significant decrease in the regression correlation coefficient (Appendix 2) relative to those observed using a flame thermospray-microatomizer interface (Appendix 1). Thus, removing the 5 ng points from the regression resulted in correlation coefficients higher than 0.9992. Peak tailing at higher analyte

Table 3. Reproducibility of the HPLC-AAS at Varying Analytes Levels.

Amount (ng)	Me_3Pb^+ r.s.d.(%)[a]	Et_3Pb^+ r.s.d.(%)	Me_2Pb^{2+} r.s.d.(%)	Et_2Pb^{2+} r.s.d.(%)
0.1	6.3	10.7	8.8	9.4
0.3	1.6	5.2	6.8	5.9
1.0	0.6	5.3	5.7	3.0
5.0	5.6	8.1	5.5	4.1

[a] r.s.d. = relative standard deviation based on triplicate analyses.

Figure 17. HPLC-AAS chromatograms of (a) Me_3Pb^+; (b) Et_3Pb^+; (c) Me_2Pb^{2+} and (d) Et_2Pb^{2+} (injected from methanol) obtained using a Nucleosil C_{18} column eluted with methanol containing 600 µg/mL of PDTC and 25 % water. Chromatograms represents (A) 5 ng; (B) 1 ng; (C) 0.5 ng and (D) 0.3 ng of standards.

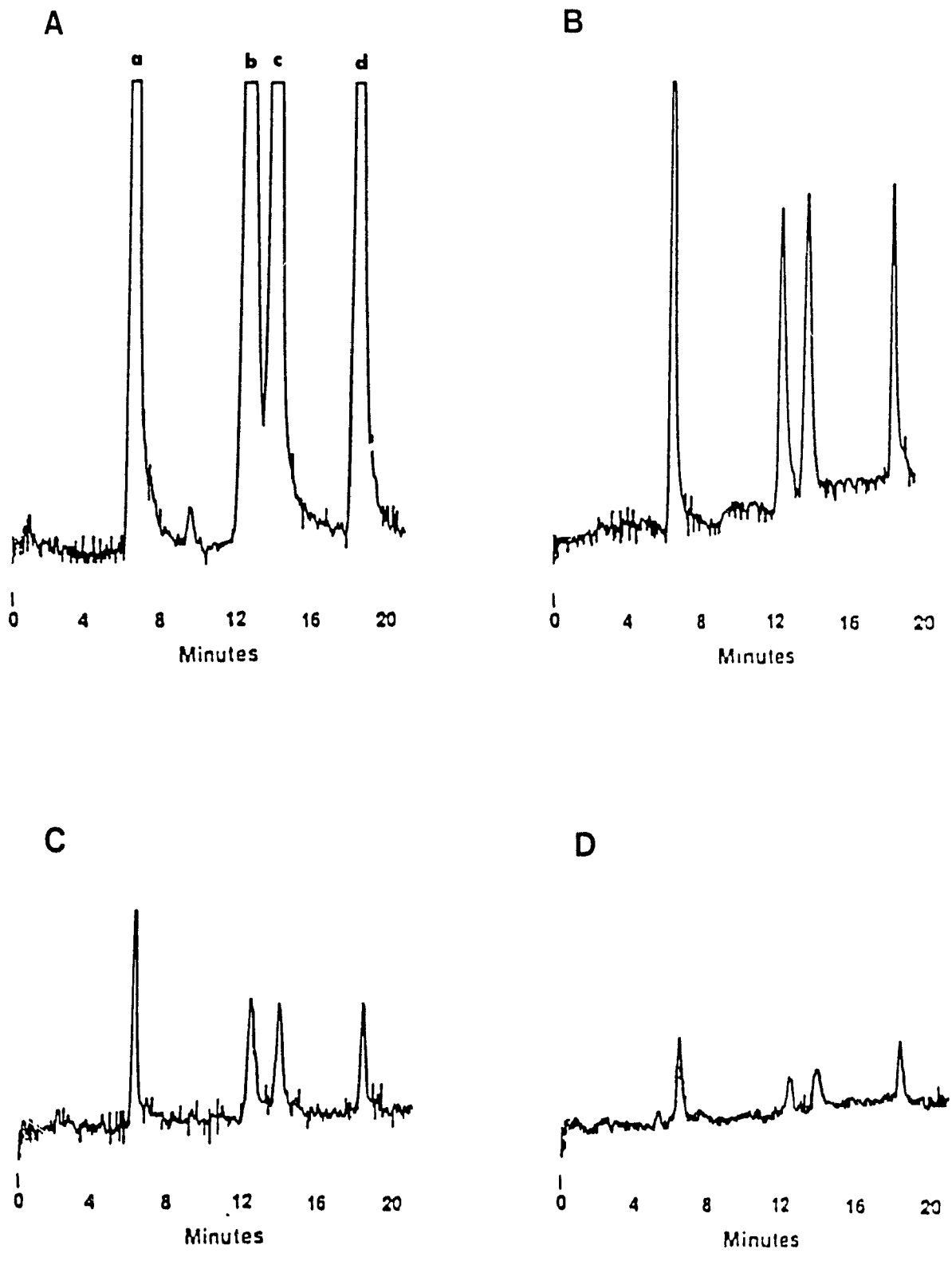
A
a
b
c
d
0
4
8
12
16
20
Minutes
B
0
4
8
12
16
20
Minutes
C
0
4
8
12
16
20
Minutes
D
0
4
8
12
16
20
Minutes

concentration (3-10 ng) reflected a saturation of the interface at lower hydrogen flow rate (50 mL/min) and was not observed if this flow rate was doubled.

As described in section 3.3.1, inorganic lead was not efficiently volatilized by $NaBEt_4$ and its limit of detection was estimated to be 100 ng (Figure 18, A). This characteristic is desirable since some environmental samples contain appreciable amounts of Pb^{2+}. High levels of inorganic lead in samples have been a persistent problem if the ionic alkyllead species were to be analyzed by gas chromatography-QTAAS (formation of actifacts during the Grignard derivatization step; Blais and Marshall, 1986). As shown in Figure 18-B the HPLC column efficiently separated the 7 mixed ionic alkylleads which may be present in environmental samples.

3.3.6 Conclusion

The ethylate generator interface decreased the LOD of ionic alkylleads 10 fold relative to a thermospray-microatomizer interface (Section 2), with a practical analyte concentration range (at optimum H_2 flow rate) of 0.1 to 3 ng. This interface was highly selective toward ionic alkylleads by a factor of at least 1000 (relative to inorganic lead) and consequently is compatible with highly lead polluted samples, especially if a selective complexometric extraction procedure (PDTC-hexane) is used (Blais and Marshall, 1986). In this case, however, an automated solvent front oxidation cycle (circulating air in the furnace for 2 min after injection) would be required since hexane is also volatilized from the interface, and would otherwise cause carbon deposition in the quartz furnace (Forsyth and Marshall, 1985). Although more expensive than a mercury column, the adoption of a precise back-pressure regulator to the GLS liquid outlet would simplify the operation of the HPLC-AAS system.

Figure 18. HPLC-AAS chromatograms of (A) 1 ng each of (a) Me_3Pb^+; (c) Et_3Pb^+; (d) Me_2Pb^{2+}; (e) Et_2Pb^{2+}; [(b) 100 ng of Pb^{2+}] and (B), synthetic ionic alkyllead mixture containing (a) Me_3Pb^+; (b) $EtMe_2Pb^+$; (c) Et_2MePb^+; (d) Et_3Pb^+; (e) Me_2Pb^{2+}; (f) $EtMePb^{2+}$ and (g) Et_2Pb^{2+}.

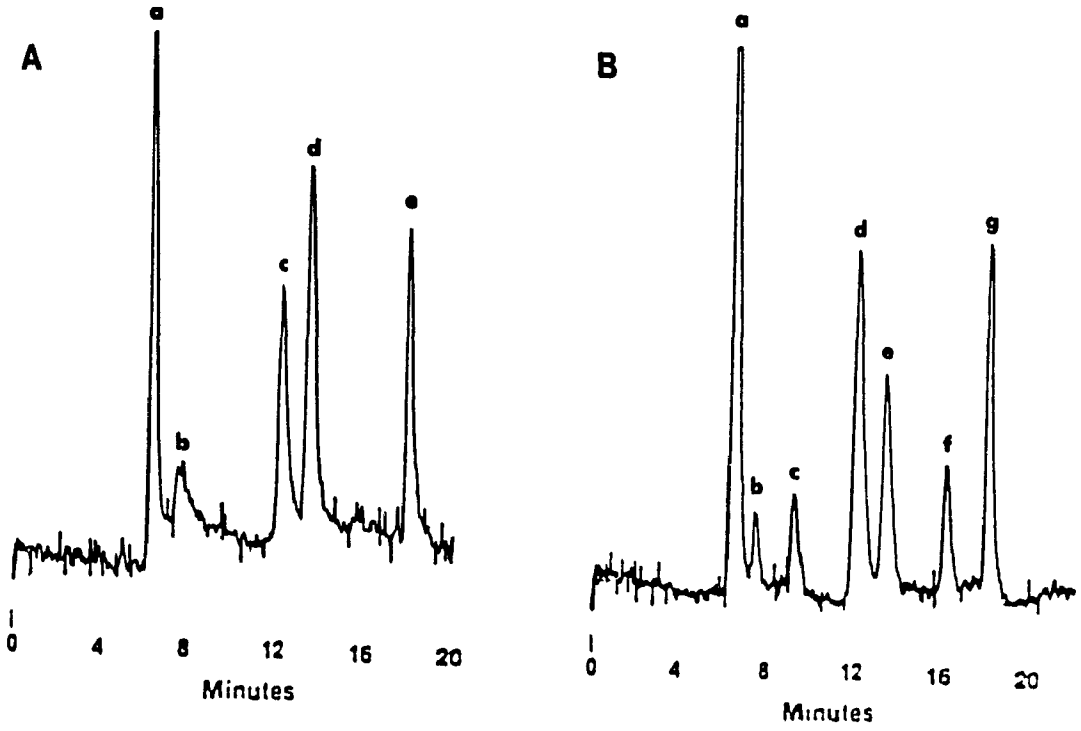
A
a
b
c
d
e
0
4
8
12
16
20
Minutes
B
a
b
c
d
e
f
g
0
4
8
12
16
20
Minutes

Since final extracts can be concentrated to a final volume of 0.1 mL without appreciable analyte losses (Section 2), the practical limit of detection for the ionic alkyllead compounds was ca. 20 parts per trillion from 5 g samples, which was in the LOD range of GC-QTAAS instrumentations. With the capacity of speciating directly seven ionic alkyllead species (Figure 18, B) at sub-ng levels, without artifact prone chemical derivatization, this HPLC-ethylate generator-AAS instrument appears to be a suitable alternative to GC-QTAAS techniques for the analysis of alkylleads and possibly mercury or tin compounds.

---

4. Determination of Arsonium and Selenonium Compounds by HPLC-Thermochemical Hydride Generation-Atomic Absorption Spectrometry

4.1 Synopsis

It has been reported that for hydride forming elements the quartz electrothermal (Godden and Thomerson, 1980) and diffused (Siemer et al., 1976) flame atomization cells are several orders of magnitude more efficient than the kinetic flame. In addition to the high atomization efficiency of these devices, the absence of a kinetic flame in the optical path maximizes their signal-to-noise ratio at low atomic absorption wavelengths. However, these atomizers can not handle high flows of liquids so that the analytes have to be introduced in the gas phase, either as hydride species or alkylated organometallic derivatives. Thus, this approach has been applied to almost every physico-chemical forms of elements which form stable hydrides in the presence of reducing agents (zinc, sodium borohydride) in acidic media. However, several naturally occurring organometalloid compounds are relatively inert and are not predicted to react rapidly with reducing agents. Included are those compounds in which the metalloid occurs in its lowest oxidation state, such as arsonium [As(-III)] and selenonium species, seleno-amino acids and selenonucleosides [Se(-II)].

It was anticipated that the thermospray-microatomizer interface described earlier (Section 2) could also be used for organoselenium and organoarsenic species. There were however strong limitations to this supposition, the most important one being the fact that the most sensitive resonance lines for selenium (196.0 nm) and arsenic (193.7 nm) occur at lower UV wavelength range than the AAS resonance lines of lead (217.0 or 283.3 nm). At these lower wavelengths, the analytical flame emits an intense background signal which would decrease the

signal-to-noise ratio and consequently the limit of detection of these analytes. This problem was verified and the thermospray-microatomizer approach was rapidly abandoned for arsonium and selenonium compounds.

A novel HPLC-AAS interface based on thermospray nebulization, pyrolysis of the analytes in a methanol/oxygen flame, thermochemical hydride generation using excess hydrogen and cool diffused flame atomization has therefore been developed and optimized. The low cost of this quartz interface coupled with its relatively high sensitivity makes it a potential candidate for routine analyses of several organometallic forms of Se and As. Optimum analytical conditions for arsonium compounds [$(CH_3)_3RAs^+$ X^-; R = CH_3, CH_2CH_2OH, CH_2COOH] which have been recently detected in a variety of marine organism (Kurosawa et al., 1980; Cannon et al., 1981; Shiomi et al., 1984; Franscesconi et al., 1985; Lawrence et al., 1986, Beauchemin et al., 1988) and selenonium compounds [$(CH_3)_2Se^+$ X^- ; R = CH_3, CH_2CH_2OH] which are potential selenium metabolites in mammals (Byard, 1969; Palmer et al., 1970; Nahapetian et al., 1984; Sun et al., 1987) are presented.

4.2 Materials and Methods

4.2.1 Thermochemical Hydride Generator

Diagrams of the thermochemical hydride generator (THG) main body and of the complete assembly are presented in Figure 19-A and 19-B, respectively. The all-quartz (LaSalle Scientific Inc. Guelph, Ont.) main body (Figure 19-A) consisted of an optical tube (a, 9 mm i.d. x 11 mm o.d. x 12 cm) which was positioned in the AAS optical beam, an analytical flame tube (b, 4 mm i.d. x 6 mm o.d. x 8 cm); a combustion chamber (c, 7 mm i.d. x 9 mm o.d. x 4 cm); a thermospray tube (d, 4 mm i.d. x 6 mm o.d. x 7 cm); and oxygen/hydrogen inlets (e,f, 2 mm i.d. x 3.2 mm o.d. x 5 cm).

Figure 19. Thermochemical hydride generator: (19-A) quartz main body comprising (a) optical tube; (b) analytical flame tube; (c) combustion chamber; (d) thermospray tube and (e,f) gas inlets. The complete assembly (19-B) comprised (A) a silica transfer line; (B) a quartz insert supporting the transfer line; (C) a thermoelectric element; (D) modified Swagelok fittings and (E) analytical oxygen inlet (quartz insert).

A

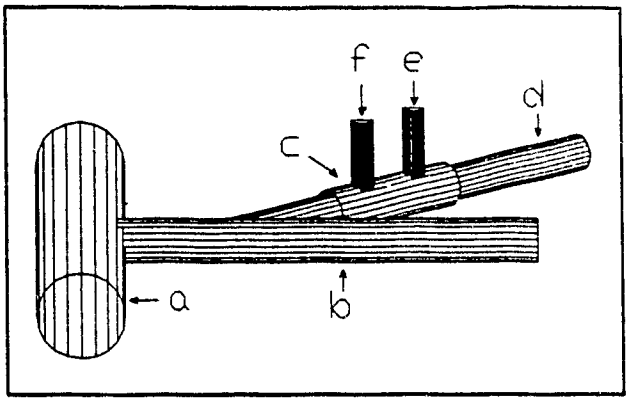

B

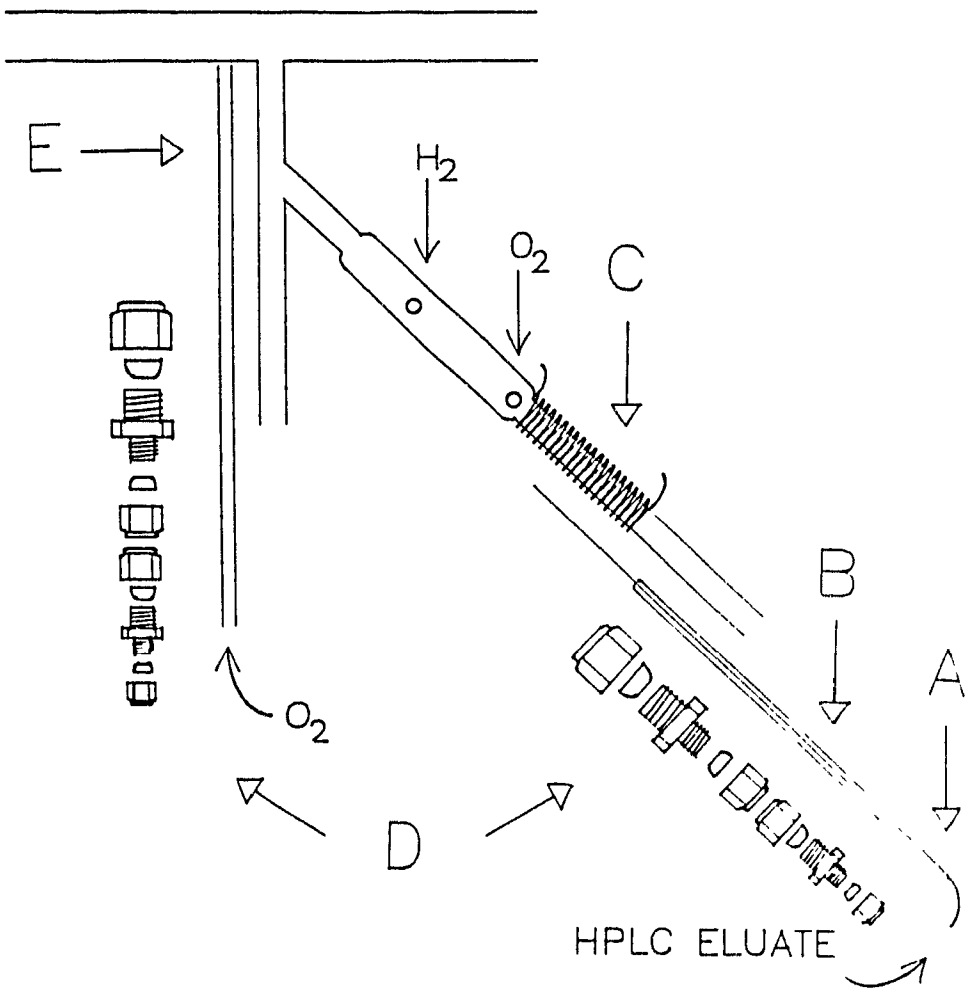

The oxygen and hydrogen inlets were spaced by 2.5 cm apart. The combustion chamber-thermospray tube assembly met the analytical flame tube at an angle of 45^{o}. All joints were glass-blown. The complete assembly (Figure 19-B) was composed of the main body, a capillary transfer line which was connected to the HPLC column outlet (A, 50 u i.d. x 20 cm deactivated silica tube, Chromatographic Specialties, Brockville, Ont.); a quartz guide tube (B, 2 mm i.d. x 3.2 mm o.d. x 10 cm, with outlet bore constricted to 1 mm by glass blowing) which served to center the capillary (A); a coil of resistance wire (C, 40 cm of 22 gauge Chromel 875 alloy, Hoskins Alloys, Toronto, Ont.) which was insulated with refractive wool (Fiberfrax, The Carborundum Co., Niagara Falls, N.Y.) and surrounded by a shaped firebrick casing held in place by a screw-clip. Two stainless steel Swagelok assemblies (D, Forsyth and Marshall, 1985) were modified to support the guide tube (B) and the analytical oxygen inlet (E; quartz tube, 2 mm i.d. x 3.2 mm o.d. x 15 cm). The guide tube B was positioned in the thermospray tube 1 cm upstream from the heating element. The tip of the analytical oxygen inlet (E) was fixed 0.5 cm from the optical tube intersection to maintain the analytical flame slightly removed from the AAS beam. Thermospray oxygen and hydrogen were channeled from flowmeters (Matheson, Toronto, Ont.) using Teflon tubing (2.48 mm i.d. x 4 mm o.d., Cole-Parmer Co., Chigaco, Ill.) which were heat fitted to the quartz tube gas inlets using a bunsen burner. Contraction of the Teflon tube upon cooling formed a tight seal. The analytical oxygen was introduced in the tube E through the modified Swagelok assembly. The optical tube was mounted in an aluminum casing as described elsewhere (Forsyth and Marshall, 1985) and secured by firebrick disks and refractive wool at both extremes, leaving most of the tube surface exposed. Both Swagelok assemblies were also supported. The heating element was powered by a AC variable transformer and current, as monitored with a standard ammeter was varied between 5 and 6 amperes (2 amps on standby).

A smooth ignition of the THG was obtained with the following sequence: (a) thermospray oxygen (OT) flow rate was adjusted to 500 mL/min; (b) heating element current was increased to 6 amperes; (c) after 1-2 min, (thermospray tube outer skin temperature 900-1000^{o}C), the capillary was introduced half way into the hot region; (d) the HPLC pump flow rate (100 % methanol) was rapidly adjusted to 0.5 mL/min (note; at lower heating element temperature, an accumulation of methanol in the interface due to an unsuccessful thermospray ignition may result in an explosive ignition); (e) the hydrogen flow rate was adjusted to 1 L/min; (f) excess hydrogen was ignited at both ends of the optical tube, using a bunsen burner; (g) the analytical oxygen (OA) flow rate was to 240 mL/min or more until ignition of the analytical flame; (h) the hydrogen flow rate was subsequently decreased until flameout of optical tube ends (the analytical flame should remain ignited); (i) the capillary depth, HPLC flow rate and OT flow rate were then adjusted to obtain a stable thermospray effect; (j) the hydrogen and OA flow rates were adjusted to optimal values. Instrument shut-down was performed smoothly by following the reversed procedure.

4.2.2 Optimization

The interface was optimized using a factorial design (half-replicate 2^5 composite design) as described previously (Appendix 2). The five variables studied were thermospray oxygen (OT) flow rate (500-800 mL/min), hydrogen flow rate (1.00-2.40 L/min), analytical oxygen (OA) flow rate (100-240 mL/min), HPLC mobile phase flow rate (0.30-1.00 mL/min) and % (v/v) diethyl ether or % (v/v) water in the methanolic mobile phase which contained also 1 % (v/v) glacial acetic acid and 0.05 % (v/v) triethylamine. These ranges were determined by preliminary experiments, searching for a maximum response. The integrations of the atomic absorption signal

for trimethylselenonium iodide or tetramethylarsonium iodide (20 µl of a 100 µg/mL methanolic solution) were recorded in triplicate for each of the 27 experimental points. For these experiments the HPLC column was replaced with a wide bore stainless steel tubing (1 mm i.d. x 20 cm) to allow proper mixing of the analytes solution with the mobile phase and to obtain a 15-30 sec. time delay between injection and response. The AAS response to equimolar amounts of different As (tetramethylarsonium iodide vs dimethylarsinic acid vs arsenic pentoxide) and Se (trimethylselenonium iodide vs selenomethionine vs selenium dioxide vs sodium selenate) standards were also recorded under these conditions. The possible interference of other organometallic cations (trimethylsulfonium iodide and trimethyllead chloride) was evaluated by co-injection at 1 and 10 fold molar excess of interferent relative to the analyte $(CH_3)_3SeI$ or $(CH_3)_4AsI$).

4.2.3 Trapping Apparatus

A diagram of the trapping apparatus is presented in Figure 20. The quartz main body of this thermochemical hydride generator was similar to the assembly presented in figure 19 except that the combustion chamber and the outlet quartz tube were smaller (4 mm i.d. x 6 mm o.d. tube and 2 mm i.d. x 4 mm o.d. x 45 cm, respectively); a third inlet was added (2.5 cm downstream from the hydrogen inlet) to permit the introduction of 1 M HCl, which was delivered by a peristaltic pump (Eyela, Model MP-3). The outlet of the modified THG train was inserted into a custom made water cooled condenser [Figure 20, E; 1.27 cm o.d x 37 cm copper tube equipped with water inlet and outlet and sealed with brass Swagelok unions (J, 1.27 cm x 0.64 cm)]. A Teflon tube (F, 2.48 mm i.d. x 4 mm o.d. x 50 cm) was connected to the quartz transfer line and the other end was connected to a 250 mL Erlenmeyer filtering flask (trap # 1) which contained 190 µmol of 2,3-naphthalenediamine in 150 mL of 1 M HCl.

Figure 20. Trapping apparatus: (A) silica transfer line; (B) quartz insert; (C) thermoelectric element; (D,J) modified Swagelok fittings; (E) vapour condenser; (F,I) Teflon tubes; (G,H) Erlenmeyer flasks containing trapping solutions.

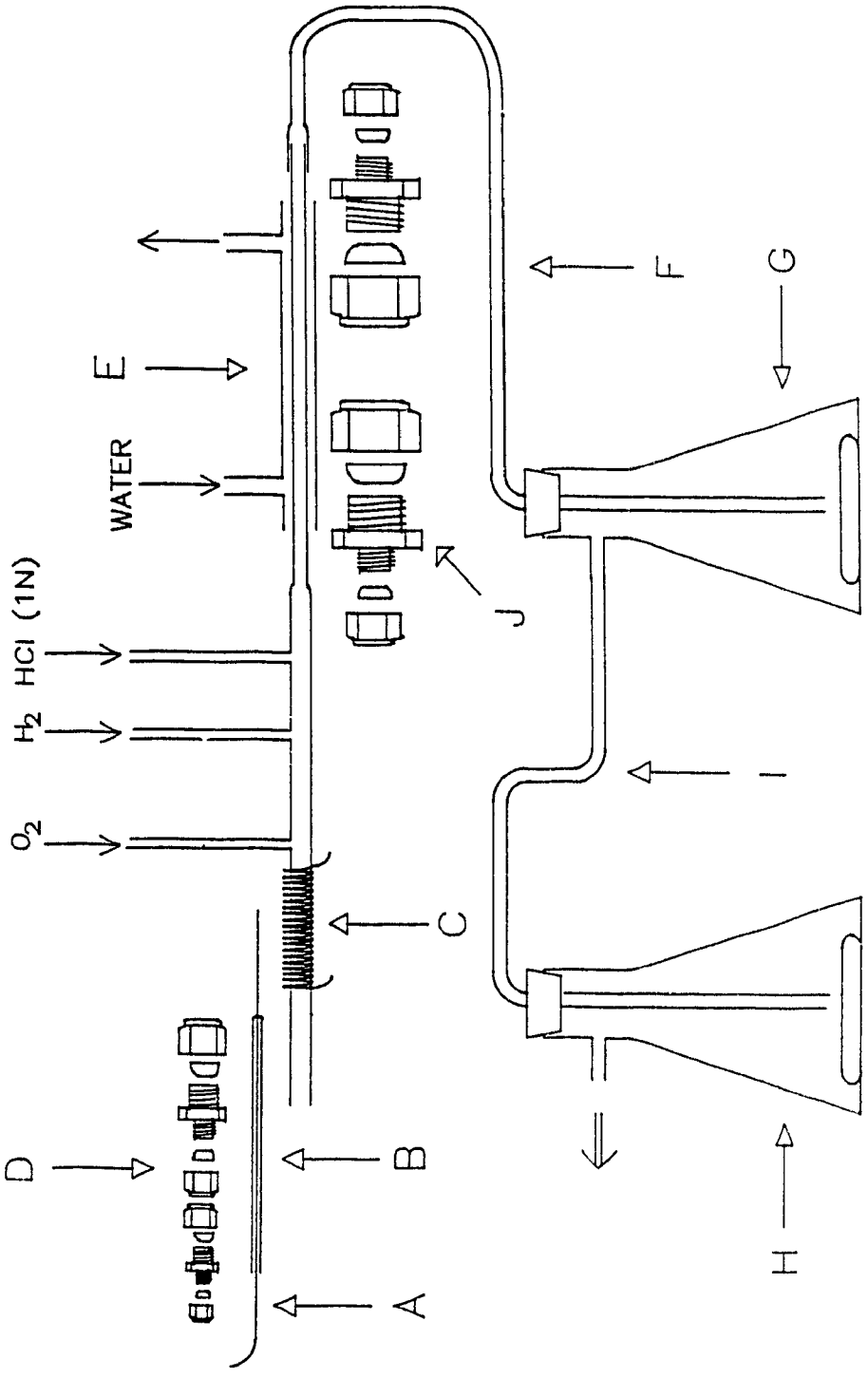
A
B
C
D
E
F
G
H
I
J
WATER
HCl (1N)
H_2
O_2

The gases emerging from trap #1 were channeled via a Teflon tube (I) into a second trap (trap #2) filled with 150 mL of 7:3 DMF:water containing 18 mmol of $NaHCO_3$ and 500 umol of 1-fluoro 2,4-dinitrobenzene (DNFB). Both trapping solutions were magnetically stirred. The experiments were carried out by injecting twenty 0.2 mL volumes of trimethylselenonium iodide (0.537 µmol/mL in methanol) and selenium oxide (0.955 µmol/mL) into the system via a HPLC injection valve, under the following conditions: methanol flow rate 0.5 mL/min; heating element current 6 amps; oxygen flow rate 600 mL/min, hydrogen flow rate 1.7 L/min; 1 M HCl flow rate 2 mL/min.

At the termination of the experiment the trapping solution # 1 was stirred for 30 min and extracted three times with 50 mL benzene. The organic phases were combined, washed with 3 x 50 mL of 1 M HCl, dried with generous amounts of Na_2SO_4, filtered through Whatman # 1 filter paper, and then evaporated to dryness under vacuum. The residue was diluted to 1 mL with methanol.

Excess DNFB in the trapping solution # 2 was reacted at room temperature with 1 mmol of glycine for 2 hours and diluted to 400 mL with $NaOH_{(aq)}$ (pH 12.00). The solution was extracted with three successive 50 mL aliquots of benzene, which were combined and washed with three 100 mL portions of dilute NaOH. The resulting benzene extract was treated as described for solution # 1. The final extracts were analyzed (20 µl injections) by HPLC-THG-AAS.

4.2.4 Instruments

The instrumentation used for this study comprised an HPLC system (Beckman Model 100 A), an autosampler (LKB, model 2157) and an atomic absorption spectrometer (Phillips, PU9100) which was equipped with high energy

AAS lamps (Photron super lamps system, Australia) and a deuterium background correction system. The optimization experiments (without chromatography) were performed with deuterium background correction. Because background correction almost tripled the electronic background signal of the AAS detector, the chromatographic calibrations were performed without deuterium background correction. Narrow-bore stainless-steel tubing (0.007 cm i.d.) was used post-injector. The 50 u i.d. silica transfer line was connected to HPLC tubing through a capillary reducing union (Chromatographic Specialties, Brockville Ont.).

4.2.5 Reagents and Standards

All solvents used were "distilled in glass" grade or better (Caledon Inc., Georgetown, Ont.). Certified ACS reagent grade hydrochloric and acetic acid were used. Triethylamine was purified Gold Label grade (Aldrich Chemical Co., Milwaukee, Wis.). Other chemicals were reagent grade or better (Aldrich Chemical Co., Milwaukee, Wis.). Water was double-distilled and deionized. The synthesis, purification and characterization of tetramethylarsonium iodide (TMAs), arsenobetaine iodide (AsBet), arsenocholine iodide (AsChol), trimethylselenonium iodide (TMSe) and selenocholine tetraphenylborate (SeChol) standards have been described elsewhere (Huyghes-Despointes, 1990; Momplaisir, 1990). Naphthylpiazselenole and bis-2,4-dinitrophenyl selenide were prepared and purified as described previously (Bayfield and Romalis, 1985; Ganther and Kraus, 1984). The purity of the standards was assessed by mass spectrometry. Stock solutions (TMAs 1.08×10^{-4} g/mL; AsBet 1.00×10^{-4} g/mL; AsChol 1.12×10^{-4} g/mL; TMSe 1.01×10^{-4} g/mL; SeChol 2.06×10^{-4} g/mL) of these standards were prepared in methanol and kept at -40 ^{o}C. The addition of 10% (v/v) acetone was necessary to dissolve the selenocholine tetraphenylborate. Dilution of these standards in methanol or methanol containing 1% (v/v) acetic acid and 0.05% (v/v) triethylamine provided the working standards.

4.2.6 HPLC Conditions

Naphthylpiazselenole and bis-2,4-dinitrophenyl selenide were separated on a Nucleosil C_{18} column (0.46 cm x 15 cm, 3 µ diameter particles, CSC Inc. Montreal, Qc) using 100 % methanol as mobile phase (0.5 mL/min).

Arsonium and selenonium standards were separated on a cyano-propyl bonded phase (5 µ diameter silica support, 0.46 mm i.d. x 15 cm, LC-CN, Supelco Inc., Bellefonte, PA). Arsonium compounds were eluted using methanol containing 30% (v/v) diethyl ether, whereas selenonium analytes were separated with 100% methanol (0.65 mL/min). In both methods, a silanol masking agent combination consisting of 0.05 % triethylamine and 1 % acetic acid was added in the mobile phase. The injection volume in all cases was 100 µL.

A number of other chromatographic approaches (ion pairing, reversed-phase, cation exchange) were tested. Ion pairing agents tested included methanesulphonic acid, ethanesulphonic acid, toluenesulphonic acid (Aldrich Chemical, Milwaukee, Wis.) and ammonium tetraphenylborate, which was synthesized by precipitation of aqueous sodium tetraphenylborate with ammonium acetate. The crude product was purified by reprecipitation from methanol by water. Stationary phases tested included Bondapak C_{18} (0.21 cm i.d. x 30 cm, 10 u particle size, Waters Chromato. Div., Milford, MA), Nucleosil C_{18} (0.46 cm i.d. x 15 cm, 5 µ particle size, CSC Ltd, Montreal, Qc), and a weak cation exchanger, (ICW, 0.32 cm i.d. x 5 cm, BDH Inc. Montreal, Qc).

4.3 Results and Discussion

4.3.1 Preliminary Approach to Post-HPLC Hydride Generation

The prototype thermochemical hydride generation HPLC-AAS interface was developed as an analytical tool for studying the fate of biogenic selenonium and arsonium compounds. Although HPLC-ICP (Kurosawa et al., 1980; Franscesconi et al., 1985; Low et al., 1986; Shiomi et al., 1987), HPLC-ICP-MS (Beauchemin et al., 1988) or HPLC-graphite furnace-AAS (Stockton and Irgolic, 1979; Lawrence et al., 1986) instruments are very suitable for the analysis of these species, their high purchase price and operating costs make it difficult to justify their dedicated use for a specific procedure. Yet biological studies often require a continual access to those procedures. The criteria to be fulfilled by the projected HPLC-hydride generation AAS were similar to those of routine analytical instruments; high sensitivity and specificity, low operating cost and, if possible, a high degree of automation.

Several of the recent reports on coupled LC-FAAS have stressed simple interface systems and increased sensitivity by paying attention to the atom cell (Ebdon et al., 1987). One relatively efficient interface developed to analyze alkyllead by HPLC-AAS was a miniaturized flame atomizer which used the HPLC organic mobile phase as fuel and oxygen as oxidant (Section 2, Blais and Marshall, 1989). The HPLC eluate was vaporized by thermospray effect via a 50 u i.d. silica capillary which was inserted in an electrothermally heated quartz tube, and ignited in the presence of oxygen. The resulting analytical flame had a estimated temperature of 1400-1600^{o}C, which provided enough energy to atomize the organolead analytes efficiently, with limits of detection approaching 1 ng.

This approach was abandoned for Se, and As since their lower atomic absorption wavelengths were in the spectral range of strong emissions and/or absorption from the kinetic flame components, decreasing appreciably the signal to noise ratio of the AAS detector. Deuterium lamp background correction was ineffective in this case. However, the coupling of a Zeeman effect background correction system with this simple atomizer may represent a successful compromise.

On-line hydride generation (Burns et al., 1981; Tye et al., 1985) was not investigated since arsonium and selenonium compounds do not react readily with reducing agents and acids. On-line pyrolytic degradation of the analytes to produce hydride forming inorganic species using a thermospray microatomizer followed by condensation and chemical hydride generation was a successful preliminary approach. This apparatus was essentially similar to the assembly presented in Figure 20, in which the condensed post-thermospray solution was mixed with 1 mL/min of 1% aqueous $NaBH_4$. The resulting stream was channeled to a gas-liquid separator (Burns et al., 1981) and the vapors were introduced in a cool diffused flame quartz atomizer (CDFA) (Siemer et al., 1976; Dedina and Rubeska, 1980). Although it provided a relatively high sensitivity this apparatus was characterized by signal pulses which decreased its reproducibility. The present gas phase thermochemical hydride generator-CDFA interface provided both promising sensitivities and a pulseless background signal.

4.3.2 Thermochemical Hydride Generation Mechanism

The thermochemical hydride generator (THG) interface presented in Figure 19 represented a direct coupling of three processes: (1) thermospray pyrolysis of the organometallic analytes to the metallic state (Section 2); (2) a postulated thermochemical hydride derivatization to the hydride derivative with hydrogen radicals;

and (3) diffuse flame atomization. The latter technique has been reported to be the most efficient process for the AAS detection of metalloid hydrides (Siemer et al., 1976; Dedina and Rubeska, 1980). The diffused flame atomization process was highly compatible with the THG since massive hydrogen flow rates were required in both processes. The atomization of the analyte has been attributed to reaction with hydrogen free radicals:

$$SeH_2 + H^{\bullet} \longrightarrow HSe^{\bullet} + H_2 \qquad (1)$$

$$HSe^{\bullet} + H^{\bullet} \longrightarrow Se + H_2 \qquad (2)$$

which are generated in the reaction zone of the diffused flame:

$$H^{\bullet} + O_2 \longrightarrow OH^{\bullet} + O^{\bullet} \qquad (3)$$

$$O^{\bullet} + H_2 \longrightarrow OH^{\bullet} + H^{\bullet} \qquad (4)$$

$$OH^{\bullet} + H_2 \longrightarrow H_2O + H^{\bullet} \qquad (5)$$

These free radicals are formed in a spatially limited cloud which does not reach the AAS optical beam and consequently the background noise generated by the atomizer is negligible.

The thermochemical mechanism occuring in the interface was indicated by the fact that no AAS signal was observed in the absence of the analytical diffused flame, suggesting that the species emerging from the THG was molecular and volatile in nature. A confirmation of the thermochemical derivatization of

trimethylselenonium iodide and selenium dioxide to selenium hydride was obtained by chemical trapping experiments using the apparatus presented in Figure 20. The hot gases emerging from the THG were mixed with 1 M HCl, cooled in a condenser (E) and channeled into an acidic solution containing 2,3-diaminonaphthalene (G, trap #1) which would derivatize Se(IV) to naphthylpiazselenole (Bayfield and Romalis, 1985). The postulated hydrogen selenide which was carried through the acidic trap # 1 was channeled into an alkaline solution (H, trap #2) containing 1-fluoro 2,4-dinitrobenzene (FDNB). After the trapping experiments, excess FDNB was reacted with glycine, forming the base soluble 2,4-dinitroanilinoacetic acid (Bunnett and Hermann, 1970). The organo-soluble content of trap # 1 was extracted from the basic solution into benzene and the residue obtained after rotary-evaporation was dissolved in methanol. The postulated bis-2,4-dinitrophenyl selenide derivative (Ganther and Kraus, 1984) formed in trap #2 was extracted from the basic aqueous solution with benzene, concentrated to dryness and redissolved in methanol. These solutions where analyzed directly by HPLC-THG-AAS. Chromatograms of the derivative standards and of trapping solution products obtained after thermospray pyrolysis of $(CH_3)_3SeI$ and SeO_2 under reducing (H_2) or inert (He) post-thermospray atmospheres are presented in Figure 21. The quantitative results are recorded in Table 4.

As shown by these results both selenium dioxide and trimethylselenonium iodide were derivatized to hydrogen selenide only in the presence of hydrogen. As a result of the high gas flow rates occurring in the apparatus, the trapping of H_2Se was not considered quantitative.

Figure 21. HPLC-THG-AAS chromatograms of extracts of (1) trap #1 and (2) trap #2 from the pyrolysis-trapping experiments: (A) TMSeI pyrolyzed under H_2 atmosphere; (B) TMSeI pyrolyzed under He atmosphere; (C) SeO_2 pyrolysed under H_2 atmosphere; (D) SeO_2 pyrolysed under He atmosphere; (E) chromatogram of standards (3.9 min = $(NDP)_2Se$; 5.2 min = NPSe).

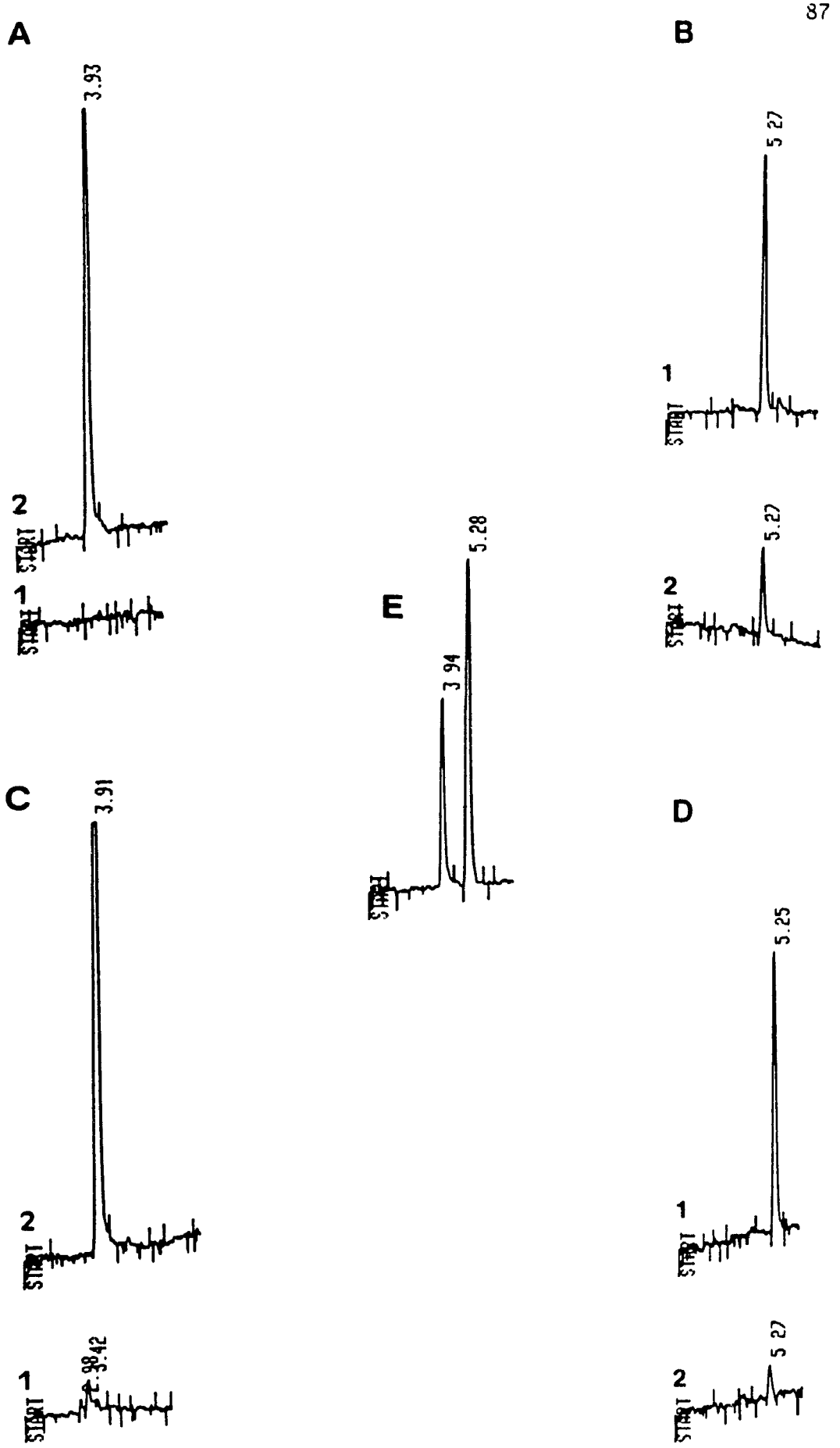
A
3.93
2
1
B
5 27
1
5.27
2
E
5.28
3 94
C
3.91
2
1
3.42
D
5.25
1
5 27
2

Table 4. Amounts and % recoveries of naphthylpiazselenole (NPSe) and bis-2,4-dinitrophenyl selenide [$(DNP)_2Se$] recovered in chemical traps during the pyrolysis of $(CH_3)_3SeI$ or SeO_2 in the presence of H_2 or He.

Analytes	Atmosphere	Trap #	Amt NPSe umol	% recov.	Amt $(DNP)_2Se$ umol	% rec
$(CH_3)_3SeI$[a]	H_2	1	nd[c]	---	nd	---
		2	nd	---	0.67	31.1
	He	1	0.36	16.6	nd	---
		2	0.20	9.3	nd	---
SeO_2[b]	H_2	1	nd	---	nd	---
		2	nd	---	1.13	29.5
	He	1	0.78	20.4	nd	---
		2	0.11	2.9	nd	---

[a] 2.15 umol of TMSe injected
[b] 3.82 umol of selenium dioxide injected
[c] nd = not detected

Under an inert post-thermospray atmosphere (He), a portion of injected selenium [Se(IV) or TMSeI] was found in trap #1 [Se(IV)], but an appreciable amount remained deposited in the condenser tube as metallic red selenium. In both cases a portion of the naphthylpiazselenole derivative was carried in trap # 2. These data corroborate the postulated thermochemical hydride generation mechanism which is most probably mediated by hydrogen radicals. It is known that metallic hydride forming elements can be derivatized to their hydrides by hydrogen radicals. The fact that no Se(IV) was detected in trap #1 under hydrogen atmosphere suggest a direct thermochemical derivatization of an oxidized species [Se(IV) in this case] to its hydride. One possible mechanism which may explain this phenomenon is initiated by hydrogen radicals:

$$H^{\cdot} + OSeO \quad <----> \quad OH^{\cdot} + SeO^{\cdot} \qquad (6)$$

$$SeO^{\cdot} + H_2 \quad <----> \quad HSe^{\cdot} + OH^{\cdot} \qquad (7)$$

$$HSe^{\cdot} + H_2 \quad <----> \quad H_2Se + H^{\cdot} \qquad (8)$$

Such a reaction sequence may occur in a hot spatially limited volume around the hydrogen inlet. In this suggested process, the final product (SeH_2) is rapidly stabilized on cooling by the massive hydrogen steam. The relevance of this hypothesis was corroborated by additional experiments with the THG-AAS interface. Replacing thermospray oxygen by nitrous oxide (producing a white flame exceeding 1665^{o}C) resulted in a complete loss of AAS signal at 500 x LOD, which may reflect a rapid degradation of the hydride at this higher post-thermospray temperature. Replacing thermospray O_2 by air decreased the AAS response by about 40 %. In this case a massive air flow rate (< 2 L/min) was necessary to maintain the thermospray flame and the lower response may be attributed to a lower residence time of the hydride in the analytical diffused flame.

Under optimum conditions for selenonium and arsonium compounds, the interface also provided vigorous responses for higher oxidation states of arsenic and for Se(IV). Relative responses observed for different representative organic and inorganic compounds of Se and As are presented in Table 5. The relatively efficient thermochemical hydride generation from As(V) contrasts with the difficult chemical derivatization of As(V) compounds to arsine (Siemer et al., 1976). Sodium selenate was poorly derivatized (18%) with the thermochemical procedure.

The relative AAS response of As (as tetramethyarsonium iodide) and Se (as trimethylselenonium iodide) co-injected with equimolar and 10 fold molar excess of the potential interferent, S (as trimethylsulfonium iodide) and Pb (as trimethyllead chloride) are presented in Table 6. Although the response of selenium remained relatively unaffected by the presence of As, the arsenic signal was decreased appreciably by the presence of a 10 fold excess of selenium. Since even the most selective extraction procedure is likely to co-extract arsonium and selenonium compounds it will be necessary to verify the relative proportion of these species in the final extract and, (in the remote probability of chromatographic co-elution), correct for this interference. As for the thermospray-microatomizer interface described earlier (Section 2), this THG device was not compatible with alkaline earth metals (degradation of quartz), halogenated solvents (halogen deposits), and high proportion of water (60-100%) in the HPLC mobile phase (thermospray disruption).

The limit of detection of selenonium and arsonium compounds (direct injection in interface) was estimated at 10 ng for As and 30 ng for Se, which justified the development of a an HPLC method which would be compatible with the interface.

Table 5. Relative AAS Responses of As and Se Compounds.

Compound	Relative Response (%)
Tetramethylarsonium iodide	100 ± 1.2[a]
Arsenobetaine iodide	98 ± 1.7
Arsenocholine iodide	103 ± 1.4
Dimethylarsinic acid	106 ± 0.8
Arsenic pentoxide	75 ± 2.4
Trimethylselenonium Iodide	100 ± 1.5
Selenocholine Tetraphenylboron	104 ± 3.3
Selenomethionine	99 ± 2.7
Selenium dioxide	101 ± 2.2
Sodium selenate	18 ± 1.2

[a] Standard deviation based on three replicate analyses

Table 6. Effect of Potential Inteferent on Response of TMA and TMSe.

Standard	Interferent	Rel. Amount (molar basis)	Response (%)
Tetramethylarsonium Iodide	-----		100 ± 1.8[a]
	Trimethylselenonium Iodide	1	88 ± 1.3
		10	52 ± 1.3
	Trimethylsulphonium Iodide	1	97 ± 4.0
		10	98 ± 2.5
	Trimethyllead Chloride	1	97 ± 1.3
		10	96 ± 9.0
Trimethylselenonium Iodide	-----		100 ± 2.1
	Tetramethylarsonium Iodide	1	100 ± 1.2
		10	96 ± 2.6
	Trimethylsulphonium Iodide	1	99 ± 0.5
		10	94 ± 2.0
	Trimethyllead Chloride	1	97 ± 1.6
		10	95 ± 0.8

[a] One standard deviation based on three replicate analyses

Table 7. Optimum Operating Parameters for As and Se Determination

Element	OT mL/min	H2 L/min	OA mL/min	FR mL/min	PE % (v/v)
Arsenic	700	2.05	205	0.65	30
Selenium	725	2.03	170	0.65	0

4.3.3 Optimization of the THG Interface

The interface operating parameters were optimized using a multivariate approach based on a half-replicate 2^5 composite design (Box and Wilson, 1951; Hill and Hunter, 1966). These experiments were carried-out by recording the response of $(CH_3)_3SeI$ and $(CH_3)_4AsI$ under different flow rates of thermospray oxygen (OT), hydrogen (H2), analytical oxygen (OA) and HPLC mobile phase (FR). A fifth variable was introduced in the model to mimic typical normal- and reversed-phase HPLC eluents [0-40% (v/v) diethyl-ether (PE) or 0-40% (v/v) water (PW) in a methanolic mobile phase].

Details of the statistical analyses, resulting quadratic models and exploratory response surface plots are presented in Appendix 3. Although variations between observed and predicted responses were generally lower than 15 %, lack-of-fit tests were statistically significant ($p < 0.05$) for the four models. This was attributed to outlier predictions which occurred at extreme parameter values and resulted from unmodeled variations in the performance of the interface. A rapid accumulation of carbon deposits (which was removed by increasing OA flow rate temporarily) was observed in the optical tube at 30-40 % ether and 500 mL/min OT. Similarly, unmodeled variations may have occurred as the capillary depth was readjusted to obtain a stable thermospray at 40% water and 500 mL/min OT.

Predicted vs observed data regressions for each model (Appendix 3) were well correlated ($0.8699 < r < 0.9886$; $0.9826 <$ slope < 1.0200). However, the significant lack-of fit calculated for each model resulted in meaningless F-tests for variables effects. Although non-ideal, the accuracy of the model was considered sufficient to estimate the effect of individual variables and to determine optimum parameters

Figure 22-A. Predicted response surfaces (Peak Area vs H_2 flow rate and Thermospray O_2 flow rate) for TMAsI at different analytical oxygen flow rates; (A) OA = 100 mL/min; (B) OA = 170 mL/min and (C) OA = 240 mL/min. The two remaining chromatographic variables were constant, (FR = 0.65 mL/min and PE = 30 %). The functions describing these surfaces are presented in Table A-8.

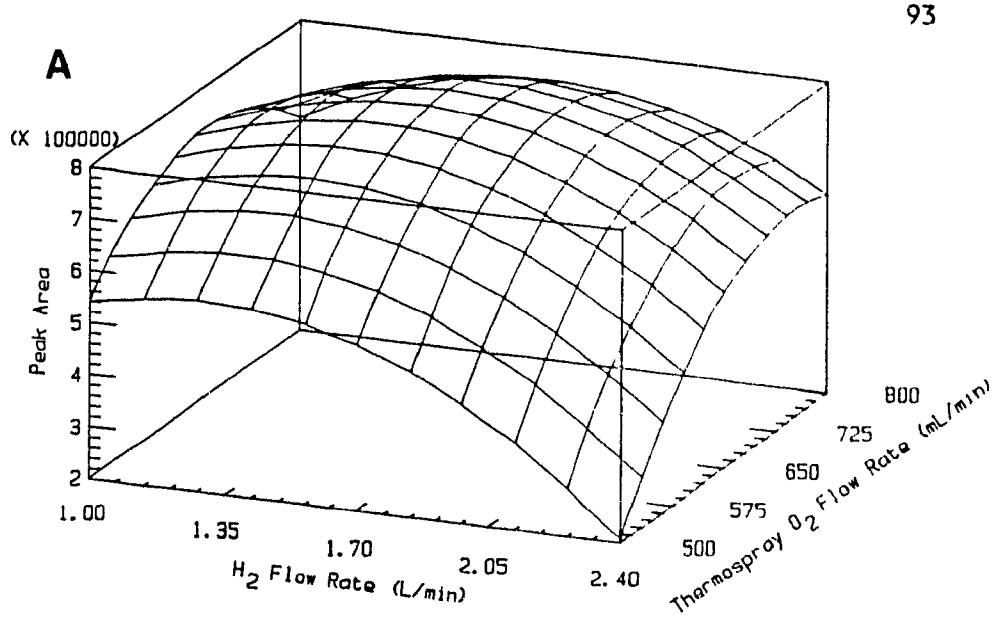
A
(X 100000)
8
7
6
5
4
3
2
Peak Area
1.00
1.35
1.70
2.05
2.40
H2 Flow Rate (L/min)
500
575
650
725
800
Thermospray O2 Flow Rate (mL/min)

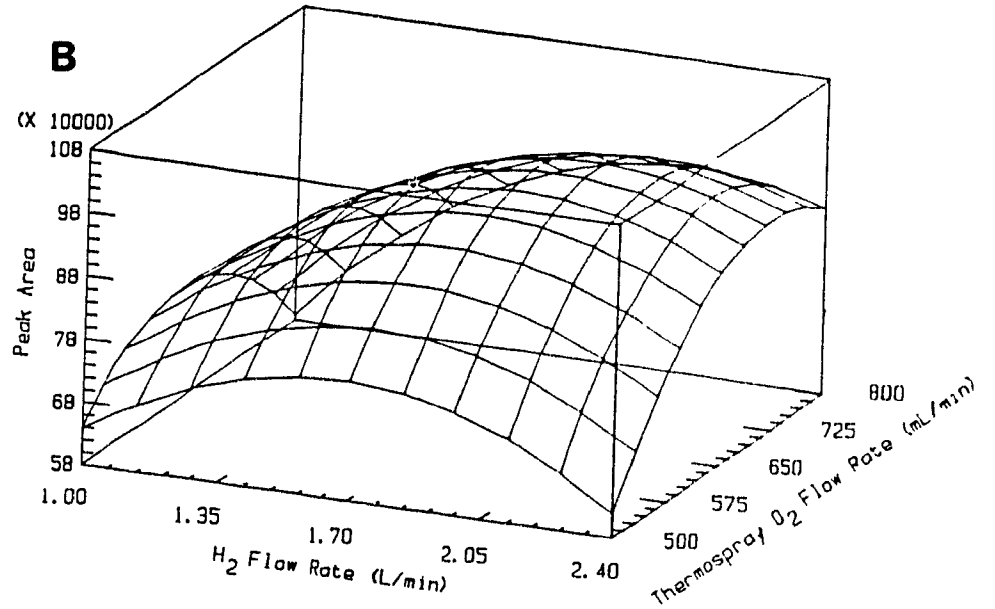
B
(X 10000)
108
98
88
78
68
58
Peak Area
1.00
1.35
1.70
2.05
2.40
H2 Flow Rate (L/min)
500
575
650
725
800
Thermospray O2 Flow Rate (mL/min)

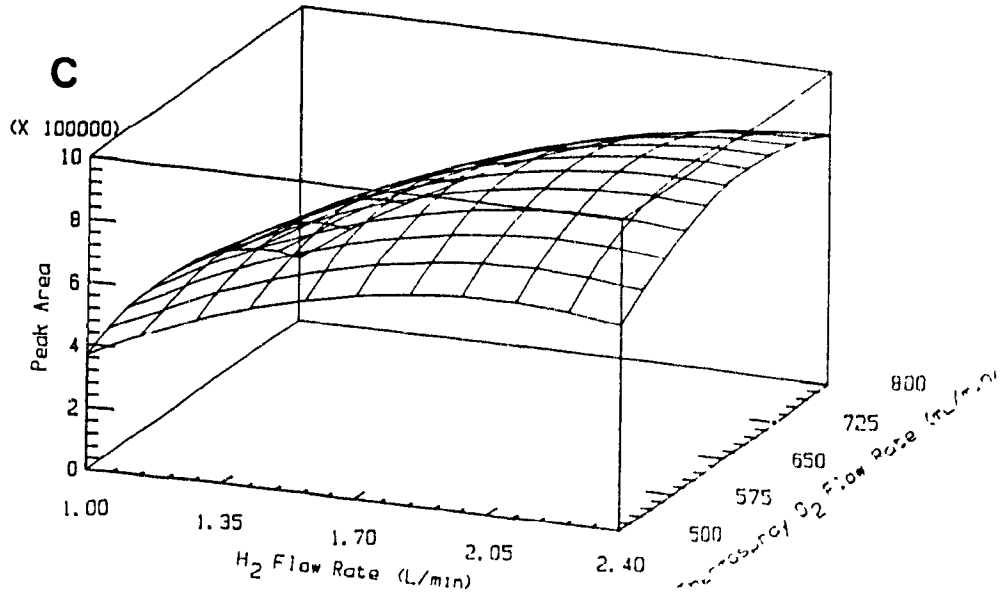
C
(X 100000)
10
8
6
4
2
0
Peak Area
1.00
1.35
1.70
2.05
2.40
H2 Flow Rate (L/min)
500
575
650
725
800

Figure 22-B. Predicted response surfaces (Peak Area vs H_2 flow rate and thermospray O_2 flow rate) for TMSeI at different analytical oxygen flow rates; (A) OA = 170 mL/min; (B) OA = 205 mL/min and (C) OA = 240 mL/min. The two remaining chromatographic variables were constant, (FR = 0.65 mL/min and PE = 30 %). The functions describing these surfaces are presented in Table A-11.

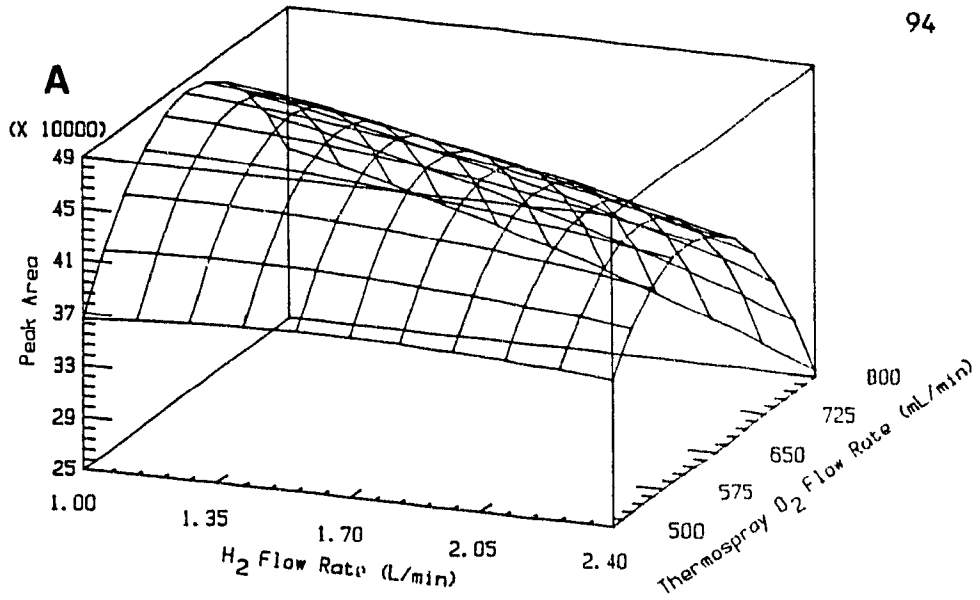
A
(X 10000)
49
45
41
37
33
29
25
Peak Area
1.00
1.35
1.70
2.05
2.40
H_2 Flow Rate (L/min)
500
575
650
725
800
Thermospray O_2 Flow Rate (mL/min)

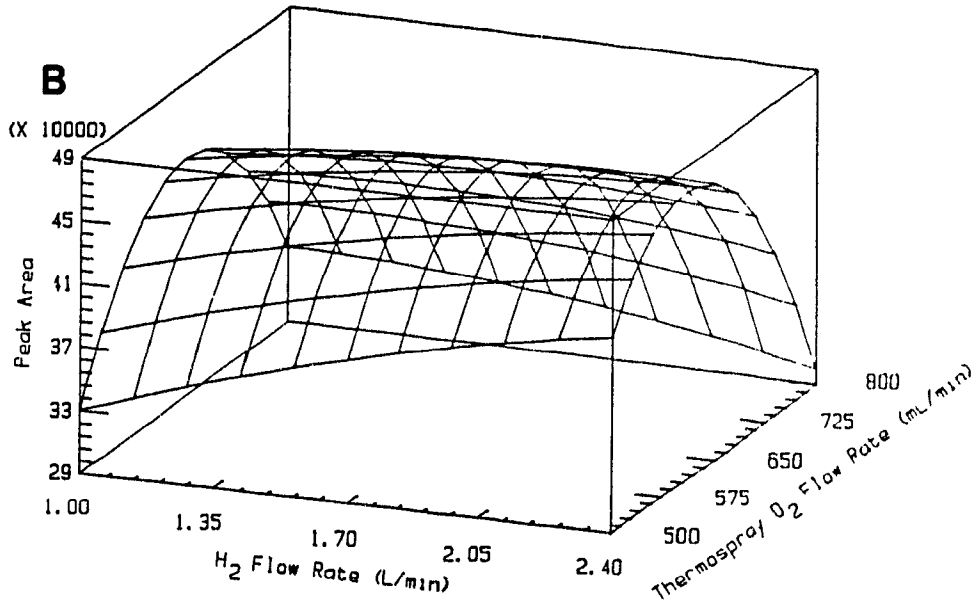
B
(X 10000)
49
45
41
37
33
29
Peak Area
1.00
1.35
1.70
2.05
2.40
H_2 Flow Rate (L/min)
500
575
650
725
800
Thermospray O_2 Flow Rate (mL/min)

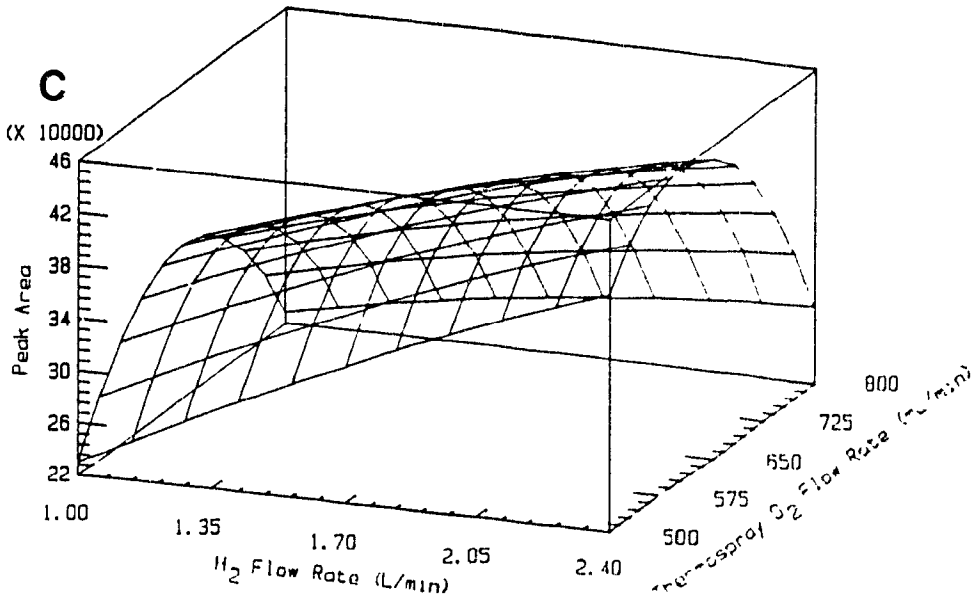
C
(X 10000)
46
42
38
34
30
26
22
Peak Area
1.00
1.35
1.70
2.05
2.40
H_2 Flow Rate (L/min)
500
575
650
725
800

visually using surface response plots. Exploratory surface response plots for each models are presented and discussed in Appendix 3.

Optimum THG parameters for analysis of Se and As analytes were determined from surface response plots of OT vs H2 at different levels of analytical oxygen (OA) with the two other parameters [mobile phase flow rate (FR) and % diethyl ether (PE)] fixed at optimum chromatographic values (FR = 0.65 mL/min; PE = 30 % for arsonium and 0 % for selenoniums compounds). The resulting plots are presented in Figure 22. Tentative explanations for the shape of these surface responses are suggested in Appendix 3. Estimates of the optimum operating parameters for the determination of the selenium and arsenic compounds studied are presented in Table 6.

4.3.4 HPLC of Arsonium and Selenonium Compounds

The main criteria to be fulfilled by the chromatographic step to be interfaced with the THG-AAS detector were: (a) baseline separation of the analytes as well resolved symmetrical peaks; (b) a methanol rich mobile phase [> 60% (v/v)] which was free of alkaline earth cations; (c) chromatographic performance which remained unaffected by other cationic species which may be co-extracted during the isolation of the analytes; and (d) an isochratic elution, to facilitate automation of the instrument.

Arsenobetaine and arsenocholine have been separated by ion-pair reversed-phase HPLC (Beauchemin et al., 1988). Although this particular approach was not considered compatible with our criteria (mobile phase containing sodium dodecyl sulfate; double peak for arsenobetaine), different ion-pairing approaches were investigated for separating the three test arsonium compounds. A microbore

Bondapak C_{18} (2.1 mm x 30 cm) column (flow rate 0.2-0.5 mL/min) was used for this purpose with different combinations of methanol (0-100 %), water (0-100 %), methanesulphonic acid, ethane sulphonic acid, toluenesulphonic acid and ammonium tetraphenylborate (100-2000 µg/mL). The methanol content of the chromatographic effluent was maintained at 80-90 % (v/v) by post-column methanolic enrichment using a T-union. Although highly soluble in methanol/water, the analytes remained immobilized in the column in the absence of pairing agents, indicating a strong adsorption affinity for the stationary phase. The separation of arsenobetaine and arsenocholine was readily achieved (in less than 10 min) using a high water content (60-90 %) and moderate pairing ion concentrations (500-1000 µg/mL). However, tetramethylarsonium and arsenocholine were invariably co-eluted even using concentration gradients of water and ion-pairing agents.

Arsenobetaine (AsBet) and arsenocholine (AsChol) have also been separated on a Bondapak C_{18} column using a methanolic mobile phase (10% water) acidified at pH 3.5 with acetic acid (Lawrence et al., 1986). These conditions were highly effective for the separation of AsBet and AsChol, but co-elution of AsChol and tetramethylarsonium (TMAs) remained a problem. In this case the analytes appeared to be separated mainly by a silanophilic mechanism (ion exchange interactions of analyte with underivatized silanol groups on the surface of the stationary phase particles). The capacity factors of AsBet and AsChol were highly dependent on the acidity of the mobile phase. The addition (500-1000 µg/mL) to the mobile phase of different alkylamines (triethylamine, ethylenediamine), mixed with varying amounts of acetic acid (5-15 %) and water (10-40 %) in methanol resulted in the co-elution of the three analytes with the solvent front. Under conditions of lower masking agent concentrations or gradients (0-30 µg/mL), a complete separation of AsChol from TMAs was possible but the resulting chromatographic

bands were broad and asymmetric. A similar pattern was observed using a weak cation exchanger (resin based column; Polyspher ICW). Under these conditions, selenocholine (SeChol) and trimethylselenonium (TMSe) behaved as their arsenic homologs, and were even more difficult to separate.

The strong cation exchanger (sulphonated support) appears to be the medium of choice for separating AsBet, AsChol and TMAs (Shiomi et al. 1987) or selenonium compounds (Kraus et al., 1985). However, this approach was incompatible with the THG interface because of the high proportion of water and required in the mobile phase. The relatively high proportion of organic buffer used in this technique (typically 0.1 M formate-pyridine) would also be difficult to pyrolyse efficiently. In principle, post-column methanol enrichment could be used in this case. Since the maximum capacity of the THG interface was estimated to be 1.5 mL/min, this approach implies a lowering of the flow rate of the chromatographic eluent to 0.6 mL/min or less (to allow 0.8 mL/min methanol enrichment), resulting in an appreciable loss in resolution and a longer analysis time. With optimum flow rates of 0.2 to 0.5 mL/min, a microbore (0.21 cm i.d.) strong cation exchange column would have been desirable in this particular case. However, this packing was not commercially available in this format.

The four defined chromatographic criteria were met using a normal-phase HPLC approach; a cyano-propyl stationary phase eluted with a methanolic mobile phase containing a silanol masking agent [0.05 % (v/v) triethylamine + 1 % (v/v) acetic acid]. Chromatograms of arsonium and selenonium analytes recorded under optimum chromatographic and THG conditions are presented in Figures 23 and 24. Arsonium (AsBet, AsChol, TMAs) and selenonium (SeChol, TMSe) analytes were

Figure 23-A. HPLC-THG-AAS of (A) 0.05 μg; (B) 0.1 μg; (C) 0.5 μg and (D) 1.0 μg each of (a) arsenobetaine iodide; (b) arsenocholine iodide and (c) tetramethylarsonium iodide recorded under optimized conditions (s = solvent front).

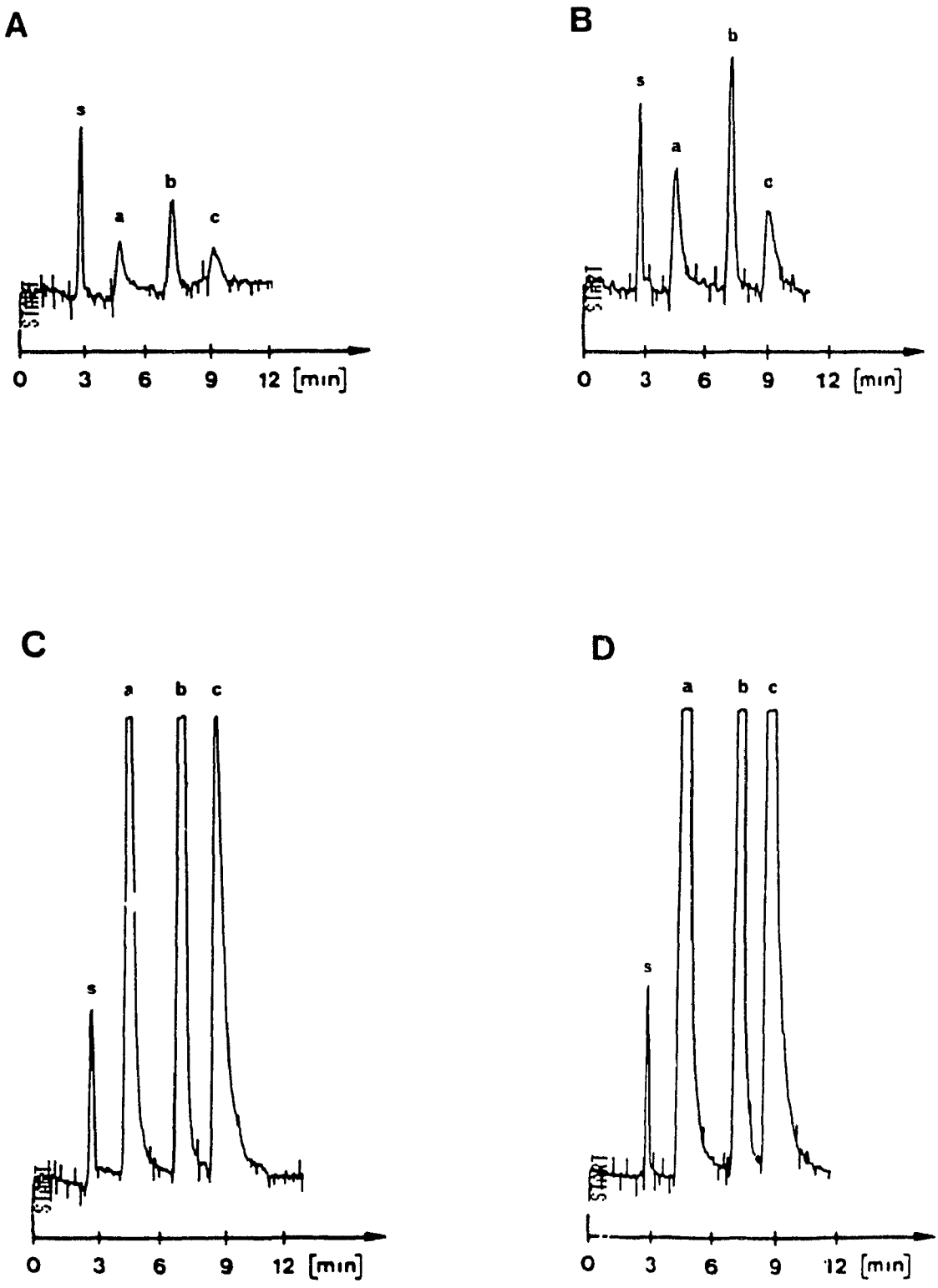
A
s
a
b
c
START
0 3 6 9 12 [min]
B
s
a
b
c
START
0 3 6 9 12 [min]
C
s
a
b
c
START
0 3 6 9 12 [min]
D
s
a
b
c
START
0 3 6 9 12 [min]

Figure 23-B. HPLC-THG-AAS of (A) 0.1 ug; (B) 0.5 ug; (C) 1.0 ug and (D) 2.5 ug each of (a) selenocholine tetraphenylboron (quantified as iodide) and (b) trimethylselenonium iodide recorded under optimized conditions (s = solvent front).

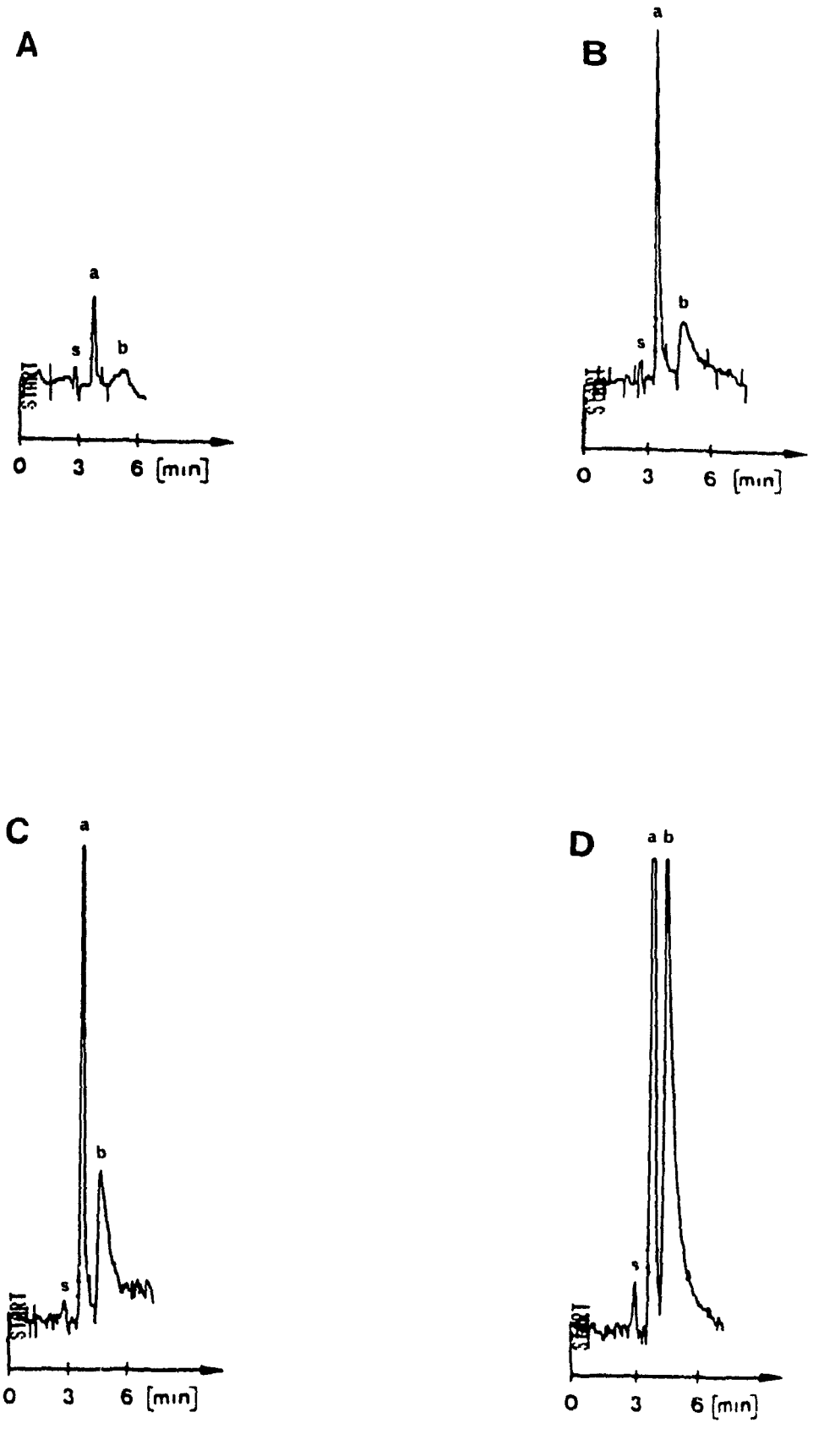
A
a
s
b
START
0 3 6 [min]
B
a
b
s
START
0 3 6 [min]
C
a
b
s
START
0 3 6 [min]
D
a b
s
START
0 3 6 [min]

separated isochratically using methanol:diethyl ether (7:3) and methanol, respectively. Although the two selenonium analytes were well resolved (Figure 24), trimethylselenonium was eluted as a broader peak with these chromatographic conditions, which increased substantially its limit of detection. The addition of up to a 500 fold molar excess of ammonium acetate did not affect the retention times of the analytes.

4.3.5 Linearity, Reproducibility and Limits of Detection

The limits of detection for each each analytes were calculated from their calibration curves under optimized conditions, as described in Appendix 1. The linear calibration models were highly correlated ($0.9989 < p < 0.9997$) in the concentration range studied (50 ng to 1 µg for arsonium; 100 ng to 2.5 µg for selenoniums). Analyses of variance and linear regression parameters for each analyte are presented in Appendix 3.

The calculated limits of detection of each analyte (as the iodide salts) were as follows: AsBet = 22.7 ng; AsChol = 26.7 ng; TMAs = 14.8 ng; SeChol = 59.1 ng; TMSe = 88.9 ng. These LOD's may be expressed in terms of the free cations (which is more appropriate to real samples); $(CH_3)_3As^+CH_2COOH$ = 13.3 ng; $(CH_3)_3As^+CH_2OH$ = 14.5 ng; $(CH_3)_4As^+$ = 7.6 ng; $(CH_3)_2Se^+CH_2OH$ = 31.0 ng; $(CH_3)_3Se^+$ = 43.9 ng, or in terms of As or Se; AsBet = 5.5 ng; AsChol = 7.2 ng; TMAs = 4.2 ng; SeChol = 17.5 ng; TMSe = 27.9 ng. These LOD's were similar to those observed using HPLC-ICP systems for the As analytes (Irgolic et al., 1983).

Table 8.Reproducibility of the HPLC-THG-AAS at Varying Analyte Levels.

Amount (ng)	AsBetaine r.s.d.(%)[a]	AsCholine r.s.d.(%)	TMeAs r.s.d.(%)	SeCholine r.s.d.(%)	TMeSe r.s.d.(%)
50	12.9	14.6	13.5	--	--
100	1.5	2.2	5.0	10.7	11.6
500	1.4	2.6	6.2	2.5	1.4
1000	4.2	2.0	1.0	1.9	2.8
2500	---	---	---	0.6	1.2

[a] r.s.d.=relative standard deviation based on three replicate analyses.

The short-term reproducibility of the THG interface (based on three replicate analyses) for different concentrations of each analyte is reported in Table 8. The long-term reproducibility (6 hours; n=6) recorded at 10 x LOD was: AsBet = 6.0 %, AsChol = 2.3 %, TMAs = 6.5 %, SeChol = 3.1 % and TMSe = 5.8 %. The limits of detection provided by this automated HPLC-THG-AAS were considered sufficient for routine analysis of arsonium metabolites in marine organisms where they may occur at relatively high concentrations (typically 0.1 - 16 µg/g). Concentrations of selenonium metabolites in varying bilogical samples remain to be determined. Clearly, in order to provide a LOD in the 10-50 ppb range, the extraction methodology to be developed for these analytes should be designed to allow the treatment of large (5-25 g) samples and concentration to a 1 mL methanolic extract.

4.3.7 Conclusion

Since the cool diffused flame atomizer has been shown to provide picogram sensitivities for As at gas flow rates exceeding 5 l/min (Siemer et al., 1976; Dedina and Rubeska, 1980), it may be assumed that the performance of this interface is limited by the efficiency of the thermochemical hydride generation and hydride transport processes. As suggested by the efficient quenching of this process in a nitrous oxide supported flame, the post-thermospray performance of the THG interface appears to be strongly affected by excessive post-thermospray temperatures. Thus, it is reasonable to predict that further research on this aspect may result in sub nanogram limits of detections for hydride forming elements. Although different physical and thermochemical approaches can be developed empirically to control this thermochemical hydride generation, high resolution emission spectroscopy or mass spectrometry of this process may provide valuable information to more fully characterize and optimize this novel approach to HPLC-AAS interfacing.

Contribution to Original Knowledge

Section 2

- The first reported miniaturized quartz flame atomizer.
- The lowest limits of detection for ionic alkyllead compounds by HPLC-flame AAS (c.a. 1 ng).
- The first successful separation of four ionic alkylleads and inorganic lead by reverse-phase HPLC using dithizone or ammonium pyrrolidinedithiocarbamate as complexing agents.
- The successful development of a speciation approach for alkyllead salts (at sub-mg/kg concentrations) in water, soils and sediments. This method involve a selective complexometric extraction step followed by the determination of ionic alkylleads by direct injection of the extract in the HPLC-AAS instrument.

Section 3

- The first post-column continuous flow interface derivatizing ionic alkylleads to ethylated derivatives and volatilizing these tetraalkyllead derivatives in an electrothermal quartz atomizer.
- The first successful HPLC-electrothermal quartz atomization-AAS interfacing.
- The lowest limits of detection for the determination of ionic alkylleads by HPLC-AAS (c.a. 0.1 ng).
- The first successful separation of seven ionic alkylleads by reverse-phase ion pairing HPLC.

Section 4

- The first report of a thermochemical hydride generation process in an analytical approach.
- The first successful separation of selenocholine/trimethylselenonium and arsenobetaine/arsenocholine/tetramethylarsonium mixtures by normal-phase HPLC.

APPENDICES

Appendix 1. Limits of Detection of the HPLC-AAS Interfaces

The limits of detection (LOD) provided by the HPLC-AAS interfaces presented in Sections 2, 3 and 4 were determined using a linear model based on first order error propagation (Foley and Dorsey, 1984):

$$LOD = 3\ (Sb^2 + Si^2\ (i/S)^2\ Ss^2)^{1/2} / S \qquad (1)$$

where S, i, are the slope and intercept of the calibration curve; Ss and Si are the relative standard errors on S and i; and Sb is the standard deviation of the spectroscopic blank signal.

The factor 3 in the numerator of equation (1) gives a practical confidence level (between 90 and 99.7 %) which is proportional to the goodness of fit of the probability distribution of the blank signal and the accuracy of Sb. The standard deviation of the baseline noise was given by:

$$Sb = Np\text{-}p / r \qquad (2)$$

where Np-p is the peak-to-peak noise (integrated on a 30 min blank run) and r is a parameter dependent on the type of noise. In all cases, baseline noise was normally distributed ($p < 0.005$) and consequently $r = 5$ (Foley and Dorsey, 1984).

The resulting regression plots and analyses of variance (for the thermospray-microatomizer interface) are presented in Figure A-1.

Figure A-1-a. Regression analysis related to the determination of the limit of detection of $Pb(NO_3)_2$.

Simple Regression of Pb on Amount

Parameter	Estimate	Standard Error	T Value	Prob. Level
Intercept	2197.7	1148.86	1.91294	0.0780387
Slope	1041.18	9.35397	111.309	0

Analysis of Variance

Source	Sum of Squares	Df	Mean Square	F-Ratio
Model	1.2781E0011	1	1.2781E0011	1.2390E0004
Error	1.3411E0008	13	1.0316E0007	
Total (Corr.)	1.2794E0011	14		

Correlation Coefficient = 0.999476
Stnd. Error of Est. = 3211.83

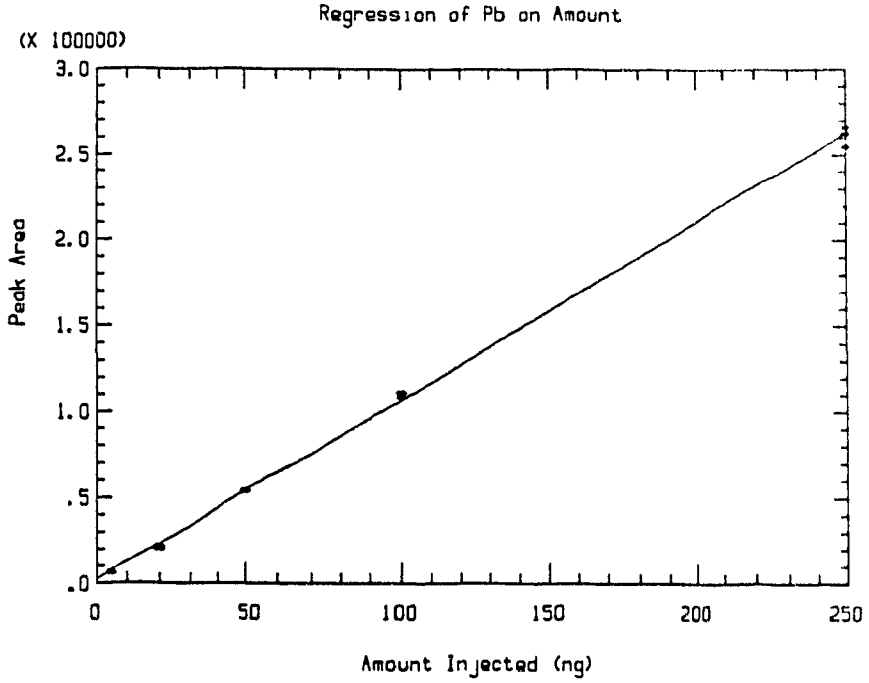

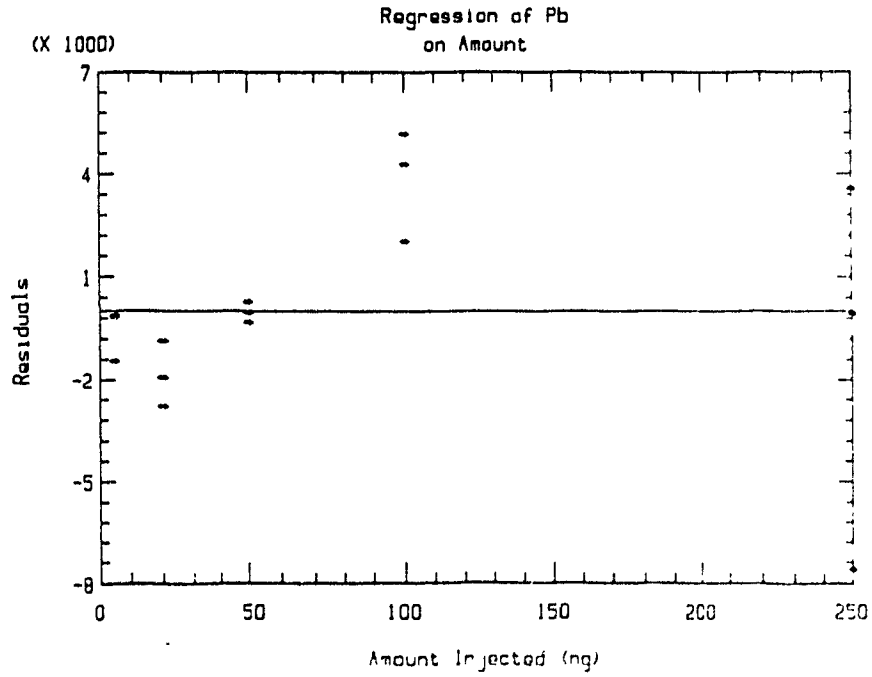

Figure A-1-b. Regression analysis related to the determination of the limit of detection of Me_3PbCl.

Simple Regression of Me3PbCl on Amount

Parameter	Estimate	Standard Error	T Value	Prob. Level
Intercept	2440.26	416.721	5.85587	5.63057E-5
Slope	1534.36	3.39291	452.225	0

Analysis of Variance

Source	Sum of Squares	Df	Mean Square	F-Ratio
Model	2.7757E0011	1	2.7757E0011	2.0451E0005
Error	17644243	13	1357249	
Total (Corr.)	2.7758E0011	14		

Correlation Coefficient = 0.999968
Stnd. Error of Est. = 1165.01

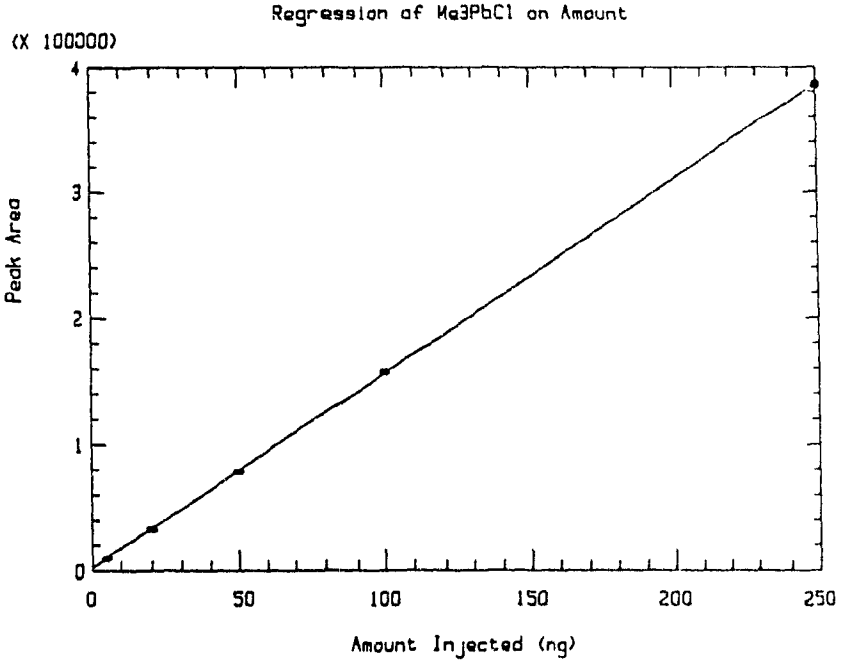

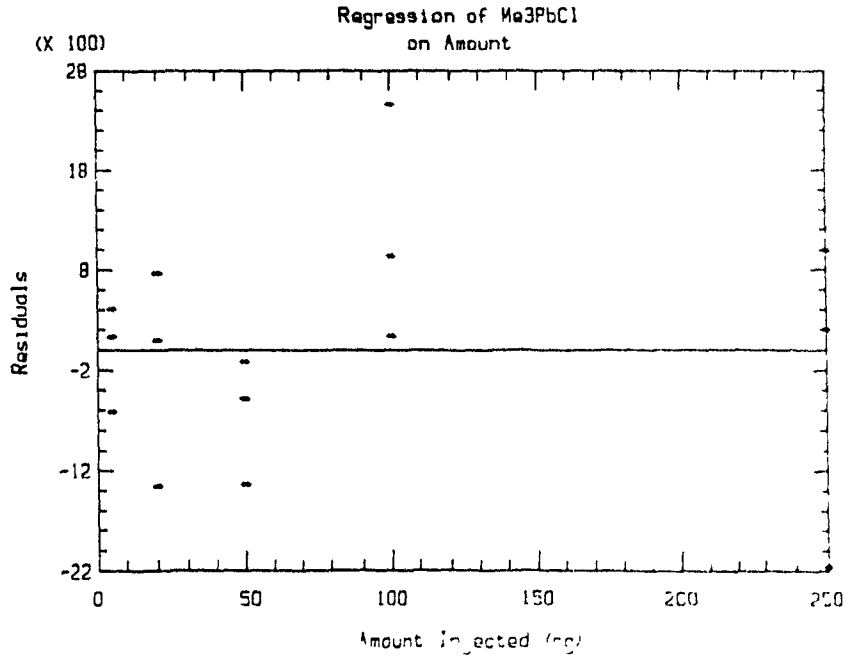

Figure A-1-d. Regression analysis related to the determination of the limit of detection of Et_3PbCl.

Simple Regression of Et3PbCl on Amount

Parameter	Estimate	Standard Error	T Value	Prob. Level
Intercept	1873.37	373.303	5.01835	2.3521E-4
Slope	1404.29	3.03941	462.028	0

Analysis of Variance

Source	Sum of Squares	Df	Mean Square	F-Ratio
Model	2.3250E0011	1	2.3250E0011	2.1347E0005
Error	14159092	13	1089161	
Total (Corr.)	2.3252E0011	14		

Correlation Coefficient = 0.99997
Stnd. Error of Est. = 1043.63

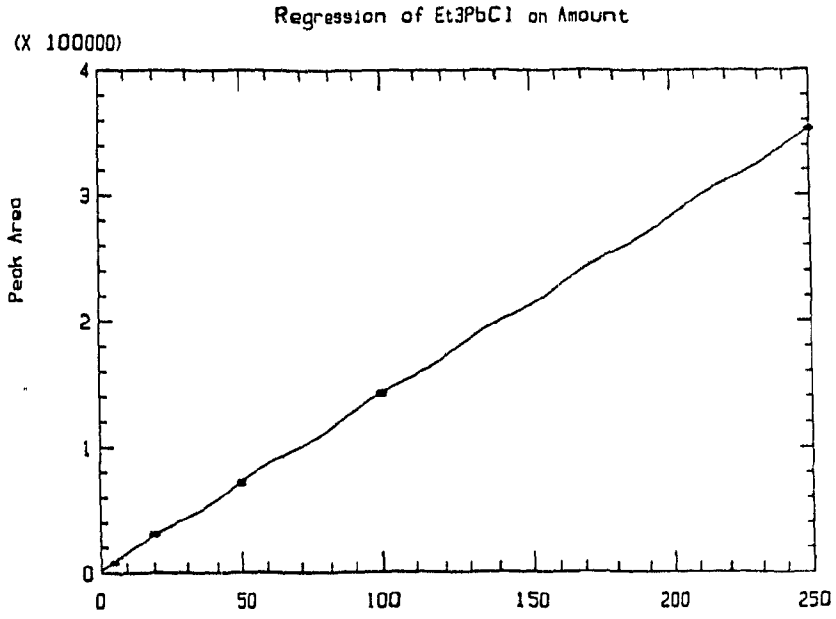

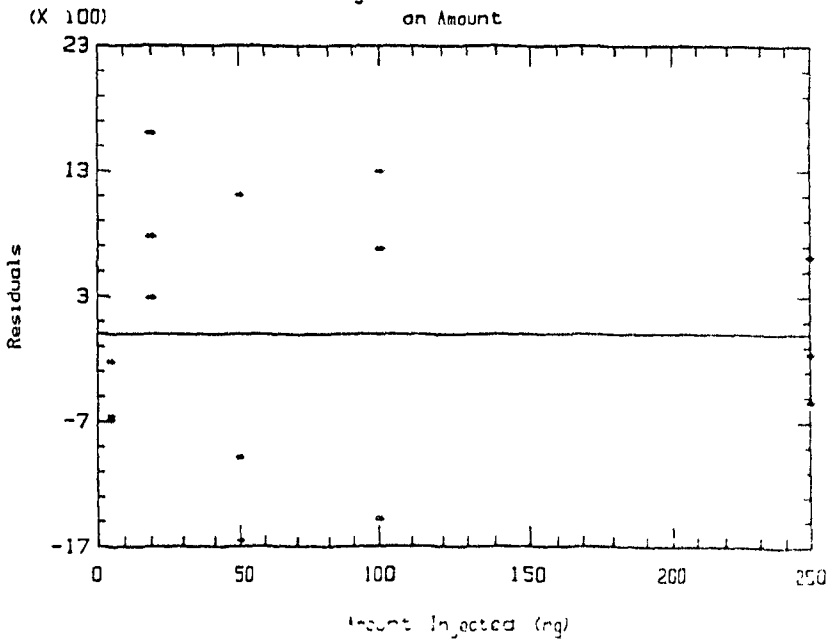

Figure A-1-c. Regression analysis related to the determination of the limit of detection of Me_2PbCl_2.

Simple Regression of Me2PbCl2 on Amount

Parameter	Estimate	Standard Error	T Value	Prob. Level
Intercept	965.708	683.689	1.4125	0.181294
Slope	1333.26	5.56655	239.513	0

Analysis of Variance

Source	Sum of Squares	Df	Mean Square	F-Ratio
Model	2.0958E0011	1	2.0958E0011	5.7366E0004
Error	47492981	13	3653306	
Total (Corr.)	2.0962E0011	14		

Correlation Coefficient = 0.999887
Stnd. Error of Est. = 1911.36

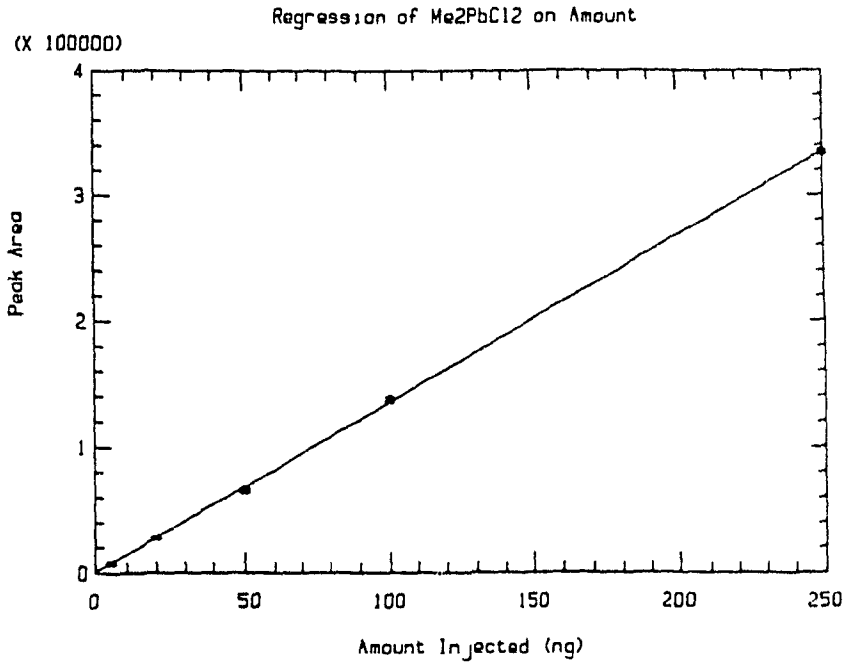

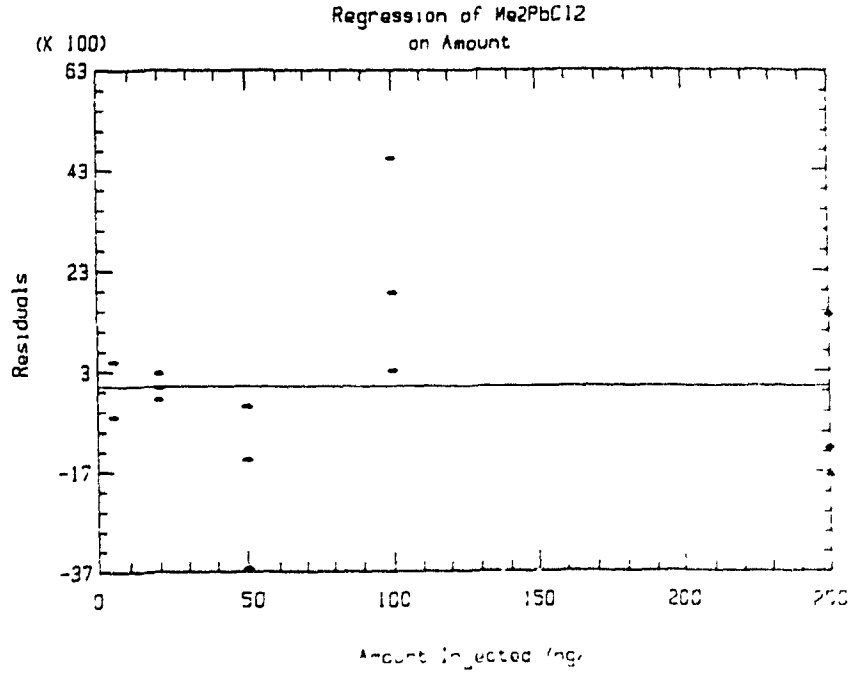

Figure A-1-e. Regression analysis related to the determination of the limit of detection of Et_2PbCl_2.

Simple Regression of Et2PbCl2 on Amount

Parameter	Estimate	Standard Error	T Value	Prob. Level
Intercept	2282.21	645.812	3.53386	3.66826E-3
Slope	1190.35	5.25816	226.382	0

Analysis of Variance

Source	Sum of Squares	Df	Mean Square	F-Ratio
Model	1.6706E0011	1	1.6706E0011	5.1249E0004
Error	42376450	13	3259727	
Total (Corr.)	1.6710E0011	14		

Correlation Coefficient = 0.999873
Stnd. Error of Est. = 1805.47

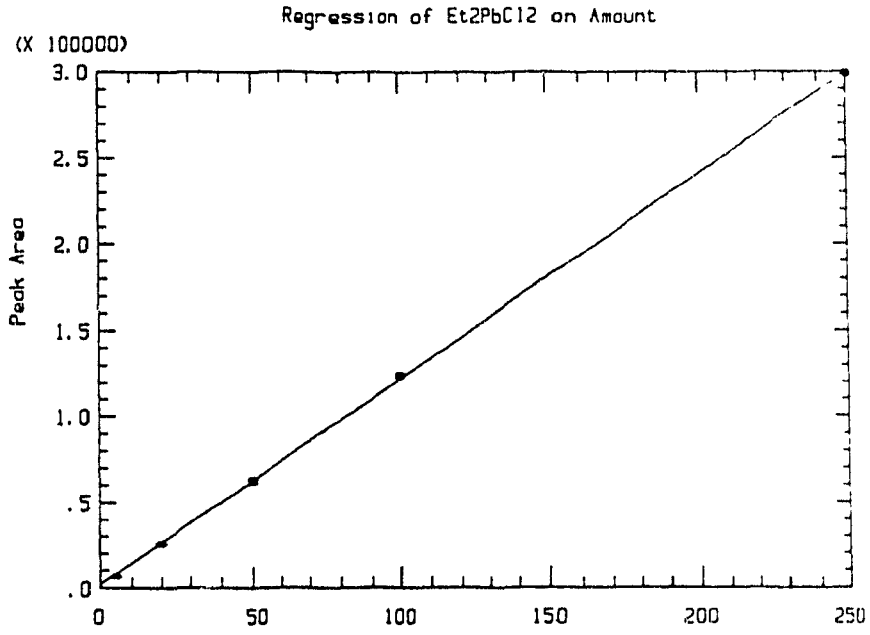

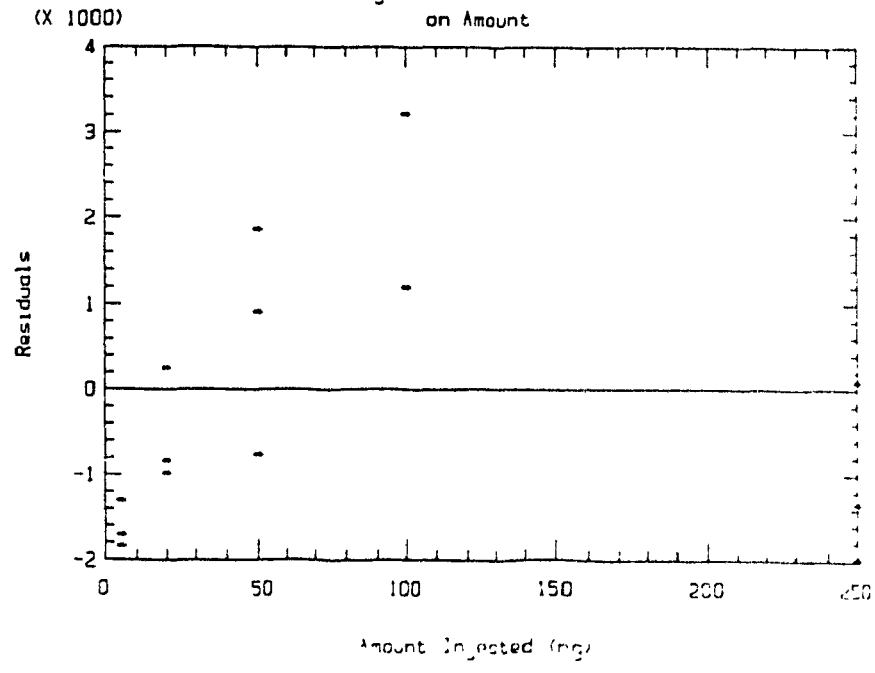

Appendix 2. Details of the Statistical Analyses Associated with the Optimization of the HPLC-Ethylate Generation-AAS Instrument

A-2.1 Optimization by Response Surface Analysis

A-2.1.1 Introduction

Multivariate optimization designs are generally used for optimizing multi-variables processes including variables which are expected to interact with each other. Although Simplex optimization algorithms (Nakai and Kaneko, 1985) are less time consuming than factorial designs (Box and Wilson, 1951), the later methodology provides additional information on variable interactions which may facilitate the characterization of the process under study. Thus, the resulting fitted factorial equation may be used to plot a tri-dimensional contour map of a response (response surface) as a function of two interacting variables (keeping the other variables constant).

As described in section 3.3.4, the process to be optimized included 5 variables. A complete 3^5 (3 levels, 5 variables) factorial design would be suitable for estimating all linear, quadratic and interaction effects. However, this design would require excessive experimentation (the 243 points required must at least be duplicated), promoting time-dependent response variations which are not included in the model. Composite designs (Box and Wilson, 1951) have been introduced to reduce the number of experimental points (3^5 = 243 vs 2^5 + (2 x 5 + 1) = 43) required for the optimization of complex processes. In this design, 2n + 1 (n = number of variables) points are added to the first order 2^n factorial design (which is suitable only for estimating interaction and linear effects), allowing the fitting of a second order model (including quadratic effects) searching for optimum response. The (2n+1) extr. points are added so that one of them is at the origin (center) of the design and

the remaining (2n) at a magnitude of x units from the origin, distributed equally along the n axis of the design.

Even for composite design, the number of experimental points is increasing rapidly as the number of variables (n) increases. Hence, the composite designs that will maximize the information quality/experimentation time ratio are those in which the 2^n factorial design is replaced by a fractional replicate of 2^n. In keeping with the aims of composite designs, fractional replications are normally designed to permit the estimation of all the linear and quadratic effects and, if possible (depending on the fractionation factor), all the interactions effects. To accomplish this, the fractional replicate should be defined so that no main effect is confounded with the grand mean (Hill and Hunter, 1961). One desirable property of a second order design is rotability. In a rotatable design, the standard error of the estimated response is, in theory, homogeneous for all points at the same magnitude (x) from the center of the experimented response region. In order to obtain a rotatable half-replicate composite design, x must be equal to $2^{(n-1)/4}$.

A-2.1.2 Method

A half-replicate 2^5 factorial experiment was designed to optimize the 5 variables of the HPLC-ethylate generator-AAS interface. The basic half-replicate 2^5 design was augmented by (2n+1) = 11 points; one central point (coded 0) and 10 equally spaced points with magnitudes of $\pm 2^{(5-1)/4} = \pm 2$, to make the design rotatable and permit the estimation of all linear, quadratic and interaction effects. The coded design matrix is presented in Table A-1. The resulting data were analyzed by the RSREG procedure of the SAS software (SAS Institute Inc., Cary, N.J.).

A-2.1.3 Results and Discussion

The experimental and predicted responses (in term of absolute peak area) are presented in Table A-2. The resulting statistical analyses and estimated regression parameters are presented in Table A-3. The statistical lack of fit was unsignificant at the 0.05 level of significance, but significant at the 0.01 level, which allowed a relatively accurate (with a confidence of 95 %) estimation of effects. The regression analysis of observed vs predicted values (r = 0.9918) is presented in Figure A-2. As presented in Section 3.3.4, the maximum response calculated from the fitted model was not considered optimum.

The optimum conditions were estimated using tri-dimensional response surface plots of the statistically significant parameters. These response surface plots (2 variables vs response) were generated from the second order equations obtained by keeping the three other variables constant, at the center of the factorial design. These equations and their corresponding plots are presented in Table A-4 and Figure 16 (Section 3.3.4) respectively. Generally, the curvature of the response surface reflected the magnitude of the probability factor associated with the interaction of the two variables considered (Table A-3). From the information obtained in these response surface plots, the optimum parameters (sections 3.3.4) were estimated on the basis of response, post-chromatographic transfer efficiency (symmetrical peak shape,) and economy (high cost of the derivatizing agent) criteria.

A-2.2 Calibration

The calibration regressions and related statistics from which limits of detections (Section 3.3.5) were calculated are presented in Figure A-3.

Table A-1. Matrix of the Augmented 1/2 replicate 2^5 Factorial Design.

Point	Flow Rate $NaBEt_4$	Flow rate H_2	Temp. Furnace	Temp. Coil	Conc. $NaBEt_4$
1	1[a]	-1	-1	-1	-1
2	-1	1	-1	-1	-1
3	-1	-1	1	-1	-1
4	1	1	1	-1	-1
5	-1	-1	-1	1	-1
6	1	1	-1	1	-1
7	1	-1	1	1	-1
8	-1	1	1	1	-1
9	-1	-1	-1	-1	1
10	1	1	-1	-1	1
11	1	-1	1	-1	1
12	-1	1	1	-1	1
13	1	-1	-1	1	1
14	-1	1	-1	1	1
15	-1	-1	1	1	1
16	1	1	1	1	1
17	0	0	0	0	0
18	-2	0	0	0	0
19	2	0	0	0	0
20	0	-2	0	0	0
21	0	2	0	0	0
22	0	0	-2	0	0
23	0	0	2	0	0
24	0	0	0	-2	0
25	0	0	0	2	0
26	0	0	0	0	-2
27	0	0	0	0	2

[a] Coded value

Table A-2. Observed and Predicted Results of the Factorial Experiment.

Point	Flow Rate $NaBEt_4$ mL/min	Flow Rate H_2 mL/min	Current Furnace amp.	Temp. Coil ^oC	Conc. $NaBEt_4$ w/v	Observed response Area	Predicted response Area
1	0.775	32.5	4.375	36.2	0.325	167760	166543
1	0.775	32.5	4.375	36.2	0.325	166985	166543
1	0.775	32.5	4.375	36.2	0.325	171220	166543
2	0.325	77.5	4.375	36.2	0.325	84011	87859
2	0.325	77.5	4.375	36.2	0.325	91154	87859
2	0.325	77.5	4.375	36.2	0.325	91239	87859
3	0.325	32.5	5.125	36.2	0.325	133890	131566
3	0.325	32.5	5.125	36.2	0.325	132220	131566
3	0.325	32.5	5.125	36.2	0.325	136950	131566
4	0.775	77.5	5.125	36.2	0.325	102170	95522
4	0.775	77.5	5.125	36.2	0.325	99949	95522
4	0.775	77.5	5.125	36.2	0.325	90327	95522
5	0.325	32.5	4.375	58.7	0.325	156330	155648
5	0.325	32.5	4.375	58.7	0.325	151950	155648
5	0.325	32.5	4.375	58.7	0.325	162600	155648
6	0.775	77.5	4.375	58.7	0.325	103920	102549
6	0.775	77.5	4.375	58.7	0.325	103700	102549
6	0.775	77.5	4.375	58.7	0.325	101480	102549
7	0.775	32.5	5.125	58.7	0.325	168000	156347
7	0.775	32.5	5.125	58.7	0.325	148680	156347
7	0.775	32.5	5.125	58.7	0.325	159350	156347
8	0.325	77.5	5.125	58.7	0.325	88725	87670
8	0.325	77.5	5.125	58.7	0.325	88607	87670
8	0.325	77.5	5.125	58.7	0.325	89154	87670
9	0.325	32.5	4.375	36.2	0.775	104160	106485
9	0.325	32.5	4.375	36.2	0.775	100310	106485
9	0.325	32.5	4.375	36.2	0.775	115210	106485
10	0.775	77.5	4.375	36.2	0.775	89570	92248
10	0.775	77.5	4.375	36.2	0.775	90416	92248
10	0.775	77.5	4.375	36.2	0.775	94500	92248
11	0.775	32.5	5.125	36.2	0.775	137300	138410
11	0.775	32.5	5.125	36.2	0.775	149120	138410
11	0.775	32.5	5.125	36.2	0.775	132090	138410
12	0.325	77.5	5.125	36.2	0.775	60560	61301
12	0.325	77.5	5.125	36.2	0.775	60409	61301
12	0.325	77.5	5.125	36.2	0.775	62704	61301
13	0.775	32.5	4.375	58.7	0.775	161510	168546
13	0.775	32.5	4.375	58.7	0.775	170140	168546
13	0.775	32.5	4.375	58.7	0.775	172840	168546
14	0.325	77.5	4.375	58.7	0.775	81099	78581
14	0.325	77.5	4.375	58.7	0.775	72653	78581
14	0.325	77.5	4.375	58.7	0.775	77332	78581
15	0.325	32.5	5.125	58.7	0.775	108980	105727
15	0.325	32.5	5.125	58.7	0.775	102950	105727
15	0.325	32.5	5.125	58.7	0.775	106130	105727

Table A-2. Observed and Predicted Results of the Factorial Experiment.

Point	Flow Rate $NaBEt_4$ mL/min	Flow Rate H_2 mL/min	Current Furnace amp.	Temp. Coil °C	Conc. $NaBEt_4$ w/v	Observed response Area	Predicted response Area
16	0.775	77.5	5.125	58.7	0.775	72710	78335
16	0.775	77.5	5.125	58.7	0.775	80216	78335
16	0.775	77.5	5.125	58.7	0.775	80474	78335
17	0.550	55.0	4.750	47.5	0.550	129240	120431
17	0.550	55.0	4.750	47.5	0.550	129900	120431
17	0.550	55.0	4.750	47.5	0.550	120660	120431
17	0.550	55.0	4.750	47.5	0.550	118810	120431
17	0.550	55.0	4.750	47.5	0.550	117860	120431
17	0.550	55.0	4.750	47.5	0.550	114550	120431
18	0.100	55.0	4.750	47.5	0.550	62293	64651
18	0.100	55.0	4.750	47.5	0.550	63458	64651
18	0.100	55.0	4.750	47.5	0.550	65012	64651
19	1.000	55.0	4.750	47.5	0.550	109080	110567
19	1.000	55.0	4.750	47.5	0.550	108014	110567
19	1.000	55.0	4.750	47.5	0.550	109360	110567
20	0.550	10.0	4.750	47.5	0.550	172740	174540
20	0.550	10.0	4.750	47.5	0.550	170460	174540
20	0.550	10.0	4.750	47.5	0.550	170210	174540
21	0.550	100.0	4.750	47.5	0.550	60220	63239
21	0.550	100.0	4.750	47.5	0.550	62122	63239
21	0.550	100.0	4.750	47.5	0.550	69147	63239
22	0.550	55.0	4.000	47.5	0.550	131440	132537
22	0.550	55.0	4.000	47.5	0.550	132290	132537
22	0.550	55.0	4.000	47.5	0.550	134740	132537
23	0.550	55.0	5.500	47.5	0.550	104030	106642
23	0.550	55.0	5.500	47.5	0.550	102819	106642
23	0.550	55.0	5.500	47.5	0.550	103780	106642
23	0.550	55.0	4.750	25.0	0.550	106974	110827
24	0.550	55.0	4.750	25.0	0.550	109723	110827
24	0.550	55.0	4.750	25.0	0.550	107788	110827
25	0.550	55.0	4.750	70.0	0.550	120360	124194
25	0.550	55.0	4.750	70.0	0.550	124950	124194
25	0.550	55.0	4.750	70.0	0.550	126830	124194
26	0.550	55.0	4.750	47.5	0.100	145060	149427
26	0.550	55.0	4.750	47.5	0.100	142940	149427
26	0.550	55.0	4.750	47.5	0.100	144870	149427
27	0.550	55.0	4.750	47.5	1.000	112770	110909
27	0.550	55.0	4.750	47.5	1.000	113580	110909
27	0.550	55.0	4.750	47.5	1.000	113350	110909

Figure A-2 Regression Analysis of Observed vs Predicted Values

Simple Regression of OBSERVED on PREDICTED

Parameter	Estimate	Standard Error	T Value	Prob. Level
Intercept	-0.435494	1691.15	-2.57514E-4	0.999795
Slope	1	0.0142461	70.1948	0

Analysis of Variance

Source	Sum of Squares	Df	Mean Square	F-Ratio
Model	8.5392E0010	1	8.5392E0010	4.9273E0003
Error	1.4211E0009	82	1.7330E0007	
Total (Corr.)	8.6813E0010	83		

Correlation Coefficient = 0.991781
Stnd. Error of Est. = 4162.97

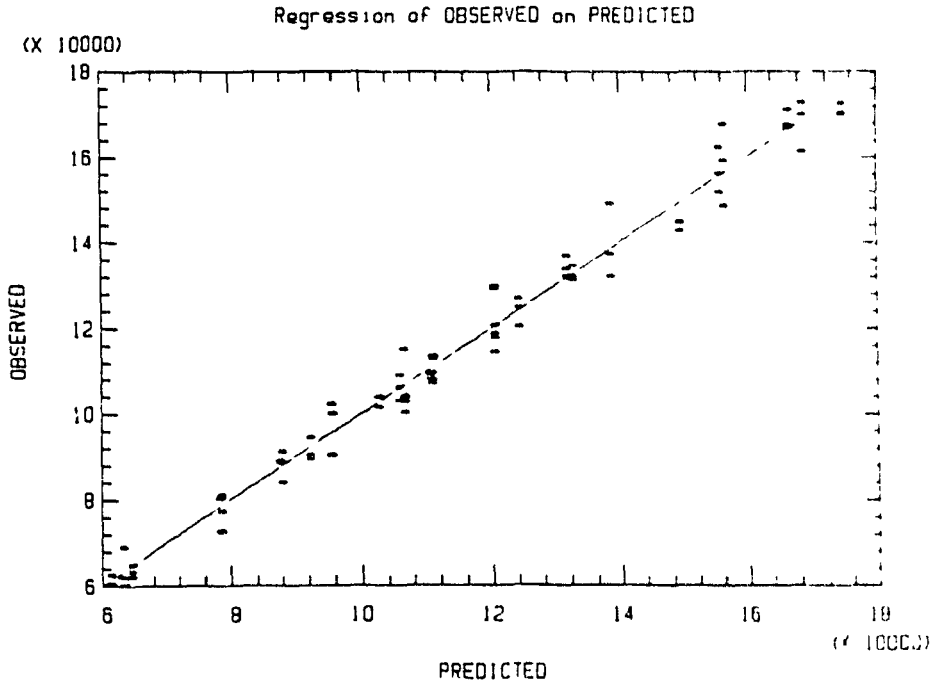

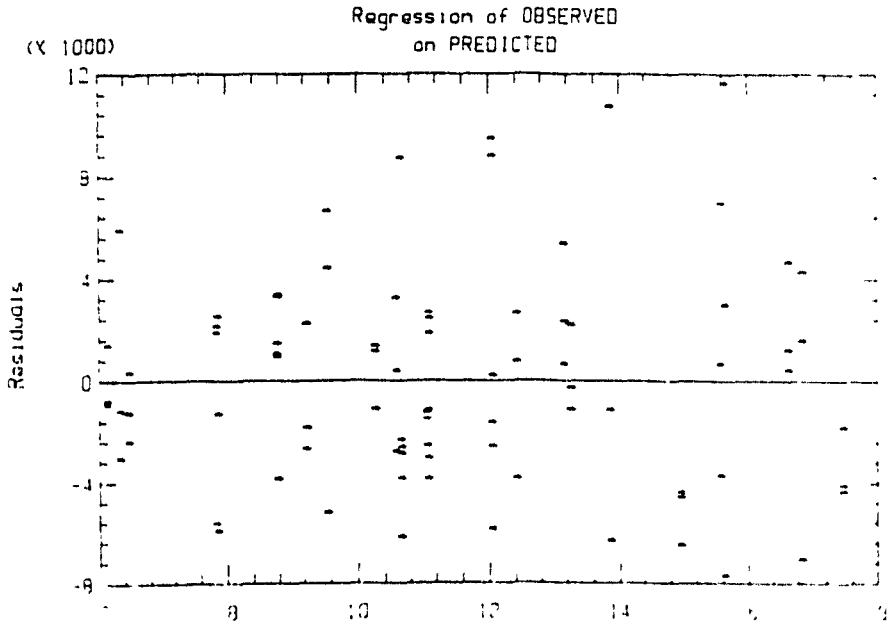

Table A-3. Analysis of variance and regression estimates.

Response Mean: 114347.4
Root MSE : 4749.415
R-square : 0.9836305
Coef.of Var. : 0.04153495

Regression	Df	Type I SS	R-Square	F-Ratio	Prob.
Linear	5	75731817978	0.8724	671.47	0.0001
Quadratic	5	6411408259	0.0739	56.85	0.0001
Crossproduct	10	3248660626	0.0374	14.40	0.0001
Tot. Regress	20	85391886863	0.9836	189.28	0.0001

Residual	Df	SS	Mean Square	F-Ratio	Prob.
Lack of fit	6	297171383	49528563.90	2.512	0.0316
Pure error	57	1123915776	19717820.63		
Total error	63	1421087159	22556939.04		

Parameters	Df	Estimate	Std Dev	T-Ratio	Prob.
Intercept	1	-51220.58870	115564.97	-0.44	0.6591
FD[a]	1	334872.74	44026.84856	7.61	0.0001
H2[b]	1	-1371.55247	440.25849	-3.12	0.0028
CF[c]	1	37986.28394	41595.80607	0.91	0.3646
TC[d]	1	5084.99547	929.17115	5.47	0.0001
CD[e]	1	-101867.22	44026.84856	-2.31	0.0240
FD*FD	1	-162083.33	11726.94963	-13.82	0.0001
H2*FD	1	-952.79835	135.41115	-7.04	0.0001
H2*H2	1	-0.76125514	1.17269496	-0.65	0.5186
CF*FD	1	-14045.92593	8124.66903	-1.73	0.0887
CF*H2	1	198.23704	81.24669030	2.44	0.0175
CF*CF	1	-1496.07407	4221.70187	-0.35	0.7242
TC*FD	1	-675.55556	270.82230	-2.49	0.0152
TC*H2	1	-8.16329218	2.70822301	-3.01	0.0037
TC*CF	1	-754.23210	162.49338	-4.64	0.0001
TC*TC	1	-5.76897119	4.69077985	-1.23	0.2233
CD*FD	1	82995.06173	13541.11505	6.13	0.0001
CD*H2	1	343.21811	135.41115	2.53	0.0138
CD*CF	1	-15251.85185	8124.66903	-1.88	0.0651
CD*TC	1	296.82305	270.82230	1.10	0.2772
CD*CD	1	48083.74486	11726.94963	4.10	0.0001

[a] FD = Flow rate of aqueous $NaBEt_4$ (0.1-1.0 mL/min)
[b] H2 = Flow rate of hydrogen (10-100 mL/min)
[c] CF = Current applied on the furnace (4.000-5.500 ampere)
[d] TC = Temperature of the reaction coil (25-70 ^{o}C)
[e] CD = Concentration of aqueous $NaBEt_4$ (0.1-1.0 % w/v)

Table A-4. Factorial Second Order Equations Predicting the Effects of Selected Variables on Analytes Response (plots presented in Fig.16).

1) H2 and FD vs Area; CD = 0.55 %, CF = 4.375 ampere and TC = 47.5 ^{o}C

$$Area = 87688.8263 - 703.2382 \times H2 + 286980.2079 \times FD - 0.7612 \times H2^2 - 162083.33 \times FD^2 - 952.7983 \times H2 \times FD$$

2) CD and TC vs Area; H_2 = 55 mL/min, CF = 4.375 ampere and FD=0.55 mL/min

$$Area = 128826.0161 - 122758.0177 \times CD + 964.6930 \times TC + 48083 \times CD^2 - 5.7690 \times TC^2 + 296.8230 \times CD \times TC$$

3) CD and FD vs Area; H_2 = 55 mL/min, CF = 4.375 ampere and TC = 47.5 ^{o}C

$$Area = 106751.8712 - 135617.9836 \times CD + 188929.0167 \times FD + 48083.7449 \times CD - 162083.33 \times FD^2 + 82995.0617 \times CD \times FD$$

4) FD and TC vs Area; H2 = 55 mL/min, CF = 4.375 ampere and CD = 0.55 %

$$Area = -11502.6884 + 266665.1916 \times FD + 1499.5012 \times TC - 162083.33 \times FD^2 - 5.7689 \times TC^2 - 675.5556 \times FD \times TC$$

5) H2 and TC vs Area; CD = 0.55 %, CF = 4.375 ampere and FD = 0.55 mL/min

$$Area = 134610.0002 - 839.5347 \times H2 + 1576.9271 \times TC - 0.7612 \times H2^2 - 5.7690 \times TC^2 - 8.1633 \times H2 \times TC$$

6) H2 and CD vs Area; TC = 47.5 ^{o}C, CF = 4.375 ampere and FD = 0,55 mL/min

$$Area = 241818.6324 - 1416.0641 \times H2 - 108847.6952 \times CD - 0.7612 \times H2^2 + 48083.7449 \times CD^2 + 343.2181 \times H2 \times CD$$

FD = Flow rate of aqueous $NaBEt_4$ (0.1-1.0 mL/min)
H2 = Flow rate of hydrogen (10-100 mL/min)
CF = Current applied on the furnace (4.000-5.500 ampere)
TC = Temperature of the reaction coil (25-70 ^{o}C)
CD = Concentration of aqueous $NaBEt_4$ (0.1-1.0 % w/v)

Figure A-3-a. Regression analysis related to the determination of the limit of detection of Me_3PbCl.

Simple Regression of Me3PbCl on Amount

Parameter	Estimate	Standard Error	T Value	Prob. Level
Intercept	2278.36	4569.17	0.498637	0.62882
Slope	112091	1788.74	62.6649	2.59792E-14

Analysis of Variance

Source	Sum of Squares	Df	Mean Square	F-Ratio
Model	5.9782E0011	1	5.9782E0011	3.9269E0003
Error	1.5224E0009	10	1.5224E0008	
Total (Corr.)	5.9934E0011	11		

Correlation Coefficient = 0.998729
Stnd. Error of Est. = 12338.4

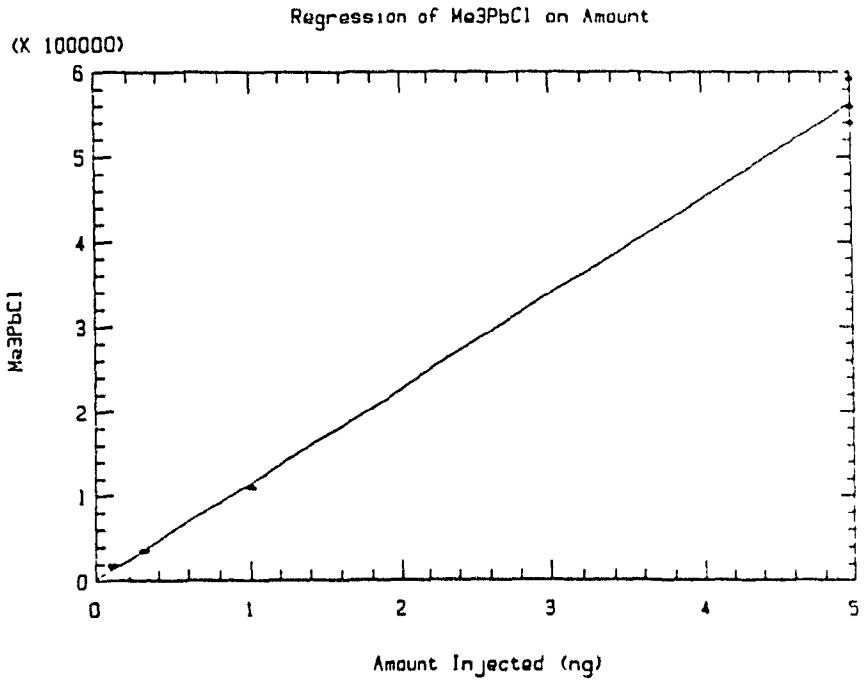

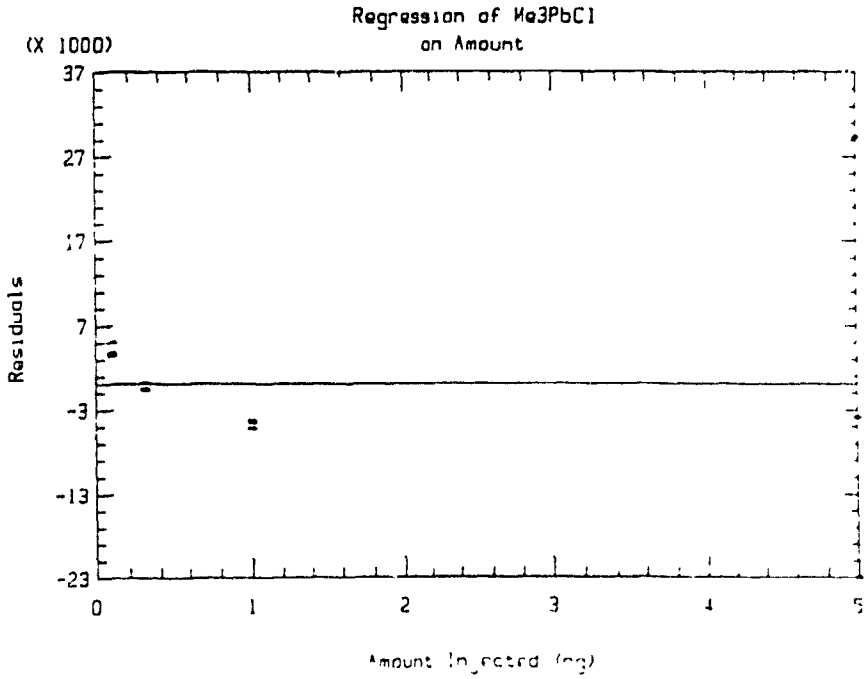

Figure A-3-c. Regression analysis related to the determination of the limit of detection of Et_3PbCl.

Simple Regression of Et3PbCl on Amount

Parameter	Estimate	Standard Error	T Value	Prob. Level
Intercept	-1499.79	4662.82	-0.321648	0.754342
Slope	94242.9	1825.4	51.6285	1.79856E-13

Analysis of Variance

Source	Sum of Squares	Df	Mean Square	F-Ratio
Model	4.2259E0011	1	4.2259E0011	2.6655E0003
Error	1.5854E0009	10	1.5854E0008	
Total (Corr.)	4.2418E0011	11		

Correlation Coefficient = 0.998129
Stnd. Error of Est. = 12591.3

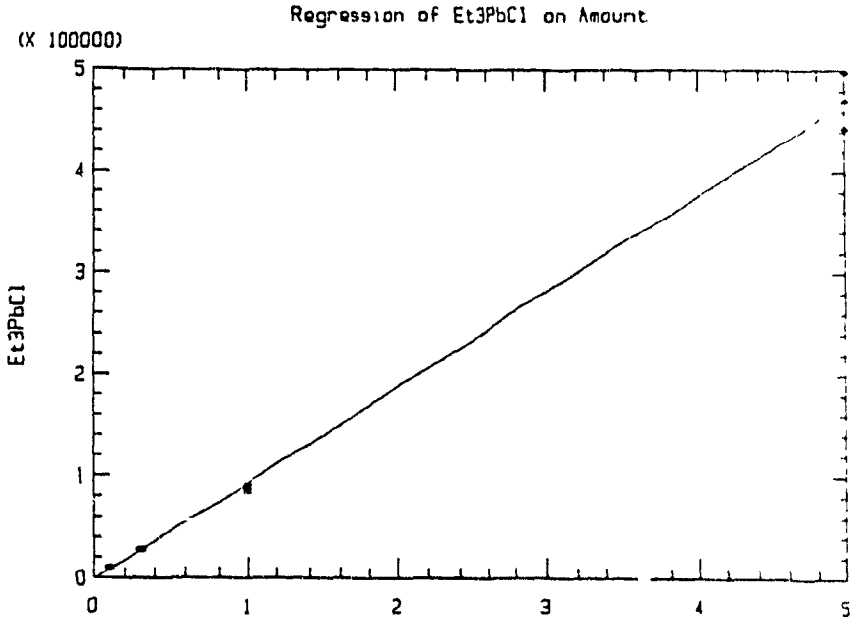

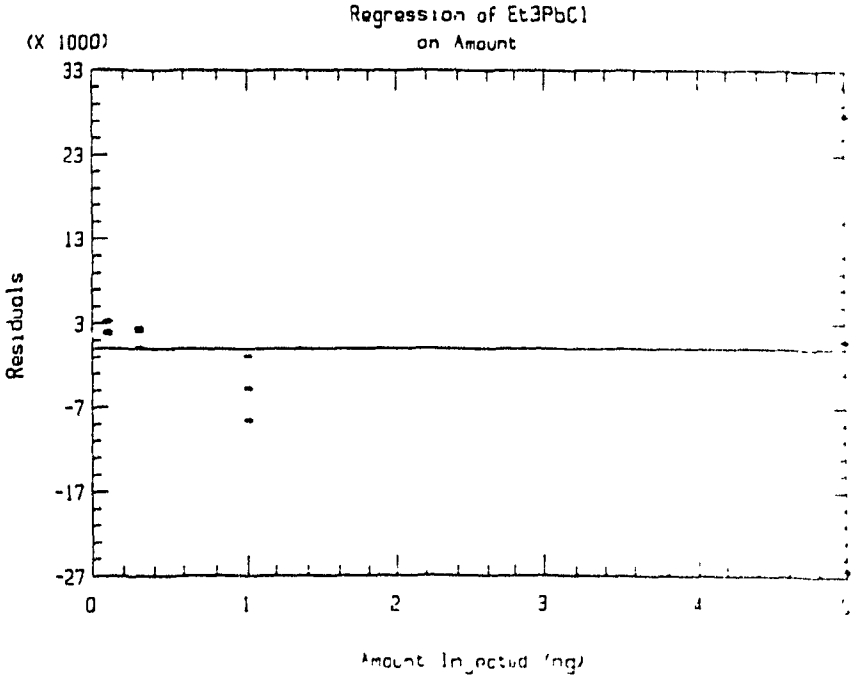

Figure A-3-d. Regression analysis related to the determination of the limit of detection of Et_2PbCl_2.

Simple Regression of Et2PbCl2 on Amount

Parameter	Estimate	Standard Error	T Value	Prob. Level
Intercept	2045.88	2823.74	0.724526	0.485349
Slope	63498.2	1105.44	57.4415	6.19504E-14

Analysis of Variance

Source	Sum of Squares	Df	Mean Square	F-Ratio
Model	1.9184E0011	1	1.9184E0011	3.2995E0003
Error	5.8143E0008	10	5.8143E0007	
Total (Corr.)	1.9242E0011	11		

Correlation Coefficient = 0.998488
Stnd. Error of Est. = 7625.13

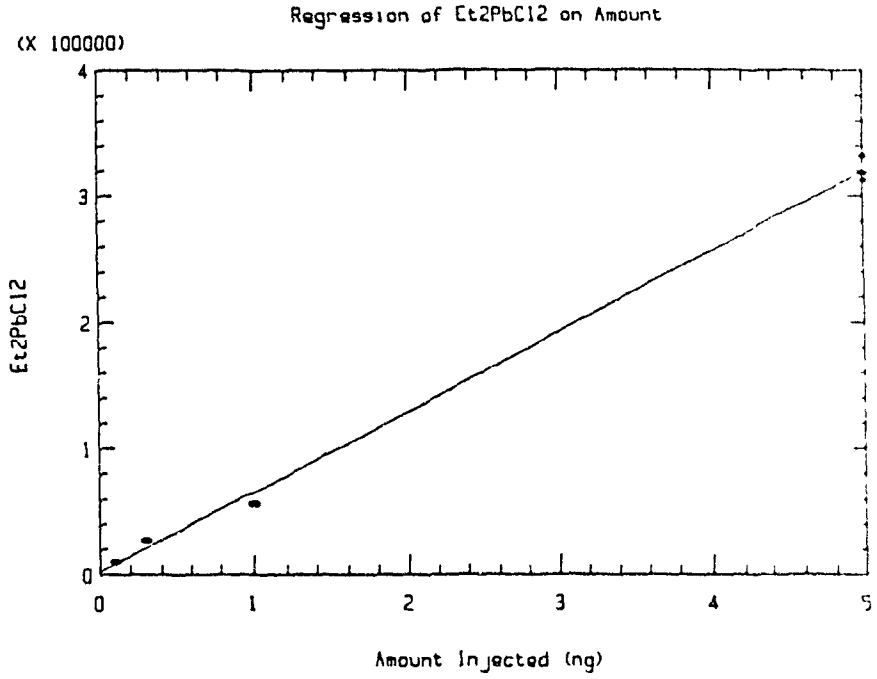

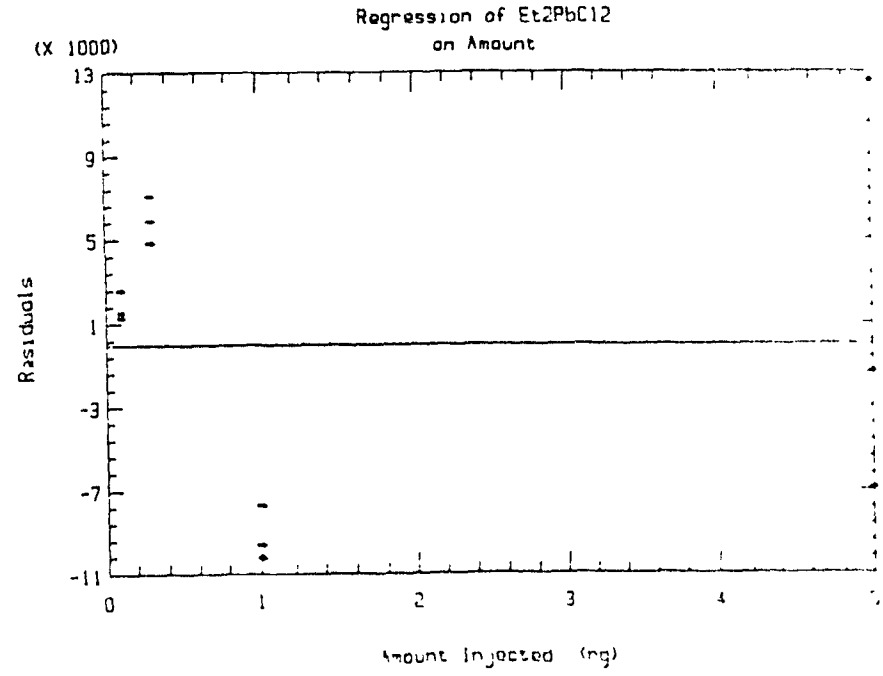

Figure A-3-b. Regression analysis related to the determination of the limit of detection of Me_2PbCl_2.

Simple Regression of Me2PbCl2 on Amount

Parameter	Estimate	Standard Error	T Value	Prob. Level
Intercept	-1374.58	3058.54	-0.449422	0.662711
Slope	87317	1197.36	72.9248	5.77316E-15

Analysis of Variance

Source	Sum of Squares	Df	Mean Square	F-Ratio
Model	3.6276E0011	1	3.6276E0011	5.3180E0003
Error	6.8214E0008	10	6.8214E0007	
Total (Corr.)	3.6344E0011	11		

Correlation Coefficient = 0.999061
Stnd. Error of Est. = 8259.16

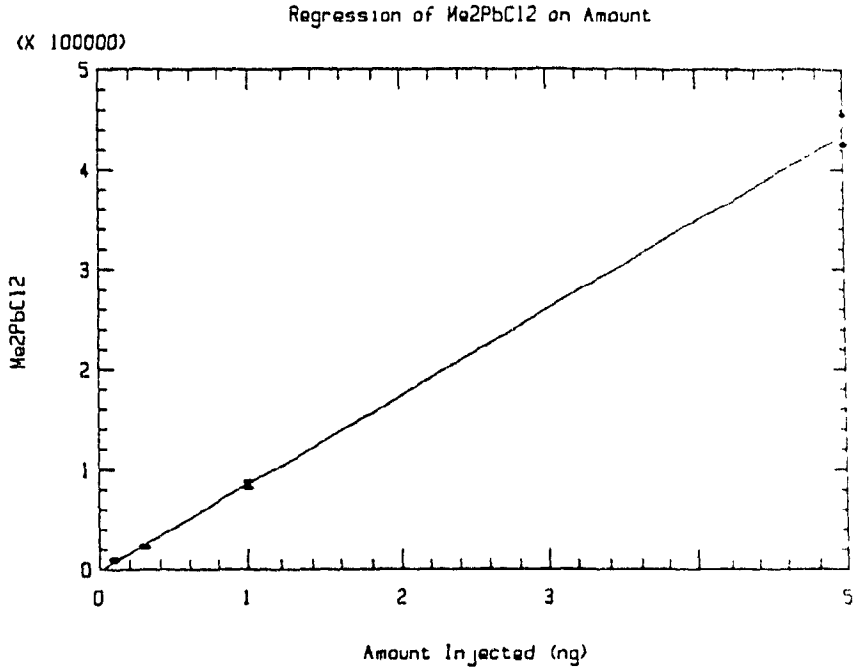

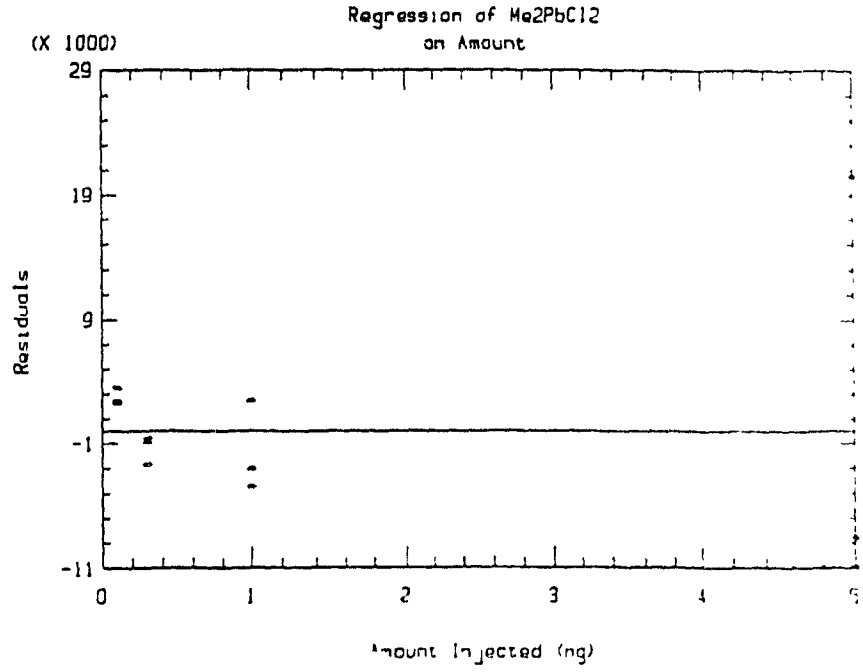

Appendix 3. Details of the Statistical Analyses Associated with the Optimization of the HPLC-Thermochemical Hydride Generator-AAS Instrument

A-3.1 Introduction

The statistical analyses associated to the characterization, optimization and performance of the HPLC-THG-AAS (Section 4) are presented. Tentative explanations for the effect of different variables on the THG performance are also suggested.

A-3.2 Method

As described in sections 4.2.1 and 4.3.2, a half-replicate 2^5 composite design was used to fit a theoretical model for predicting the performances of the THG interface. The principles of this approach are presented in Appendix 2. The limits of detection for each selenonium and arsonium analytes were determined as described previously (Appendix 1).

A-3.3 Results and Discussion

A-3.3.1 THG Performances

The matrix of the half-replicate 2^5 composite design is presented in Table A-5. The performance of the THG interface was modeled for both arsonium and selenonium analytes. Since the HPLC method to be used had not been developed at this time, two HPLC mobile phase modifiers, diethyl ether for normal phase HPLC or water for reversed phase HPLC, were tested individually. This combination resulted in four models, which were characterized by a significant lack of fit ($p < 0.05$). However, as discussed in Section 4.3.2 the accuracy of these models [based on correlation coefficients of predicted vs observed regressions (Figures A-4, A-6, A-8 and A-10)] was considered adequate for estimating the optimum operating

parameter from surface response plots. The curvature of these plots provided valuable information for a tentative characterization of the simple, quadratic and interaction effects provided by the variables.

The effects of the five variables [flow rate of thermospray (OT) and analytical oxygen (OA), hydrogen (H2), mobile phase (FR) and the proportion of modifier (PE for ether or PW for water) were characterized by plotting two selected variables vs response while keeping the three other variables constant at the center of the design.

A-3 3.2 Effects of Variables with Ether as HPLC Eluent Modifier

The experimental results, statistical analyses, quadratic surface response equations and plots resulting from these experiments are presented in Tables A-6 to A-11 and Figures A-4 to A-7. The combined effects of mobile phase (FR) and thermospray oxygen (OT) flow rates (with PE at 20 %, H2 at 1.7 L/min and OA at 170 mL/min) were similar for both analytes (As, Figure A-5-a; Se Figure A-7-a). The response was maximized at ca. intermediate values (OT = 650 mL/min; FR = 0.62 mL/min). The minimum response occurred at low OT and high FR; visually, these conditions resulted in a short thermospray flame and a slow accumulation of carbon deposits in the THG combustion chamber. A similar pattern was observed when the proportion of ether (PE) was combined with OT (Figures A-5-b and A-7-b). In this case, the THG-AAS response was decreased by about 40 % (relative to maximum) at high PE and low OT, reflecting an incomplete combustion of the mobile phase. When combined with a proper level of OT, the presence of diethyl ether appeared to be beneficial. Thus, the optimum response for both analytes were obtained when OT, FR and PE values were around the center of the design.

The interaction between the effects of H2 and OT was demonstated in the resulting surface response (Figures A-5-c and A-7-c). At low OT the response was generally lower (with a maxima occuring at 1.7 L/min H2), which was presumably the results of a cooler thermospray flame (affecting analytes derivatization). At high OT and low H2, this flame was vigorous but a minimum response was still observed, most probably reflecting a rapid consumption of H_2 by excess oxygen. Increasing the flow rate of hydrogen resulted in higher responses; at higher H2 and OT levels, a secondary H_2/O_2 flame was ignited at the H_2 inlet tube. The detrimental effect of this secondary flame corroborated previous observations suggesting that excessive post-thermospray temperatures were decreasing the performance of the interface. Again, the maximum response occurred at intermediate levels of H_2 and thermospray O_2.

The interaction between H2 and the level of analytical oxygen (Figures A-5-d and A-7-d) demonstrated the previously reported characteristics of this atomization mechanism (Dedina and Rubeska, 1980), which requires a fuel rich flame. The minimum observed at low OA was resulting from a appreciable reduction in the volume of the analytical flame. Over the variable ranges studied, the difference between minimum and maximum responses was generally less than 50% (relative to maximum). Thus, the performance of this interface was only slightly affected by appreciable variations in the levels of the five variables. This characteristic was reflected in the relatively high long term reproducibility of the instrument (Table 7). Once optimum normal-phase chromatographic conditions were known (FR and PE then became constants), these two models (for As and Se) were applied to optimise response of the interface (Section 4, Figure 22).

A-3.3.3 Effects of Variables with Water as HPLC Eluent Modifier

The experimental results, statistical analyses, quadratic surface responses equations and plots resulting from these experiments are presented in Tables A-12 to A-17 and Figures A-8 to A-11. The presence of water in the mobile phase was generally detrimental for both analytes. For arsenic (Figure A-9-a), the flow rate of the mobile phase (FR, containing 20 % water) affected (in a ca. proportional relationship) the sensitivity when combined with high thermospray oxygen flow rates (OT). Surprisingly, this effect was inversely proportional for the Se analyte (maximum response observed at low FR and high OT, Figure A-11-a). The latter condition resulted in a relatively cool thermospray flame (fuel deficient). Since the temperature of this flame may affect the thermochemical hydride generation in at least three steps (pyrolysis of analyte, formation of the hydride, post-thermospray thermal decomposition of the hydride) it is difficult to provide a clear explanation for this difference. However, from these observations it can be speculated that this difference results from the relative thermal stability of the two hydrides (i.e. arsine would be less susceptible to thermal decomposition than selenium hydride). The combined effects of water content (PW) and OT somewhat support this hypothesis (Figures A-9-b vs A-11-b). For arsenic, a maximum response was obtained at higher flame temperature (low water content) whereas selenium was most efficiently detected in a cooler (high water content) environment.

The combined effects of H2 and OT on the response of TMAsI (Figure A-9-c) was relatively small, with a maximum around high H2 and OT levels. These latter conditions resulted in a secondary H_2/O_2 flame at the H_2 inlet which increased appreciably the temperatures of post-thermospray gases. These same conditions were detrimental to the response for selenium (Figure A-11-c). For this analyte, a maximum response occurred at high OT and low H2 (cooler post-thermospray

environment). At low OT, the thermospray flame was barely burning (20 % water was present in the mobile phase), resulting in a low response for both analytes.

The interaction between H2 and the level of analytical oxygen (OA) (Figure A-9-d and A-11-d) was somewhat independent of the type of mobile phase modifier present (ether or water). Again, within the variable ranges studied, the difference between the minimum and the maximum responses was relatively small (less than 55%, relative to maximum). Thus, the THG interface is also compatible with reversed-phase HPLC. One approach to minimize the detrimental effect of water on sensitivity would be to combine a micro-HPLC method (optimum flow rate 0.3 to 0.5 mL/min) with post-column methanol enrichment (0.5 to 0.7 mL/min).

A-3.3.4 Calibration

The limits of detections for the arsonium and selenonium analytes (Section 4.3.5) were determined from the linear regressions statistics presented in Figures A-13 and A-14.

Table A-5. Matrix of the Augmented 1/2 replicate 2^5 Factorial Design.

Point	Flow Rate Thermo O_2	Flow rate H_2	Flow Rate Analyt O_2	Flow Rate Eluent	% Water or Ether
1	1[a]	-1	-1	-1	-1
2	-1	1	-1	-1	-1
3	-1	-1	1	-1	-1
4	1	1	1	-1	-1
5	-1	-1	-1	1	-1
6	1	1	-1	1	-1
7	1	-1	1	1	-1
8	-1	1	1	1	-1
9	-1	-1	-1	-1	1
10	1	1	-1	-1	1
11	1	-1	1	-1	1
12	-1	1	1	-1	1
13	1	-1	-1	1	1
14	-1	1	-1	1	1
15	-1	-1	1	1	1
16	1	1	1	1	1
17	C	0	0	0	0
18	-2	0	0	0	0
19	2	0	0	0	0
20	0	-2	0	0	0
21	0	2	0	0	0
22	0	0	-2	0	0
23	0	0	2	0	0
24	0	0	0	-2	0
25	0	0	0	2	0
26	0	0	0	0	-2
27	0	0	0	0	2

[a] Coded value

Table A-6. Observed and Predicted Results of the Factorial Experiment. Arsonium Analyte with Ether as Eluent Modifier

Point	F.R. T-O_2 mL/min	F.R H_2 L/min	F.R. A-O_2 mL/min	F.R. Eluent mL/min	PE % (v/v)	Response Observed	Response Predicted	Deviation[a] %
1	725	1.35	135	0.47	10	837720	910827	8.71
1	725	1.35	135	0.47	10	865540	910827	5.23
1	725	1.35	135	0.47	10	851730	910827	6.94
2	575	2.05	135	0.47	10	896040	971489	8.42
2	575	2.05	135	0.47	10	900420	971489	7.89
2	575	2.05	135	0.47	10	885980	971489	9.65
3	575	1.35	205	0.47	10	880090	988549	12.32
3	575	1.35	205	0.47	10	888030	988549	11.32
3	575	1.35	205	0.47	10	879220	988549	12.43
4	725	2.05	205	0.47	10	834990	903344	8.19
4	725	2.05	205	0.47	10	820140	903344	10.15
4	725	2.05	205	0.47	10	835290	903344	8.15
5	575	1.35	135	0.82	10	704720	686391	2.60
5	575	1.35	135	0.82	10	713070	686391	3.74
5	575	1.35	135	0.82	10	714910	686391	3.99
6	725	2.05	135	0.82	10	827960	763696	7.76
6	725	2.05	135	0.82	10	830950	763696	8.09
6	725	2.05	135	0.82	10	804400	763696	5.06
7	725	1.35	205	0.82	10	709200	685846	3.29
7	725	1.35	205	0.82	10	717940	685846	4.47
7	725	1.35	205	0.82	10	716340	685846	4.26
8	575	2.05	205	0.82	10	697980	686565	1.64
8	575	2.05	205	0.82	10	706270	686565	2.79
8	575	2.05	205	0.82	10	686850	686565	0.04
9	575	1.35	135	0.47	30	866560	972825	12.26
9	575	1.35	135	0.47	30	883590	972825	10.10
9	575	1.35	135	0.47	30	879480	972825	10.61
10	725	2.05	135	0.47	30	870160	913037	4.93
10	725	2.05	135	0.47	30	824300	913037	10.77
10	725	2.05	135	0.47	30	854500	913037	6.85
11	725	1.35	205	0.47	30	673660	768444	14.07
11	725	1.35	205	0.47	30	689160	768444	11.50
11	725	1.35	205	0.47	30	666080	768444	15.37
12	575	2.05	205	0.47	30	916980	1030095	12.34
12	575	2.05	205	0.47	30	914950	1030095	12.58
12	575	2.05	205	0.47	30	927390	1030095	11.07
13	725	1.35	135	0.82	30	759350	720936	5.06
13	725	1.35	135	0.82	30	753960	720936	4.38
13	725	1.35	135	0.82	30	764900	720936	5.75
14	575	2.05	135	0.82	30	514920	489867	4.87
14	575	2.05	135	0.82	30	501300	489867	2.20
14	575	2.05	135	0.82	30	514250	489867	4.74
15	575	1.35	205	0.82	30	521860	522421	0.11
15	575	1.35	205	0.82	30	504720	522421	3.51
15	575	1.35	205	0.82	30	515270	522421	1.39

Table A-6.Observed and Predicted Results of the Factorial Experiment. Arsonium Analyte with Ether as Eluent Modifier.

Point	F.R. $T\text{-}O_2$ mL/min	F.R H_2 L/min	F.R. $A\text{-}O_2$ mL/min	F.R. Eluent mL/min	PE %(v/v)	Response Observed	Response Predicted	Deviation[a] %
16	725	2.05	205	0.82	30	851950	818842	3.89
16	725	2.05	205	0.82	30	837280	818842	2.20
16	725	2.05	205	0.82	30	840580	818842	2.59
17	650	1.70	170	0.65	20	944300	999946	5.89
17	650	1.70	170	0.65	20	952250	999946	5.01
17	650	1.70	170	0.65	20	961920	999946	3.95
17	650	1.70	170	0.65	20	975950	999946	2.46
17	650	1.70	170	0.65	20	946930	999946	5.60
17	650	1.70	170	0.65	20	947860	999946	5.50
17	650	1.70	170	0.65	20	952350	999946	5.00
17	650	1.70	170	0.65	20	956360	999946	4.56
18	500	1.70	170	0.65	20	948510	841167	11.32
18	500	1.70	170	0.65	20	949850	841167	11.44
18	500	1.70	170	0.65	20	959200	841167	12.31
19	800	1.70	170	0.65	20	893290	875360	2.01
19	800	1.70	170	0.65	20	891080	875360	1.76
19	800	1.70	170	0.65	20	869310	875360	0.70
20	650	1.00	170	0.65	20	888150	816057	8.12
20	650	1.00	170	0.65	20	893400	816057	8.66
20	650	1.00	170	0.65	20	891610	816057	8.47
21	650	2.40	170	0.65	20	950220	896231	5.68
21	650	2.40	170	0.65	20	934340	896231	4.08
21	650	2.40	170	0.65	20	940800	896231	4.74
22	650	1.70	100	0.65	20	832530	819244	1.60
22	650	1.70	100	0.65	20	830390	819244	1.34
22	650	1.70	100	0.65	20	847240	819244	3.30
23	650	1.70	240	0.65	20	928930	813004	12.48
23	650	1.70	240	0.65	20	904740	813004	10.14
23	650	1.70	240	0.65	20	914570	813004	11.11
24	650	1.70	170	0.30	20	1274600	986862	22.57
24	650	1.70	170	0.30	20	1256600	986862	21.47
24	650	1.70	170	0.30	20	1265480	986862	22.02
25	650	1.70	170	1.00	20	305920	465850	52.28
25	650	1.70	170	1.00	20	307660	465850	51.42
25	650	1.70	170	1.00	20	309532	465850	50.50
26	650	1.70	170	0.65	0	1055500	996382	5.60
26	650	1.70	170	0.65	0	1015900	996382	1.92
26	650	1.70	170	0.65	0	1029100	996382	3.18
27	650	1.70	170	0.65	40	982340	906322	7.74
27	650	1.70	170	0.65	40	987640	906322	8.23
27	650	1.70	170	0.65	40	999290	906322	9.30

[a] Deviation of observed from predicted values (|obs-pred.|)/obs x 100

Figure A-4-a. Regression Analysis of Observed vs Predicted Values (arsonium analyte with ether as modifier).

Simple Regression of OBSERVED on PREDICTED

Parameter	Estimate	Standard Error	T Value	Prob. Level
Intercept	-11463.9	36722.4	-0.312131	0.7566
Slope	1.01694	0.115304	8.8191	0.0000

Analysis of Variance

Source	Sum of Squares	DF	Mean Square	F-Ratio
Model	6.6636E0011	1	6.6636E0011	77.7782
Error	2.1424E0011	25	8.5694E0009	
Total (Corr.)	8.8060E0011	26		

Correlation Coefficient = 0.868392
Stnd. Error of Est. = 92572.1

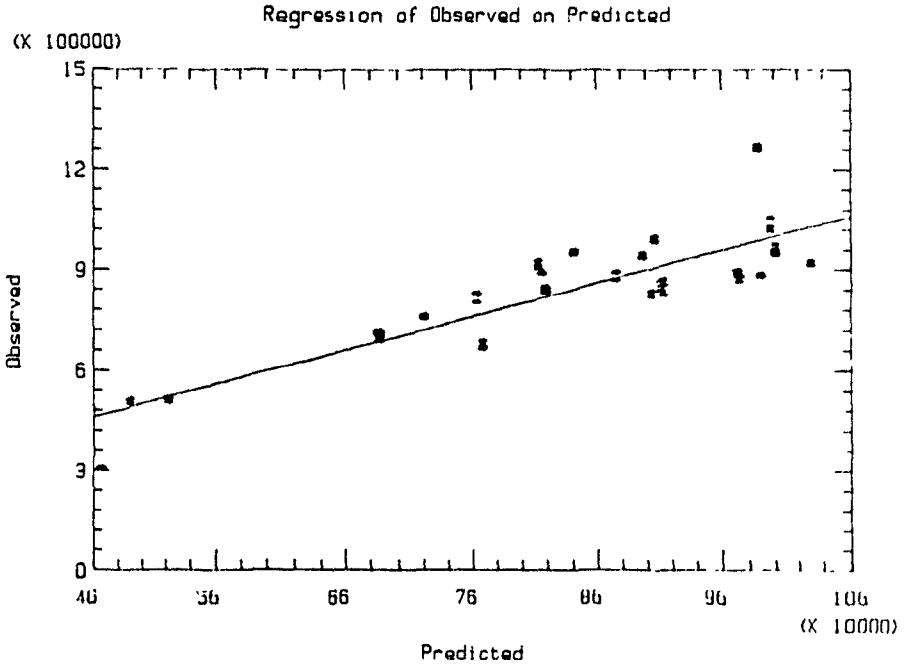

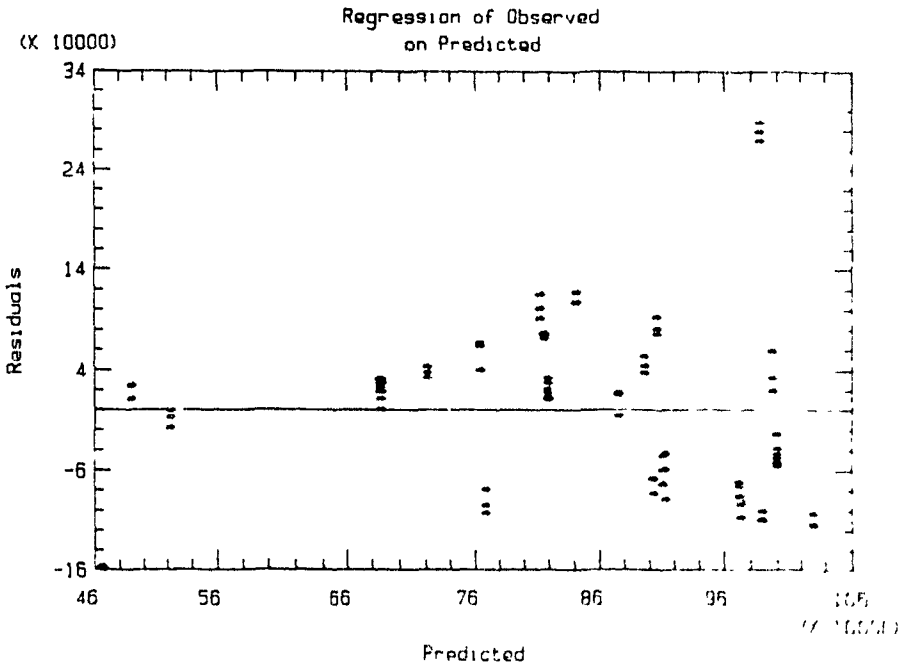

Table A-7. Analysis of Variance and Regression Estimates. Arsonium Analyte with Ether as Eluent Modifier.

Response Mean: 834285.7
Root MSE : 100108.8
R-square : 0.760965
Coef.of Var. : 0.1199934

Regression	Df	Type I SS	R-Square	F-Ratio	Prob.
Linear	5	1.29240E+12	0.4742	25.79	0.0001
Quadratic	5	429769744972	0.1577	8.58	0.0001
Crossproduct	10	351603537804	0.1290	3.51	0.0010
Tot. Regress	20	2.07377E+12	0.7610	10.35	0.0001

Residual	Df	SS	Mean Square	F-Ratio	Prob.
Lack of fit	6	645059217809	107509869635	997.998	0.0001
Pure error	59	6355807909	107725558		
Total error	65	651415025718	10021769626		

Parameters	Df	Estimate	Std Dev	T-Ratio	Prob.
Intercept	1	999946.73	33637.62951	29.73	0.0001
OT[a]	1	8548.19444	11797.93392	0.72	0.4713
H2[b]	1	20043.47222	11797.93392	1.70	0.0941
OA[c]	1	-1560.13889	11797.93392	-0.13	0.8952
FR[d]	1	-130252.86	11797.933^2	-11.04	0.0001
PE[e]	1	-22515.13889	11797.93392	-1.91	0.0608
OT*OT	1	-35420.59005	11892.69797	-2.98	0.0041
H2*OT	1	19064.79167	14449.45906	1.32	0.1917
H2*H2	1	-35950.59005	11892.69797	-3.02	0.0036
OA*OT	1	-14942.29167	14449.45906	-1.03	0.3049
OA*H2	1	39154.79167	14449.45906	2.71	0.0086
OA*OA	1	-45955.59005	11892.69797	-3.86	0.0003
FR*OT	1	66961.45833	14449.45906	4.63	0.0001
FR*H2	1	-2121.45833	14449.45906	-0.15	0.8837
FR*OA	1	8158.12500	14449.45906	0.56	0.5743
FR*FR	1	-68397.59007	11892.69797	-5.75	0.0001
PE*OT	1	17208.12500	14449.45906	1.19	0.2380
PE*H2	1	13358.54167	14449.45906	0.92	0.3586
PE*OA	1	6952.29167	14449.45906	0.48	0.6320
PE*FR	1	-11288.95833	14449.45906	-0.78	0.4375
PE*PE	1	-12148.50672	11892.69797	-1.02	0.3108

[a]OT = Flow rate of thermospray oxygen (500-800 mL/min)
[b]H2 = Flow rate of hydrogen (1.00-2.40 L/min)
[c]OA = Flow rate of analytical oxygen (100-240 mL/min)
[d]FR = Flow rate of eluent (0.3-1.0 mL/min)
[e]PE = Proportion of diethyl ether in eluent (0-40 % v/v)

Table A-8. Factorial Second Order Equations Predicting the Effects of Selected Variables on Analyte Response. Arsonium Analyte with Ether as Eluent Modifier.

1) H2 and OT v Area; FR=0[a] (0.65 mL/min), OA=-2 (100 mL/min), PE=1 (30 %)
Ref. Figure 22-A-1

$$Area = 770676.4 - 44907.5 \times H2 + 55640.9 \times OT - 35950.5 \times H2^2 - 35420.5 \times OT^2 + 19064.79 \times H2 \times OT$$

2) H2 and OT v Area; FR=0 (0.65 mL/min), OA=0 (170 mL/min), PE=1 (30 %)
Ref. Figure 22-A-2

$$Area = 965283.0 + 33402.01 \times H2 - 25756.31 \times OT - 35950.5 \times H2^2 - 35420.5 \times OT^2 + 19064.79 \times H2 \times OT$$

3) H2 and OT v Area; FR=0 (0.65 mL/min), OA=2 (240 mL/min), PE=1 (30 %)
Ref. Figure 22-A-3

$$Area = 792245.0 + 111711.5 \times H2 - 4128.26 \times OT - 35950.5 \times H2^2 - 35420.5 \times OT^2 + 19064.79 \times H2 \times OT$$

4) OT and FR vs Area; H2=0 (1.7 L/min), OA=0 (170 mL/min), PE=0 (20 %)
Ref. Figure A-5-a

$$Area = 999946.7 + 8548.194 \times OT - 130252.3 \times FR - 35420.5 \times OT2 - 68397.5 \times FR2 + 66961.45 \times OT \times FR$$

5) PE and OT vs Area; FR=0(0.65 mL/min), H2=0(1.7 L/min),OA=0(170 mL/min)
Ref. Figure A-5-b

$$Area = 999946.7 - 22515.1 \times PE + 25756.31 \times OT - 12148.5 \times PE^2 - 35420.5 \times OT^2 + 17208.12 \times PE \times OT$$

6) H2 and OT v Area; FR=0 (0.65 mL/min), OA=0 (170 mL/min), PE=0 (20 %)
Ref. Figure A-5-c

$$Area = 999946.7 + 20043.47 \times H2 + 8548.194 \times OT - 35950.5 \times H2^2 - 35420.5 \times OT^2 + 19064.79 \times H2 \times OT$$

7) H2 and OA vs Area; FR=0 (0.65 mL/min), OT=0 (650 mL/min), PE=0 (20 %)
Ref. Figure A-5-d

$$Area = 999946.7 + 20043.47 \times H2 - 1560.13 \times OA - 35950.5 \times H2^2 - 45955.5 \times OA^2 + 39154.79 \times H2 \times OA$$

[a] Variables expressed in coded values (Table A-5)
OT = Flow rate of thermospray oxygen (500-800 mL/min)
H2 = Flow rate of hydrogen (1.00-2.40 L/min)
OA = Flow rate of analytical oxygen (100-240 mL/min)
FR = Flow rate of eluent (0.3-1.0 mL/min)
PE = Proportion of diethyl ether in eluent (0-40 % v/v)

Figure A-5-a. Exploratory response surfaces (arsonium analyte with ether as modifier) of peak area versus two selected variables. The three other variables were kept constant at the center (coded value of 0) of the factorial design. The quadratic functions describing these surfaces are presented in Table A-8.

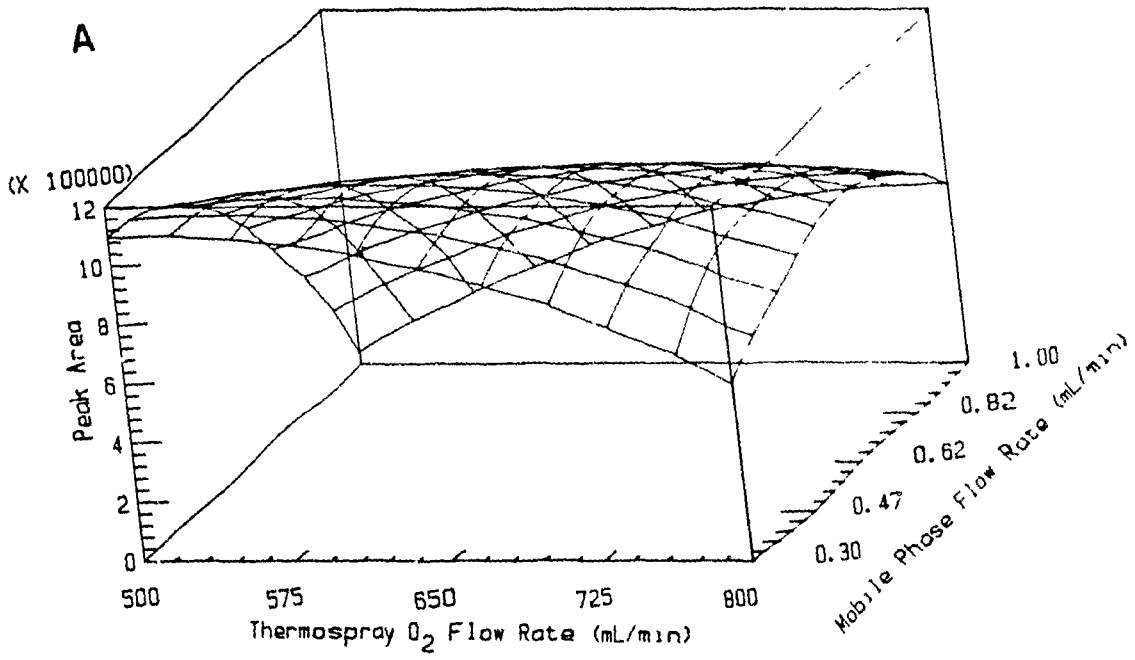
A
(X 100000)
12
10
8
6
4
2
0
Peak Area
500
575
650
725
800
Thermospray O_2 Flow Rate (mL/min)
1.00
0.82
0.62
0.47
0.30
Mobile Phase Flow Rate (mL/min)

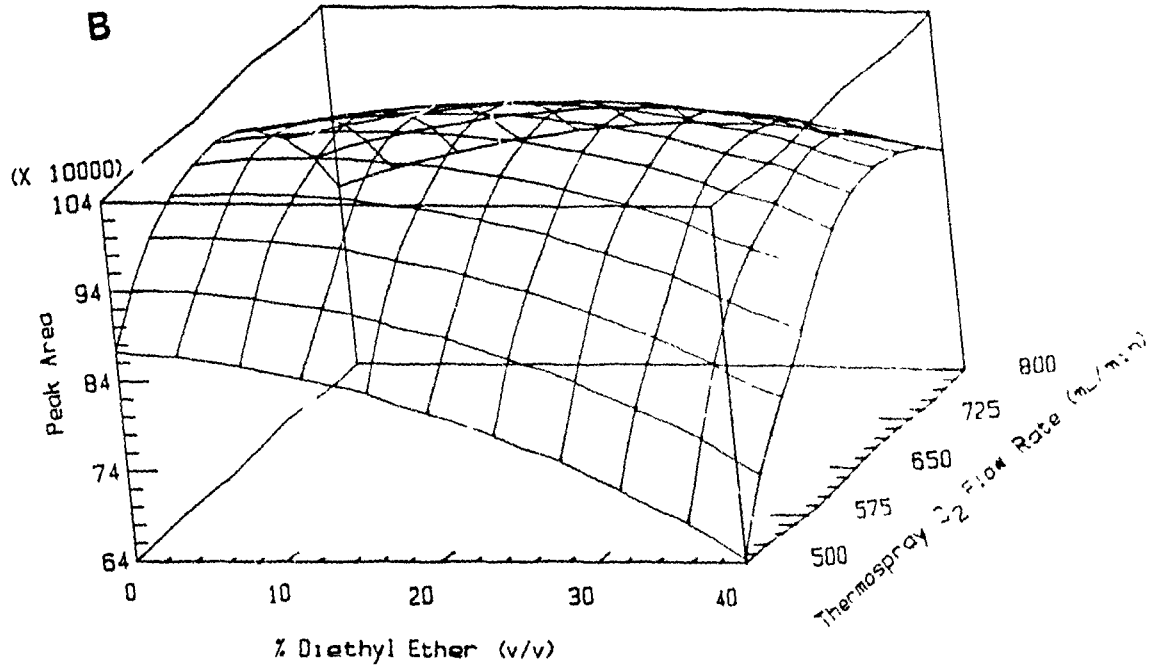
B
(X 10000)
104
94
84
74
64
Peak Area
0
10
20
30
40
% Diethyl Ether (v/v)
800
725
650
575
500
Thermospray O_2 Flow Rate (mL/min)

Figure A-5-b. Exploratory response surfaces (arsonium analyte with ether as modifier) of peak area versus two selected variables. The three other variables were kept constant at the center (coded value of 0) of the factorial design. The quadratic functions describing these surfaces are presented in Table A-8.

C

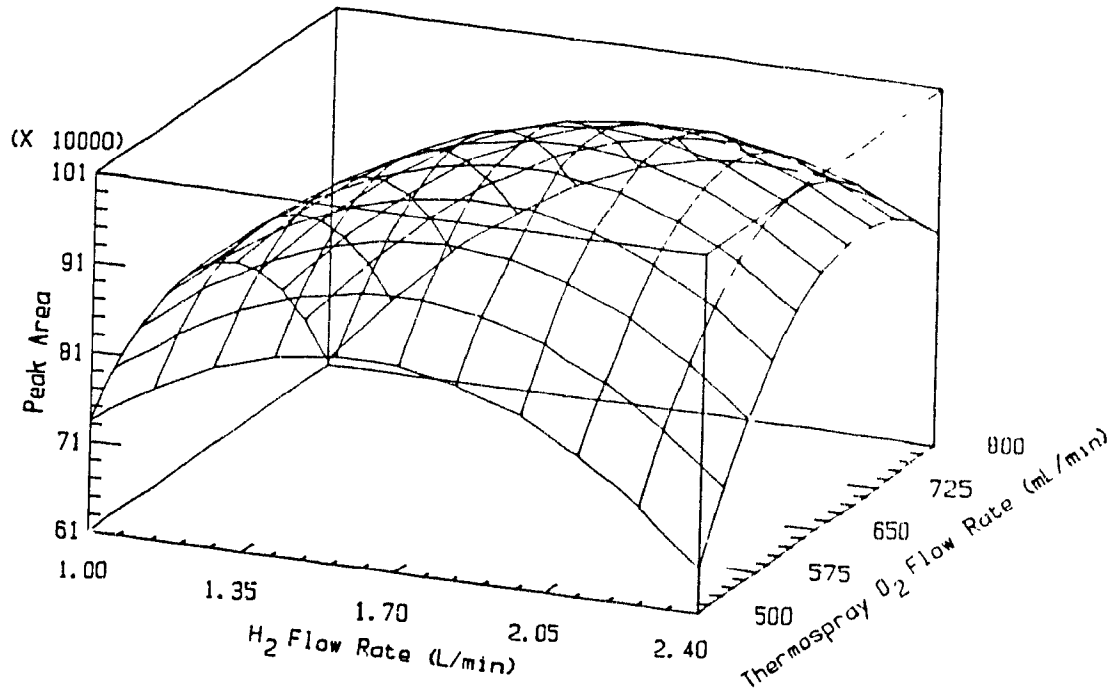
(X 10000)
101
91
81
71
61
Peak Area
1.00
1.35
1.70
2.05
2.40
H2 Flow Rate (L/min)
500
575
650
725
800
Thermospray O2 Flow Rate (mL/min)

D

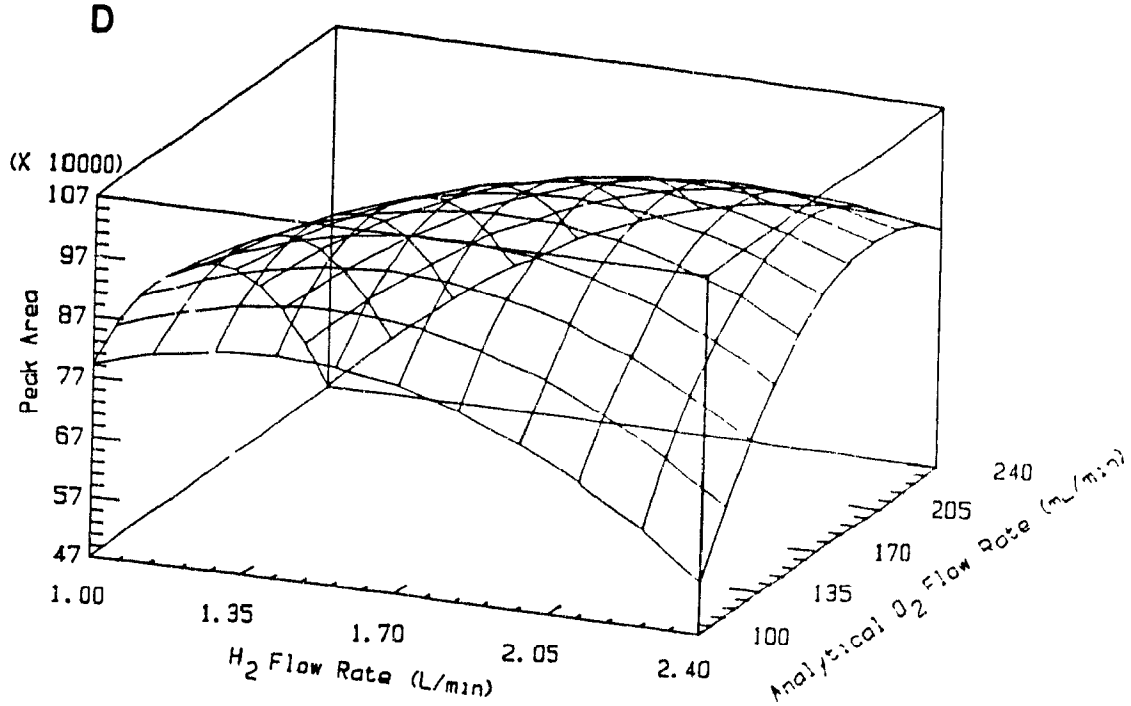
(X 10000)
107
97
87
77
67
57
47
Peak Area
1.00
1.35
1.70
2.05
2.40
H2 Flow Rate (L/min)
100
135
170
205
240
Analytical O2 Flow Rate (mL/min)

Table A-9. Observed and Predicted Results of the Factorial Experiment. Selenonium Analyte with Ether as Eluent Modifier.

Point	F.R. $T\text{-}O_2$ mL/min	F.R H_2 L/min	F.R. $A\text{-}O_2$ mL/min	F.R. Eluent mL/min	PE % (v/v)	Response Observed	Response Predicted	Deviation[a] %
1	725	1.35	135	0.47	10	446840	454657	1.75
1	725	1.35	135	0.47	10	456310	454657	0.36
1	725	1.35	135	0.47	10	433550	454657	4.87
2	575	2.05	135	0.47	10	364580	401874	10.23
2	575	2.05	135	0.47	10	366540	401874	9.64
2	575	2.05	135	0.47	10	363940	401874	10.42
3	575	1.35	205	0.47	10	481950	500499	3.85
3	575	1.35	205	0.47	10	484030	500499	3.40
3	575	1.35	205	0.47	10	492030	500499	1.72
4	725	2.05	205	0.47	10	438960	464500	5.82
4	725	2.05	205	0.47	10	442070	464500	5.07
4	725	2.05	205	0.47	10	443590	464500	4.71
5	575	1.35	135	0.82	10	268470	280835	4.61
5	575	1.35	135	0.82	10	267360	280835	5.04
5	575	1.35	135	0.82	10	269200	280835	4.32
6	725	2.05	135	0.82	10	259290	280750	8.28
6	725	2.05	135	0.82	10	257170	280750	9.17
6	725	2.05	135	0.82	10	262920	280750	6.78
7	725	1.35	205	0.82	10	382410	379661	0.72
7	725	1.35	205	0.82	10	381080	379661	0.37
7	725	1.35	205	0.82	10	379700	379661	0.01
8	575	2.05	205	0.82	10	341700	370231	8.35
8	575	2.05	205	0.82	10	345660	370231	7.11
8	575	2.05	205	0.82	10	344250	370231	7.55
9	575	1.35	135	0.47	30	402190	434939	8.14
9	575	1.35	135	0.47	30	407730	434939	6.67
9	575	1.35	135	0.47	30	403180	434939	7.88
10	725	2.05	135	0.47	30	354260	393384	11.04
10	725	2.05	135	0.47	30	353060	393384	11.42
10	725	2.05	135	0.47	30	355720	393384	10.59
11	725	1.35	205	0.47	30	486780	500899	2.90
11	725	1.35	205	0.47	30	485560	500899	3.16
11	725	1.35	205	0.47	30	480320	500899	4.28
12	575	2.05	205	0.47	30	452480	499996	10.50
12	575	2.05	205	0.47	30	462180	499996	8.18
12	575	2.05	205	0.47	30	452000	499996	10.62
13	725	1.35	135	0.82	30	348870	363089	4.08
13	725	1.35	135	0.82	30	343490	363089	5.71
13	725	1.35	135	0.82	30	352880	363089	2.89
14	575	2.05	135	0.82	30	172840	213278	23.40
14	575	2.05	135	0.82	30	171200	213278	24.58
14	575	2.05	135	0.82	30	168480	213278	26.59
15	575	1.35	205	0.82	30	253920	275760	8.60
15	575	1.35	205	0.82	30	257980	275760	6.89
15	575	1.35	205	0.82	30	255140	275760	8.08

Table A-9 Observed and Predicted Results of the Factorial Experiment. Selenonium Analyte with Ether as Eluent Modifier.

Point	F.R. T-O_2 mL/min	F.R H_2 L/min	F.R. A-O_2 mL/min	F.R. Eluent mL/min	PE % (v/v)	Response Observed	Response Predicted	Deviation[a] %
16	725	2.05	205	0.82	30	394640	429865	8.93
16	725	2.05	205	0.82	30	404450	429865	6.28
16	725	2.05	205	0.82	30	404870	429865	6.17
17	650	1.70	170	0.65	20	463410	481576	3.92
17	650	1.70	170	0.65	20	463390	481576	3.91
17	650	1.70	170	0.65	20	440130	481576	9.42
17	650	1.70	170	0.65	20	435860	481576	10.49
17	650	1.70	170	0.65	20	441430	481576	9.09
17	650	1.70	170	0.65	20	440270	481576	9.38
17	650	1.70	170	0.65	20	441810	481576	9.00
17	650	1.70	170	0.65	20	442600	481576	8.81
18	500	1.70	170	0.65	20	399230	337776	15.39
18	500	1.70	170	0.65	20	405910	337776	16.79
18	500	1.70	170	0.65	20	407940	337776	17.20
19	800	1.70	170	0.65	20	445860	410125	8.01
19	800	1.70	170	0.65	20	438240	410125	6.42
19	800	1.70	170	0.65	20	430240	410125	4.68
20	650	1.00	170	0.65	20	488430	490098	0.34
20	650	1.00	170	0.65	20	505940	490098	3.13
20	650	1.00	170	0.65	20	509100	490098	3.75
21	650	2.40	170	0.65	20	539850	455983	15.54
21	650	2.40	170	0.65	20	529790	455983	13.93
21	650	2.40	170	0.65	20	548850	455983	16.92
22	650	1.70	100	0.65	20	329590	277488	15.81
22	650	1.70	100	0.65	20	336740	277488	17.60
22	650	1.70	100	0.65	20	333460	277488	16.78
23	650	1.70	240	0.65	20	463350	427139	7.81
23	650	1.70	240	0.65	20	473570	427139	9.80
23	650	1.70	240	0.65	20	460890	427139	7.32
24	650	1.70	170	0.30	20	577720	520960	9.82
24	650	1.70	170	0.30	20	579370	520960	10.08
24	650	1.70	170	0.30	20	585140	520960	10.97
25	650	1.70	170	1.00	20	282770	256640	9.24
25	650	1.70	170	1.00	20	311750	256640	17.68
25	650	1.70	170	1.00	20	279770	256640	8.27
26	650	1.70	170	0.65	0	482490	457250	5.23
26	650	1.70	170	0.65	0	485770	457250	5.87
26	650	1.70	170	0.65	0	474350	457250	3.60
27	650	1.70	170	0.65	40	526710	451801	14.22
27	650	1.70	170	0.65	40	517900	451801	12.76
27	650	1.70	170	0.65	40	523650	451801	13.72

[a] Deviation of observed from predicted values (|obs-pred.|)/obs x 100

Figure A-6-a. Regression Analysis of Observed vs Predicted Values (selenonium analyte with ether as modifier).

Simple Regression of OBSERVED on PREDICTED

Parameter	Estimate	Standard Error	T Value	Prob. Level
Intercept	-6000.30	36489.7	-0.164494	0.870665
Slope	1.00001	0.0890469	11.4547	1.93345E-11

Analysis of Variance

Source	Sum of Squares	Df	Mean Square	F-Ratio
Model	2.0930E0011	1	2.0930E0011	1.3121E0002
Error	3.9879E0010	25	1.5952E0009	
Total (Corr.)	2.4918E0011	26		

Correlation Coefficient = 0.916493
Stnd. Error of Est. = 39939.6

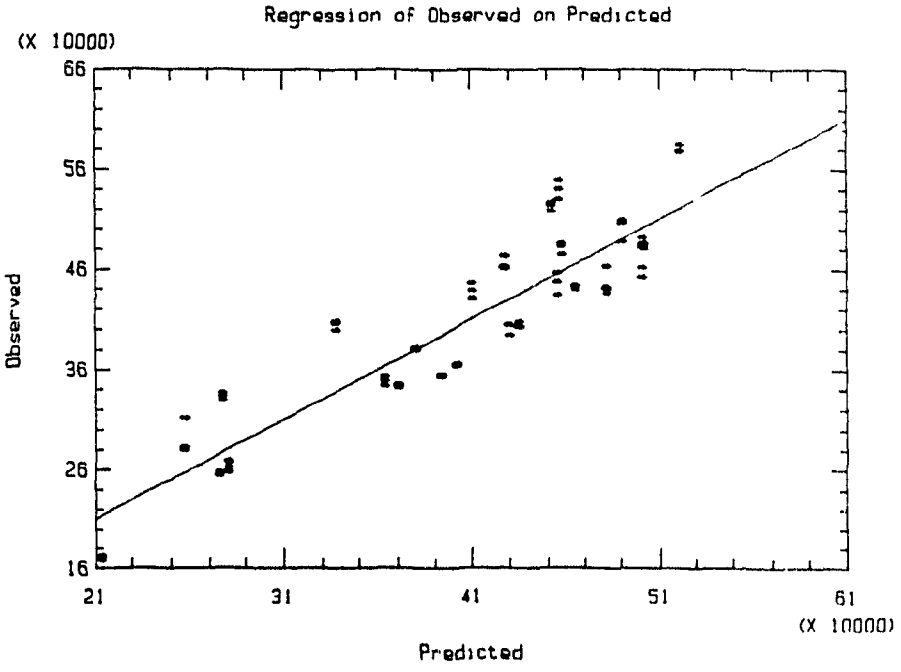

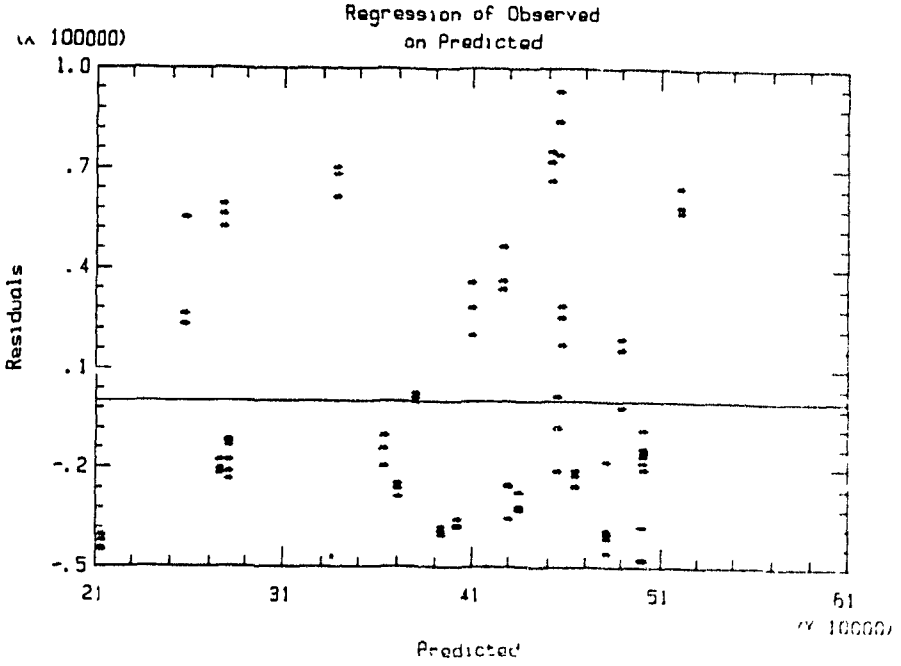

Table A-10. Analysis of Variance and Regression Estimates. Selenonium Analyte with Ether as Eluent Modifier.

Response Mean: 405129.0
ROOT MSE : 44571.72
R-square : 0.829949
Coef.of Var. : 0.1100186

Regression	Df	Type I SS	R-Square	F-Ratio	Prob.
Linear	5	444097983156	0.5848	44.71	0.0001
Quadratic	5	123841405537	0.1631	12.47	0.0001
Crossproduct	10	62298339250	0.0820	3.14	0.0025
Tot. Regress	20	630237727943	0.8299	15.86	0.0001

Residual	Df	SS	Mean Square	F-Ratio	Prob.
Lack of fit	6	126229605046	21038267508	427.743	0.0001
Pure error	59	2901874817	49184318.93		
Total error	65	12931479863	1986638152		

Parameters	Df	Estimate	Std Dev	T-Ratio	Prob.
Intercept	1	481576.77	14976.57691	32.16	0.0001
OT[a]	1	18087.22222	5252.82748	3.44	0.0010
H2[b]	1	-8528.88889	5252.82748	-1.62	0.1093
OA[c]	1	37412.77778	5252.82748	7.12	0.0001
FR[d]	1	-66080.00000	5252.82748	-12.58	0.0001
PE[e]	1	-1362.22222	5252.82748	-0.26	0.7962
OT*OT	1	-26906.45161	5295.01954	-5.08	0.0001
H2*OT	1	-7697.08333	6433.37352	-1.20	0.2359
H2*H2	1	-2133.95161	5295.01954	-0.40	0.6883
OA*OT	1	-2032.08333	6433.37352	-0.32	0.7531
OA*H2	1	22000.41667	6433.37352	3.42	0.0011
OA*OA	1	-32315.61828	5295.01954	-6.10	0.0001
FR*OT	1	21070.41667	6433.37352	3.28	0.0017
FR*H2	1	7876.25000	6433.37352	1.22	0.2253
FR*OA	1	2282.91667	6433.37352	0.35	0.7238
FR*FR	1	-23193.95161	5295.01954	-4.38	0.0001
PE*OT	1	14820.83333	6433.37352	2.30	0.0244
PE*H2	1	3758.33333	6433.37352	0.58	0.5611
PE*OA	1	315.83333	6433.37352	0.05	0.9610
PE*FR	1	-2323.33333	6433.35352	-0.36	0.7192
PE*PE	1	-6762.70161	5295.01954	-1.28	0.2061

[a]OT = Flow rate of thermospray oxygen (500-800 mL/min)
[b]H2 = Flow rate of hydrogen (1.00-2.40 L/min)
[c]OA = Flow rate of analytical oxygen (100-240 mL/min)
[d]FR = Flow rate of eluent (0.3-1.0 mL/min)
[e]PE = Proportion of diethyl ether in eluent (0-40 % v/v)

Table A-11. Factorial Second Order Equations Predicting the Effects of Selected Variables on Analyte Response. Selenonium Analyte with Ether as Eluent Modifier.

---

1) H2 and OT vs Area; FR=0[a] (0.65 mL/min), OA=0 (170 mL/min), PE=-2 (0 %)
Ref. Figure 22-B-1

$$Area = 457250.1 - 16045.5 \times H2 - 11554.4 \times OT - 2133.95 \times H2^2 - 26906.4 \times OT^2 - 7697.08 \times H2 \times OT$$

2) H2 and OT vs Area; FR=0 (0.65 mL/min), OA=1 (205 mL/min), PE=-2 (0 %)
Ref. Figure 22-B-2

$$Area = 461715.8 + 5954.861 \times H2 - 13586.5 \times OT - 2133.95 \times H2^2 - 26906.4 \times OT^2 - 7697.08 \times H2 \times OT$$

3) H2 and OT vs Area; FR=0^ (0.65 mL/min), OA=2 (240 mL/min), PE=0 (0 %)
Ref. Figure 22-B-3

$$Area = 401550.1 + 27995.27 \times H2 - 15618.6 \times OT - 2133.95 \times H2^2 - 26906.4 \times OT^2 - 7697.08 \times H2 \times OT$$

4) OT and FR vs Area; H2=0 (1.7 L/min), OA=0 (170 mL/min), PE=0 (20 %)
Ref. Figure A-7-a

$$Area = 481576.7 + 18087.22 \times OT - 66080.0 \times FR - 26906.4 \times OT^2 - 23193.9 \times FR^2 + 21070.41 \times OT \times FR$$

5) PE and OT vs Area; FR=0(0.65 mL/min), H2=0(1.7 L/min),OA=0(170 mL/min)
Ref. Figure A-7-b

$$Area = 481576.7 - 1362.22 \times PE + 32908.05 \times OT - 6762.7 \times PE^2 - 26906.4 \times OT^2 + 14820.83 \times PE \times OT$$

6) H2 and OT vs Area; FR=0^ (0.65 mL/min), OA=0 (170 mL/min), PE=0 (20 %)
Ref. Figure A-7-c

$$Area = 481576.7 - 8528.88 \times H2 + 18087.22 \times OT - 2133.95 \times H2^2 - 26906.4 \times OT^2 - 7697.08 \times H2 \times OT$$

7) H2 and OA vs Area; FR=0 (0.65 mL/min), OT=0 (650 mL/min), PE=0 (20 %)
Ref. Figure A-7-d

$$Area = 481576.7 - 8528.88 \times H2 + 37412.77 \times OA - 2133.95 \times H2^2 - 32315.6 \times OA^2 + 22000.41 \times H2 \times OA$$

---

[a] Variables expressed in coded values (Table A-5)
OT = Flow rate of thermospray oxygen (500-800 mL/min)
H2 = Flow rate of hydrogen (1.00-2.40 L/min)
OA = Flow rate of analytical oxygen (100-240 mL/min)
FR = Flow rate of eluent (0.3-1.0 mL/min)
PE = Proportion of diethyl ether in eluent (0-40 % v/v)

Figure A-7-a. Exploratory response surfaces (selenonium analyte with ether as modifier) of peak area versus two selected variables. The three other variables were kept constant at the center (coded value of 0) of the factorial design. The quadratic functions describing these surfaces are presented in Table A-11.

A

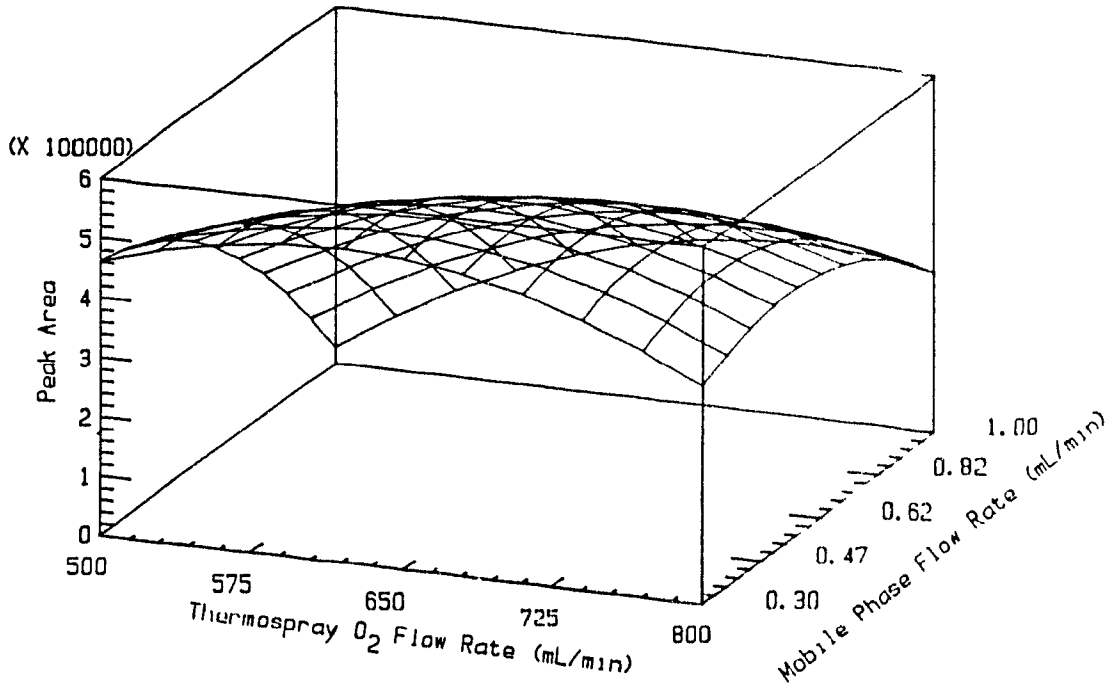
(X 100000)
6
5
4
3
2
1
0
Peak Area
500
575
650
725
800
Thermospray O_2 Flow Rate (mL/min)
0.30
0.47
0.62
0.82
1.00
Mobile Phase Flow Rate (mL/min)

B

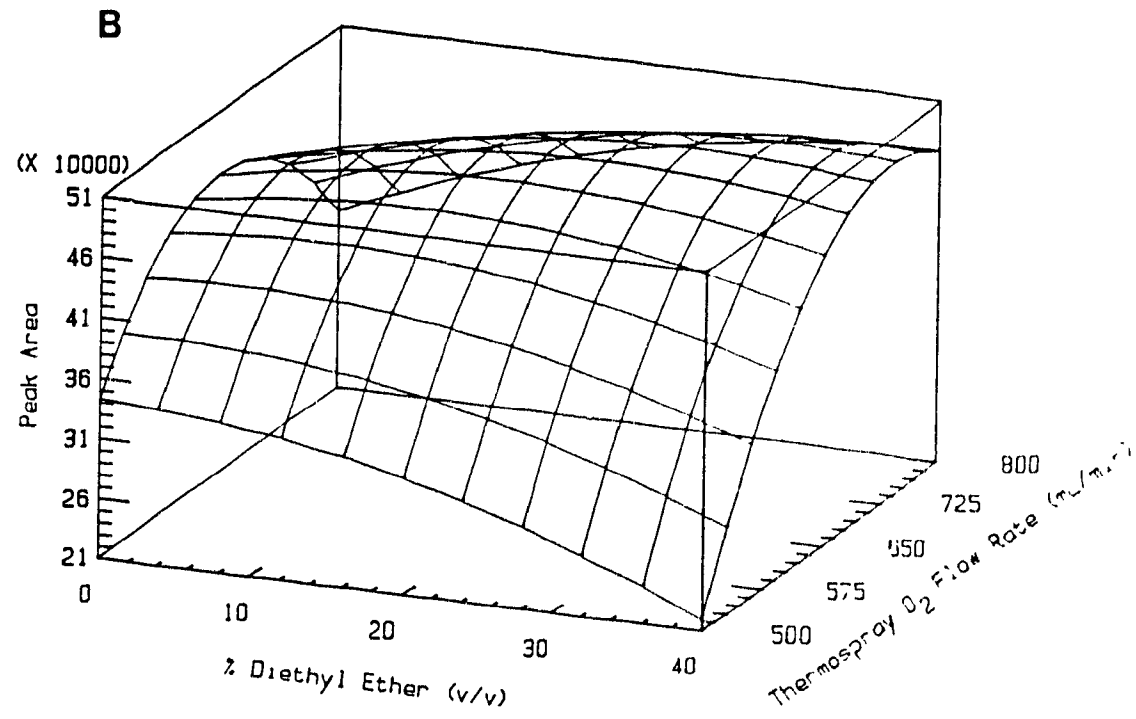
(X 10000)
51
46
41
36
31
26
21
Peak Area
0
10
20
30
40
% Diethyl Ether (v/v)
500
575
650
725
800
Thermospray O_2 Flow Rate

Figure A-7-b. Exploratory response surfaces (selenonium analyte with ether as modifier) of peak area versus two selected variables. The three other variables were kept constant at the center (coded value of 0) of the factorial design. The quadratic functions describing these surfaces are presented in Table A-11.

C

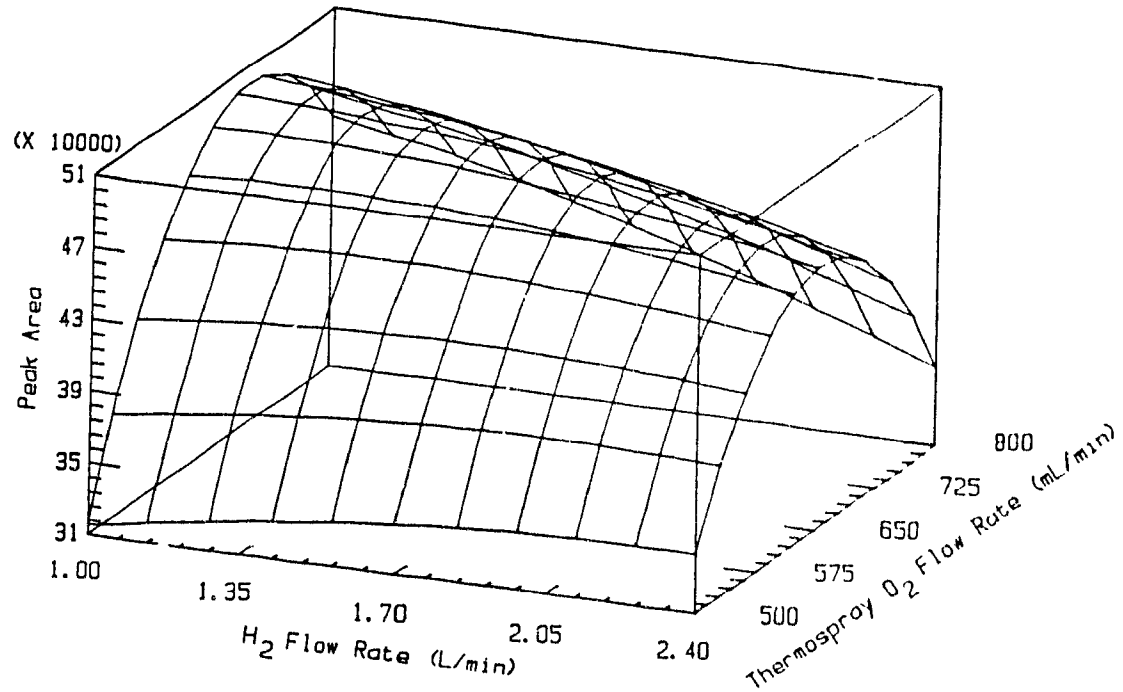
(X 10000)
51
47
43
39
35
31
Peak Area
1.00
1.35
1.70
2.05
2.40
H2 Flow Rate (L/min)
800
725
650
575
500
Thermospray O2 Flow Rate (mL/min)

D

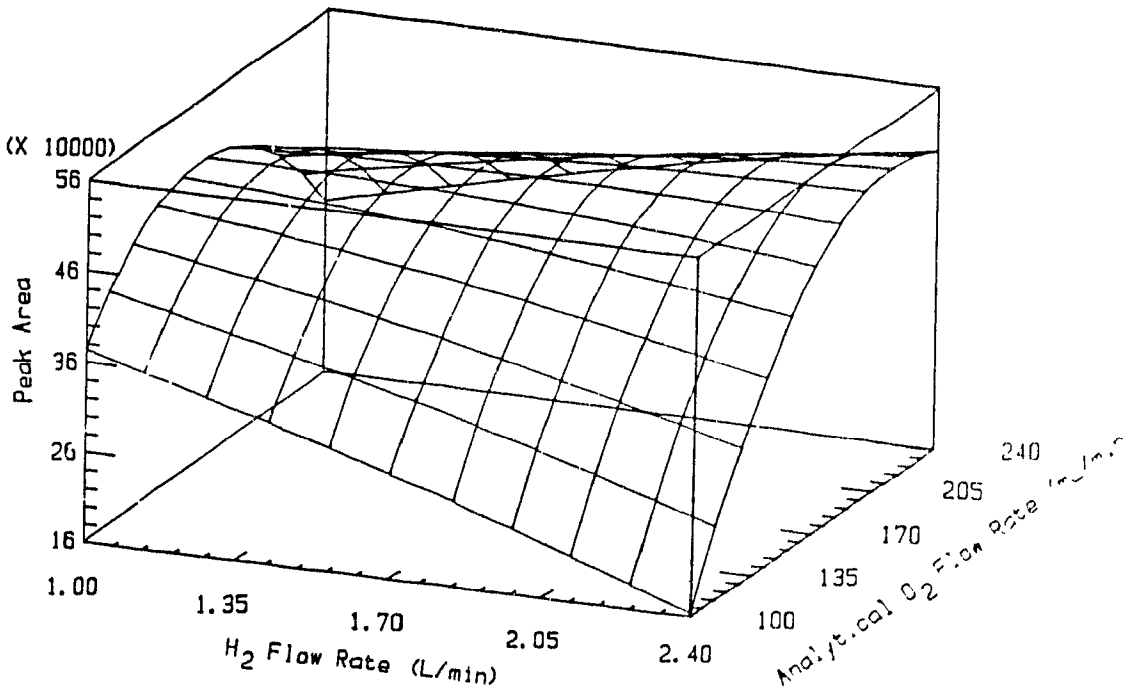
(X 10000)
56
46
36
26
16
Peak Area
1.00
1.35
1.70
2.05
2.40
H2 Flow Rate (L/min)
240
205
170
135
100

Table A-12. Observed and Predicted Results of the Factorial Experiment. Arsonium Analyte with Water as Eluent Modifier.

Point	F.R. $T\text{-}O_2$ mL/min	F.R H_2 L/min	F.R. $A\text{-}O_2$ mL/min	F.R. Eluent mL/min	PW % (v/v)	Response Observed	Response Predicted	Deviation[a] %
1	725	1.35	135	0.47	10	684640	674149	1.53
1	725	1.35	135	0.47	10	691120	674149	2.46
1	725	1.35	135	0.47	10	688400	674149	2.07
2	575	2.05	135	0.47	10	826080	817417	1.05
2	575	2.05	135	0.47	10	813840	817417	0.44
2	575	2.05	135	0.47	10	824210	817417	0.82
3	575	1.35	205	0.47	10	615900	627944	1.96
3	575	1.35	205	0.47	10	615190	627944	2.07
3	575	1.35	205	0.47	10	602600	627944	4.21
4	725	2.05	205	0.47	10	636100	652831	2.63
4	725	2.05	205	0.47	10	660570	652831	1.17
4	725	2.05	205	0.47	10	598270	652831	9.12
5	575	1.35	135	0.82	10	800390	768274	4.01
5	575	1.35	135	0.82	10	784400	768274	2.06
5	575	1.35	135	0.82	10	797030	768274	3.61
6	725	2.05	135	0.82	10	719160	697279	3.04
6	725	2.05	135	0.82	10	715560	697279	2.55
6	725	2.05	135	0.82	10	720700	697279	3.25
7	725	1.35	205	0.82	10	703996	712617	1.22
7	725	1.35	205	0.82	10	713210	712617	0.08
7	725	1.35	205	0.82	10	722210	712617	1.35
8	575	2.05	205	0.82	10	784260	788531	0.54
8	575	2.05	205	0.82	10	776010	788531	1.61
8	575	2.05	205	0.82	10	777050	788531	1.48
9	575	1.35	135	0.47	30	574520	532593	7.30
9	575	1.35	135	0.47	30	534220	532593	0.30
9	575	1.35	135	0.47	30	552510	532593	3.60
10	725	2.05	135	0.47	30	525500	520548	0.94
10	725	2.05	135	0.47	30	537830	520548	3.21
10	725	2.05	135	0.47	30	549450	520548	5.26
11	725	1.35	205	0.47	30	168280	170544	1.35
11	725	1.35	205	0.47	30	168790	170544	1.04
11	725	1.35	205	0.47	30	163680	170544	4.19
12	575	2.05	205	0.47	30	588950	612340	3.97
12	575	2.05	205	0.47	30	603580	612340	1.45
12	575	2.05	205	0.47	30	602690	612340	1.60
13	725	1.35	135	0.82	30	643710	611365	5.02
13	725	1.35	135	0.82	30	657900	611365	7.07
13	725	1.35	135	0.82	30	648740	611365	5.76
14	575	2.05	135	0.82	30	722010	689340	4.52
14	575	2.05	135	0.82	30	726100	689340	5.06
14	575	2.05	135	0.82	30	705250	689340	2.26
15	575	1.35	205	0.82	30	663970	659274	0.71
15	575	1.35	205	0.82	30	663340	659274	0.61
15	575	1.35	205	0.82	30	673830	659274	2.16

Table A-12 Observed and Predicted Results of the Factorial Experiment. Arsonium Analyte with Water as Eluent Modifier.

Point	F.R. T-O_2 mL/min	F.R H_2 L/min	F.R. A-O_2 mL/min	F.R. Eluent mL/min	PW % (v/v)	Response Observed	Response Predicted	Deviation[a] %
16	725	2.05	205	0.82	30	616250	613105	0.51
16	725	2.05	205	0.82	30	617400	613105	0.70
16	725	2.05	205	0.82	30	616650	613105	0.57
17	650	1.70	170	0.65	20	640780	623606	2.68
17	650	1.70	170	0.65	20	643150	623606	3.04
17	650	1.70	170	0.65	20	637540	623606	2.19
17	650	1.70	170	0.65	20	624330	623606	0.12
17	650	1.70	170	0.65	20	632220	623606	1.36
17	650	1.70	170	0.65	20	630380	623606	1.07
17	650	1.70	170	0.65	20	627230	623606	0.58
17	650	1.70	170	0.65	20	641110	623606	2.73
18	500	1.70	170	0.65	20	728050	729897	0.25
18	500	1.70	170	0.65	20	710440	729897	2.74
18	500	1.70	170	0.65	20	724760	729897	0.71
19	800	1.70	170	0.65	20	500040	519079	3.81
19	800	1.70	170	0.65	20	498740	519079	4.08
19	800	1.70	170	0.65	20	497010	519079	4.44
20	650	1.00	170	0.65	20	471940	507218	7.48
20	650	1.00	170	0.65	20	476610	507218	6.42
20	650	1.00	170	0.65	20	485910	507218	4.39
21	650	2.40	170	0.65	20	654100	665875	1.80
21	650	2.40	170	0.65	20	675100	665875	1.37
21	650	2.40	170	0.65	20	667730	665875	0.28
22	650	1.70	100	0.65	20	590340	663624	12.41
22	650	1.70	100	0.65	20	592630	663624	11.98
22	650	1.70	100	0.65	20	596670	663624	11.22
23	650	1.70	240	0.65	20	584140	545179	6.67
23	650	1.70	240	0.65	20	592410	545179	7.97
23	650	1.70	240	0.65	20	582330	545179	6.38
24	650	1.70	170	0.30	20	436530	422122	3.30
24	650	1.70	170	0.30	20	436940	422122	3.39
24	650	1.70	170	0.30	20	435940	422122	3.17
25	650	1.70	170	1.00	20	612150	654977	7.00
25	650	1.70	170	1.00	20	612970	654977	6.85
25	650	1.70	170	1.00	20	608880	654977	7.57
26	650	1.70	170	0.65	0	985647	972899	1.29
26	650	1.70	170	0.65	0	956854	972899	1.68
26	650	1.70	170	0.65	0	993265	972899	2.05
27	650	1.70	170	0.65	40	602110	640416	6.36
27	650	1.70	170	0.65	40	621170	640416	3.10
27	650	1.70	170	0.65	40	593010	640416	7.99

[a] Deviation of observed from predicted values (|obs-pred.|)/obs x 100

Figure A-8. Regression Analysis of Observed vs Predicted Values (arsonium analyte with water as modifier).

Simple Regression of OBSERVED on PREDICTED

Parameter	Estimate	Standard Error	T Value	Prob. Level
Intercept	11034.2	24953.9	0.442182	0.662159
Slope	0.982624	0.038485	25.5326	0

Analysis of Variance

Source	Sum of Squares	Df	Mean Square	F-Ratio
Model	5.3604E0011	1	5.3604E0011	6.5192E0002
Error	2.0556E0010	25	8.2225E0008	
Total (Corr.)	5.5660E0011	26		

Correlation Coefficient = 0.98136
Stnd. Error of Est. = 28674.9

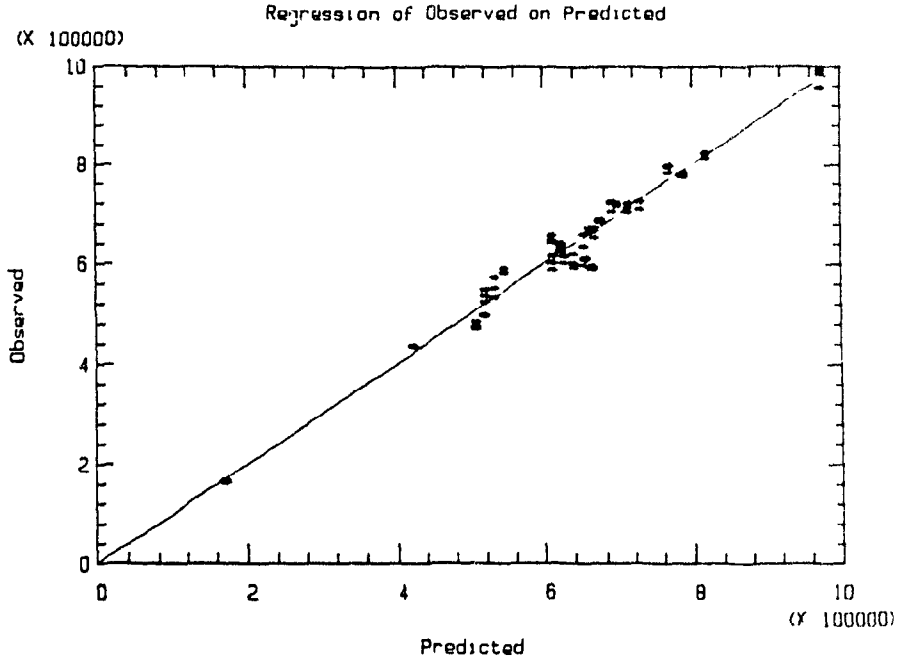

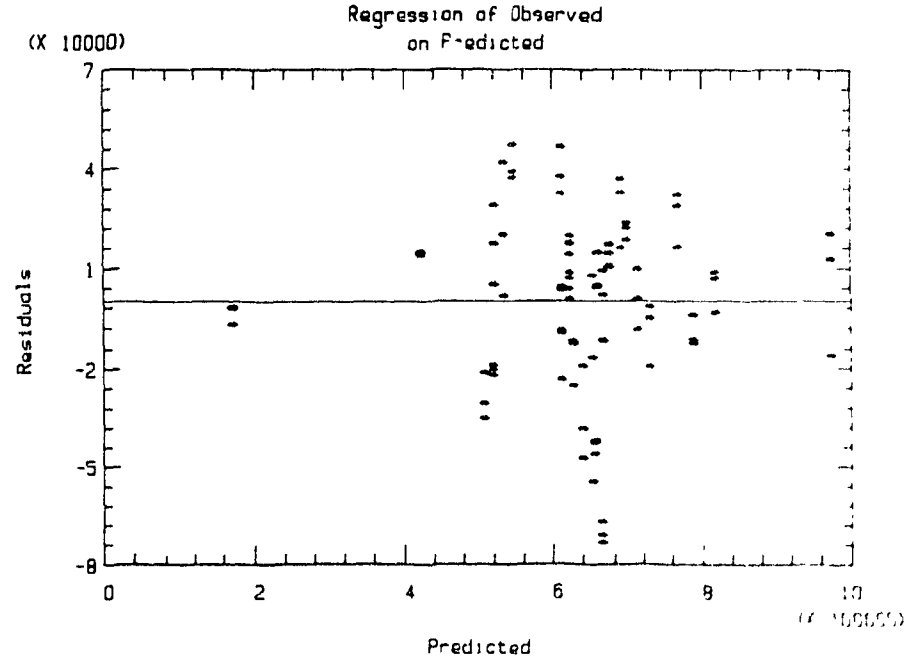

Table A-13. Analysis of Variance and Regression Estimates.
Arsonium Analyte with Water as Eluent Modifier.

Response Mean: 632252.6
ROOT MSE : 29805.52
R-square : 0.9655491
Coef.of Var. : 0.04712145

Regression	Df	Type I SS	R-Square	F-Ratio	Prob.
Linear	5	1.11786E+12	0.6669	251.66	0.0001
Quadratic	5	253518883900	0.1513	57.08	0.0001
Crossproduct	10	247004688591	0.1474	27.80	0.0001
Tot. Regress	20	1.61838E+12	0.9655	91.09	0.0001

Residual	Df	SS	Mean Square	F-Ratio	Prob.
Lack of fit	6	51429480711	8571580118	80.089	0.0001
Pure error	59	6314511112	107025612		
Total error	65	57743991823	888369105		

Parameters	Df	Estimate	Std Dev	T-Ratio	Prob.
Intercept	1	623606.02	10014.97567	62.27	0.0001
OT[a]	1	-52704.63889	3512.61438	-15.00	0.0001
H2[b]	1	39664.36111	3512.61438	11.29	0.0001
OA[c]	1	-29611.30556	3512.61438	-8.43	0.0001
FR[d]	1	58213.69444	3512.61438	16.57	0.0001
PW[e]	1	-83120.80556	3512.61438	-23.66	0.0001
OT*OT	1	220.65726	3540.82860	0.06	0.9505
H2*OT	1	-278.45883	4302.05645	-0.06	0.9486
H2*H2	1	-9264.75941	3540.82860	-2.62	0.0110
OA*OT	1	-14669.04167	4302.06545	-3.41	0.0011
OA*H2	1	22389.04167	4302.05645	5.20	0.0001
OA*OA	1	-4801.00941	3540.82860	-1.36	0.1798
FR*OT	1	18823.04167	4302.05645	4.38	0.0001
FR*H2	1	-35073.87500	4302.05645	-8.15	0.0001
FR*OA	1	30519.70833	4302.05645	7.09	0.0001
FR*FR	1	-21263.92608	3540.82860	-6.01	0.0001
PW*OT	1	-19453.45833	4302.05645	-4.52	0.0001
PW*H2	1	18030.12500	4302.05645	4.19	0.0001
PW*OA	1	-7711.79167	4302.05645	-1.79	0.0777
PW*FR	1	33918.62500	4302.05645	7.88	0.0001
PW*PW	1	45762.99059	3540.82860	12.92	0.0001

[a]OT = Flow rate of thermospray oxygen (500-800 mL/min)
[b]H2 = Flow rate of hydrogen (1.00-2.40 L/min)
[c]OA = Flow rate of analytical oxygen (100-240 mL/min)
[d]FR = Flow rate of eluent (0.3-1.0 mL/min)
[e]PW = Proportion of water in eluent (0-40 % v/v)

Table A-14. Factorial Second Order Equations Predicting the Effects of Selected Variables on Analytes Response. Arsonium Analytes with Water as Eluent Modifier.

---

1) OT and FR vs Area; H2=0[a] (1.7 L/min), OA=0 (170 mL/min), PW=0 (20 %)
   Ref. Figure A-9-a

$$Area = 623606.0 - 52704.6 \times OT + 58213.69 \times FR + 220.6572 \times OT^2 - 21263.9 \times FR^2 + 18823.04 \times OT \times FR$$

2) PW and OT vs Area; FR=0(0.65 mL/min), H2=0(1.7 L/min),OA=0(170 mL/min)
   Ref. Figure A-9-b

$$Area = 623606.0 - 83120.8 \times PW - 72248.01 \times OT + 45762.99 \times PW^2 + 220.6572 \times OT^2 - 19453.4 \times PW \times OT$$

3) H2 and OT vs Area; FR=0 (0.65 mL/min), OA=0 (170 mL/min), PW=0 (20 %)
   Ref. Figure A-9-c

$$Area = 623606.0 + 39664.36 \times H2 - 52704.6 \times OT - 9264.75 \times H2^2 + 220.6572 \times OT^2 - 278.458 \times H2 \times OT$$

4) H2 and OA vs Area; FR=0 (0.65 mL/min), OT=0 (650 mL/min), PW=0 (20 %)
   Ref. Figure A-9-d

$$Area = 623606.0 + 39664.36 \times H2 - 29611.3 \times OA - 9264.75 \times H2^2 - 4801.0 \times OA^2 + 22389.04 \times H2 \times OA$$

---

[a] Variables expressed in coded values (Table A-5)
OT = Flow rate of thermospray oxygen (500-800 mL/min)
H2 = Flow rate of hydrogen (1.00-2.40 L/min)
OA = Flow rate of analytical oxygen (100-240 mL/min)
FR = Flow rate of eluent (0.3-1.0 mL/min)
PW = Proportion of water in eluent (0-40 % v/v)

Figure A-9-a. Exploratory response surfaces (arsonium analyte with water as modifier) of peak area versus two selected variables. The three other variables were kept constant at the center (coded value of 0) of the factorial design. The quadratic functions describing these surfaces are presented in Table A-15.

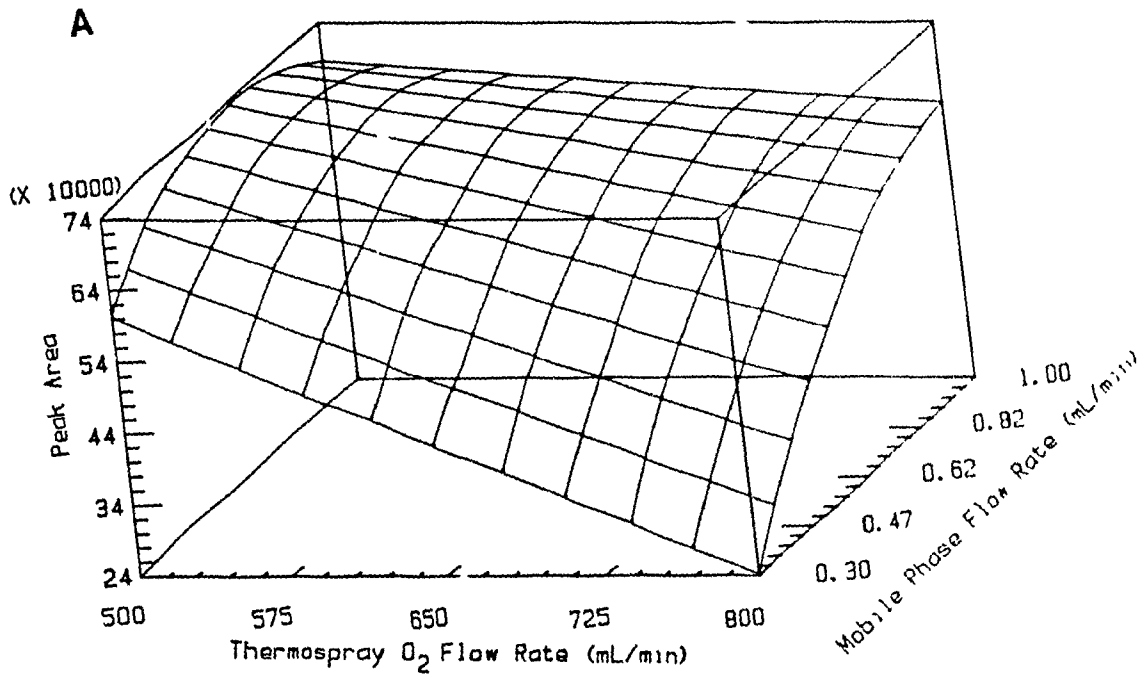
A
(X 10000)
74
64
54
44
34
24
Peak Area
500
575
650
725
800
Thermospray O_2 Flow Rate (mL/min)
1.00
0.82
0.62
0.47
0.30
Mobile Phase Flow Rate (mL/min)

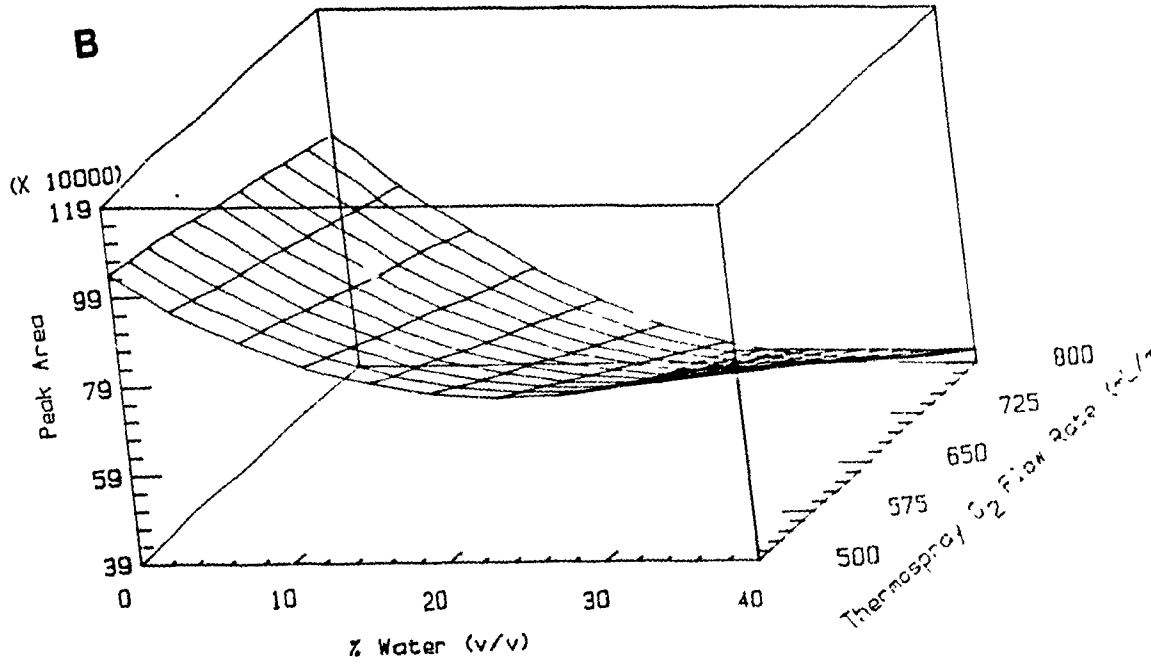
B
(X 10000)
119
99
79
59
39
Peak Area
0
10
20
30
40
% Water (v/v)
800
725
650
575
500

Figure A-9-b. Exploratory response surfaces (arsonium analyte with water as modifier) of peak area versus two selected variables. The three other variables were kept constant at the center (coded value of 0) of the factorial design. The quadratic functions describing these surfaces are presented in Table A-15.

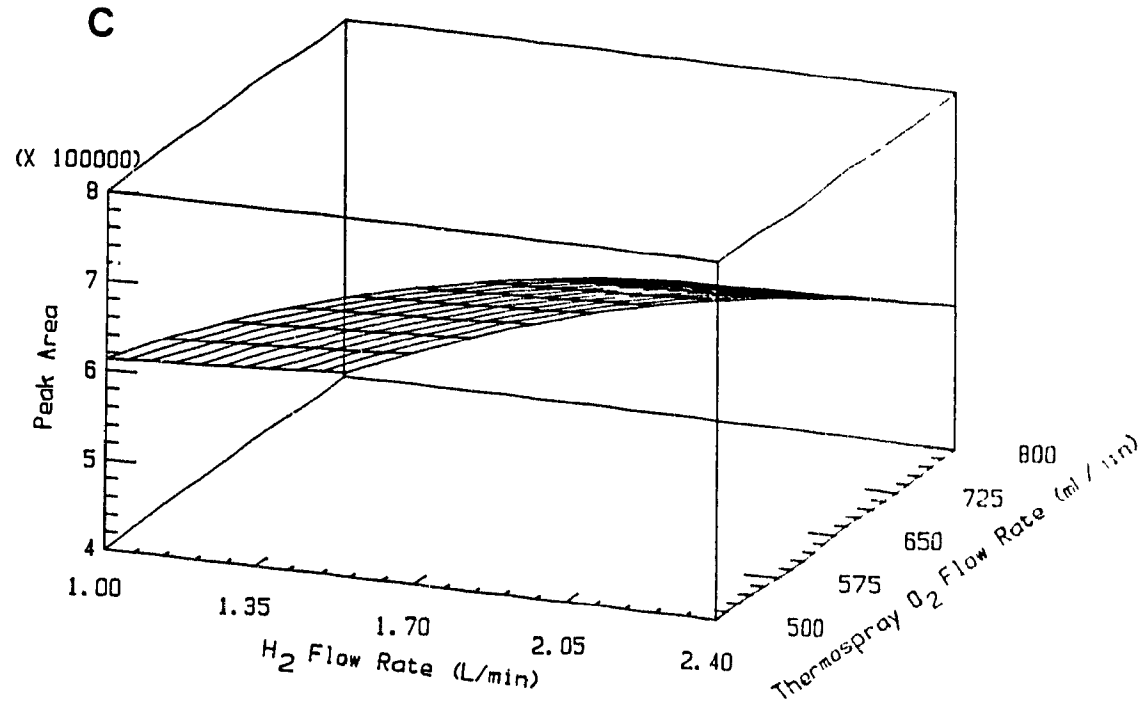
C
(X 100000)
8
7
6
5
4
Peak Area
1.00
1.35
1.70
2.05
2.40
H2 Flow Rate (L/min)
500
575
650
725
800
Thermospray O2 Flow Rate (ml / min)

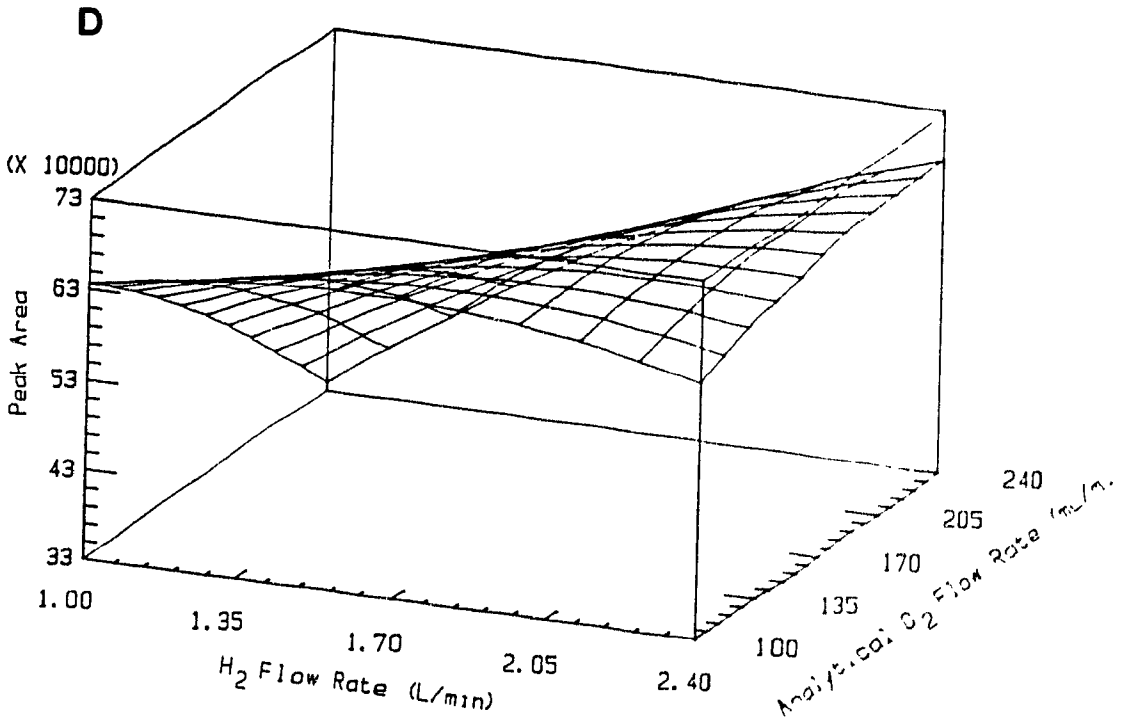
D
(X 10000)
73
63
53
43
33
Peak Area
1.00
1.35
1.70
2.05
2.40
H2 Flow Rate (L/min)
100
135
170
205
240
Analytical O2 Flow Rate (mL/m

Table A-15. Observed and Predicted Results of the Factorial Experiment. Selenonium Analytes with Water as Eluent Modifier.

Point	F.R. $T\text{-}O_2$ mL/min	F.R H_2 L/min	F.R. $A\text{-}O_2$ mL/min	F.R. Eluent mL/min	PW % (v/v)	Response Observed	Response Predicted	Deviation[a] %
1	725	1.35	135	0.47	10	578950	583956	0.86
1	725	1.35	135	0.47	10	580480	583956	0.60
1	725	1.35	135	0.47	10	588370	583956	0.75
2	575	2.05	135	0.47	10	422920	429581	1.58
2	575	2.05	135	0.47	10	418070	429581	2.75
2	575	2.05	135	0.47	10	424290	429581	1.25
3	575	1.35	205	0.47	10	407950	449621	10.21
3	575	1.35	205	0.47	10	415930	449621	8.10
3	575	1.35	205	0.47	10	411520	449621	9.26
4	725	2.05	205	0.47	10	514750	525863	2.16
4	725	2.05	205	0.47	10	510120	525863	3.09
4	725	2.05	205	0.47	10	523580	525863	0.44
5	575	1.35	135	0.82	10	374740	366543	2.19
5	575	1.35	135	0.82	10	375650	366543	2.42
5	575	1.35	135	0.82	10	369390	366543	0.77
6	725	2.05	135	0.82	10	323170	290759	10.03
6	725	2.05	135	0.82	10	326300	290759	10.89
6	725	2.05	135	0.82	10	327280	290759	11.16
7	725	1.35	205	0.82	10	431800	432292	0.11
7	725	1.35	205	0.82	10	434660	432292	0.54
7	725	1.35	205	0.82	10	444890	432292	2.83
8	575	2.05	205	0.82	10	383840	376974	1.79
8	575	2.05	205	0.82	10	377810	376974	0.22
8	575	2.05	205	0.82	10	364350	376974	3.46
9	575	1.35	135	0.47	30	509300	513835	0.89
9	575	1.35	135	0.47	30	523040	513835	1.76
9	575	1.35	135	0.47	30	491410	513835	4.56
10	725	2.05	135	0.47	30	426970	411574	3.61
10	725	2.05	135	0.47	30	436410	411574	5.69
10	725	2.05	135	0.47	30	437910	411574	6.01
11	725	1.35	205	0.47	30	666480	682231	2.36
11	725	1.35	205	0.47	30	672560	682231	1.44
11	725	1.35	205	0.47	30	684220	682231	0.29
12	575	2.05	205	0.47	30	568480	578852	1.82
12	575	2.05	205	0.47	30	563190	578852	2.78
12	575	2.05	205	0.47	30	562060	578852	2.99
13	725	1.35	135	0.82	30	426060	387513	9.05
13	725	1.35	135	0.82	30	423700	387513	8.54
13	725	1.35	135	0.82	30	422960	387513	8.38
14	575	2.05	135	0.82	30	376950	337034	10.59
14	575	2.05	135	0.82	30	362980	337034	7.15
14	575	2.05	135	0.82	30	361960	337034	6.89
15	575	1.35	205	0.82	30	484600	482538	0.43
15	575	1.35	205	0.82	30	479970	482538	0.54
15	575	1.35	205	0.82	30	483830	482538	0.27

Table A-15. Observed and Predicted Results of the Factorial Experiment. Selenonium Analytes with Water as Eluent Modifier.

Point	F.R. $T\text{-}O_2$ mL/min	F.R H_2 L/min	F.R. $A\text{-}O_2$ mL/min	F.R. Eluent mL/min	PW % (v/v)	Response Observed	Response Predicted	Deviation[a] %
16	725	2.05	205	0.82	30	427010	401073	6.07
16	725	2.05	205	0.82	30	432350	401073	7.23
16	725	2.05	205	0.82	30	428970	401073	6.50
17	650	1.70	170	0.65	20	442710	433746	2.02
17	650	1.70	170	0.65	20	448570	433746	3.30
17	650	1.70	170	0.65	20	440960	433746	1.64
17	650	1.70	170	0.65	20	435520	433746	0.41
17	650	1.70	170	0.65	20	441950	433746	1.86
17	650	1.70	170	0.65	20	440440	433746	1.52
17	650	1.70	170	0.65	20	437120	433746	0.77
17	650	1.70	170	0.65	20	441060	433746	1.66
18	500	1.70	170	0.65	20	461780	436651	5.44
18	500	1.70	170	0.65	20	462370	436651	5.56
18	500	1.70	170	0.65	20	460340	436651	5.15
19	800	1.70	170	0.65	20	438760	481722	9.79
19	800	1.70	170	0.65	20	435950	481722	10.50
19	800	1.70	170	0.65	20	437560	481722	10.09
20	650	1.00	170	0.65	20	561440	552357	1.62
20	650	1.00	170	0.65	20	568260	552357	2.80
20	650	1.00	170	0.65	20	563120	552357	1.91
21	650	2.40	170	0.65	20	385650	415652	7.78
21	650	2.40	170	0.65	20	383210	415652	8.47
21	650	2.40	170	0.65	20	383990	415652	8.25
22	650	1.70	100	0.65	20	253730	301860	18.97
22	650	1.70	100	0.65	20	251360	301860	20.09
22	650	1.70	100	0.65	20	256240	301860	17.80
23	650	1.70	240	0.65	20	482280	454022	5.86
23	650	1.70	240	0.65	20	486639	454022	6.70
23	650	1.70	240	0.65	20	479040	454022	5.22
24	650	1.70	170	0.30	20	654910	621701	5.07
24	650	1.70	170	0.30	20	665908	621701	5.64
24	650	1.70	170	0.30	20	667260	621701	6.83
25	650	1.70	170	1.00	20	284170	346504	21.94
25	650	1.70	170	1.00	20	284940	346504	21.61
25	650	1.70	170	1.00	20	289070	346504	19.87
26	650	1.70	170	0.65	0	400250	398688	0.39
26	650	1.70	170	0.65	0	410430	398688	2.86
26	650	1.70	170	0.65	0	432550	398688	7.83
27	650	1.70	170	0.65	40	442090	483454	9.36
27	650	1.70	170	0.65	40	449780	483454	7.49
27	650	1.70	170	0.65	40	452968	483454	6.73

[a] Deviation of observed from predicted values (|obs-pred.|)/obs x 100

Figure A-10. Regression Analysis of Observed vs Predicted Values (selenonium analyte with water as modifier).

Simple Regression of OBSERVED on PREDICTED

Parameter	Estimate	Standard Error	T Value	Prob. Level
Intercept	3639.15	32368.8	0.112428	0.911382
Slope	0.989431	0.0701881	14.0968	2.11386E-13

Analysis of Variance

Source	Sum of Squares	Df	Mean Square	F-Ratio
Model	2.2929E0011	1	2.2929E0011	1.9872E0002
Error	2.8845E0010	25	1.1538E0009	
Total (Corr.)	2.5813E0011	26		

Correlation Coefficient = 0.942472
Stnd. Error of Est. = 33967.7

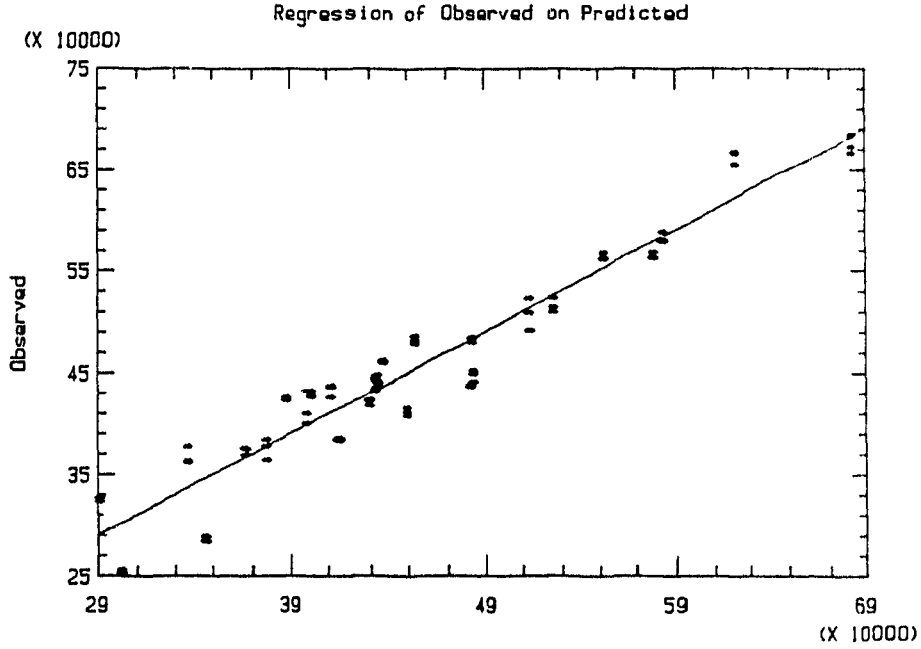

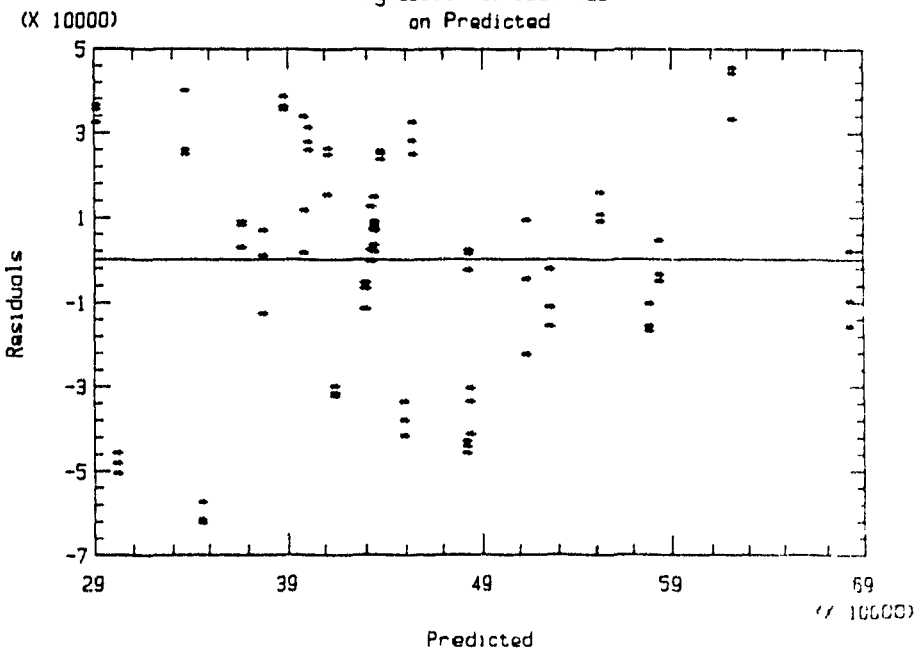

Table A-16. Analysis of Variance and Regression Estimates.
Selenonium Analytes with Water as Eluent Modifier.

Response Mean: 449983.2
ROOT MSE : 31364.95
R-square : 0.9177213
Coef.of Var. : 0.06970248

Regression	Df	Type I SS	R-Square	F-Ratio	Prob.
Linear	5	870559783569	0.7342	116.00	0.0001
Quadratic	5	48642225176	0.0626	9.89	0.0001
Crossproduct	10	94021839533	0.1210	9.56	0.0001
Tot. Regress	20	713223848279	0.9177	36.25	0.0001

Residual	Df	SS	Mean Square	F-Ratio	Prob.
Lack of fit	6	61592917357	10265486226	257.568	0.0001
Pure error	59	2351471493	39855449.04		
Total error	65	63944388851	983759828		

Parameters	Df	Estimate	Std Dev	T-Ratio	Prob.
Intercept	1	433746.217	10538.95906	41.16	0.0001
OT[a]	1	11267.77778	3696.39432	3.05	0.0033
H2[b]	1	-34176.11111	3696.39432	-9.25	0.0001
OA[c]	1	38040.52778	3696.39432	10.29	0.0001
FR[d]	1	-68799.11111	3696.39432	-18.61	0.0001
PW[e]	1	21191.33333	3696.39432	5.73	0.0001
OT*OT	1	6360.12769	3726.08471	1.71	0.0926
H2*OT	1	-22914.16667	4527.13998	-5.06	0.0001
H2*H2	1	12564.71102	3726.08471	3.37	0.0013
OA*OT	1	7916.66667	4527.13998	1.75	0.0851
OA*H2	1	13686.25000	4527.13998	3.02	0.0036
OA*OA	1	-13951.16398	3726.08471	-3.74	0.0004
FR*OT	1	-17699.16667	4527.13998	-3.91	0.0002
FR*H2	1	1295.41667	4527.13998	0.29	0.7757
FR*OA	1	837.91667	4527.13998	0.19	0.8537
FR*FR	1	12589.21102	3726.08471	3.38	0.0012
PW*OT	1	-15001.25000	4527.13998	-3.31	0.0015
PW*H2	1	-8021.66667	4527.13998	-1.77	0.0811
PW*OA	1	23801.66667	4527.13998	5.26	0.0001
PW*FR	1	-3492.50000	4527.13998	-0.77	0.4432
PW*PW	1	1831.29435	3726.08471	0.49	0.6247

[a]OT = Flow rate of thermospray oxygen (500-800 mL/min)
[b]H2 = Flow rate of hydrogen (1.00-2.40 L/min)
[c]OA = Flow rate of analytical oxygen (100-240 mL/min)
[d]FR = Flow rate of eluent (0.3-1.0 mL/min)
[e]PW = Proportion of water in eluent (0-40 % v/v)

Table A-17. Factorial Second Order Equations Predicting the Effects of Selected Variables on Analytes Response. Selenonium Analytes with Water as Eluent Modifier.

---

1) OT and FR vs Area; H2=0 (1.7 L/min), OA=0 (170 mL/min), PW=0 (20 %)
Ref. Figure A-11-a

$$\text{Area} = 433746.2 + 11267.77 \times OT - 68799.1 \times FR + 6360.127 \times OT^2 + 12589.21 \times FR^2 - 17699.1 \times OT \times FR$$

2) PW and OT vs Area; FR=0(0.65 mL/min),H2=0 (1.7 L/min),OA=0(170 mL/min)
Ref. Figure A-11-b

$$\text{Area} = 433746.2 + 21191.33 \times PW - 3733.47 \times OT + 1831.293 \times PW^2 + 6360.127 \times OT^2 - 15001.2 \times PW \times OT$$

3) H2 and OT v Area; FR=0 (0.65 mL/min), OA=0 (170 mL/min), PW=0 (20 %)
Ref. Figure A-11-c

$$\text{Area} = 433746.2 - 34176.1 \times H2 + 11267.77 \times OT + 12564.71 \times H2^2 + 6360.127 \times OT^2 - 22914.1 \times H2 \times OT$$

4) H2 and OA vs Area; FR=0 (0.65 mL/min), OT=0 (650 mL/min), PW=0 (20 %)
Ref. Figure A-11-d

$$\text{Area} = 433746.2 - 34176.1 \times H2 + 38040.5 \times OA + 12564.7 \times H2^2 - 13950.1 \times OA^2 + 13686.25 \times H2 \times OA$$

---

[a] Variables expressed in coded values (Table A-5)
OT = Flow rate of thermospray oxygen (500-800 mL/min)
H2 = Flow rate of hydrogen (1.00-2.40 L/min)
OA = Flow rate of analytical oxygen (100-240 mL/min)
FR = Flow rate of eluent (0.3-1.0 mL/min)
PW = Proportion of water in eluent (0-40 % v,)

Figure A-11-a. Exploratory response surfaces (selenonium analyte with water as modifier) of peak area versus two selected variables. The three other variables were kept constant at the center (coded value of 0) of the factorial design. The quadratic functions describing these surfaces are presented in Table A-17.

A

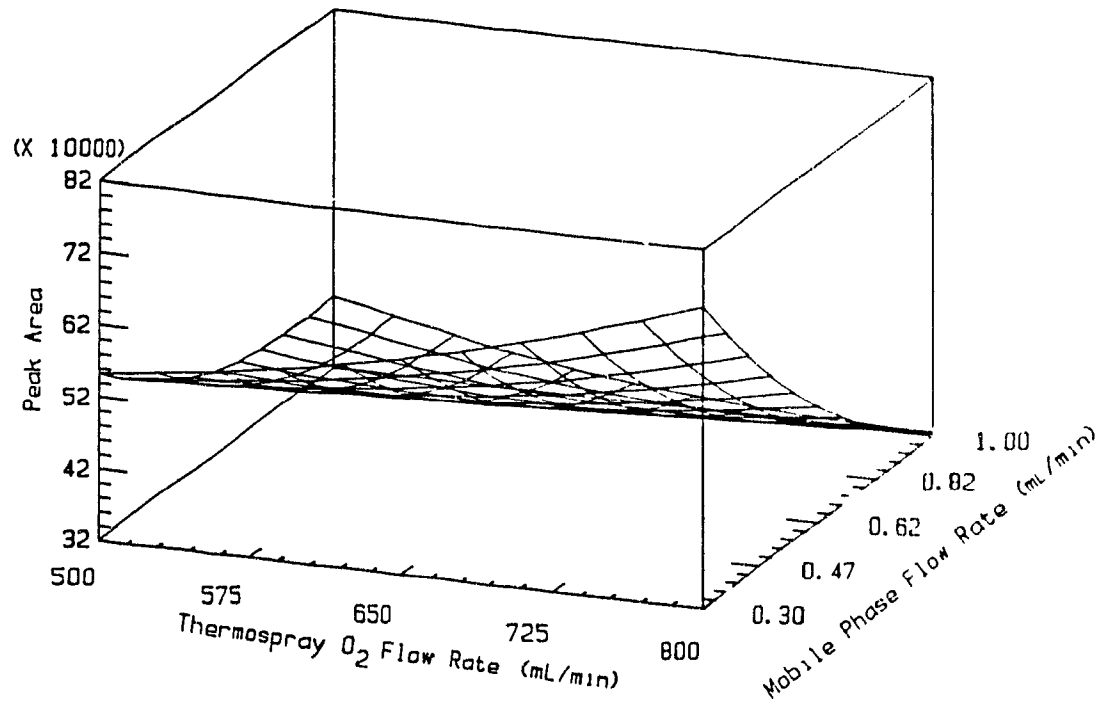
(X 10000)
82
72
62
52
42
32
Peak Area
500
575
650
725
800
Thermospray O_2 Flow Rate (mL/min)
0.30
0.47
0.62
0.82
1.00
Mobile Phase Flow Rate (mL/min)

B

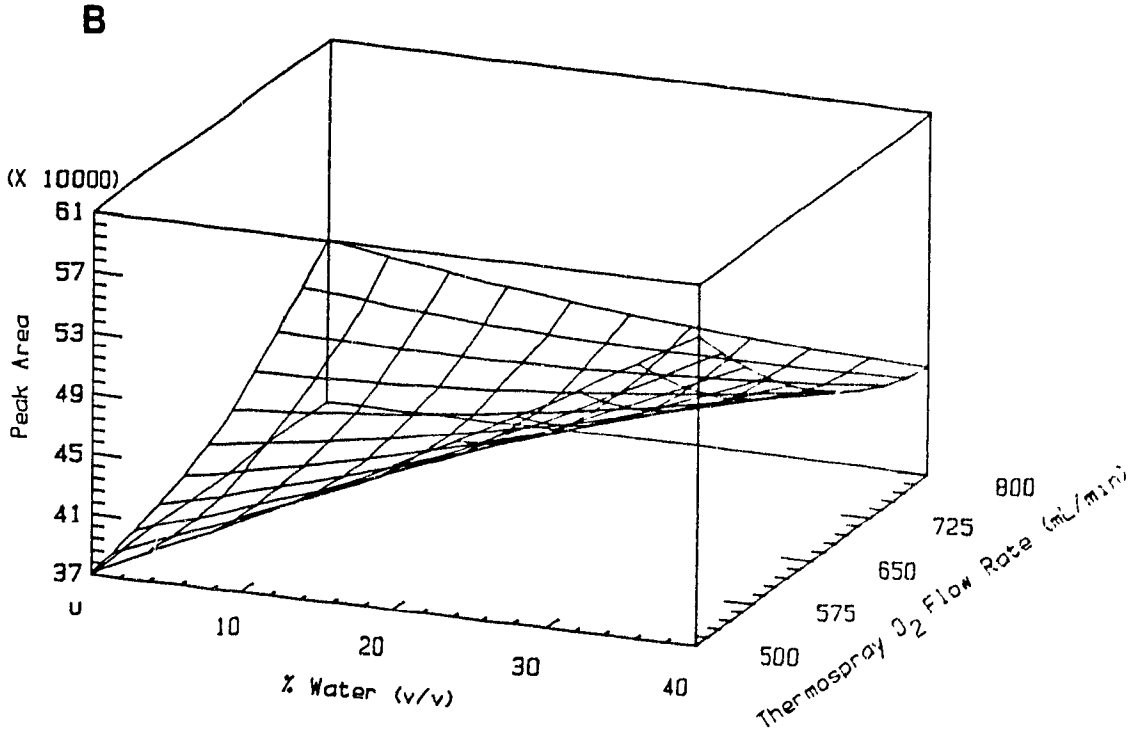
(X 10000)
61
57
53
49
45
41
37
Peak Area
0
10
20
30
40
% Water (v/v)
500
575
650
725
800
Thermospray O_2 Flow Rate (mL/min)

Figure A-11-b. Exploratory response surfaces (selenonium analyte with water as modifier) of peak area versus two selected variables. The three other variables were kept constant at the center (coded value of 0) of the factorial design. The quadratic functions describing these surfaces are presented in Table A-17.

C

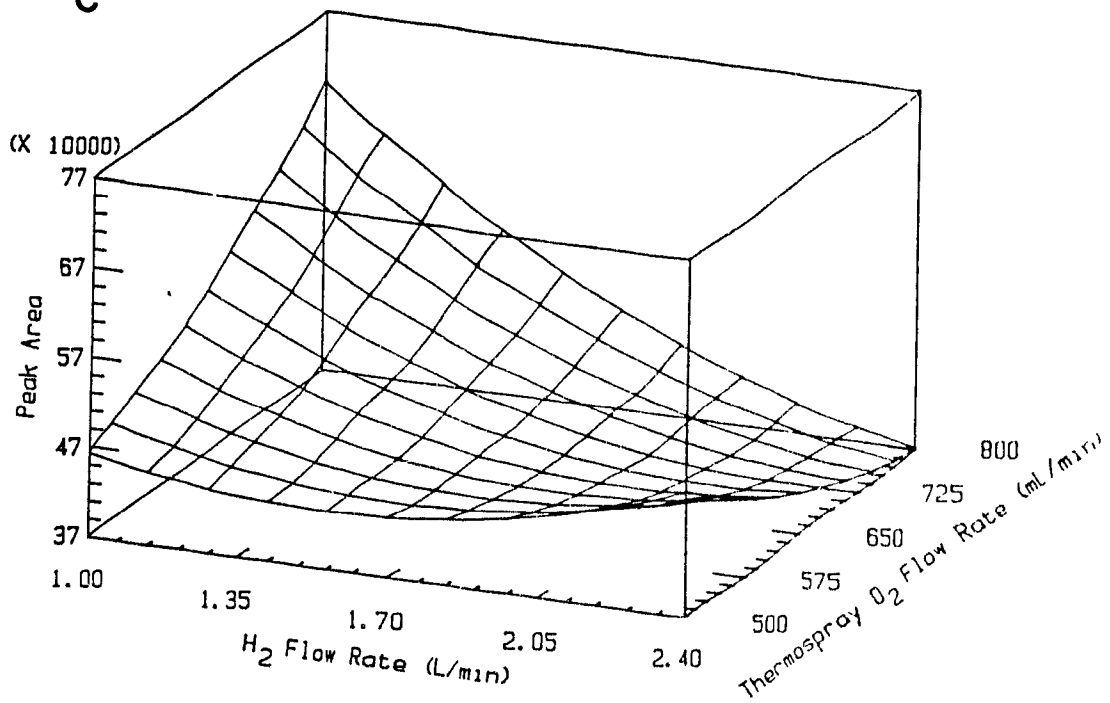
(X 10000)
77
67
57
47
37
Peak Area
1.00
1.35
1.70
2.05
2.40
H_2 Flow Rate (L/min)
500
575
650
725
800
Thermospray O_2 Flow Rate (mL/min)

D

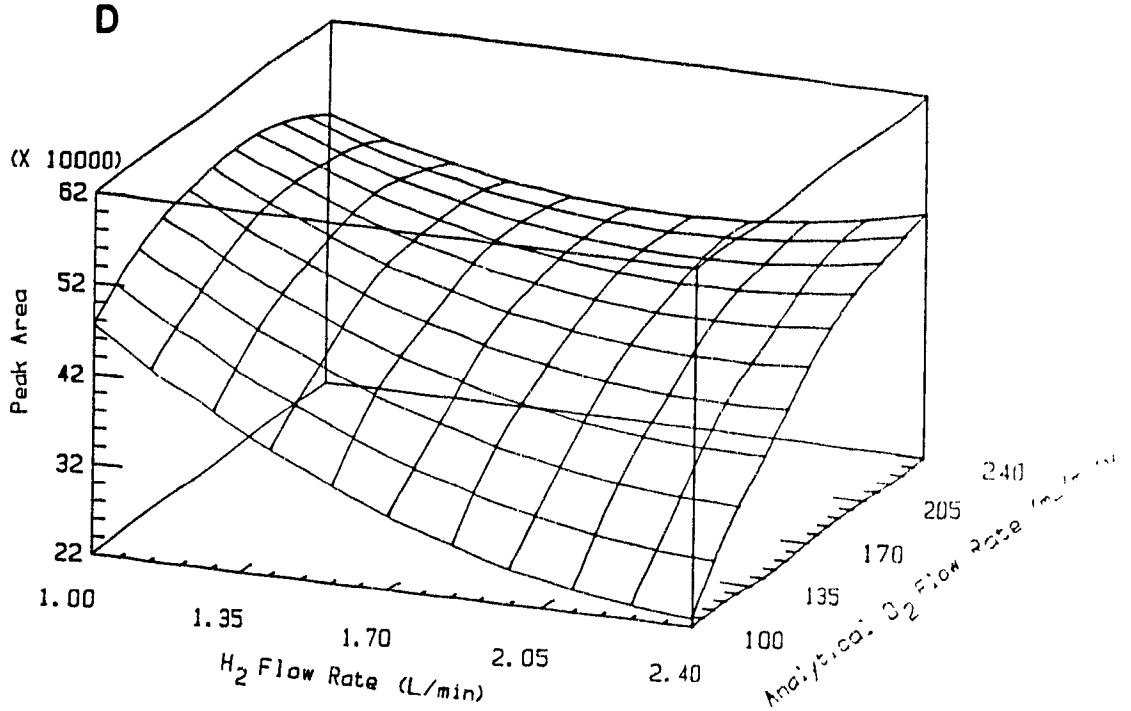
(X 10000)
62
52
42
32
22
Peak Area
1.00
1.35
1.70
2.05
2.40
H_2 Flow Rate (L/min)
100
135
170
205
240

Figure A-12-a. Regression analysis related to the determination of the limit of detection of arsenobetaine.

Simple Regression of AsBetaine on Amount

Parameter	Estimate	Standard Error	T Value	Prob. Level
Intercept	9500.75	4382.21	2.16803	0.0553541
Slope	644536	7800.23	82.6304	1.55431E-15

Analysis of Variance

Source	Sum of Squares	Df	Mean Square	F-Ratio
Model	7.2518E0011	1	7.2518E0011	6.8278E0003
Error	1.0621E0009	10	1.0621E0008	
Total (Corr.)	7.2624E0011	11		

Correlation Coefficient = 0.999269
Stnd. Error of Est. = 10305.8

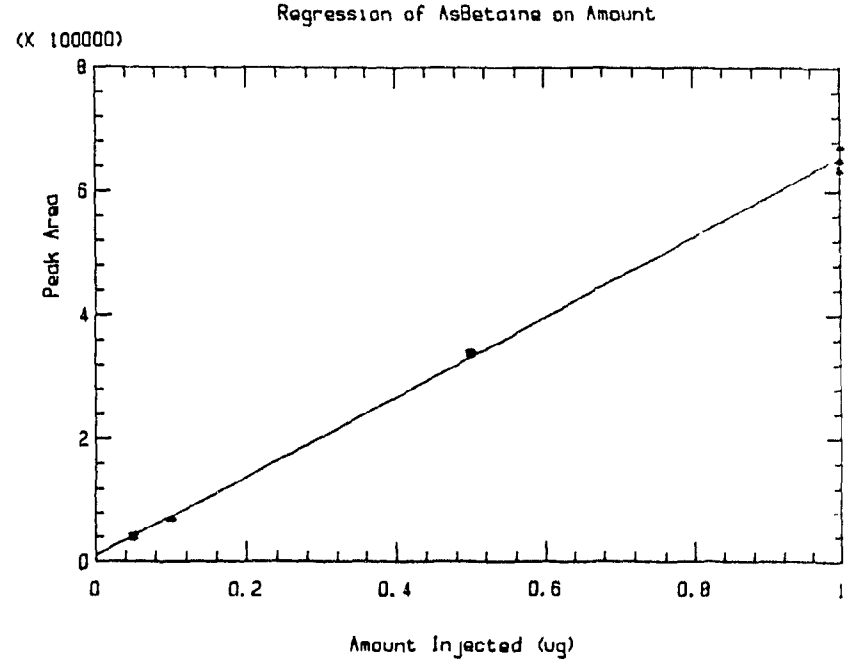

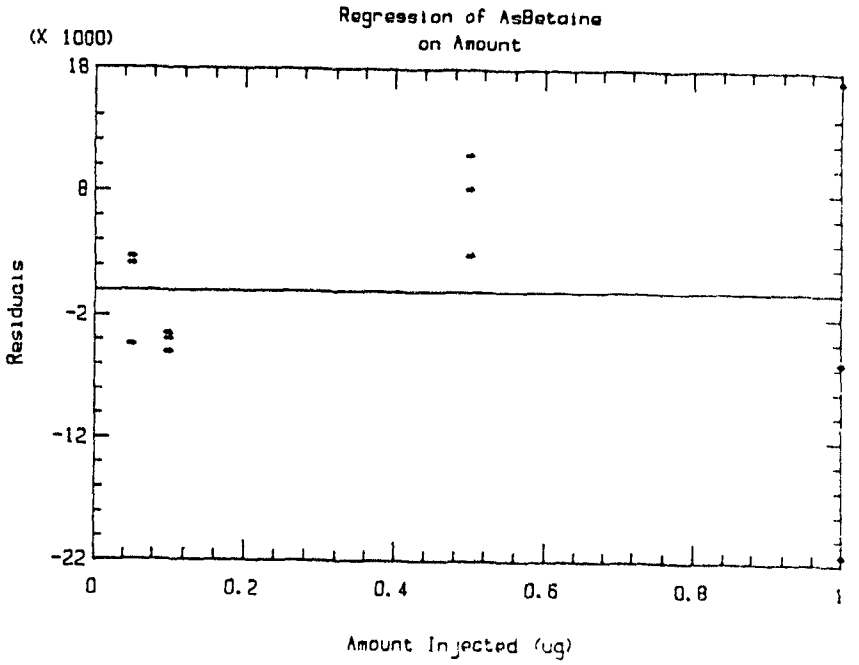

Figure A-12-b. Regression analysis related to the determination of the limit of detection of arsenocholine.

Simple Regression of AsCholine on Amount

Parameter	Estimate	Standard Error	T Value	Prob. Level
Intercept	11844.2	6259.36	1.89223	0.0877393
Slope	744051	11141.6	66.7816	1.37668E-14

Analysis of Variance

Source	Sum of Squares	Df	Mean Square	F-Ratio
Model	9.6640E0011	1	9.6640E0011	4.4598E0003
Error	2.1669E0009	10	2.1669E0008	
Total (Corr.)	9.6857E0011	11		

Correlation Coefficient = 0.998881
Stnd. Error of Est. = 14720.5

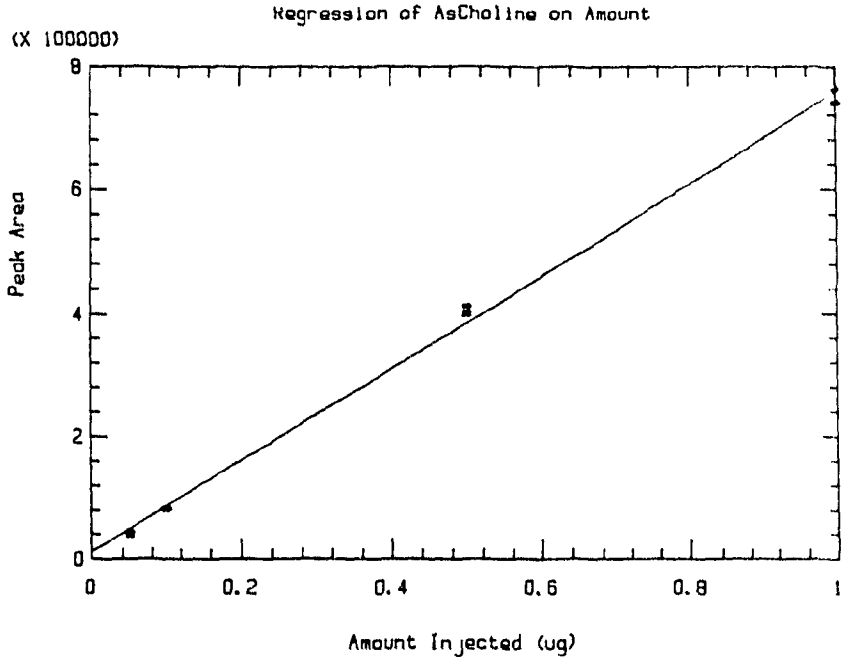

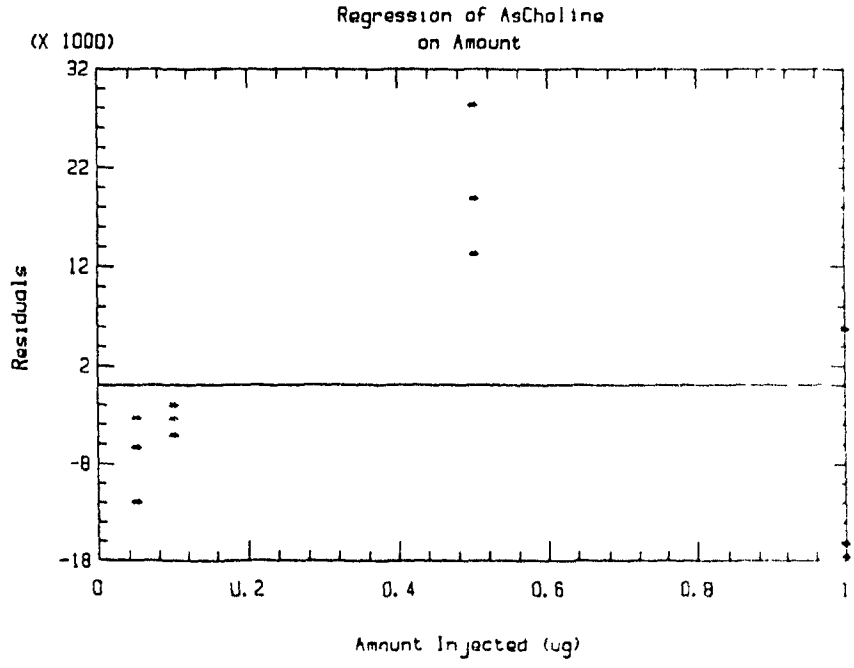

Figure A-12-c. Regression analysis related to the determination of the limit of detection of tetramethylarsonium.

Simple Regression of TMeAs on Amount

Parameter	Estimate	Standard Error	T Value	Prob. Level
Intercept	-5258.02	3463.98	-1.51791	0.159996
Slope	658028	6165.8	106.722	2.22045E-16

Analysis of Variance

Source	Sum of Squares	Df	Mean Square	F-Ratio
Model	7.5586E0011	1	7.5586E0011	1.1390E0004
Error	6.6364E0008	10	6.6364E0007	
Total (Corr.)	7.5652E0011	11		

Correlation Coefficient = 0.999561
Stnd. Error of Est. = 8146.38

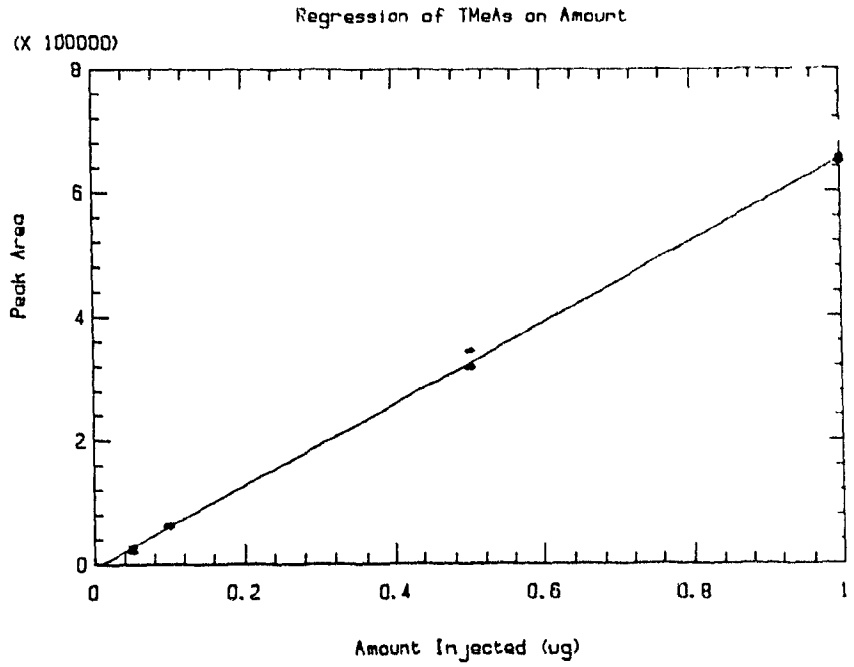

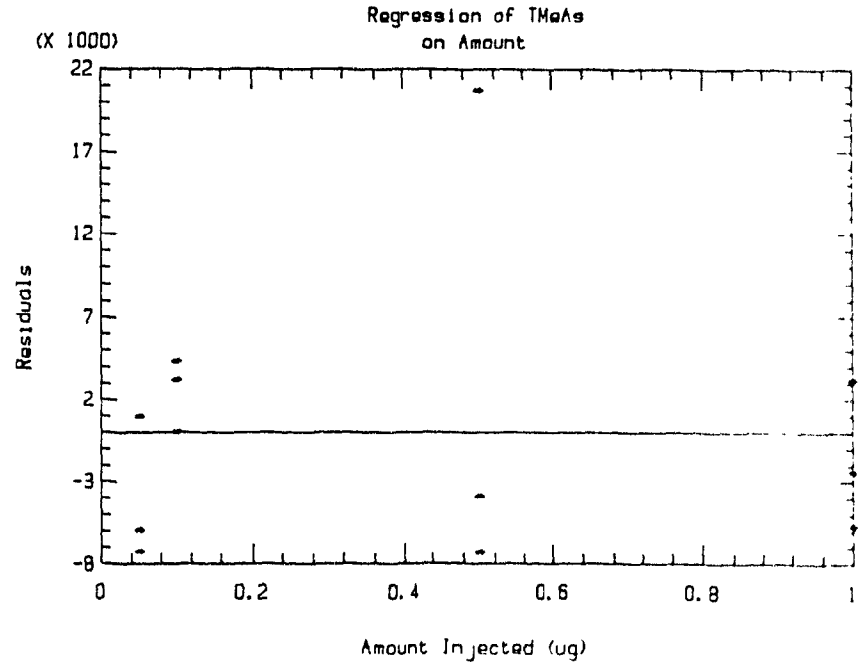

Figure A-13-a. Regression analysis related to the determination of the limit of detection of selenocholine.

Simple Regression of SeCholine on Amount

Parameter	Estimate	Standard Error	T Value	Prob. Level
Intercept	7108.66	1394.02	5.09939	4.64439E-4
Slope	124498	1017.37	122.372	0

Analysis of Variance

Source	Sum of Squares	Df	Mean Square	F-Ratio
Model	1.5380E0011	1	1.5380E0011	1.4975E0004
Error	1.0270E0008	10	1.0270E0007	
Total (Corr.)	1.5390E0011	11		

Correlation Coefficient = 0.999666
Stnd. Error of Est. = 3204.72

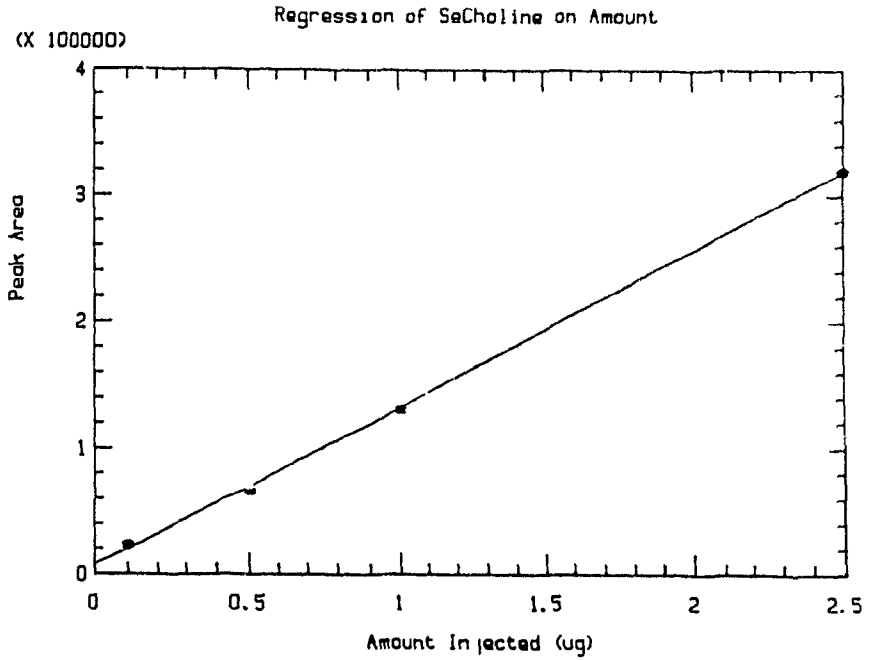

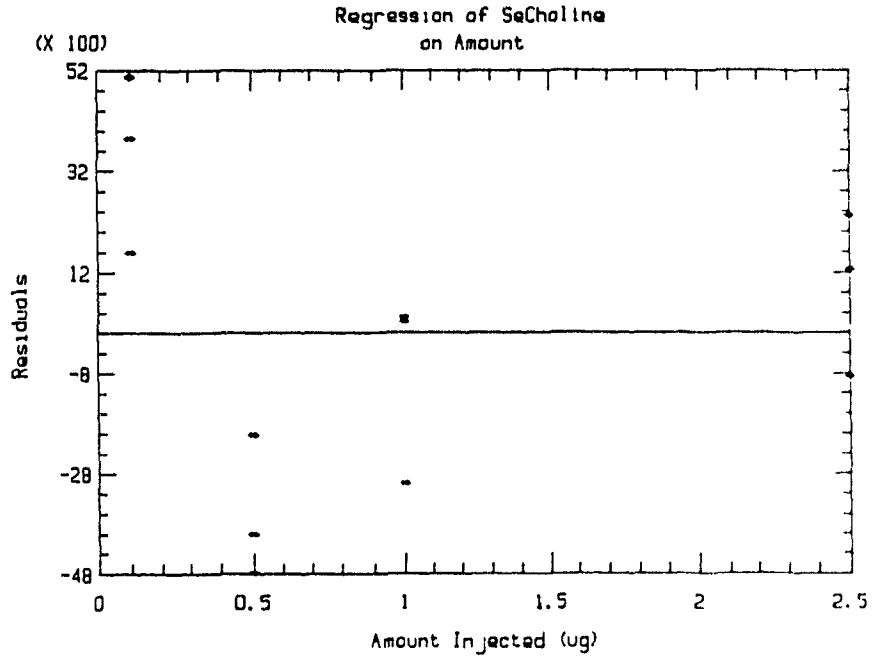

Figure A-13-b. Regression analysis related to the determination of the limit of detection of trimethylselenonium.

Simple Regression of TMSe on Amount

Parameter	Estimate	Standard Error	T Value	Prob. Level
Intercept	-7496.76	2458.15	-3.04976	0.0122567
Slope	107313	1793.98	59.8182	4.15223E-14

Analysis of Variance

Source	Sum of Squares	Df	Mean Square	F-Ratio
Model	1.1427E0011	1	1.1427E0011	3.5782E0003
Error	3.1934E0008	10	3.1934E0007	
Total (Corr.)	1.1459E0011	11		

Correlation Coefficient = 0.998606
Stnd. Error of Est. = 5651.04

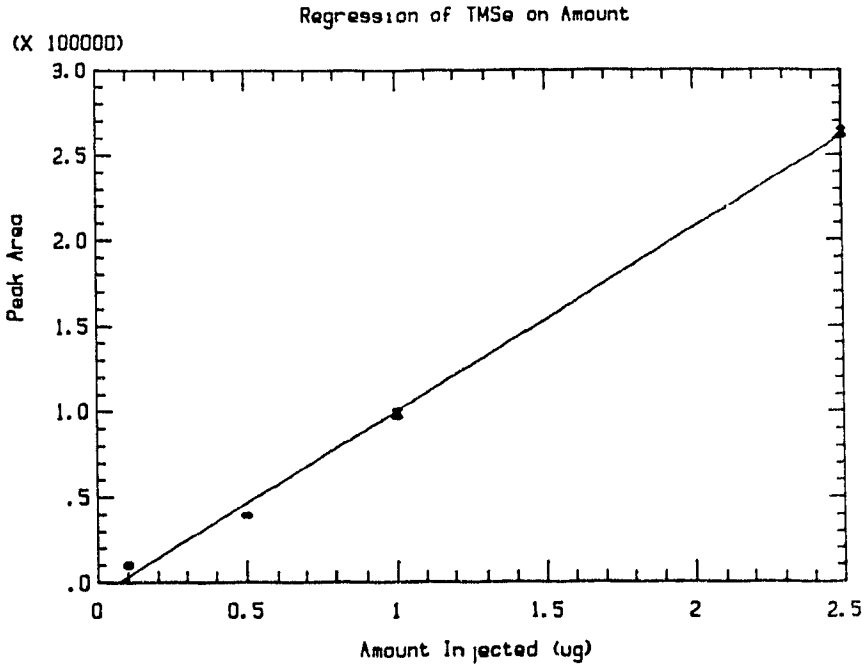

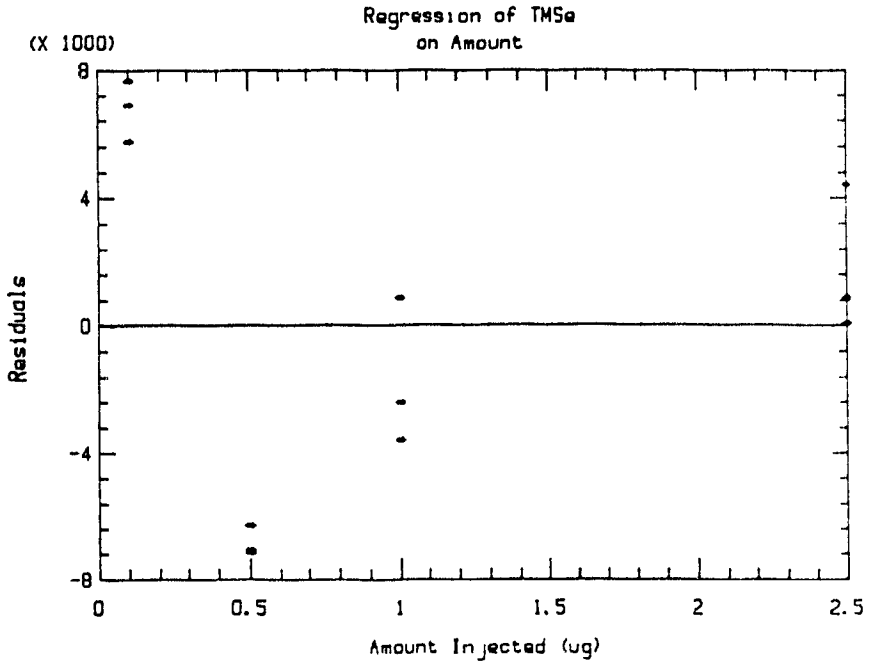

REFERENCES

Ashby, J., S. Clark and P.J. Craig. 1988. Methods for the production of volatile organometallic derivatives for application to the analysis of environmental samples. J. Anal. At. Spectrom. 3:735-736.

Bank, P.C., M.T.C. De Loos-Vollebregt and L. De Galan. 1988. Flow injection thermospray sample deposition for electrothermal atomization atomic absorption spectrometry. Spectrochimica Acta 43B:983-987.

Beauchemin, D., M.E. Bednas, S.S. Berman, J.W. McLaren, K.W.M. Siu and R.E. Sturgeon. 1988. Identification and quantification of arsenic species in dogfish muscle reference material for trace elements. Anal. Chem. 60:2209-2212.

Bayer, E. and A. Paulus. 1987. Silanophilic interactions in reversed-phase high performance chromatography. J. Chromatogr. 400:1-4.

Bayfield, R.F. and L.F. Romalis. 1985. pH control in the fluorometric assay for selenium with 2,3-diaminonaphtalene. Anal. Biochem. 144:569-576.

Belcher, R., W.I. Stephen, I.J. Thompson and P.C. Uden. 1971. Volatile metal chelates of monothioacetylacetone. J. Inorg. Nucl. Chem. 33:1851-1860.

Blais, J.S. and W.D. Marshall. 1986. Determination of alkyllead salts in runoff, soils and street dust containing high levels of lead. J. Environ. Qual. 15:255-260.

Blais, J.S. and W.D. Marshall. 1987. Synthesis of ^{14}C-radiolabelled trimethyllead chloride. Appl. Organomet. Chem. 1:251-260.

Blais, J.S. and W.D. Marshall. 1988a. Synthesis of [^{210}Pb]$(CH_3)_3$PbCl. Appl. Radiat. Isot. 39:1259-1264.

Blais, J.S., W.D. Marshall and R. Knowles. 1988b. Toxicity of alkyllead salts to anaerobic nitrogen transformations in sediments. J. Environ. Qual. 17:457-462

Blais, J.S., G.M. Momplaisir, and W.D. Marshall. 1989a. Synthesis, storage, and transfer of [^{210}Pb]$(CH_3)_3$PbCl across tomato fruit cuticle. Appl. Organomet. Chem. 3:89-98.

Blais, J.S. and W.D. Marshall. 1989b. Determination of ionic alkyllead compounds in water, soil and sediment by HPLC-Quartz tube atomic absorption spectrometry. J. Anal. At. Spectrom. 4:271-277.

Blackley, C.R., J.J. Carmony and M.L. Vestal. 1980. Liquid chromatograph-Mass Spectrometer for the analysis of non-volatile samples. Anal. Chem. 52:1636-1641.

Blaszkewicz, M., G. Baumhoer and B. Neidhart. 1984. Coupling of HPLC and chemical reaction detector for the separation and determination of organolead compounds. Fresenius Z. Anal. Chem. 317:221-225.

Bond, A.M. and G.G Wallace. 1981. Determination of copper as dithiocarbamate by reversed-phase liquid chromatography with electrochemical detection. Anal. Chem. 53:1209-1213.

Bond, A.M. and Y. Nagaosa. 1985. Determination of aluminum, copper, iron and manganese in biological and other samples as 8-quinolinol complexes by high-performance liquid chromatography with electrochemical detection. Anal. Chim. Acta 178:197-208.

Bonilla, M., L. Rodriguez and C. Camara. 1987. Determination of lead in biological materials by atomic absorption spectrometry sensitized with hydride generation J. Anal. At. Spectrom. 2:157-161.

Boorn, A.W. and R.F. Browner. 1982. Effects of organic solvents in inductively coupled plasma emission spectroscopy. Anal. Chem. 54:1402-1410.

Botre, C., F. Cacace and R. Cozzani. 1976. Direct combination of high performance liquid chromatography and atomic absorption spectroscopy for the analysis of metalorganic compounds. Anal. Lett. 9:825-830

Box, G.E.P and K.B. Wilson. 1951. On the experimental attainment of optimum conditions J. Roy Stat Soc (B) 13:1-14.

Brinckman, F.E., W.R. Blair, K.L. Jewett and W.P. Inverson. 1977. Application of a liquid chromatograph coupled with a flameless atomic absorption detector for the speciation of organometallic compounds J. Chromatogr. Sci. 15: 493-503.

Brinckman, F.E., K.L. Jewett, W.P. Inverson, K.J. Irgolic, K.C. Ehrhrart and R A Stockton 1980 Graphite-furnace atomic absorption spectroscopy as automated element specific detector for HPLC The determination of arsenite, arsenate, methylarsonic acid and dimethylarsinic acid. J. Chromatogr. 191:31-46

Brown, A.A., D.J. Roberts and K.V. Kahokola. 1987. Methods for improving the sensitivity in flame atomic absorption spectrometry. J. Anal. At. Spectrom. 2:201-204.

Bunnett, J.F. and D.H. Hermann. 1970. Kinetics of dinitrophenylation of amino acids. Biochemistry 9:816-822.

Burns, D.T., F. Glockling and M. Harriott. 1981. Investigation of the determination of tin tetraalkyls and alkyltin chlorides by atomic absorption spectrometry after separation by gas-liquid chromatography or high-performance liquid chromatography. Analyst 106:921-930.

Byard, J.L. 1969. Trimethyl selenide. A urirary metabolite of selenite. Arch. Biochem Biophys 130 556-560

Cannon, J.R., J.S. Edmonds, K.A. Francesconi, C.L. Raston, J.B. Saunders, B.W Skelton and A H. White 1980 Isolation, crystal structure and synthesis of arsenobetaine, a constituent of the western rock lobster, the dusty shark and some samples of human urine. Aust. J. Chem. 34:787-798.

Cardwell, T.J., J. Terence, D.J. Desarro and P.C. Uden. 1976. Gas chromatography of some volatile metal diethyldithiocarbamates. Anal.Chim. Acta 85:415-419.

Cardwell, T.J., P.J. Marriot and P.S. McDonough. 1980. Gas chromatography of volatile metal dialkylthiophosphates. J.Chromatogr. 193:53-60.

Carvajal, N.J. and R.H. Zienius. 1986. Gas chromatographic analysis of trace metals isolated from aqueous solutions as diethyldithiocarbamates. J. Chromatogr. 355:107-116.

Chau, Y.K., P.T.S. Wong and H. Saitoh. 1976a. Determination of tetraalkyl lead compounds in the atmosphere J. Chromatogr. Sc. 14:162-164.

Chau Y.K., P.T.S. Wong and P.D. Goulden. 1976b. Gas chromatography-atomic aborption spectrometry for the determination of tetraalkyllead compounds. Anal. Chim. Acta 85:421-424.

Chau, Y.K., P.T.S. Wong and P.D. Goulden. 1979. Determination of tetraalkyllead compounds in water, sediment and fish samples Anal. Chem. 51:186-188.

Chau, Y.K., P.T.S. Wong, O. Kramar, G.A. Bergert, R.B. Cruz, J.O. Kinrade, J. Lye and J C Van Loon 1980 Occurence of tetraalkyllead compounds in the aquatic environment. Bull. Environ Contam Toxicol 24 265-269.

Chau. Y.K., P.T.S. Wong, and O. Kramar. 1983. Determination of dialkyllead, trialkyllead, tetraalkyllead and lead(II) ions in water by chelation/extraction and gas chromatography/atomic absorption spectrometry. Anal. Chim. Acta 146:211-217.

Chau Y.K., P.T.S. Wong, G.A. Bergert and J.L. Dunn. 1984. Determination of dialkyllead, trialkyllead, tetraalkyllead and lead(II) compounds in sediment and biological samples. Anal. Chem. 56:271-274.

Chakraborti, D., S.G. Jiang, P. Surkijn, W. De Jongue and F. Adams. 1981. Determination of tetraalkyllead compounds in environmental samples by gas chromatography-graphite furnace atomic absorption spectrometry. Anal. Proc. 18:347-351.

Chakraborti, D., W.R.A. De Jongue, W.E. Van Mol, R.J.A. Van Cleuvenberger and F.C. Adams. 1984. Determination of ionic alkyllead compounds in water by gas chromatography/atomic absorption spectrometry. Anal. Chem. 56:2692-2697

Dedina, J. and I. Rubeska. 1980. Hydride atomization in a cool hydrogen-oxygen flame burning in a quartz tube atomiser. Spectrochim. Acta 35B:199-128.

Drash, G., L.V. Meyer and G. Kauer. 1982. Detection of lead and cadmium by HPLC after chelate extraction with Na-diethyldithiocarbamate. Fresenius Z. Anal. Chem. 311:695-696.

De Jonghe, W.R.A., D Chakraborti and F. Adams. 1980. Graphite furnace atomic absorption spectrometry as a metal-specific detection system for tetraalkyllead compounds separated by gas-liquid chromatography. Anal. Chim. Acta 115:89-101.

Huyghues-Despointes, A. 1990. Synthesis and determination of trimethylselenonium and selenocholine. M.Sc. Thesis, McGill University, Montreal, Quebec, Canada.

D'Ulivo, A., R. Fuoko and P Papoff. 1986. Behavior of some dialkyl and trialkyl-lead compounds in the hydride generation procedure using a non-dispersive atomic fluorescence detector. Talanta 33:401-405.

Ebdon, L., R.W. Ward and D.A. Leathard. 1982. Approaches to trace metals speciation in environmental samples. Anal. Proc. 19:110-113.

Ebdon, L., S.J. Hill and P. Jones. 1985. Speciation of tin in natural waters using high performance liquid chromatography-flame atomic absorption spectrometry. Analyst 110:515-517.

Ebdon, L., S.J. Hill and R.W. Ward. 1986. Directly coupled gas chromatography-atomic spectroscopy. Analyst 111:1113-1138.

Ebdon, L., S. Hill and R.W. Ward. 1987. Directly coupled liquid chromatography-atomic spectroscopy. Analyst 112:1-16.

Elgersma, J.W., F.J. Maessen and W.M. Niessen. 1986. Low consumption thermospray nebulizer with a fused silica vaporizer for inductively coupled plasma atomic emission spectroscopy. Spectrochim. Acta 41B:1217-1220.

Estes, S.A., P.C. Uden and R.M. Barnes. 1981. High resolution gas chromatography of trialkyllead chloride with an inert solvent interface for microwave excited helium plasma detection. Anal. Chem. 53:1336-1340.

Estes, S.A., P.C. Uden and R.M. Barnes. 1982a. Plasma emission spectral detection for high resolution gas chromatographic study of group IV organometallic compounds. J. Chromatogr. 239:181-189.

Estes, S.A., P.C. Uden and R.M. Barnes. 1982b. Determination of n-butylated trialkyllead complunds by gas chromatography with microwave plasma emission detection. Anal. Chem. 54:2402-2405.

Flemming, H.D. and R.G. Ide. 1976. Determination of volatile-hydride-forming metals in steel by atomic absorption spectrometry Anal. Chim. Acta 83:67-82.

Foley, J.P. and Dorsey J.G. 1984. Clarification of the limit of detection in chromatography. Chromatographia 18:503-512.

Forsyth, D.S. and W.D. Marshall. 1983. Determination of alkyllead salts in water and whole eggs by capillary column gas chromatography with electron capture detection. Anal. Chem. 55:2132-2137.

Forsyth, D.S. and W.D. Marshall. 1985. Performance of an automated gas chromatograph-silica furnace-atomic absortion spectrometer for the determination of alkyllead compounds. Anal. Chem. 57:1299-1305

Forsyth, D.S. and W.D. Marshall. 1986. Ionic alkylleads in Herring Gulls from the Great Lakes regions Environ. Sci. Technol. 20:1033-1037.

Francesconi, K.A., P. Mick, R.A. Stockton and K.J. Irgolic. 1985. Quantitative determination of arsenobetaine, the major water-soluble arsenical in three species of crab, using high pressure liquid chromatography and an inductively coupled argon plasma emission spectrometer as the arsenic-specific detector Chemosphere 14 1443-1453.

Ganther, H.E. and R.J. Kraus. 1984 Identification of hydrogen selenide and other volatile selenols by derivatization with 1-fuoro-2,4-dinitropbenzene. Anal. Biochem. 138:396-403.

Gast, C.H., J.C. Kraak, H. Poppe and F.J.M.J. Maessen. 1979. Capabilities of on-line element specific detection in HPLC using an inductively coupled argon plasma emission source detector. J. Chromatogr. 185 549-561.

Godden, R.G. and D.R. Thomerson. 1980 Generation of covalent hydrides in atomic absorption spectroscopy. A review. Analyst 105:1137-62.

Gouw, T.H., R.E. Jentoft and E.J. Gallegos. 1979. High pressure science and technology, Sixth AIRAPT Conference. (K.D. Timmerhaus and M.S. Barber, ed's), Plenum Press, N.Y. Vol 1, p. 583.

Greandjean, P. and T. Nielsen. 1979. Organolead compounds: Environmental health aspects. Residue Rev 72:97-154.

Griffing, M.E., A. Rozek, L.J. Snyder and H.R. Henderson. 1957 Determination of trace amounts of lead in gasolines and naphthas. Anal. Chem. 29:190-195.

Harrison, R.M. and D.H.P. Laxen. 1978. Natural source of tetraalkyllead in air. Nature 275:738-739

Hatfield, D.B. 1987. Electrically heated quartz atomisation cell for hydride generation absorption spectrometry Anal. Chem. 59:1887-1888.

Hausler, D.W. and L.T. Taylor. 1981. On-line determination of metals by size exclusion chromatography with induced coupled plasma atomic emission spectrometry detection. Anal. Chem. 53 1223-1227

Heizmann, P. and K. Ballschmiter. 1977 High performance liquid chromatography of metal 1,2-diketobisthiobenzylhydrazone, metal dialkyldithiocarbamates and 1,2-diketobisthiosemicarbazones. J. Chromatogr. 137:153-163.

Hill, S., Ebdon, L. and P. Jones. 1986. Novel approaches to directly coupled high performance liquid chromatography-flame atomic absorption spectrometry for trace metals speciation. Anal. Proc. 23:6-8.

Hill, WJ. and W.G. Hunter. 1966. A review of response surface methodology: A litterature survey. Technometrics 8:571-587.

Hubis, W. and R.O. Clark. 1955. Rapid polarographic determination of lead in gasoline. Anal. Chem. 27:1009-1110.

Honeycutt, J.B. and J.M. Riddle. 1960. Preparation and reactions of sodium tetraethylborate and related compounds. J. Am. Chem. Soc. 82:3051-3052.

Honeycutt, J.B. and J.M. Riddle. 1961. Preparation and reactions of sodium tetraethylborate and related compounds. J. Am. Chem. Soc. 83:369-373.

Iadevaia, R., N. Aharonson and E.A. Woolson. 1980. Extraction and clean-up of soil arsenical residues. J. Assoc. Off. Anal. Chem. 6:742-746.

Ikeda, M., F. Palacios, J. Nishibe, S. Hamada and R. Tujino. 1981. Dtermination of lead at the ng level by reduction tp plumbane and measurement by inductively coupled plasma emission spectrometry. Anal. Chim. Acta. 125:109-115.

Irgolic, K.J., R.A. Stockton, D. Chakrabarti and W. Bayer. 1983. Simultaneous induced-coupled argon plasma emission spectroscopy as a multi-element-specific detector for high performance liquid chromatography determination of arsenic, selenium and phosphorus compounds. Spetrochim. Acta 38B:437-445.

Irving, H. and U.S Manhot. 1967. Interaction of dithizone with allegedly purified dioxane. Chem. Ind. (London) 193-194.

Jin, U. and M. Taga. 1982. Determination of lead by continuous flow hydride generation atomic absorption spectrometry. Anal. Chim. Acta 143:229-236.

Jinno, K., H. Tsuchida, S. Nakanishi, Y. Hirata and C. Fujimoto. 1983. Micro-high performance liquid chromatography-inductively coupled plasma combination technique in analysis of organometallic compounds. Appl. Spectroc. 37:258-261.

Jones, D.R., H.C. Tung and S.E. Manahan. 1976. Mobile phase effects on atomic absorption detectors for high speed liquid chromatography. Anal. Chem. 48:7-10.

Katz, E.D. and R.P. Scott. 1985. Peak dispersion in a liquid chromatography-atomic absorption spectrometry system. Analyst 110:253-261.

Koropchack, J.A., H. Aryamanya-Mugisha and D.H. Winn. 1988. Effect of capillary diameter on the thermospray sample introduction to inductively coupled plasma atomic emission spetrometry. J. Anal. At. Spectrom. 3:799-802

Koizumi, H., T. Hadeishi and R. McLaughlin. 1978. Speciation of organometallic compounds by Zeeman attomic absorption spectrometry with liquid chromatography. Anal. Chem. 50:1700-1701.

Kraus, R.J., S.J. Foster and H.E. Ganther. 1985. Analysis of trimethylselenonium ion in urine by high performance liquid chromatography. Anal. Biochem. 147:432-436.

Kurosawa, S., K. Yasuda, M. Tagushi, S. Yamasaki, S. Toda, M. Morita, T. Uehiro and K. Fuwa. 1980. Identification of arsenobetaine, a water soluble compound in muscle and liver of a Shark, *Prionace glaucus*. Agric. Biol. Chem. 44:1993-1994.

LaFreniere, K.E., V.A. Fassel and D.E. Eckels. 1987. Elemental speciation via high performance liquid chromatography combined with inductively coupled plasma atomic emission spectrometric detection Anal Chem. 59:879-887.

Lawrence, J.F., P. Michalik, G. Tam and H.B.S. Conacher. 1986. Identification of arsenobetaine and arsenocholine in Canadian fish and shellfish by high performance liquid chromatography with atomic absorption detection and fast atom bombardment mass spectrometry. J. Agric. Food Chem. 34:315-319

Lawrence, K.E., G.W. Rice and V.A. Fassel. 1984. Direct liquid sample introduction for flow injection analysis and liquid chromatography with induced coupled argon plasma spectrometric detector. Anal Chem 56:289-292.

Lederer, M. 1955. Separation of rare heart elements. Nature 176:462-463.

Lohmuller, H., P. Heizmann and K. Ballschmiter. 1977. High performance liquid chromatography of metal dithizonates. J. Chromatogr. 137:165-170.

Low, G.K.C., G.E. Batley and S.T. Buchanan. 1986. Application of column switching in high performance liquid chromatography to arsenic speciation analysis with inductively coupled argon plasma spectrometric detection J Chromatogr. 368:423-426.

Masaryk, J., J. Krupcik, J. Garaj and M. Kosik. 1975. Gas chromatographic separation of some metals J Chromatogr. 115:256-258.

Messman, J.D., and T.C. Rains. 1981. Determination of tetraalkyllead compounds in gasoline Anal Chem 53:1632-1636.

Mooney, J.P., M. Meaney, M.R. Smyth, R.G. Leonard and G.G. Wallace. 1987. Determination of copper(II) and iron(III) in some anaerobic adhesive formulations using high-performance liquid chromatography Analyst 112:1555-1558.

Momplaisir, G.M., 1990. Synthesis and determination of arsenobetaine, arsenocholine and tetramethylarsonium. M.Sc. Thesis, McGill University, Montreal, Quebec, Canada.

Nahapetian, A.T., M. Janghorbani and V R. Young. 1983 Urinary trimethylselenonium excretion by the rat effect of source and level of selenium-75. J. Nutr. 113:401-411.

Nahum, A. and C. Horvath. 1983. Dual retention mechanism in reversed-phase chromatography. J Chromatogr. 203:53-64.

Nakai, S. and T. Kaneko. 1985. Standardization of mapping simplex optimization. J. Food Sci. 50:845-846

Nygren, O., C.A. Nilsson and W. French. 1988. On-line interfacing of a liquid chromatograph to a continuously heated graphite furnace atomic absorption spectrophotometer for element-specific detection Anal. Chem. 60:2204-2208.

Palmer, I.S., S. Gunsalus, A.W. Halverson and O E. Olson. 1970 Trimethylselenonium ion as a general excretion product from selenium metabolism in the rat. Biochim. Biophys Acta 108 260-266

Parks, E.J., F.E. Brinckman and W.R. Blair. 1979. Application of a graphite furnace-atomic absroption spectrometry detector automatically coupled to a HPLC. J.Chromatogr. 185:563-572.

Purdue, J.P., R.E. Enrione, R.J. Thompson and B.A. Bonfield. 1973. Determination of organic and total lead in the atmosphere by atomic absorption spectrometry. Anal. Chem. 45:527-530.

Rapsomanikis, S., O.F.X. Donard and J.H. Weber. 1986. Speciation of lead and methyllead ions in water by gas chromatography after ethylation with sodium tetraethylborate. Anal. Chem. 58:35-38.

Ricci, G.R., L.S Shepard, G. Colovos and N.E. Hester. 1981. Ion chromatography with atomic absorption spectrometry for determination of organic and inorganic arsenic species. Anal.Chem. 53:611-613.

Robinson, J W. and E.L. Kiesel. 1977. Concentrations of molecular and organic lead in the atmosphere. J. Environ. Sci. Health A12:411-422.

Robinson, J.W. and D.S. Choi. 1987. The development of a thermospray flame atomizer for AA improved sensitivity, interfacing witth HPLC Spectrosc. Lett. 20:375-390.

Schwartz, S.A. and G.A. Meyer. 1986. Characterisation of aerosols generated by thermospray nebulization for atomic spectroscopy. Spectrochimica Acta 41B:1287-1298.

Shiomi, K., Kakehashi, Y., Yamanaka, H. and T. Kikushi. 1987. Identification of arsenobetaine and tetramethylarsonium in the clam *Meretrix lusoria*. Appl. Organomet. Chem. 1:177-183.

Siemer, D.D and L. Hageman. 1975. Improved hydride generation apparatus for selenium determination. Anal. Lett. 8:323-337.

Siemer, D.D , P. Koteel and V. Jawiwala. 1976. Optimization of arsine generation in atomic absorption arsenic determinations. Anal. Chem. 48:836-840.

Siemer, D.D. and P. Koteel. 1977. comparison of methods of hydride generation atomic absorption spectrometric analysis of arsenic and selenium determination. Anal. Chem. 49:1096-1099.

Smith, R. 1981. Use of a hydride generation technique for the atomic absorption determination of lead in drinking water, At. Spectrosc. 2:155-158.

Snyder, L.J. and S.R Henderson. 1961. A new field method for the determination of organolead compounds in air. Anal. Chem. 33:1175-1180.

Stary, J and J Ruzicka. 1968 Extraction and exchange constants of dithizonates and diethyldithiocarbamates. Talanta 15:505-514.

Stockton, R.A. and K.J. Irgolic. 1979. The Hitachi graphite furnace-Zeeman atomic absorption spectrometer as an automated element-specific detector for high pressure liquid chromatography. Int. J. Anal. Chem. 6:313-319.

Sun, X F , B T.G. Ting and M. Janghorbani. 1987. Excretion of trimethylselenonium in human urine. Anal. Biochem. 167:304-311.

Tavlaridis, A. and A. Neeb. 1978. Dialkyldithiocarbamates as reagents for the gas chromatographic determination of metals. I. Thermal behavior, vapor pressure and gas chroamtography of some dialkyldithiocarbamate chelates. Fresenium Z. Anal. Chem. 293:211-219.

Tye, C.T., S.J. Haswell, P. O'Neil and K.C.C. Bancroft. 1985. High performance liquid chromatography with hydride generation/atomic absorption spectrometry for the determination of arsenic species with application to some water samples. Anal. Chim. Acta 169:195-200.

Uden, P.C., D.E. Henderson and A. Kamalized. 1974. Electron capture gas chromatographic determination of cupper and nickel beta-ketoamines chelates. J. Chromatogr. Sci. 12:591-598

Vermeiren, K.A., P.D.P. Taylor and R.J. Dams. 1987. Use of a thermospray nebulizer as a sample introduction system for inductively coupled plasma-atomic emission spectrometry. J. Anal. At. Spectrom. 2.383-387

Vickrey, T.M. and W.J. Eue. 1979. A microprocessor controlled liquid chromatograph/atomic absorption sampling system. J. Autom. Chem. 1:198-202.

Vickrey, T.M., H.E. Howell, G.V. Harrison and G.J. Ramelow. 1980. Post-column digestion methods for liquid chromatography-graphite furnace atomic absorption speciation of organolead and organotin compounds Anal Chem. 52:1743-1746.

Vijan, P.N. and G.R. Wood. 1976. Semi-autometed determination of lead by hydride generation and atomic absorption spectrophotometry. Analyst 101:966-973.

Vlacil, F. and V. Hamplova. 1985. A contribution to the description of the retention of metal chelates during their reversed-phase chromatography. Collection Czechoslovak Chem. Commun 50:2221-2227

Welz, B. and M. Melcher. 1983. Volatile hydride-forming elements in a heated quarzt cell Part 1 Gas-phase and surface effects; decomposition and atomisation of arsine. Analyst 108:213-222.
